

---

# Large-Scale Load Tests and Data Base of Spread Footings on Sand

---

PUBLICATION NO. FHWA-RD-97-068

NOVEMBER 1997



U.S. Department of Transportation  
**Federal Highway Administration**

Research and Development  
Turner-Fairbank Highway Research Center  
6300 Georgetown Pike  
McLean, VA 22101-2296

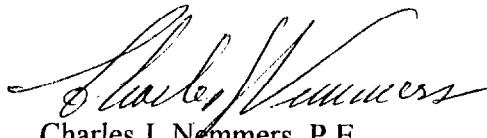


## FOREWORD

This report, "Large-Scale Load Tests and Data Base of Spread Footings on Sand", documents research which had a goal of improving the reliability of design rules for spread footings; accomplishment of the goal was seen as a way of increasing the confidence of engineers in the judicious use of spread footings instead of deep foundations, thus effecting economies in foundation engineering.

The research included: 1) the development of a data base for spread footings, including case histories and load tests, 2) evaluation of the performance of large-scale footings in sand, 3) evaluation of accuracy of footing performance prediction methods, and 4) new prediction methods.

The report will be of interest to engineers and technologists charged with the design and construction of foundations.



Charles J. Nemmers, P.E.  
Director, Office of Engineering  
Research and Development

## NOTICE

This document is disseminated under the sponsorship of the Department of Transportation in the interest of information exchange. The United States Government assumes no liability for its contents or use thereof. This report does not constitute a standard, specification, or regulation.

The United States Government does not endorse products or manufacturers. Trademarks or manufacturers' names appear herein only because they are considered essential to the object of this document.

### Technical Report Documentation Report

1. Report No. FHWA-RD-97-068		2. Government Accession No.		3. Recipient's Catalog No.	
4. Title and Subtitle LARGE SCALE LOAD TESTS AND DATA BASE OF SPREAD FOOTINGS ON SAND				5. Report Date November 1997	
				6. Performing Organization Code 14G604	
7. Author(s) Jean-Louis BRIAUD and Robert GIBBENS				8. Performing Organization Report No.	
9. Performing Organization Name and Address Geotest Engineering, Inc. Texas A&M University 5600 Bintliff Drive Civil Engineering Dept. Houston, Texas 77036 College Station, Texas 77843				10. Work Unit No. (TRAIS) 3E3A0291	
				11. Contract or Grant No. DTFH61-92-Z-00050	
12. Sponsoring Agency Name and Address Federal Highway Administration, HNR 10 Turner Fairbank Highway Research Center 6300 Georgetown Pike McLean, Virginia 22101				13. Type of Report and Period Covered Final Report	
				14. Sponsoring Agency Code	
15. Supplementary Notes Contracting Officer's Technical Representative (COTR): A.F. Dimillio FHWA Technical Consultants: M.T. Adams, R. Cheney and J. Dimaggio Contractor Project Manager: V.N. Vijayvergia					
16. Abstract  Spread Footings are most often less expensive than deep foundations. In an effort to improve the reliability of spread footings, this research project was undertaken. The results consist of:  <ol style="list-style-type: none"> <li>1. A user friendly microcomputer data base of spread footings, case histories and load tests.</li> <li>2. The performance of five large scale square footings in sand.</li> <li>3. An evaluation of the current accuracy of settlement and bearing capacity prediction methods.</li> <li>4. Observations on the scale effect, the zone of influence, the creep settlement, and soil heterogeneity.</li> <li>5. A new and simple method to predict the complete load settlement curve for a footing as well as several correlations.</li> <li>6. Evaluation of the WAK test, a dynamic test for spread footings.</li> </ol>					
17. Key Words Spread footings, load tests, data base, sand, in situ testing, instrumentation, dynamic testing, finite element analysis, shallow foundations.			18. Distribution Statement No Restrictions. This document is available to the public from the National Technical Information Service, Springfield, Virginia 22161		
19. Security Classif. (of this report) Unclassified		20. Security Classif. (of this page) Unclassified		21. No. of Pages 228	22. Price

## UNIT CONVERSIONS

Acceleration	$9.81 \text{ m/s}^2 = 386.22 \text{ in./s}^2 = 32.185 \text{ ft/s}^2$ , Paris: $g = 9.80665 \text{ m/s}^2$ London: $g = 3.2174 \times 10^1 \text{ ft/s}^2$
Area	$1 \text{ m}^2 = 1.5500 \times 10^3 \text{ in.}^2 = 1.0764 \times 10^1 \text{ ft}^2 = 1.196 \text{ yd}^2 = 10^6 \text{ mm}^2$ $= 10^4 \text{ cm}^2 = 2.471 \times 10^{-4} \text{ acres}^2 = 3.861 \times 10^{-7} \text{ mi}^2$
Coefficient of Consolidation	$1 \text{ m}^2/\text{s} = 10^4 \text{ cm}^2/\text{s} = 6 \times 10^5 \text{ cm}^2/\text{min} = 3.6 \times 10^7 \text{ cm}^2/\text{h}$ $= 8.64 \times 10^8 \text{ cm}^2/\text{day} = 2.628 \times 10^{10} \text{ cm}^2/\text{month}$ $= 3.1536 \times 10^{11} \text{ cm}^2/\text{year}$ $= 1.550 \times 10^3 \text{ in.}^2/\text{s} = 4.0734 \times 10^9 \text{ in.}^2/\text{month}$ $= 1.3392 \times 10^8 \text{ in.}^2/\text{day} = 4.881 \times 10^{10} \text{ in.}^2/\text{year}$ $= 9.4783 \times 10^5 \text{ ft}^2/\text{day} = 2.8830 \times 10^7 \text{ ft}^2/\text{month}$ $= 3.3945 \times 10^8 \text{ ft}^2/\text{year}$
Flow	$1 \text{ m}^3/\text{s} = 10^6 \text{ cm}^3/\text{s} = 8.64 \times 10^4 \text{ m}^3/\text{day} = 8.64 \times 10^{10} \text{ cm}^3/\text{day}$ $= 3.5314 \times 10^1 \text{ ft}^3/\text{s} = 3.0511 \times 10^6 \text{ ft}^3/\text{day}$
Force	$10 \text{ kN} = 2.2482 \times 10^3 \text{ lb} = 2.2482 \text{ kip} = 1.1241 \text{ t}$ (short ton = 2000 lb) $= 1.0194 \times 10^3 \text{ kg} = 1.0194 \times 10^6 \text{ g} = 1.0194 \text{ T}$ (metric ton = 1000 kg) $= 10^9 \text{ dynes} = 3.5971 \times 10^4 \text{ ounces} = 1.0221 \text{ t}$ (long ton = 2200 lb)
Force per Unit Length	$1 \text{ kN/m} = 6.8526 \times 10^1 \text{ lb/ft} = 6.8526 \times 10^{-2} \text{ kip/ft}$ $= 3.4263 \times 10^{-2} \text{ t/ft}$ $= 1.0194 \times 10^2 \text{ kg/m} = 1.0194 \times 10^{-1} \text{ T/m}$
Length	$1 \text{ m} = 3.9370 \times 10^1 \text{ in.} = 3.2808 \text{ ft} = 1.0936 \text{ yd}$ $= 10^{10} \text{ Angstrom} = 10^6 \text{ microns} = 10^3 \text{ mm} = 10^2 \text{ cm}$ $= 10^{-3} \text{ km} = 6.2137 \times 10^{-4} \text{ mile} = 5.3996 \times 10^{-4} \text{ nautical mile}$
Moment or Energy	$1 \text{ kN.m} = 7.3759 \times 10^2 \text{ lb.ft} = 7.3759 \times 10^{-1} \text{ kip.ft} = 3.6879 \times 10^{-1} \text{ t.ft}$ $= 1.0194 \times 10^3 \text{ g.cm} = 1.0194 \times 10^2 \text{ kg.m} = 1.0194 \times 10^{-1} \text{ T.m}$ $= 10^3 \text{ N.m} = 10^3 \text{ Joule}$
Moment of Inertia	$1 \text{ m}^4 = 2.4025 \times 10^6 \text{ in}^4 = 1.1586 \times 10^2 \text{ ft}^4 = 6.9911 \times 10^{-1} \text{ yd}^4$ $= 10^8 \text{ cm}^4 = 10^{12} \text{ mm}^4$
Moment per Unit Length	$1 \text{ kN.m/m} = 2.2482 \times 10^2 \text{ lb.ft/ft} = 2.2482 \times 10^{-1} \text{ kip.ft/ft}$ $= 1.1241 \times 10^{-1} \text{ t.ft/ft} = 1.0194 \times 10^2 \text{ kg.m/m} = 1.0194 \times 10^{-1} \text{ T.m/m}$
Pressure	$100 \text{ kPa} = 10^2 \text{ kN/m}^2 = 1.4503 \times 10^1 \text{ lb/in.}^2 = 2.0885 \times 10^3 \text{ lb/ft}^2$ $= 1.4503 \times 10^{-2} \text{ kip/in.}^2 = 2.0885 \text{ kip/ft}^2 = 1.0442 \text{ t/ft}^2$ $= 7.5003 \times 10^1 \text{ cm of Hg (0}^\circ \text{ C)} = 1.0197 \text{ kg/m}^2 = 1.0197 \times 10^1 \text{ T/m}^2$ $= 9.8689 \times 10^{-1} \text{ Atm} = 3.3455 \times 10^1 \text{ ft of H}_2\text{O (4}^\circ \text{ C)}$ $= 1.0000 \text{ bar} = 10^6 \text{ dynes/cm}^2$
Temperature	$^\circ\text{C} = 5/9(^\circ\text{F} - 32)$ , $^\circ\text{K} = ^\circ\text{C} + 273.15$
Time	$1 \text{ yr.} = 12 \text{ mo.} = 365 \text{ day} = 8760 \text{ hr} = 5.256 \times 10^5 \text{ min} = 3.1536 \times 10^7 \text{ s}$
Unit Weight, Coefficient of Subgrade Reaction	$10 \text{ kN/m}^3 = 6.3654 \times 10^1 \text{ lb/ft}^3 = 3.6837 \times 10^{-2} \text{ lb/in.}^3$ $= 1.0196 \text{ g/cm}^3 = 1.0196 \text{ T/m}^3 = 1.0196 \times 10^3 \text{ kg/m}^3$
Velocity or Permeability	$1 \text{ m/s} = 3.6 \text{ km/h} = 2.2369 \text{ mile/h} = 6 \times 10^1 \text{ m/min} = 10^2 \text{ cm/s}$ $= 1.9685 \times 10^2 \text{ ft/min} = 3.2808 \text{ ft/s} = 1.0346 \times 10^8 \text{ ft/year} = 2.8346 \times 10^5 \text{ ft/day}$
Volume	$1 \text{ m}^3 = 6.1024 \times 10^4 \text{ in.}^3 = 3.5315 \times 10^1 \text{ ft}^3 = 1.308 \text{ yd}^3 = 10^9 \text{ mm}^3 = 10^6 \text{ cm}^3 = 10^3 \text{ dm}^3$ $= 10^3 \text{ liter} = 2.1998 \times 10^2 \text{ gallon (U.K.)} = 2.6417 \times 10^2 \text{ gallon (U.S.)}$
Volume Loss in a Tubing	$1 \text{ cm}^3/\text{m/kPa} = 8.91 \times 10^{-4} \text{ in.}^3/\text{ft/psf}$

## TABLE OF CONTENTS

	Page
1. SUMMARY.....	1
1.1 GOALS.....	1
1.2 RESULTS.....	3
2. INTRODUCTION.....	8
3. SHALDB: DATA BASE OF SPREAD FOOTINGS.....	10
3.1 THE DATA BASE FILES.....	10
3.1.1 General Information.....	10
3.1.2 Footing Data.....	11
3.1.3 Footing Behavior.....	11
3.1.4 Soil Data.....	11
3.1.5 Settlement Predictions.....	12
3.1.6 Case Histories Listed in the Data Base.....	13
3.2 THE DATA BASE PROGRAM.....	15
3.2.1 System Requirements.....	16
3.2.2 Installation.....	16
3.2.3 The Maintenance Section.....	17
3.2.3.1 Adding a New Case History.....	18
3.2.3.2 Modifying an Existing Case History.....	18
3.2.4 The Inquires Section.....	20
3.2.4.1 The Parameter Based Search.....	20
3.2.4.2 Viewing a Footing.....	21
3.2.5 The Data Analysis Section.....	21
3.2.5.1 Background Calculations.....	21
3.2.5.2 Unit Conversions.....	21
3.2.5.3 Averages and Standard Deviation.....	22
3.2.5.4 Unit Weight and Overburden Pressure.....	22
3.2.6 Settlement Prediction Methods.....	23
3.2.7 Data Analysis.....	25
4. LOAD TESTING OF FIVE LARGE-SCALE FOOTINGS ON SAND.....	26
4.1 LOAD TEST SETUP.....	26
4.1.1 Spread Footing Construction.....	26
4.1.2 Reaction Shaft Construction.....	28
4.1.3 Horizontal Displacement Measurements (Inclinometers).....	28
4.1.4 Vertical Displacement Measurements (Extensometer).....	31
4.1.5 Footing Displacement Measurements.....	31
4.1.6 Load Measurements.....	33

## TABLE OF CONTENTS (continued)

	Page
4.2 SOIL INVESTIGATION.....	33
4.2.1 General Soil Description.....	33
4.2.2 Laboratory Tests.....	33
4.2.3 Field Tests.....	35
4.2.3.1 Standard Penetration Tests w/ Energy Measurements.....	36
4.2.3.2 PiezoCone Penetration Tests.....	36
4.2.3.3 Pressuremeter Tests.....	36
4.2.3.4 Dilatometer Tests.....	39
4.2.3.5 Borehole Shear Test.....	39
4.2.3.6 Cross-Hole Wave & Step Blade Tests.....	39
4.3 RESULTS.....	39
4.3.1 Load Settlement Curves.....	39
4.3.2 Creep Curves.....	39
4.3.3 Inclinometer Profiles.....	41
4.3.4 Telltale Profiles.....	47
5. COMPARISON BETWEEN PREDICTED AND MEASURED RESULTS.....	51
5.1 PREDICTION SYMPOSIUM EVENT USING THE FIVE FOOTINGS.....	51
5.1.1 Introduction.....	51
5.1.2 The Prediction Request.....	51
5.1.3 Prediction Results and Comparisons.....	52
5.1.4 Predicted Design Loads and Factor of Safety.....	62
5.1.5 General Observations.....	63
5.2 EVALUATION OF 18 PREDICTION METHODS USING THE FIVE FOOTINGS.....	67
5.2.1 Settlement Prediction Methods.....	68
5.2.2 Bearing Capacity Methods.....	69
5.2.3 Best Method.....	69
6. WAK TEST.....	71
6.1 PROCEDURES.....	71
6.2 DATA ANALYSIS.....	75
6.3 COMPARISON WITH LOAD TESTS.....	75
7. ANALYSIS OF THE DATA.....	83
7.1 SCALE EFFECT.....	83
7.2 CREEP SETTLEMENT.....	89
7.3 STRAIN VERSUS DEPTH.....	92
7.4 SOIL MASS DEFORMATION.....	95
8. NEW LOAD SETTLEMENT CURVE METHOD.....	100
8.1 THE IDEA.....	100
8.2 DEVELOPEMENT OF THE METHOD.....	101
8.3 STEP BY STEP PROCEDURE.....	108

**TABLE OF CONTENTS (continued)**

	<b>Page</b>
<b>9. CONCLUSIONS</b> .....	111
<b>APPENDIX A: Soil Data</b> .....	117
<b>APPENDIX B: Load Settlement Curves</b> .....	159
<b>APPENDIX C: Creep Curves</b> .....	170
<b>APPENDIX D: Inclinator Results</b> .....	193
<b>APPENDIX E: Telltale Results</b> .....	209
<b>REFERENCES</b> .....	214

## LIST OF FIGURES

Figure	Page
4.1 Footing/Pier Layout.....	27
4.2 Load Test Setup.....	29
4.3 In Situ Field Testing Layout with Auger Hole Location.....	30
4.4 Cross Sectional View of Telltale.....	32
4.5 General Soil Layering.....	34
4.6 Grain Size Analysis.....	37
4.7 Range of STP Results.....	38
4.8 Range of 5 CPT Soundings.....	38
4.9 Range of PMT Results.....	40
4.10 Range of DMT Results.....	40
4.11 Range of BHST Results.....	41
4.12 30-Minute Monotonic Load Settlement Curves for All Footings.....	42
4.13 Individual Creep Exponent Curves for 1.5-m Footing, 1.34 MN - 2.80 MN.....	43
4.14 Individual Creep Exponent Curves for 1.5-m Footing - 24-Hour Creep Test.....	44
4.15 Individual Creep Exponent Curves for 3.0-m(n) Footing, 6.23 MN - 10.24 MN.....	45
4.16 Individual Creep Exponent Curves for 3.0-m(n) Footing - 24-Hour Creep Test.....	46
4.17 Inclinator Test - 1.78-MN Fail Load - N-S Direction, 1.0-m Footing.....	48
4.18 Inclinator Test - 8.90-MN Fail Load - N-S Direction, 3.0-m Footing.....	49
4.19 Settlement Versus Depth for 3.0-m(s) Footing With Varying Percentages of B.....	50
5.1 Load-Settlement Curve.....	52
5.2 Distribution of $Q_{pred}/Q_{meas}$ for 25-mm Settlement: 3-m North Footing.....	57
5.3 Distribution of $Q_{pred}/Q_{meas}$ for 25-mm Settlement: 3-m South Footing.....	57
5.4 Distribution of $Q_{pred}/Q_{meas}$ for 25-mm Settlement: 2.5-m Footing.....	58
5.5 Distribution of $Q_{pred}/Q_{meas}$ for 25-mm Settlement: 1.5-m Footing.....	58
5.6 Distribution of $Q_{pred}/Q_{meas}$ for 25-mm Settlement: 1.0-m Footing.....	59
5.7 Distribution of $Q_{pred}/Q_{meas}$ for 150-mm Settlement: 3-m North Footing.....	59
5.8 Distribution of $Q_{pred}/Q_{meas}$ for 150-mm Settlement: 3-m South Footing.....	60
5.9 Distribution of $Q_{pred}/Q_{meas}$ for 150-mm Settlement: 2.5-m Footing.....	60
5.10 Distribution of $Q_{pred}/Q_{meas}$ for 150-mm Settlement: 1.5-m Footing.....	61

LIST OF FIGURES (continued)

Figure		Page
5.11	Distribution of $Q_{pred}/Q_{meas.}$ for 150-mm Settlement: 1.5-m Footing.....	61
6.1	Soil-Footing Model.....	72
6.2	The WAK Test.....	72
6.3	Sample of Time Domain Plot.....	73
6.4	Sample of Mobility Curve: Theoretical vs, Measured.....	74
6.5	Typical Load-Settlement Curve.....	76
6.6	Predicted Stiffness on 1.0-m Footing Before Load Test.....	78
6.7	Predicted Stiffness on 1.5-m Footing Before Load Test.....	79
6.8	Predicted Stiffness on 2.5-m Footing Before Load Test.....	80
6.9	Predicted Stiffness on 3.0-m North Footing Before Load Test.....	81
6.10	Predicted Stiffness on 3.0-m South Footing Before Load Test.....	82
7.1	Pressure vs. Settlement Curves.....	84
7.2	Scale Effect at Large Displacement.....	84
7.3	Triaxial Test/Spread Footing Analogy.....	85
7.4	Pressure vs. Settlement/Width Curves.....	85
7.5	Scale Effect on Modulus of Subgrade Reaction.....	89
7.6	Creep Exponent Curve for 3.0-m North Footing - $Q_u = 12.50$ MN.....	91
7.7	Lateral Strain vs. Strain.....	95
7.8	Comparison of the Horizontal and Vertical Soil Movement.....	96
7.9	Schematic of the Volume Change Under Footing.....	98
8.1	Pressuremeter Curve (PMT 1, $z = 0.6$ m).....	102
8.2	Influence Factor Distribution with Depth.....	103
8.3	Recommended Influence Factor Distribution, and Example of the Determination of the $a_i$ Factors.....	103
8.4	FEM Results for Medium Dense Sand.....	105
8.5	FEM Results for Dense Sand.....	105
8.6	The Correction Function $\Gamma$ (s/B).....	107
8.7	Pressuremeter Modulus as a Function of Time.....	108
8.8	Generating the Average PMT Curve for a Footing.....	109
8.9	Predicted Footing Response by Proposed PMT Method.....	110
8.10	Measured Versus PMT Predicted Load Settlement Curves.....	110
A.1	SPT-1.....	118
A.2	SPT-2.....	119
A.3	SPT-3.....	120

LIST OF FIGURES (continued)

Figure		Page
A.4	SPT-4.....	121
A.5	SPT-5.....	122
A.6	SPT-6.....	123
A.7	Grain Size Distribution.....	124
A.8	DMT-1 Test Results w/o Axial Thrust Measurements.....	125
A.9	DMT-2 Test Results w/o Axial Thrust Measurements.....	126
A.10	DMT-3 Test Results w/ Axial Thrust Measurements.....	127
A.11	Axial Thrust Versus Depth for DMT-3.....	128
A.12	Stress Strain Curve for 0.6-m Sample.....	129
A.13	Volume Change Curve for 0.6-m Sample.....	130
A.14	Stress Strain Curve for 3.0-m Sample.....	131
A.15	Volume Change Curve for 3.0-m Sample.....	132
A.16	Mohr's Circles From Triaxial Tests.....	133
A.17	Resonant Column Test Results @ 0.0-m.....	134
A.18	Resonant Column Test Results @ 1.6-m.....	135
A.19	Resonant Column Test Results @ 3.3-m.....	136
A.20	Resonant Column Test Results @ 6.0-m.....	137
A.21	Graph of Blow Counts N Versus Depth for SPT 1, 3 & 4.....	138
A.22	Graph of Blow Counts N Versus Depth for SPT 2, 5 & 6.....	139
A.23	Graph of $\phi$ Versus Depth From Borehole Shear Results.....	140
A.24	Cone Penetrometer Test Results for CPT-1.....	141
A.25	Cone Penetrometer Test Results for CPT-2.....	142
A.26	Cone Penetrometer Test Results for CPT-5.....	143
A.27	Cone Penetrometer Test Results for CPT-6.....	144
A.28	Cone Penetrometer Test Results for CPT-7.....	145
A.29	Pressuremeter Test Results for PMT-1.....	146
A.30	Pressuremeter Test Results for PMT-2.....	147
A.31	Pressuremeter Test Results for PMT-3.....	148
A.32	Pressuremeter Test Results for PMT-4.....	149
A.33	Determination of the Creep Exponent for PMT-1.....	150
A.34	Determination of the Creep Exponent for PMT-2.....	151

LIST OF FIGURES (continued)

Figure		Page
B.1	Load Settlement Curve for 1.0-m Footing - Total History.....	160
B.2	Load Settlement Curve for 1.0-m Footing - Avg. 30-Minute Curve.....	161
B.3	Load Settlement Curve for 1.5-m Footing - Total History.....	162
B.4	Load Settlement Curve for 1.5-m Footing - Avg. 30-Minute Curve.....	163
B.5	Load Settlement Curve for 2.5-m Footing - Total History.....	164
B.6	Load Settlement Curve for 2.5-m Footing - Avg. 30-Minute Curve.....	165
B.7	Load Settlement Curve for 3.0-m(n) Footing - Total History.....	166
B.8	Load Settlement Curve for 3.0-m(n) Footing - Avg. 30-Minute Curve.....	167
B.9	Load Settlement Curve for 3.0-m(s) Footing - Total History.....	168
B.10	Load Settlement Curve for 3.0-m(s) Footing - Avg. 30-Minute Curve.....	169
C.1	Individual Creep Exponent Curves for 1.0-m Footing, 0.09 MN - 0.71 MN.....	171
C.2	Individual Creep Exponent Curves for 1.0-m Footing, 0.71 MN - 1.25 MN.....	172
C.3	Individual Creep Exponent Curves for 1.0-m Footing, 1.25 MN - 1.78 MN.....	173
C.4	Individual Creep Exponent Curves for 1.0-m Footing - 24-Hour Creep Test	174
C.5	Individual Creep Exponent Curves for 1.5-m Footing, 0.27 MN - 1.34 MN.....	175
C.6	Individual Creep Exponent Curves for 1.5-m Footing, 1.34 MN - 2.80 MN.....	176
C.7	Individual Creep Exponent Curves for 1.5-m Footing, 3.07 MN - 3.29 MN.....	177
C.8	Individual Creep Exponent Curves for 1.5-m Footing - 24-Hour Creep Test.....	178
C.9	Individual Creep Exponent Curves for 2.5-m Footing, 0.62 MN - 3.12 MN.....	179
C.10	Individual Creep Exponent Curves for 2.5-m Footing, 4.36 MN - 7.03 MN.....	180
C.11	Individual Creep Exponent Curves for 2.5-m Footing - 24-Hour Creep Test.....	181
C.12	Individual Creep Exponent Curves for 3.0-m(n) Footing, 0.89 MN - 5.34 MN.....	182
C.13	Individual Creep Exponent Curves for 3.0-m(n) Footing, 6.23 MN - 10.24 MN.....	183
C.14	Individual Creep Exponent Curves for 3.0-m(n) Footing - 24-Hour Creep Test.....	184
C.15	Individual Creep Exponent Curves for 3.0-m(s) Footing, 0.89 MN - 5.34 MN.....	185
C.16	Individual Creep Exponent Curves for 3.0-m(s) Footing, 6.23 MN - 8.90 MN.....	186
C.17	Individual Creep Exponent Curves for 3.0-m(s) Footing - 24-Hour Creep Test	187
C.18	Creep Exponent Curve for 1.0-m Footing - $Q_u = 1.48$ MN.....	188
C.19	Creep Exponent Curve for 1.5-m Footing - $Q_u = 3.38$ MN.....	189
C.20	Creep Exponent Curve for 2.5-m Footing - $Q_u = 8.50$ MN.....	190
C.21	Creep Exponent Curve for 3.0-m(n) Footing - $Q_u = 12.50$ MN.....	191
C.22	Creep Exponent Curve for 3.0-m(s) Footing - $Q_u = 11.50$ MN.....	192

LIST OF FIGURES (continued)

Figure		Page
D.1	Inclinometer Test - 1.78 MN Failure Load - N-S Direction, 1.0-m Footing.....	194
D.2	Inclinometer Test - 1.47 & 3.29 MN Loads - N-S Direction, 1.5-m Footing.....	195
D.3	Inclinometer Test - 1.47 & 3.29 MN Loads - E-W Direction, 1.5-m Footing.....	196
D.4	Inclinometer Test - 3.12-MN Creep Load - N-S Direction, 2.5-m Footing.....	197
D.5	Inclinometer Test - 7.03-MN Failure Load - N-S Direction, 2.5-m Footing.....	198
D.6	Inclinometer Test - 3.12-MN Creep Load - E-W Direction, 2.5-m Footing.....	199
D.7	Inclinometer Test - 7.03-MN Failure Load - E-W Direction, 2.5-m Footing.....	200
D.8	Inclinometer Test - 4.45-MN Creep Load - N-S Direction, 3.0-m(n) Footing.....	201
D.9	Inclinometer Test - 8.90-MN Failure Load - N-S Direction, 3.0 m(n) Footing.....	202
D.10	Inclinometer Test - 4.45-MN Creep Load - E-W Direction, 3.0-m(n) Footing.....	203
D.11	Inclinometer Test - 8.90-MN Failure Load - E-W Direction, 3.0-m(n) Footing.....	204
D.12	Inclinometer Test - 4.45-MN Creep Load - N-S Direction, 3.0-m(s) Footing.....	205
D.13	Inclinometer Test - 8.90-MN Failure Load - N-S Direction, 3.0-m(s) Footing.....	206
D.14	Inclinometer Test - 4.45-MN Creep Load - E-W Direction, 3.0-m(s) Footing.....	207
D.15	Inclinometer Test - 8.90-MN Failure Load - E-W Direction, 3.0-m(s) Footing.....	208
E.1	Settlement Versus Depth for 1.0-m Footing With Varying Percentages of B.....	210
E.2	Settlement Versus Depth for 1.5-m Footing With Varying Percentages of B.....	211
E.3	Settlement Versus Depth for 3.0-m(n) Footing With Varying Percentages of B.....	212
E.4	Settlement Versus Depth for 3.0-m(s) Footing With Varying Percentages of B.....	213

## LISTING OF TABLES

Table	Page
3.1 General Information Data Files.....	10
3.2 Footing Data Files.....	11
3.3 Footing Behavior Data Files.....	11
3.4 Soil Data Files.....	12
3.5 Prediction Method Data Files.....	13
3.6 Case Histories Listed in the Data Base.....	13
3.7 Minimal System Requirements.....	16
3.8 Relationship Between SPT Blow Count and Soil Properties.....	23
3.9 Data Files Corresponding to Prediction Methods.....	24
4.1 As-Built Footing Dimensions.....	28
4.2 Test Dates & People Involved.....	35
4.3 Dry Hand Augered Samples: Test Results.....	36
5.1 Methods Used.....	53
5.2 Soil Tests Used.....	53
5.3 Prediction Results for $Q_{25}$ and $Q_{150}$ in kN.....	54
5.4 Prediction Results for $\Delta_s$ and $S_{2014}$ .....	55
5.5 Measured Results.....	56
5.6 Predicted Design Loads.....	64
5.7 Factors of Safety $F = Q_p/Q_d$ .....	65
5.8 Settlement Under Design Load, $S_d$ .....	66
5.9 Tabulated Settlement Prediction Values.....	68
5.10 Tabulated Bearing Capacity Prediction Values.....	68
5.11 Best Prediction Method Determination.....	70
6.1 Summary of WAK Test Results.....	77
A1 Stepped Blade Test Results.....	152
A2 Cross-Hole Test Results.....	153
A3 Summary of Field Results for SPT Energy Movements.....	154
A4 Physical Properties.....	155
A5 Moisture Content with Depth for SPT 2 & 3.....	156
A6 Moisture Content with Depth for SPT 4 & 5.....	157
A7 Moisture Content with Depth for SPT-6.....	158



## 1. SUMMARY

Tasks 1 through 6 described in section 1.1 below correspond to 6 of the 10 chapters in this report which summarize the work done in each of the 6 tasks. Five separate reports give more detail concerning this project. These reports are: ((Nasr & Briaud, 1995), (Gibbens & Briaud, 1995), (Briaud & Gibbens), 1994, (Ballouz, Maxwell & Briaud, 1995), and (Jeanjean & Briaud, 1994)).

### 1.1 GOALS

In most cases shallow foundations are less expensive than deep foundations (Briaud, 1992). The FHWA is therefore making efforts to ensure that spread footings are considered as a viable alternative for all bridges. Part of this effort is in the form of research on spread footings to improve the reliability of the design rules thereby increasing the confidence of engineers across the country in this economical solution.

There are approximately 600,000 bridges in the country. If those bridges had to be replaced today by new bridges it would cost approximately \$300 billion. Therefore the average cost of a bridge is \$500,000. About 50% of that cost is in the foundation. For such an average bridge the difference in cost between shallow foundations and deep foundations is \$90,000 (Briaud, 1993).

Each year 6,000 new bridges are built for a yearly national bridge budget of \$3 billion. Approximately 85% of the existing 600,000 bridges in the inventory are over water. This percentage is probably more like 50% when considering the bridges built in the last few years. If one assumes that all 6,000 bridges built yearly are on deep foundations and if one further assumes that all bridges that are not over water can be placed on shallow foundations, the numbers above indicate a yearly saving to taxpayers of  $90,000 \times 6000 \times 0.5 = \$270$  million. Even if the saving is only a fraction of this number, say 100 million, the potential saving is significant. If 5% of the

potential saving is invested in research, a budget of \$5 million per year is not unreasonable to make serious progress towards this economic goal.

This research project sets the beginning of this effort and aims at the following goals:

1. Develop a user friendly computerized addressable data base for spread footings. Such a data base will help identify what load tests have been performed, thereby identifying what load tests are missing and need to be performed. Such a data base will also help in evaluating the precision of current design procedures, modify them if necessary or develop new ones. Therefore this data base would be a design tool as well as a research tool.
2. Perform a series of large-scale footing tests on sand. These footings will vary in size from 1 to 3 m, will be square and embedded 0.76 m. The load settlement curve will be obtained for each footing and the soil will be instrumented so that the vertical and horizontal movement of the soil mass can be monitored during the test. Such a series of tests will be used to evaluate the influence of footing scale on footing behavior including settlement and bearing capacity.
3. Use the results of these large-scale tests to evaluate the existing settlement prediction methods for footings on sand. A prediction symposium will be organized with wide national and international participation. Prediction packages will be distributed and predictions will be collected prior to the load tests. Comparisons will be made between predicted and measured response for all footings.
4. Perform a series of impact tests on the footings. The five footings will be tested with the Wave Activated stiffness or WAK test before the load test. An instrumented sledgehammer, two geophones and a data acquisition system will be used. The data collected will be used to predict the initial stiffness of the load settlement curve. Predicted and measured stiffness will be compared.
5. Perform the analysis of the load test data. The raw data collected during the five footing load tests will be reduced and corrected. The data will be analyzed to shed light on the scale effect, the creep settlement and the soil deformation versus depth both in vertical and horizontal directions.

6. Develop, if necessary, a new method to predict the settlement of footings on sand. A new method may be developed if it is clear from the load test results that a significant improvement can be achieved.

## 1.2 RESULTS

1. A spread footing data base has been developed. This data base comes in the form of an IBM PC compatible computer program called SHALDB. The program is in two parts: an organized set of data files follows the DBASE format and a program to manipulate these data written in Visual Basic. SHALDB version no. 4 is the version prepared as an outcome of this project. Version nos. 1 to 3 were also developed at Texas A&M University from which version no. 4 is available. SHALDB contains at the present time 77 case histories where the behavior of spread footings is documented. Some of the case histories are of the load test type where a complete load settlement curve was recorded; some of the case histories are of the performance monitoring type where the settlement versus time was recorded for the given structural load. With the program one can retrieve the data, inspect it, create a sub data base satisfying chosen criteria, compare the measurements with predictions and so on.
2. Load tests were performed on five square footings ranging in size from 1 m to 3 m. They were all embedded 0.76 m. The load settlement curve was recorded for all footings which were pushed up to 150 mm of penetration. During the tests the deformation of the soil at depth in the vertical direction was measured with telltales at 0.5B, 1B and 2B depths. At the same time the deformation of the soil at depth in the horizontal direction was measured with inclinometers at various distances from the footing edge. One of the major lessons learned from the instrumentation is that settlement beams for large footing tests may be unreliable and that the best way to measure settlement is to place a telltale through the footing near its center and anchored at a depth of 4B. A very inexpensive telltale system was developed.
3. A very successful prediction event was organized. A total of 31 predictions were received from 8 different countries, half from consultants, half from academics. The load creating

25 mm of settlement  $Q_{25}$  was under estimated by 27% on the average. The predictions were 80% of the time on the safe side. The load creating 150 mm of settlement  $Q_{150}$  was underestimated by 6% on the average. The predictions were 63% of the time on the safe side. The scale effect was not properly predicted and there was a trend towards overpredicting  $Q_{150}$  for the larger footings. The most used methods were based on the Cone Penetrometer (CPT), Standard Penetration (SPT), and Pressuremeter (PMT) tests in that order. The average true factor of safety was 5.4. Therefore it appears that our profession knows how to design spread footings very safely but could design them more economically.

4. An independent set of predictions was performed on the five load tested footings using 12 settlement calculation methods and 6 bearing capacity calculation methods. The best settlement methods were the Schmertmann DMT (1986) and the Peck & Bazarra (1967) although they are somewhat on the unconservative side. The best conservative methods are Briaud (1992) and Burland & Burbidge (1984). The best method for bearing capacity was the simple  $0.2q_c$  method from Briaud (1993). Most other methods were 25 to 42 percent conservative.
5. WAK tests were performed on the five footings before load testing them. This sledgehammer impact test allows one to determination the static stiffness of the soil-footing assembly. The stiffness predicted by the WAK test was compared to the stiffness measured at small displacements in the load tests. The comparison shows that the WAK test predicted a secant stiffness which intersects the load settlement curve at about 10 mm. Therefore the WAK test stiffness can be used to predict small settlement.
6. The medium dense sand had a mean SPT blow count of 20 blows/0.3 m, a mean CPT  $q_c$  of 7 MPa, a mean PMT limit pressure and modulus of 800 kPa and 8 MPa respectively, a mean friction angle of  $32^\circ$ , and a mean cross hole shear wave velocity of 270 m/s. In this sand the loads necessary to reach 150 mm of penetration were 1740 kN, 3400 kN, 7100 kN, and 9625 kN for the 1 m, 1.5 m, 2.5 m and 3 m footings respectively. In this sand the load necessary to reach 25 mm of penetration were 850 kN, 1500 kN, 3600 kN, and 4850 kN for the 1 m, 1.5 m, 2.5 m and 3 m footings respectively.

7. The scale effect was studied. It was found that for the five footings tested there was no scale effect; indeed when plotting the load-settlement curves as pressure vs. settlement over width curves, all such curves vanish to one curve and the scale effect disappears. This is explained by the uniqueness of the soil stress strain curve. Since the general bearing capacity equation shows a definite scale effect, the use of this equation is not recommended. The pressure  $p_u$  corresponding to a settlement over width ratio ( $s/B$ ) equal to 0.1 can be estimated as follows:

$$p_u = \frac{N}{12} \quad \text{with } N \text{ in blows/0.3 m and } p_u \text{ in MPa} \quad (1)$$

$$p_u = \frac{q_c}{4} \quad (2)$$

The allowable pressure  $p_a$  corresponding to an  $s/B$  ratio equal to 0.01 can be estimated as follows:

$$p_a = \frac{N}{36} \quad \text{with } N \text{ in blows/0.3 m and } p_a \text{ in MPa} \quad (3)$$

$$p_a = \frac{q_c}{12} \quad (4)$$

Another finding related to scale was that a sand deposit which is apparently very heterogeneous at the scale of an in situ test (say maybe 50 mm) may be quite homogeneous at the scale of a spread footing (say maybe 3000 mm).

8. The creep settlement was studied. It was found that the power law model proposed by Briaud and Garland (1985) fit the data very well:

$$\frac{s_t}{s_{t_0}} = \left( \frac{t}{t_0} \right)^n \quad (5)$$

where  $s_t$  and  $s_{t_0}$  are the settlements of the footing after a time  $t$  and  $t_0$  respectively. The exponent  $n$  was found to vary from 0.01 to 0.05. For  $n = 0.03$  the settlement at 50 years

would be 1.67 times larger than the settlement at 1 min. Therefore the creep settlement in sand cannot be neglected yet is not of dramatic proportion. The value of  $n$  for the footings increased with the load level and decreased with unload-reload cycles and was, on the average, equal to 2 times the  $n$  value obtained from the pressuremeter test:

$$n_{\text{footing}} = 2n_{\text{pressuremeter}} \quad (6)$$

9. The soil movement at depth in the vertical direction was studied. It was found that on the average 36% of the top settlement occurs between 0 and 0.5B below the footing, 42% between 0.5B and 1B, 19% between 1B and 2B, and 3% below 2B. Therefore 2B seems to be a reasonable depth of influence for such footings and the average strain below the footing is  $s/2B$ . The strain vs. depth profile obtained from the telltales shows a natural increase in strain with depth except close to the bottom of the footing where the strain decreases due to the lateral confinement brought about by the roughness of the footing.
10. The soil movement at depth in the horizontal direction was studied. It was found that the general shape of the inclinometer curves is a lateral bulging of the soil with a maximum at a depth averaging 0.73B and a bottom at a depth averaging 2.33B. The maximum horizontal movement is of the order of 15% of the footing settlement and the horizontal zone of influence extends to about 1.8B beyond the edge on each side of the footing. Approximate calculations indicate that the soil mass under the footing does not dilate but instead compresses for this medium dense sand.
11. A new method for predicting the behavior of spread footings on sand was developed using pressuremeter testing. It is drastically different from existing methods in that it gives a prediction of the complete load settlement curve. Because the deformation pattern under the footing resembles the expansion of a cavity, the pressuremeter test was chosen. The pressuremeter curve is simply transformed point by point to obtain the footing curve as follows:

$$p_{\text{footing}} = \Gamma(p_{\text{pressuremeter}}) \quad (7)$$

$$\frac{s}{B} = \frac{\Delta R_c}{4.2R_c} \quad (8)$$

where  $p_{\text{footing}}$  is the footing pressure,  $p_{\text{pressuremeter}}$  is the pressuremeter pressure,  $\Gamma$  is the transfer function recommended on the basis of the load test data and finite element analysis,  $s$  is the footing settlement corresponding to  $p_{\text{footing}}$ ,  $B$  is the footing width and  $\Delta R_c/R_c$  is the relative increase in cavity radius on the pressuremeter curve at a pressure equal to  $p_{\text{pressuremeter}}$ .

## 2. INTRODUCTION

This report is a summary report for the project. Its purpose is to summarize the project, the tests done, the results obtained, the analysis performed and the conclusions reached. It will allow the reader to go through about 100 pages and learn the essence of the project in a short time. If the reader requires more detailed information he or she can refer to the following detailed reports: ((Nasr & Briaud, 1995), (Gibbens & Briaud, 1995), (Briaud & Gibbens, 1994), (Ballouz, Maxwell & Briaud, 1995), and (Jeanjean & Briaud, 1994)).

In most cases shallow foundations are less expensive than deep foundations (Briaud, 1992). The FHWA is therefore making efforts to ensure that spread footings are considered as a viable alternative for all bridges. Part of this effort is in the form of research on spread footings to improve the reliability of the design rules thereby increasing the confidence of engineers across the country in this economical solution.

There are approximately 600,000 bridges in the country. If those bridges had to be replaced today by new bridges it would cost approximately \$300 billion. Therefore the average cost of a bridge is \$500,000. About 50% of that cost is in the foundation. For such an average bridge the difference in cost between shallow foundations and deep foundations is \$90,000 (Briaud, 1993).

Each year 6000 new bridges are built for a yearly national bridge budget of \$3 billion. Approximately 85% of the existing 600,000 bridges in the inventory are over water. This percentage is probably more like 50% when considering the bridges built in the last few years. If one assumes that all 6000 bridges built yearly are on deep foundations and if one further assumes that all bridges that are not over water can be placed on shallow foundations, the numbers above indicate a yearly saving to taxpayers of  $90,000 \times 6000 \times 0.5 = \$270$  million. Even if the saving is only a fraction of this number, say 100 million, the potential saving is significant. If 5% of the potential saving is invested in research, a budget of \$5 million per year is not unreasonable to make serious progress towards this economic goal.

This research project sets the beginning of this effort and aims at the following goals:

1. Develop a user friendly computerized addressable data base for spread footings. Such a data base will help identify what load tests have been performed, thereby identifying what load tests are missing and need to be performed. Such a data base will also help in evaluating the precision of current design procedures, modify them if necessary or develop new ones. Therefore this data base would be a design tool as well as a research tool.
2. Perform a series of large-scale footing tests on sand. These footings will vary in size from 1 to 3 m, will be square and embedded 0.76 m. The load settlement curve will be obtained for each footing and the soil will be instrumented so that the vertical and horizontal movement of the soil mass can be monitored during the test. Such a series of tests will be used to evaluate the influence of footing scale on footing behavior including settlement and bearing capacity.
3. Use the results of these large-scale tests to evaluate the existing settlement prediction methods for footings on sand. A prediction symposium will be organized with wide national and international participation. Prediction packages will be distributed and predictions will be collected prior to the load tests. Comparisons will be made between predicted and measured response for all footings.
4. Perform a series of impact tests on the footings. The 5 footings will be tested with the Wave Activated stiffness or WAK test before the load test. An instrumented sledgehammer, two geophones and a data acquisition system will be used. The data collected will be used to predict the initial stiffness of the load settlement curve. Predicted and measured stiffness will be compared.
5. Perform the analysis of the load test data. The raw data collected during the 5 footing load tests will be reduced and corrected. The data will be analyzed to shed light on the scale effect, the creep settlement and the soil deformation versus depth both in vertical and horizontal directions.
6. Develop, if necessary, a new method to predict the settlement of footings on sand. A new method may be developed if it is clear from the load test results that a significant improvement can be achieved.

### 3. SHALDB: DATA BASE OF SPREAD FOOTINGS

#### 3.1 THE DATA BASE FILES

This part of the project is detailed in Nasr and Briaud, 1995.

The shallow foundation data base is divided into two main parts; the data base program and the data base files.

The data base program enables the user to easily access and manipulate the data files that describe the many case histories stored in the data base.

The data base files are a series of data files, written, updated and modified by the program. These files are written in the DBASE IV file format and thus have the file format \*.DBF. These files can be grouped into four general types; general information, footing data, footing behavior and soil data and settlement predictions.

##### 3.1.1 General Information

General information files contain data of general interest. This consists of information as to the location of the case history, the references in which the case history is mentioned, the persons connected with the case, as well as a rating of the data quality. The general information files are listed in Table 3.1.

**Table 3.1: General Information Data Files**

FILE NAME	TYPE OF DATA STORED IN THE FILE
CONTACTS.DBF	Person familiar with the data and person who entered the data
FOOTLIST.DBF	List of footings in the data base
GENINF1.DBF	Footing location and references
RATING.DBF	Data quality ratings on a scale of 1 (mediocre) to 10 (excellent)

The rating data file contains ratings of the data on footing geometry, soil properties and in-situ tests, loads applied, as well as footing movement. Case histories are rated on a scale of zero to 10, zero being the rate of a poorly documented case, and 10 being that of a very well documented case. Since the rating method has not been completely established yet, the rating file is empty and all the values in that file are set to zero.

### 3.1.2 Footing Data

The footing data files are files that contain information on footing size, shape, and basic layout. The footing data files are displayed in Table 3.2.

**Table 3.2:** Footing Data Files

FILE NAME	TYPE OF DATA STORED IN THE FILE
FOTDAT1.DBF	Footing dimensions
INDDAT.DBF	Index table listing which type of data has been updated for which footing

### 3.1.3 Footing Behavior

Information about the loads applied on the foundation as well as about the load-settlement behavior of the foundation are contained in the footing behavior files. These files on footing behavior are listed in Table 3.3.

**Table 3.3:** Footing Behavior Data Files

FILE NAME	TYPE OF DATA STORED IN THE FILE
LOADDATA.DBF	Type and magnitude of the load applied on that footing
SETLDATA.DBF	Load settlement time data

### 3.1.4 Soil Data

The soil data files contain information about the soil layers, the physical soil properties, as well as in-situ test data. The files on soil properties data are shown in Table 3.4.

**Table 3.4: Soil Data Files**

FILE NAME	TYPE OF DATA STORED IN THE FILE
LAYERDAT.DBF LAYERDT.DBF	Soil layer data
DEFRMDAT.DBF DEFRMDT.DBF	Soil deformation data
SHEARDAT.DBF SHEARDT.DBF	Shear strength data
PROPDATA.DBF PROPDAT.DBF PROP_CAL.DBF	Soil properties data
SPTDATA.DBF SPTDAT.DBF	Standard Penetration Test data
CPTDATA.DBF CPTDAT.DBF	Cone Penetrometer Test data
PMTDATA.DBF PMTDAT.DBF	Pressuremeter Test data
DMTDATA.DBF DMTDAT.PMT	Dilatometer Test data

As shown in Table 3.4, there are two different data base files for each type of soil data file.

The first file contains the data corresponding to soil profiles. For example, the file SPTDATA.DBF, contains SPT number of blows per foot versus depth.

The second file contains averages and notes. The file SPTDAT.DBF contains the values for average number of blows per foot and standard deviation, as well as hammer type and notes on the data itself.

In the particular case of soil properties data, the third file, PROP\_CAL.DBF, contains information about automatic calculations that are sometimes carried out by the computer. More information about these automatic calculations is found in section 3.2.5.1.

### **3.1.5 Settlement Predictions**

The settlement prediction files contain the predicted settlements for all the cases. These settlements are calculated when the corresponding soil data information is input or updated. A list of these files and the reference for each of the methods is shown in Table 3.5.

It should be noted here that only methods for settlement prediction on sand that are based on in-situ testing techniques were programmed into SHALDB.

**Table 3.5: Prediction Methods Data Files**

FILE NAME	PREDICTION METHOD CORRESPONDING TO THE FILE
<i>SPT METHODS</i>	
SPT_APK.DBF	Anagnostopoulos, Papadopoulos and Kavvadas (1991)
SPT_BURL.DBF	Burland and Burbidge (1984)
SPT_MEY.DBF	Meyerhof (1965)
SPT_PAR.DBF	Parry (1971)
SPT_PKBZ.DBF	Peck and Bazaraa (1967)
SPT_SHUL.DBF	Shultze and Sherif (1973)
SPT_TZPK.DBF	Terzaghi and Peck (1967)
<i>CPT METHODS</i>	
CPT_AMAR.DBF	Amar, Baguelin and Canepa (1989)
CPT_MEY.DBF	Meyerhof (1965)
CPT_SHM.DBF	Schmertmann, Hartman and Brown (1978), and Schmertmann(1970)
<i>DMT METHODS</i>	
DMT_SHM.DBF	Schmertmann (1986)
<i>PMT METHODS</i>	
PMT_BRIO.DBF	Briaud (1992)
PMT_MNRD.DBF	Menard and Rousseau (1962)

### 3.1.6 Case Histories Listed in the Data Base

As of September 1995, the time this report was completed, the data base contained 77 case histories. These case histories and their reference are listed in Table 3.6.

**Table 3.6: Case Histories Listed in the Data Base**

Nb.	FOOTING NAME	REFERENCE
1	M5000, North Avenue Sideline Over VT127, E Abut. #1	Gifford et al. (1989) Gifford and Perkins (1989)
2	M5000, North Avenue Sideline Over VT127, E Abut. #2	Gifford et al. (1989) Gifford and Perkins (1989)
3	#131-132-11, I-691 Under Dickerman Road, S Abut. #1	Gifford et al. (1989) Gifford and Perkins (1989)
4	#131-132-11, I-691 Under Dickerman Road, N Abut #2	Gifford et al. (1989) Gifford and Perkins (1989)
5	#131-132-11, I-691 Under Dickerman Road Center Pier	Gifford et al. (1989) Gifford and Perkins (1989)
6	#931, Branch Avenue, NE Corridor, W Abut	Gifford et al. (1989) Gifford and Perkins (1989)
7	#931, Branch Avenue, NE Corridor, E Abut	Gifford et al. (1989) Gifford and Perkins (1989)
8	#931, Branch Avenue, NE Corridor, Pier 1 North	Gifford et al. (1989) Gifford and Perkins (1989)

**Table 3.6: Case Histories Listed in the Data Base (continued)**

9	#931, Branch Avenue, NE Corridor, Pier 1 South	Gifford et al. (1989) Gifford and Perkins (1989)
10	#931, Branch Avenue, NE Corridor, Pier 2 North	Gifford et al. (1989) Gifford and Perkins (1989)
11	#931, Branch Avenue, NE Corridor, Pier 2 South	Gifford et al. (1989) Gifford and Perkins (1989)
12	#931, Branch Avenue, NE Corridor, Pier 3 North	Gifford et al. (1989) Gifford and Perkins (1989)
13	#931, Branch Avenue, NE Corridor, Pier 3 North	Gifford et al. (1989) Gifford and Perkins (1989)
14	Relocated Gersoni Road- Route 28 Route 7, S Abut.	Gifford et al. (1989) Gifford and Perkins (1989)
15	Relocated Gersoni Road- Route 28 Route 7, N Abut.	Gifford et al. (1989) Gifford and Perkins (1989)
16	Route 146 Southbound Over Reloc. Lackey Dam Road: N Abut.	Gifford et al. (1989) Gifford and Perkins (1989)
17	Route 146 Southbound over Reloc. Lackey Dam Road	Gifford et al. (1989) Gifford and Perkins (1989)
18	VM Route 111 Over the Middle Branch - Willams River -- E Abut.	Gifford et al. (1989) Gifford and Perkins (1989)
19	VM Route 111 Over the Middle Branch - Willams River - W Abut.	Gifford et al. (1989) Gifford and Perkins (1989)
20	Bridge # 76-88-7 I-86 - E Abut.	Gifford et al. (1989) Gifford and Perkins (1989)
21	I-86 & CD Roadway under toll and Turnpike - W Abut.	Gifford et al. (1989) Gifford and Perkins (1989)
22	I-86 & CD Roadway under toll and Turnpike - E Abut.	Gifford et al. (1989) Gifford and Perkins (1989)
23	CD-WB Roadway & Ramp 1 Over Buckland St. (I-86) - W Abut.	Gifford et al. (1989) Gifford and Perkins (1989)
24	CD-WB Roadway & Ramp 1 Over Buckland St. (I-86) - E Abut.	Gifford et al. (1989) Gifford and Perkins (1989)
25	US501 Bypass over US501, -#4, BENT #3	Baus, R.L., (1991)
26	SC 38 Twin overpasses over US301, #1, BENT #3, EBL	Baus, R.L., (1991)
27	SC 38 Twin overpasses over US301, #3, BENT #3, EBL	Baus, R.L., (1991)
28	SC 38 Twin overpasses over US301, #1, BENT #3, WBL	Baus, R.L., (1991)
29	SC 38 Twin overpasses over US301, #1, BENT #4, EBL	Baus, R.L., (1991)
30	SC 38. Twin overpasses over US301, #3. BENT #3, WBL	Baus, R.L., (1991)
31	CS 38 Twin overpasses over US301, #3, BENT #4, EBL	Baus, R.L., (1991)
32	US501 Bypass over US501, -#1, BENT #3	Baus, R.L., (1991)
33	Alabama DOT, I-359	Lockett, L., (1981)
34	Alabama DOT, I-359-#1	Lockett, L., (1981)
35	Texas A&M University, Riverside Campus, 1.0m x 1.0m	Briaud and Gibbens (1994)
36	Texas A&M University, Riverside Campus, 1.5m x 1.5m	Briaud and Gibbens (1994)
37	Texas A&M University, Riverside Campus, 3.0m x 3.0m, North	Briaud and Gibbens (1994)
38	Texas A&M University, Riverside Campus, 3.0m x 3.0m, South	Briaud and Gibbens (1994)
39	Texas A&M University, Riverside Campus, 2.5m x 2.5m	Briaud and Gibbens (1994)
40	University of Florida, -June 1992	Skyles, D.L., (1992)

**Table 3.6: Case Histories Listed in the Data Base (continued)**

41	University of Florida, July 1992	Skyles, D.L., (1992)
42	University of Florida, September 990	Skyles, D.L., (1992)
43	University of Florida, May 1991	Skyles, D.L., (1992)
44	Swedish Geotech @ Kolbytteimon, Slab 2.30 x 2.50 m	Bergdahl et al. (1985)
45	Swedish Geotech @ Fittja, Slab 2.30 x 2.50 m	Bergdahl et al. (1985)
46	Swedish Geotech @ Kolbytteimon, Slab 1.10 x 1.30 m	Bergdahl et al. (1985)
47	Swedish Geotech @ Fittja, Slab 1.10 x 1.30 m	Bergdahl et al. (1985)
48	Swedish Geotech @ Kolbytteimon, Slab 1.60 x 1.80 m	Bergdahl et al. (1985)
49	Swedish Geotech @ Fittja, Slab 1.60 x 1.80 m	Bergdahl et al. (1985)
50	Geotechnica Load Tests, (AF6)	Garga and Quin (1974)
51	Geotechnica Load Tests, (AF7)	Garga and Quin (1974)
52	Geotechnica Load Tests, (AF8)	Garga and Quin (1974)
53	Geotechnica Load Tests, (CG6)	Garga and Quin (1974)
54	Geotechnica Load Tests, (TM1)	Garga and Quin (1974)
55	Geotechnica Load Tests, (TM2)	Garga and Quin (1974)
56	Geotechnica Load Tests, (TM3)	Garga and Quin (1974)
57	Geotechnica Load Tests, (CA 1)	Garga and Quin (1974)
58	Geotechnica Load Tests, (A 5)	Garga and Quin (1974)
59	Geotechnica Load Tests, (A 6)	Garga and Quin (1974)
60	Geotechnica Load Tests, (C 3)	Garga and Quin (1974)
61	Geotechnica Load Tests, (C 4)	Garga and Quin (1974)
62	Geotechnica Load Tests, (AF 1)	Garga and Quin (1974)
63	Geotechnica Load Tests, (AF 4)	Garga and Quin (1974)
64	Geotechnica Load Tests, (CG 4)	Garga and Quin (1974)
65	Geotechnica Load Tests, (A 4)	Garga and Quin (1974)
66	FHWA @ Fairbank - Series 95 #1195	DiMillio (1994)
67	FHWA @ Fairbank - Series 95c #15295c	DiMillio (1994)
68	FHWA @ Fairbank - series 95RA #1295RA	DiMillio (1994)
69	FHWA @ Fairbank - series 95 #15395c	DiMillio (1994)
70	FHWA @ Fairbank - series 95 #2195c	DiMillio (1994)
71	FHWA @ Fairbank - Series 95 #2295c	DiMillio (1994)
72	FHWA @ Fairbank - Series 95 #15495RA	DiMillio (1994)
73	FHWA @ Fairbank Series 95 #2395c	DiMillio (1994)
74	FHWA @ Fairbank - series 85 #3185	DiMillio (1994)
75	FHWA @ Fairbank - series 85 #2285	DiMillio (1994)
76	FHWA @ Fairbank - series 85 #1185	DiMillio (1994)
77	FHWA @ Fairbank - series 85 #15185	DiMillio (1994)

### 3.2 THE DATA BASE PROGRAM

The Shallow Foundation data base, SHALDB, is made of two main parts, a series of data base files and a data base program.

The program, SHALDB, is a front-end interface that accesses and manipulates the data written in the data base files. It is divided into three main sections: maintenance, inquiries and search.

The maintenance section consists of two parts: footing data addition and footing data modification. In order to distinguish this section from the others, the main background color of the windows in this section is set to white. A more elaborate explanation of these two options can be found in section 3.2.3.

The inquiries section is made of two parts: parameter based search and footing data viewing. The background color for the parameter based search is light gray, while that for the footing viewing is light blue. A more detailed explanation on the inquiries and footing viewing options can be found in section 3.2.4.

The data analysis section is made of only one option, which background color is dark blue. Details on this part of the program can be found in section 3.2.5.

SHALDB writes the data files in the DBASE IV format, and saves them in the C:\SHALDB directory on the hard drive.

### 3.2.1 System Requirements

The system on which the program can be installed and used should meet the minimum requirements listed in Table 3.7 below:

**Table 3.7: Minimal System Requirements**

ITEM	REQUIREMENTS
System Description	Intel Compatible 386/33
Operating System	Windows 3.1 running over DOS 5.0 or higher
Memory	4 MB of hard disk space

### 3.2.2 Installation

SHALDB comes as an easy to install, two diskettes package. In order to install the program, one should follow the procedure described below:

1. Run Windows,

2. Insert disk 1 in drive A,
3. Select the Windows "PROGRAM MANAGER" icon by double clicking on it, in case the program manager is minimized,
4. From the "PROGRAM MANAGER" menu, select "FILE",
5. Under "FILE", select the option marked "RUN",
6. A window appears titled "RUN". In the box labeled "Command Line", type the following:

a:\setup.exe

7. The setup utility is then launched. A window titled "SHALDB SETUP" will then appear. In the box labeled "INSTALL TO", the name of the address directory is written.

The default directory is "C:\SHALDB". The user should not attempt to change the default. Even though the installation would then run successfully, the program will not. Queries and file addressing routines in the program have all been programmed to look for the files in that exact directory. If these files have all been installed somewhere else, the program will not find them. It could then crash, get stuck in an infinite loop, or even display wrong and meaningless values.

### **3.2.3 The Maintenance Section**

The data base maintenance section is the first of the three sections in the program. This section enables the user to enter new case histories in the data base, as well as access and modify existing data.

As with every other section in the program, it is color coded to give the user a feel that differentiates it from other sections. The pop-up windows in this particular section will appear with a white background.

### 3.2.3.1 Adding a New Case History

In order to add a new case history to the data base, one must select the option marked "ADD A FOOTING" from the main menu. A window titled "FOOTING LOCATION AND LITERATURE REFERENCES" will appear.

The program, after counting the cases stored in the data base, automatically assigns a footing number to the case history, and displays it on every pop-up window. The footing number is written next to the title of the window

In this particular section, the user is prompted to enter general information on the case history: the title of the case, its location, and the references from which all data has been obtained. The user is limited to 4 references. The user can choose from a list of countries, or type in and enter any of those that are not on display.

Once the button marked "ADD THIS FOOTING" is selected, the program accesses and updates the files GENINF1.DBF and FOOTLIST.DBF.

A window titled "DATABASE UPDATE" is then displayed with the new footing number. Buttons that correspond to data that has just been updated are marked with a check next to them to show that the corresponding data has been entered.

Since a case record would be meaningless with no footing data, the program disables all the other buttons until such information has been entered. The two buttons labeled "CONTACT PERSONS" and "DATA RATING" would be enabled because the data files that they correspond to are not as essential.

The procedure to enter the remaining data is essentially the same as that for updating information and is described in the next section.

### 3.2.3.2 Modifying an Existing Case History

In order to modify an existing case history, one must select the option marked "MODIFY AND DELETE FOOTINGS" from the main menu. A window will then appear entitled "LIST OF FOOTINGS FOR DATA MODIFICATION" which will list all footings in the data base.

One would then have to double-click on the number of the footing that has to be modified. When this is done, the window described in the previous section would appear. The user can then select the type of data that needs to be modified or updated.

The modification example that will be discussed here will be SPT data modification. Once the button marked "STANDARD PENETRATION TEST" is selected, a pop-up window titled "STANDARD PENETRATION TEST DATA" will then appear.

It is possible to view and enter data in units other than the SI units. This option is explained in detail in section 3.2.5.2.

This window lists all SPT data for one particular borehole, and shows buttons marked "UPDATE", "PRINT", "VIEW NOTE", and "QUIT", as well as a help button.

When the button marked "UPDATE" is selected, the user will be first prompted to confirm the update. When this is done, the program will remove the points that have been marked for deletion, and calculate averages and standard deviations.

The data is marked or unmarked for deletion by double clicking on the gray square next to the row of values considered. The sign displayed will then change from a "+" (unmarked for deletion) to a "-" (marked for deletion). When the update button is selected, the program will delete the data point marked with a "-" sign, and will not display it again.

Calculation of averages is explained in section 3.2.5.3.

In some windows, the button marked "PLOT" enables the user to view a plot of the data. In the case of the SPT data, the plot will show the SPT blowcount versus depth.

These plot windows have a "PRINT" button that enables the user to get a scaled printout of the plot displayed.

When the "PRINT" button is selected, the program will print a simple report of the data displayed.

The "VIEW NOTE" button allows the user to view or modify a note that contains information about the data displayed. When this button is clicked, its title changes to "HIDE NOTE", and a small window marked "NOTE" is then displayed. The user can then read or write observations on the data. In the present version, the length of the note is limited to 256 characters because of the DBASE IV format.

When the "QUIT" button is clicked, the window disappears and the data update window reappears. For SPT, CPT, PMT and DMT data the program would run a settlement prediction routine that calculates the predicted settlement. This routine runs when the data has been previously updated.

Finally, all data update windows have a help button that consists of a red question mark in a yellow square. By double-clicking on the help button, one would be able to view a help window that would explain the features of that particular data update section.

In addition to that help button, some data update windows where symbolic values are shown have an additional help routine. One has to move the mouse pointer over the symbol that is not understood, then press the left mouse button. A statement giving the name or significance of that symbol is then displayed. This statement stays as long as the mouse pointer is over the symbol.

### **3.2.4 The Inquiries Section**

The second section of the program is the inquiries section, in which it is possible to either run a parameter based search, or view the data of a chosen footing.

#### **3.2.4.1 The Parameter Based Search**

The parameter based search allows searches of groups of case histories that share a similar set of parameters to be performed. This option will get more and more useful as the data base grows larger.

In order to run a parameter based search, one must select the option "PARAMETER BASED SEARCH" from the main menu. The program will then access the data base, reading the footing names and numbers and counting them. A window titled "PARAMETER BASED SEARCH" will then appear.

It is then possible to select or deselect parameters by viewing the list of parameters in the search pull-down menu. Once a parameter is selected, the program will prompt the user to set the maximum and minimum values that this parameter can have. A window will appear in which one can enter the parameter boundaries and decide on the course of action to follow. One can proceed with the search or abort, or remove previously selected parameters from the list of parameters.

Once all chosen parameters have been set and selected, the search can be initiated by selecting "SEARCH" from the pull-down menu. The program will then go through all the relevant

files and compare recorded data to the parameters, by choosing only the cases that meet the search requirements.

When the program is done browsing through the files, a new window will appear that shows a list of the footings that the program found to meet the search requirements. This window is entitled "SEARCH BY PARAMETER RESULTS"

#### 3.2.4.2 Viewing a Footing

This option works in the same way as the data update option, except that the user is not allowed to perform any data update or unit changes while browsing, nor is he confined to selecting it from the main menu.

The option to view data from a footing is available to the user at different stages of the program. One can select the option to view the data of a particular footing not only from the main menu, but also from within either a parameter based search option, or a data analysis.

In order to view data from the main menu, one must select the "VIEW A FOOTING" option from under the "INQUIRIES" section.

### **3.2.5 The Data Analysis Section**

The Data Analysis Section is divided in three parts; Background Calculations, Settlement Prediction Calculations, and the Data Analysis section itself.

#### 3.2.5.1 Background Calculations

Background calculations are performed automatically by the program every time the units are changed or the data is updated.

#### 3.2.5.2 Unit Conversions

When a data entry window is open, the values in the data base are first stored in an array, then displayed in tables. The units can be changed by double clicking on the legend at the top of a table. Only units whose legend are in colors other than black can be changed.

Units of variables displayed in black will not change, and modifying them will have no effect on the content of the data base. They correspond to values calculated by the program and

displayed to provide the user additional information. The units of the data stored in the files are always System International Metric (SI).

When the unit of a variable is modified, all values corresponding to that particular variable are converted. The buttons marked "UPDATE" and "QUIT" are disabled. These buttons will be re-enabled when all the units of all the variables in that particular window are set back in SI. This will ensure that no data saved will be in units other than SI.

#### 3.2.5.3 Averages and Standard Deviation

Weighted averages and standard deviations are another type of background calculations performed by the program.

The weighted average of a variable is calculated with respect to depth, and for the whole depth of testing, as well as for depth values equal to one, two, and three times the width of the footing under its base.

The standard deviation is also automatically calculated once the data is updated, not based on a weighted average, but on a straight average.

Since these depths are measured starting from the bottom of the footing, the computer adjusts automatically for the difference in borehole elevation, footing embedment, footing thickness, and ground surface elevation.

Averages are computed automatically once the "UPDATE" button is selected. Since an update directly affects the data stored in the data base, it is final. After the update has been selected, there is no going back. All the data listed in that window is stored in an array. Then, upon quitting the data entry window, a query is launched that deletes all old data in the corresponding files. The new data in the array is then copied into the file.

Because of that, the user will be prompted to confirm this in case the "UPDATE" button has been selected by mistake.

#### 3.2.5.4 Unit Weight and Overburden Pressure

Once "STANDARD PENETRATION TEST" has been entered and updated, the program checks to see if any soil property data such as total unit weight and relative density have been entered by verifying their overall average value in the soil physical properties file named

PROPDAT.DBF. In case these averages are equal to zero, which could mean that none of these data have been entered, the program then calculates the values of total unit weight,  $\gamma_T$  in ( $\text{kN/m}^3$ ), relative density,  $D_R$  in (%), and angle of internal friction,  $\phi$

The calculations for relative density are based on a relationship derived, for saturated sands, by Gibbs and Holtz (1957), and those for unit weight are based on data published by Bowles (1988). These values are shown in Table 3.8.

**Table 3.8: Relationship Between SPT Blow Count and Soil Properties**

DESCRIPTION	Very Loose	Loose	Medium	Dense	Very Dense
SPT Blowcount (Blows/ft)	-	4	10	30	50
Relative Density (%)	0	0.15	0.35	0.65	0.85
Total Unit Weight ( $\text{kN/m}^3$ )	11	16	18	20	22

The values expressed in Table 3.8 are only approximate. However, prediction methods often necessitate determination of the overburden pressure at a certain depth and sometimes require knowledge of the relative density of the sand. Furthermore, few case histories are found with results from extensive laboratory testing.

It was therefore necessary to "commit" such approximations in order for the program to run smoothly and for the data entry to be facilitated. The program warns the user of the fact that an approximation was done, by writing a note that can be viewed once the soil physical properties window is accessed. The user can, upon reading that note, modify the data displayed in the Soil Physical and Engineering Properties window.

That note can be viewed by clicking on the button labeled "VIEW A NOTE" in the Soil Physical and Engineering Properties window.

### 3.2.6 Settlement Prediction Methods

Of the many methods available for predicting the settlement of footings on sand, 13 have been selected to be incorporated in the program. They are based on four different in-situ tests;

Standard Penetration (SPT), Cone Penetrometer (CPT), Dilatometer (DMT), and Pressuremeter (PMT).

The SPT based methods considered are the ones developed by Anagnostopoulos et al. (1982), Burland & Burbridge (1984), Meyerhof (1965), Parry (1971), Peck & Bazarraa (1967), Schultze & Sherif (1973), and Terzaghi & Peck (1967). The CPT Based methods were derived by Amar et al. (1989), Meyerhof (1965) and Schmertmann et al. (1970, 1978). The PMT based methods considered were developed by Briaud (1992) and Menard & Rousseau (1962). Finally, the DMT based method programmed is the one developed by Schmertmann (1986).

Once relevant data has been updated, the program runs the corresponding prediction routines. Table 3.9 shows this relationship.

**Table 3.9: Data Files Corresponding to Prediction Methods**

DATA TYPE	METHOD TYPE
Footing Dimensions	All Methods
Load-Settlement	All Methods
Soil Properties	All Methods
Standard Penetration Test	SPT Methods
Cone Penetrometer Test	CPT Methods
Dilatometer Test	DMT Methods
Pressuremeter Test	PMT Methods

When the routine that computes settlement predictions is started, the program will first access the in-situ test file in order to read the relevant test data and the borehole elevation. It will then access the footing geometry file in order to read the footing width, length, embedment depth and natural ground elevation. Then the load settlement file is accessed, and data from the pressure versus normalized settlement (ratio of settlement over footing width) curve is read.

The program will then compute a predicted normalized settlement value for each of the recorded pressure points on the pressure versus normalized settlement curve. The resulting predicted pressure versus normalized settlement curve is then stored in a data file that corresponds to the prediction method. For most methods, this curve will be a straight line.

Once the program has carried out the calculations, it is possible to view the predicted settlement curves. In order to do that, one must select the load-settlement data window, and select the load-settlement option by clicking on the button marked "LOAD-SETTLEMENT PLOT" A window titled "LOAD-SETTLEMENT PLOT" will appear.

On the load-settlement plot screen, the pressure versus normalized settlement curve will be displayed. By selecting the button marked "METHODS", a window titled "SETTLEMENT PREDICTION METHODS" will appear with a list of methods that can be plotted. The user has to select the adequate method or methods, and then select the button marked "DONE", in order for the predicted curves to be plotted.

### **3.2.7 Data Analysis**

The program enables the user to run simple data analysis. In order to start a data analysis, the user has to select the option "DATA ANALYSIS" from the main menu.

The user has then the option of viewing either a simple x-y plot, or a frequency distribution plot, by selecting the corresponding plot type from the "Plot Type" option from the menu of the window displayed.

After the plot type has been selected from the "Plot Type" option, the user has to select "Start Data Analysis" from the "Start Analysis" option in order to launch the plot utility. The x axis variable is chosen, then the y axis variable is chosen and the x-y plot is viewed.

## **4. LOAD TESTING OF FIVE LARGE-SCALE FOOTINGS ON SAND**

### **4.1 LOAD TEST SETUP**

This part of the project is detailed in Gibbens and Briaud, 1995.

Five spread footings and five reaction shafts (Figure 4.1) were built at the sand site on the Texas A&M University National Geotechnical Experimentation Site (NGES). Two 3 by 3 by 1.2-m footings, one 2.5 by 2.5 by 1.2-m footing, one 1.5 by 1.5 by 1.2-m footing and one 1 by 1 by 1.2-m footings were built along with four 0.91-m diameter, 21.3-m long drilled shafts with 2.7-m - 60° underreamed bells and one 0.91-m diameter, 5-m long straight drilled shaft. The exact as-built dimensions are shown in Table 4.1.

The four drilled and belled shafts were founded at depths ranging from 19.6 to 20.6 m as determined in the field during shaft construction. The straight shaft was founded at a depth of 5 m. The footings and reaction shafts were spaced on 8.53-m centers except for the straight shaft which was spaced as shown on Figure 4.1. Each shaft, except the straight shaft, was designed and built to minimize any effect on the surrounding soils that a column of high strength concrete might have. Figure 4.2 shows the design of the shafts which used a mix of sand and cement, designed to approximate the strength characteristics of the surrounding sand, to fill the void above the concrete shaft. Figure 4.2 also shows an overall profile of one typical load test with all soil and footing instrumentation shown.

#### **4.1.1 Spread Footing Construction**

After excavating the holes with a backhoe and hand finishing with shovels, a mat type reinforcement cage was placed just off the bottom of the footing excavation using #11 rebar, 150 mm center to center in both directions. Prior to concrete placement, three 120 mm diameter PVC sleeves were placed within the footing to serve as conduits through which the drilling of the telltales would take place. The footings were formed and poured at a rate of approximately two footings per day.

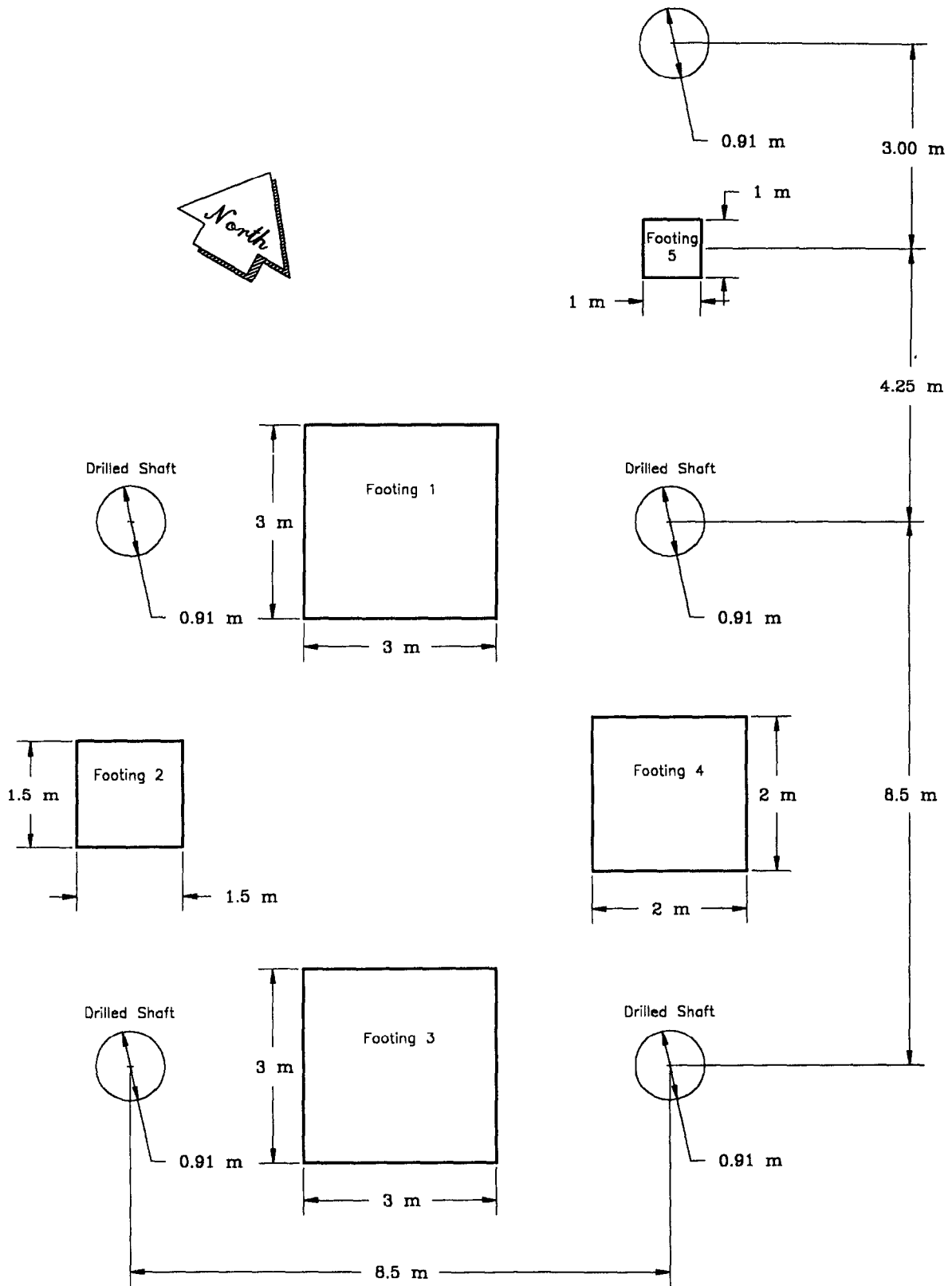


Figure 4.1: Footing/Pier Layout

**Table 4.1: As-Built Footing Dimensions**

Footing No.	Length by Width	Thickness	Embedment Depth	In Text, Referred to as
1	3.004 by 3.004	1.219	0.762	3-m North footing
2	1.505 by 1.492	1.219	0.762	1.5-m footing
3	3.023 by 3.016	1.346	0.889	3-m South footing
4	2.489 by 2.496	1.219	0.762	2.5-m footing
5	0.991 by 0.991	1.168	0.711	1.0-m footing

#### **4.1.2 Reaction Shaft Construction**

Construction of the shafts was completed at a rate of one shaft per day. A large crane mounted rotary drilling rig was used to auger the shaft holes. After installing a 1.52-m deep, 1.07-m diameter casing, placed to protect the top of the shaft, the remaining shaft hole was drilled with drilling mud until an inspection of the waste material showed definite signs that the hole was into the shale layer near a depth of 12.0-m. At this point, a second casing, 1.02 m in diameter and 14.5-m long was placed into the hole and plugged 1 m into the shale layer. With the casing plugged into the shale layer, the drilling mud was evacuated from the casing and the remaining shaft and bell drilling was done in the dry. After the diwidag bars were put in place, a 12-m tremie was used to pour concrete down the center of the bars. Concrete was poured to just above the shale layer as determined by a measuring tape. A sand plug was placed, followed by a sand/cement mixture to the ground surface.

#### **4.1.3 Horizontal Displacement Measurements (Inclinometers)**

In order to evaluate the horizontal displacement of the soil surrounding the footing group, six vertical inclinometer casings were installed at locations designated spt-1 through spt-6 on Figure 4.3. The casings were installed prior to footing construction with one casing placed at each Standard Penetration Test hole to a depth of 15.2 m. A casing consisted of 3.0-m long sections of 70-mm outside diameter PVC pipe with vertical running grooves and locking connections.

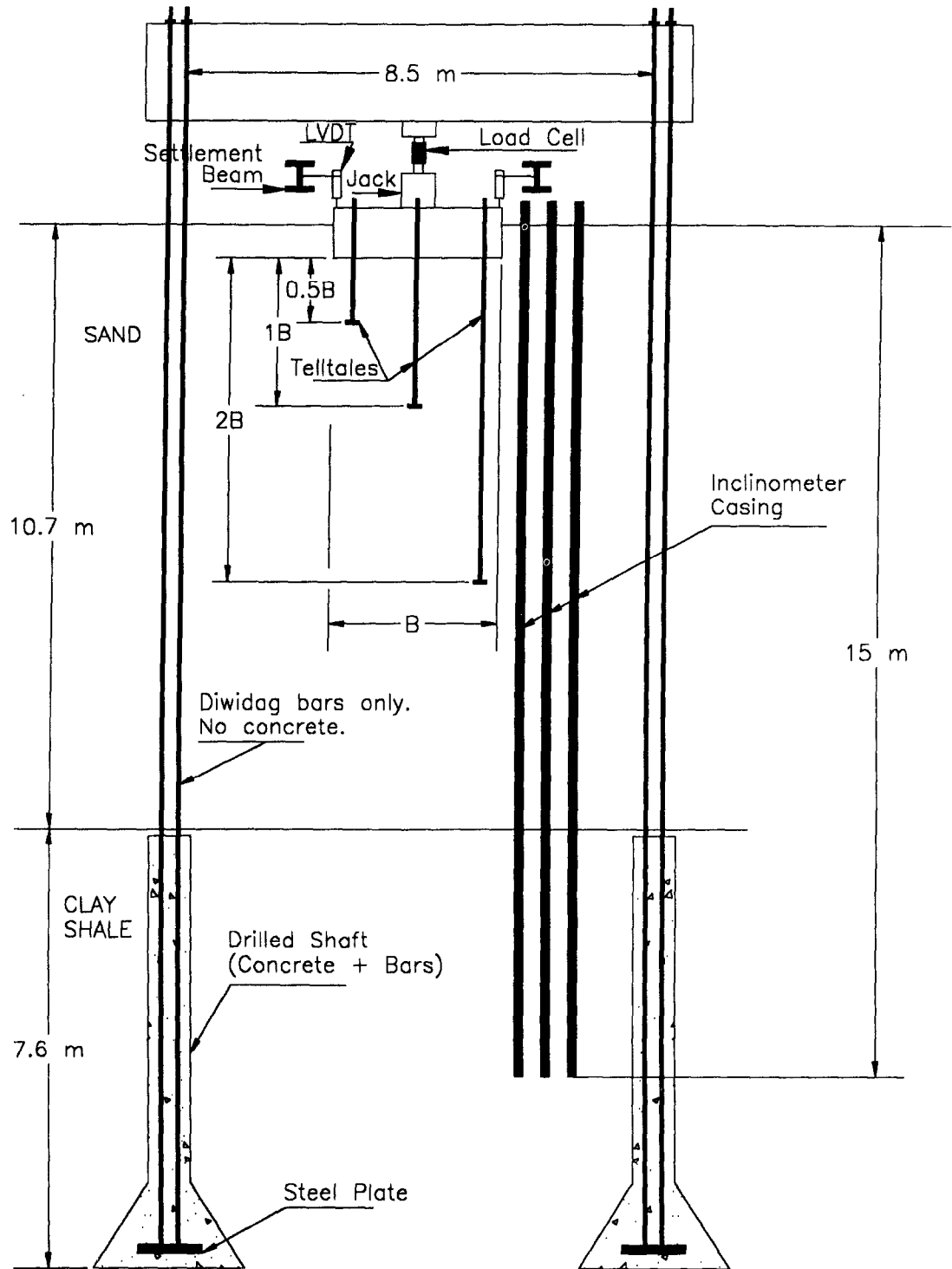


**Figure 4.2: Load Test Setup**

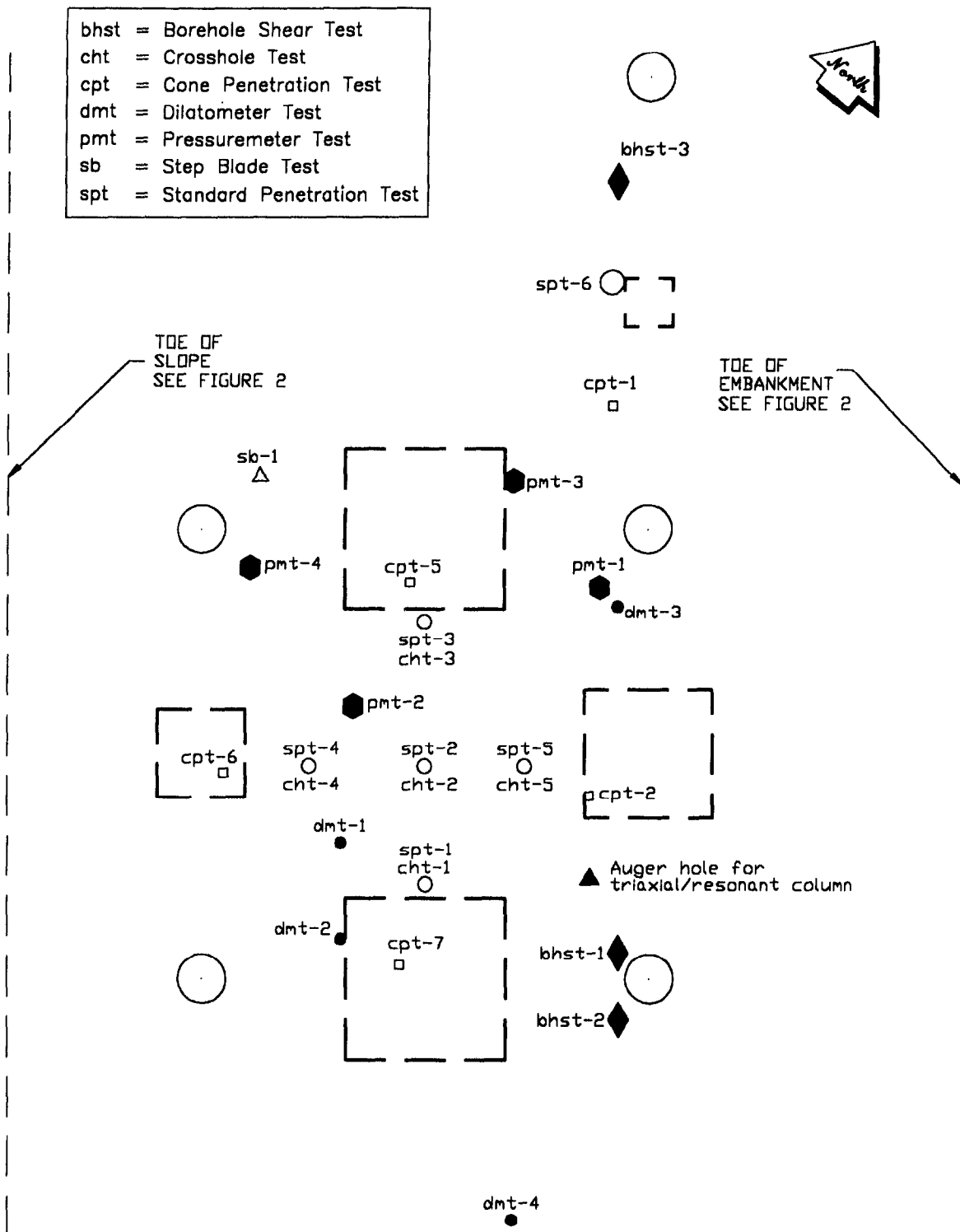


**Figure 4.3: In-Situ Field Testing Layout with Auger Hole Location**

The layout of the inclinometer casings shown on Figure 4.3 was designed primarily to facilitate the cross-hole wave test as one source hole and two recording holes were required for each test. This layout enabled multiple inclinometer tests to be performed at various distances from the footing edge for the same footing test. Single inclinometer tests were performed for the 1.0-m and 1.5-m footings.

#### **4.1.4 Vertical Displacement Measurements (Extensometer)**

Vertical displacement measurements were taken at 0.5B, 1.0B and 2.0B depths for each footing (Figure 4.2). Extensometer type telltales were designed and constructed as shown in Figure 4.4 to measure the movement at a particular depth during loading. The telltales were designed to prevent friction related settlement between the sand and telltale.

#### **4.1.5 Footing Displacement Measurements**

The movement of the footings during load testing was carefully monitored by an electronic data acquisition system supplied by the Federal Highway Administration. Linear Variable Differential Transformers (LVDT's) were used to measure the vertical displacement at each footing corner and at each telltale during load testing. The precision of measurement achieved by the LVDT's was on the order of 0.0025 mm over a total stroke of 100 mm.

The LVDT's were connected to a specially designed data acquisition box, which had the capacity of handling over 16 channels of data. Data was recorded using a portable Compaq 486DX computer which ran a program specifically designed for the data acquisition system provided by FHWA. The computer program was designed to read the LVDT's at 1, 3, 5, 7, 10, 15, 20, 25 and 30 min for normal testing and this same 30-min schedule followed by hourly readings for a total of 24 h during the creep tests.

Several crib and beam systems were used to support the data acquisition system during load testing. The initial system used wooden reference beams, constructed as I beams with stacked wooden cribs providing end support. When it was discovered that the wooden beams were creeping faster than the footings during several 24-h creep tests, the reference beams were replaced with 100-mm<sup>2</sup> steel box beams. Several crib systems were used in conjunction with the

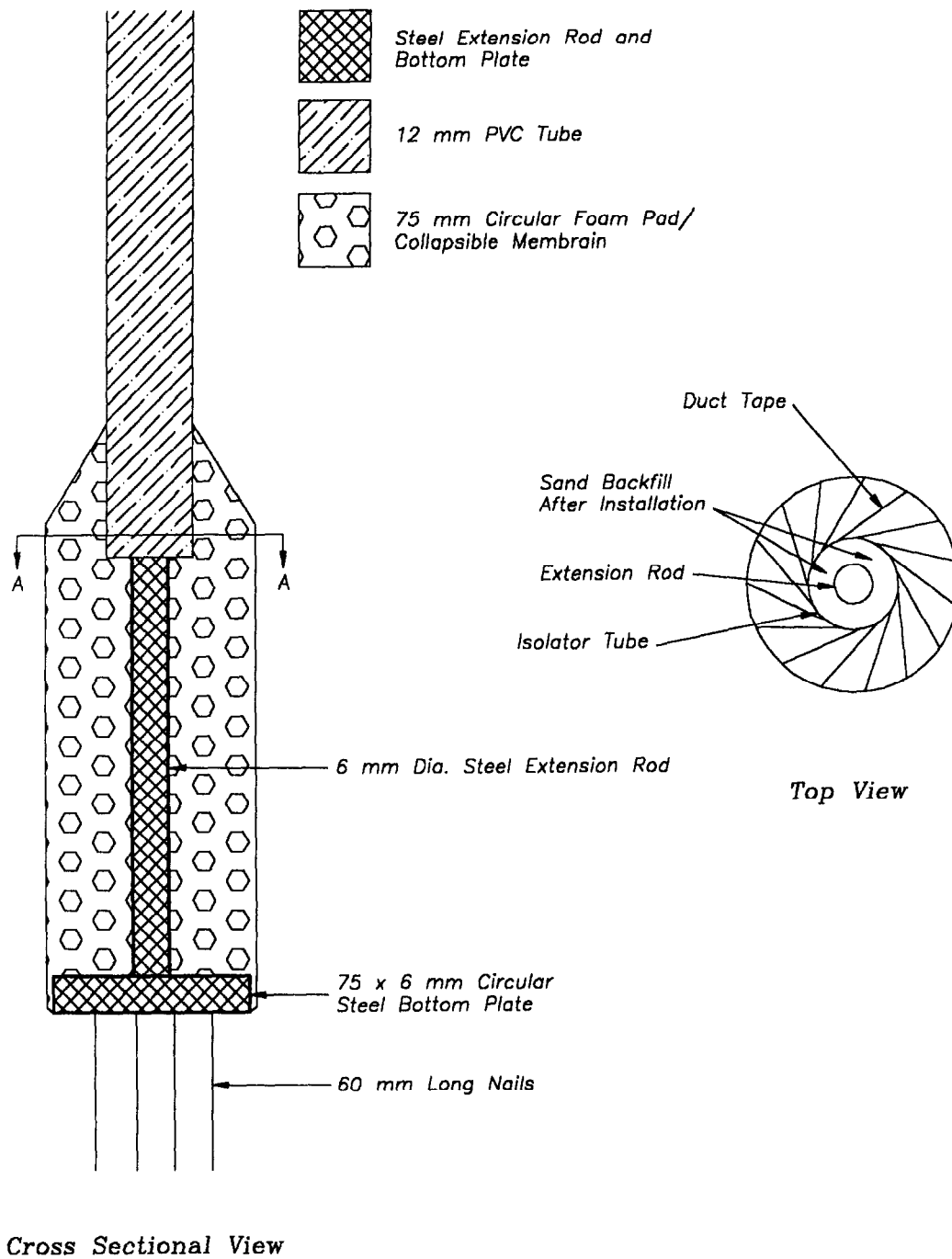


**Figure 4.4:** Cross Sectional View of Telltale

steel box beams including stacked wooden cribs, driven stakes and other footings as end supports. The different crib systems were used in an attempt to minimize any crib settlement caused by the weight of the beams.

#### **4.1.6 Load Measurements**

Figure 4.2 shows the loading system used during the load tests. The load applied to each footing was provided by a 12 MN, center piston, single acting hydraulic jack. The jack had a total stroke of 127 mm and required shims to complete the 150 mm of settlement. A 12 MN, 200 mm diameter compression load cell was placed between the jack and the shim plates in order to accurately measure the load application. The reaction beam used was actually four W33x120 beams, welded at the top flanges to produce two beams placed side by side to form one large reaction beam.

## **4.2 SOIL INVESTIGATION**

### **4.2.1 General Soil Description**

The upper soil (to a depth of 11 m) is a medium dense silty fine silica sand. The grain size distribution curve is relatively uniform with most of the grain sizes between 0.5-mm and 0.05-mm. The sand is probably lightly overconsolidated by dessication of the fines and removal of about 1 m of overburden at the location of the spread footing tests. Below the sand layer is a clay layer which exists until a depth of at least 33 m. Figure 4.5 shows the general layering at the site. A series of field and laboratory tests were performed in order to characterize the material on site. Table 4.2 gives a list of the tests performed, the dates these tests were performed and the people involved in the tests.

### **4.2.2 Laboratory Tests**

Visual classification, sieve analysis, Atterberg limits, water content, relative density, minimum and maximum void ratio, specific gravity and unit weight tests were performed at Texas A&M University on samples obtained from both a drilling rig and a hand auger. The

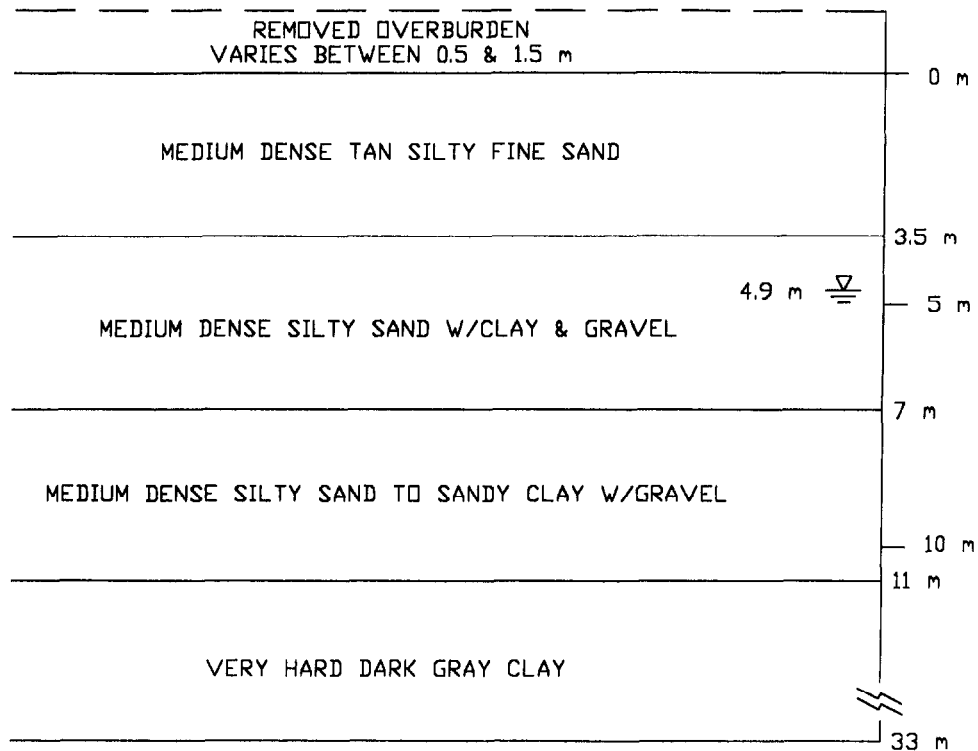


**Figure 4.5: General Soil Layering**

4.6. Tests performed on drilling rig samples include sieve analysis, Atterberg limits and water content. Sieve analysis results can be seen in Figure 4.6 while an Atterberg limit test, performed on a clay sample taken at a depth of 16.4 m, indicates a liquid limit of 40, a plastic limit of 19 and a plasticity index of 21. Water content results from samples obtained using a drilling rig ranged from 11.1% to 33.5% for the sand and 21.7% to 36.7% for the clay. The variation in moisture content between the hand augered and drilling rig samples is due to the severe seasonal moisture fluctuation which occurs in the testing area. The load tests were performed during the late summer months, as were the hand augered samples.

Consolidated/Drained Triaxial tests were also performed at Texas A&M University. These tests were performed on remolded samples of material taken from a hand auger. The values of  $\phi$  calculated from these tests are:

at 0.6 m depth:  $\phi = 34.2$  degrees  
 at 3.0 m depth:  $\phi = 36.4$  degrees

**Table 4.2: Test Dates & People Involved**

TEST	DATE	PEOPLE INVOLVED
Borehole Shear Tests	April 18 & 19, 1993	Mr. Mike Adams Dr. Allan Lutenegro Dr. Don Degroot Buchanan/Soil Mechanics
Cross-Hole Wave Tests	May 13, 1993	Dr. Derek Morris Mr. Tony Yen Mr. John Delphia
PiezoCone Penetration Test	January 27, 1993	Fugro McClelland
Dilatometer Tests	April 8 & 13, 1993	Mr. Maurizio Calabrese Mr. Robert Gibbens Buchanan/Soil Mechanics
Dilatometer Test w/Thrust Measurements	May 27, 1993	Mr. Robert Gibbens Buchanan/Soil Mechanics
Pressuremeter Tests	February 2, 1993 & May 15, 1993	Dr. Jean-Louis Briaud Mr. Philippe Jeanjean Mr. Robert Gibbens Mr. Rajan Viswanathan Buchanan/Soil Mechanics
Stepped Blade Test	April 19, 1993	Dr. Allan Lutenegro Dr. Don Degroot Buchanan/Soil Mechanics
Standard Penetration Tests	April 5-21, 1993	Mr. Robert Gibbens Dr. George Goble Buchanan/Soil Mechanics
Water Content & Unit Weights	November 1992- May 1993	Mr. Philippe Jeanjean Mr. Robert Gibbens
Atterberg Limits	May 1993	Mr. Robert Gibbens
Relative Density	November 1992	Mr. Philippe Jeanjean
Triaxial Tests	April 1993	Mr. Philippe Jeanjean
Resonant Column Tests	May 1993	Dr. Derek Morris Mr. Tony Yen

Resonant Column Tests were performed at Texas A&M University. The results of these tests can be found in Gibbens and Briaud, 1995.

#### 4.2.3 Field Tests

The location of each field test can be seen in Figure 4.3.

**Table 4.3: Dry Hand Augered Samples: Test Results**

Property	Sand 0.6 m	Sand 3.0 m
Specific Gravity	2.64	2.66
Minimum Void Ratio	0.65	0.62
Maximum Void Ratio	0.94	0.91
Maximum Dry Unit Weight (kN/m <sup>3</sup> )	15.70	16.10
Minimum Dry Unit Weight (kN/m <sup>3</sup> )	13.35	13.66
Liquid Limit	N/P	N/P
Plastic Limit	-	-
USCS Classification	SP	SP-SM
Natural Void Ratio	0.78	0.75
Dry Unit Weight (kN/m <sup>3</sup> )	14.55	14.91
Natural Moisture Content (%)	5.0	5.0
Natural Unit Weight (kN/m <sup>3</sup> )	15.28	15.65

#### 4.2.3.1 Standard Penetration Tests w/Energy Measurements

Standard Penetration Tests (SPT) were performed on site in the spring of 1993, including tests with energy measurements. Six SPT tests were performed using a safety hammer. Range plots of N-values versus depth can be seen on Figure 4.7.

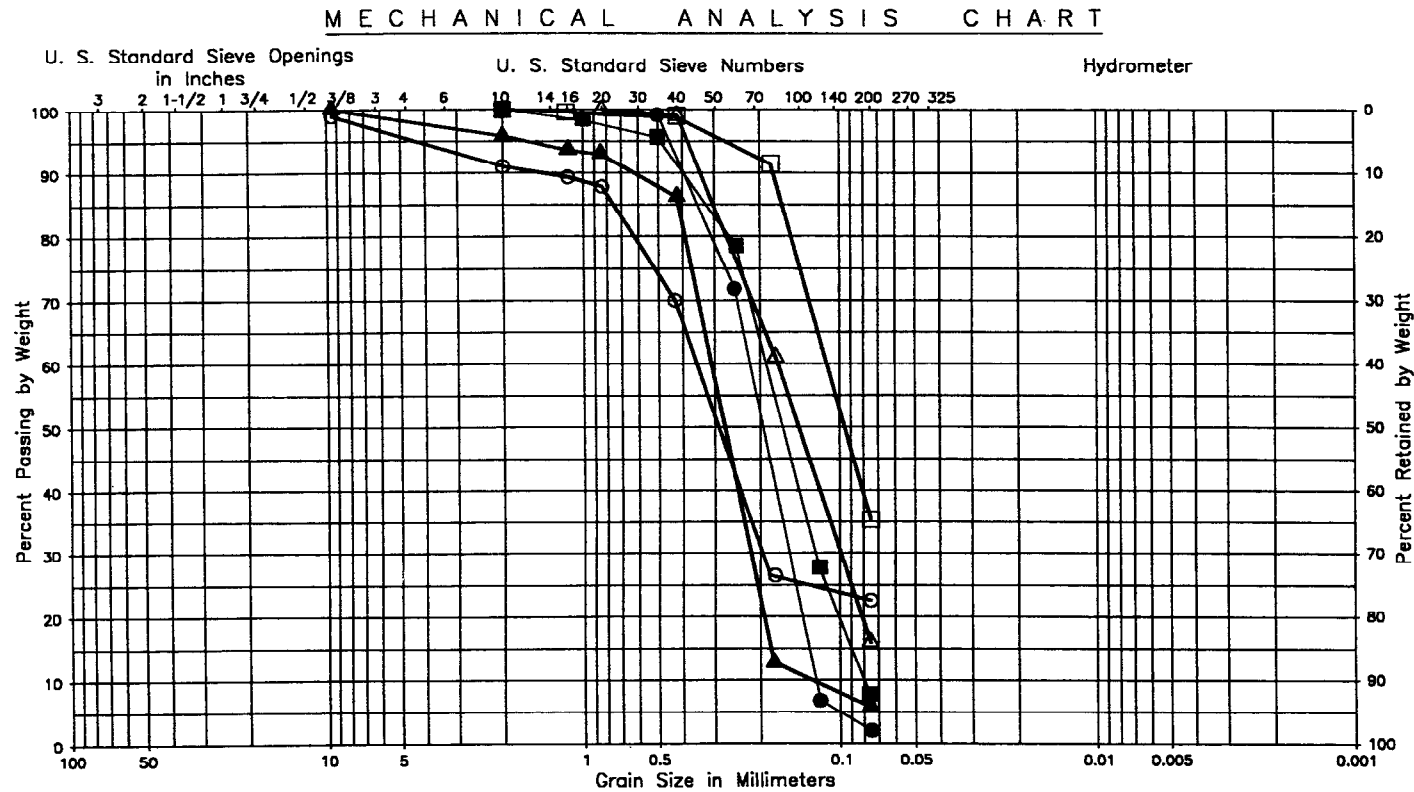
The results of energy measurements taken during one SPT test indicate that the data obtained was achieved with an average energy efficiency of 53%.

#### 4.2.3.2 PiezoCone Penetration Tests

PiezoCone Penetration Tests (CPT) were performed on site in the winter of 1993. Five CPT soundings were performed and included pore water pressure readings. Range plots of average point resistance versus depth can be seen on Figure 4.8.

#### 4.2.3.3 Pressuremeter Tests

Pressuremeter Tests (PMT) were performed on site in the winter and spring of 1993. Four PMT tests were performed using a TEXAM Pressuremeter. Range plots of initial modulus ( $E_0$ ), reload modulus ( $E_R$ ), and limit pressure ( $p_l$ ) versus depth can be seen on Figure 4.9.



GRAVEL		SAND			SILT OR CLAY
Coarse	Fine	Coarse	Medium	Fine	

UNIFIED SOIL CLASSIFICATION SYSTEM - CORPS OF ENGINEERS, U. S. ARMY

- |   |   |
|---|---|
| <p>BORING NO.: SPT-2</p> <p>DEPTH: <span style="display: inline-block; width: 20px; border-bottom: 1px solid black; margin-right: 5px;"></span> <span style="display: inline-block; width: 20px; border-bottom: 1px solid black; margin-right: 5px;"></span> <span style="display: inline-block; width: 20px; border-bottom: 1px solid black; margin-right: 5px;"></span> <span style="display: inline-block; width: 20px; border-bottom: 1px solid black; margin-right: 5px;"></span></p> <p style="margin-left: 40px;"> <span style="display: inline-block; width: 10px; height: 10px; border: 1px solid black; margin-right: 5px;"></span> 1.4m-1.8m<br/> <span style="display: inline-block; width: 10px; height: 10px; border: 1px solid black; margin-right: 5px;"></span> 3.5m-4.0m<br/> <span style="display: inline-block; width: 10px; height: 10px; border: 1px solid black; margin-right: 5px;"></span> 4.6m-5.0m<br/> <span style="display: inline-block; width: 10px; height: 10px; border: 1px solid black; margin-right: 5px;"></span> 8.7m-9.1m         </p> | <p>BORING NO.: HAND AUGERED HOLE</p> <p>DEPTH: <span style="display: inline-block; width: 20px; border-bottom: 1px solid black; margin-right: 5px;"></span> <span style="display: inline-block; width: 20px; border-bottom: 1px solid black; margin-right: 5px;"></span></p> <p style="margin-left: 40px;"> <span style="display: inline-block; width: 10px; height: 10px; border: 1px solid black; margin-right: 5px;"></span> 0.1 m<br/> <span style="display: inline-block; width: 10px; height: 10px; border: 1px solid black; margin-right: 5px;"></span> 2.5 m         </p> |
|---|---|

**TEXAS A&M RESEARCH PROJECT**  
RIVERSIDE CAMPUS

MAY 28, 1993

**Figure 4.6: Grain Size Analysis**

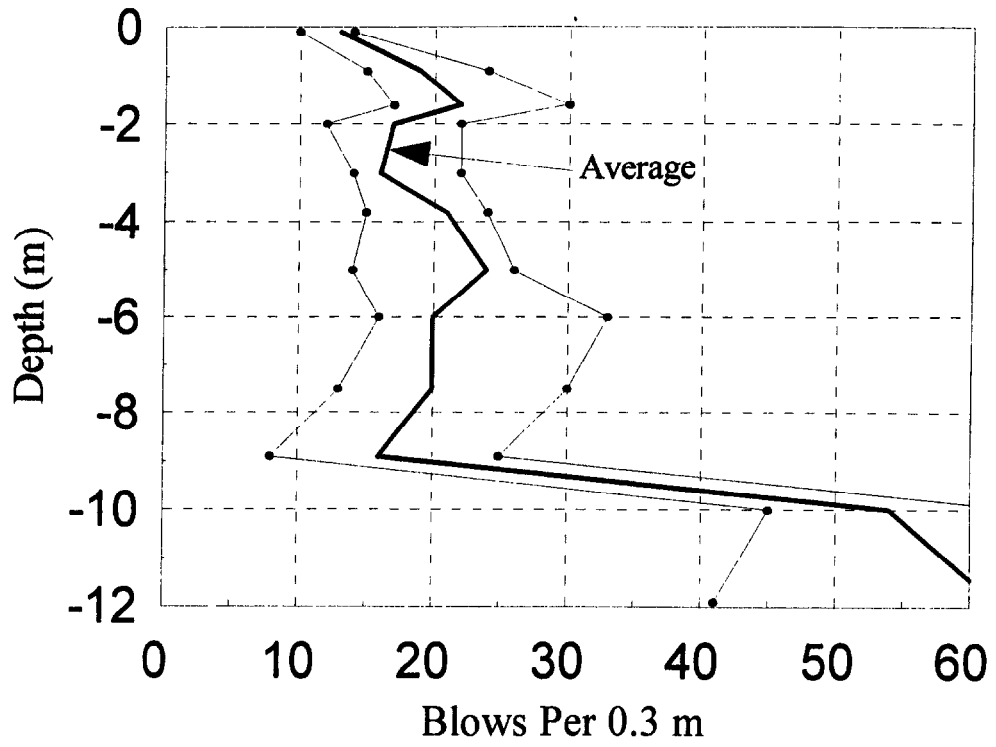


**Figure 4.7: Range of SPT Results**

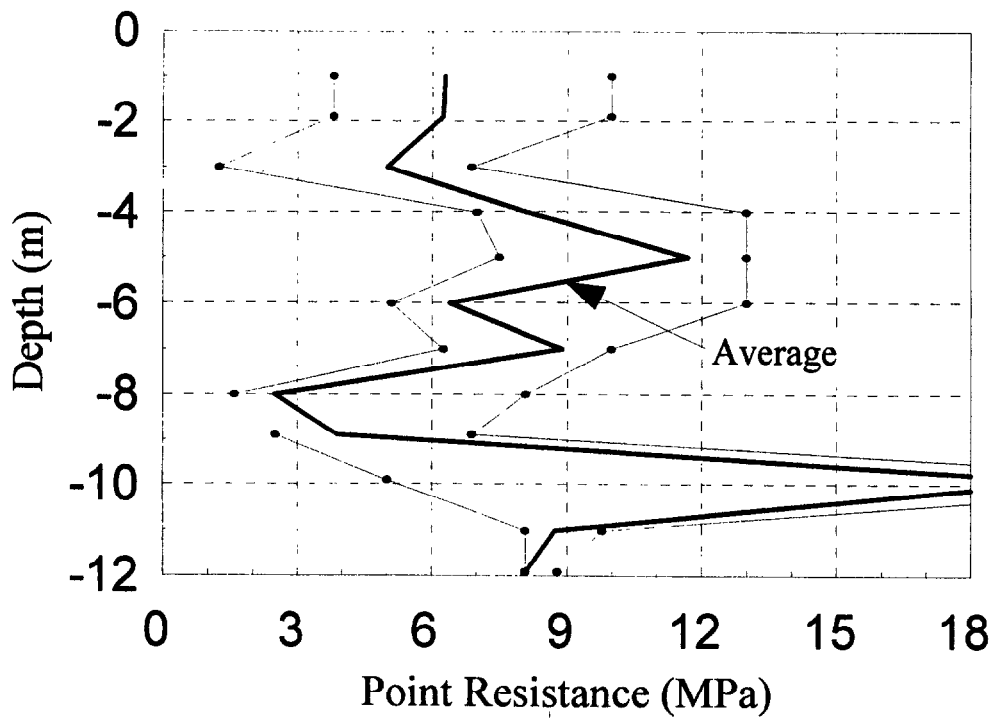


**Figure 4.8: Range of 5 CPT Soundings**

#### 4.2.3.4 Dilatometer Tests

Dilatometer Tests (DMT) were performed on site in the spring of 1993. Three DMT tests were performed with axial thrust measured during one of the three tests. Range plots of dilatometer modulus ( $E_d$ ), material index ( $I_d$ ), and horizontal stress index ( $K_d$ ) versus depth can be seen on Figure 4.10.

#### 4.2.3.5 Borehole Shear Test

Three Borehole Shear Tests (BHST) were performed on site during the spring of 1993. A range plot of phi angle,  $\phi$  versus depth can be seen on Figure 4.11.

#### 4.2.3.6 Cross-Hole Wave & Stepped Blade Tests

Cross-Hole Wave & Stepped Blade Tests were performed on site during the spring of 1993. The results of these tests can be found in the Gibbens and Briaud, 1995.

### **4.3 RESULTS**

The results of this load test program have been divided into four major areas: load settlement curves, creep curves, inclinometer profiles and telltale profiles.

#### **4.3.1 Load Settlement Curves**

Figure 4.12 shows the load settlement curves for each of the five footings. The word monotonic in Figure 4.12 refers to a load settlement curve with a constantly increasing load. All unload/reload cycles have been removed from the monotonic curve. The curves were generated by taking the settlement reached after 30 min for each load step during the tests. The settlement was the average of the settlement at the 4 corners and the load was given by the load cell. The data reduction for the load settlement curves was done in a conventional way as described in Gibbens and Briaud, 1995.

#### **4.3.2 Creep Curves**

Figures 4.13 through 4.16 show creep exponent curves generated during load testing for

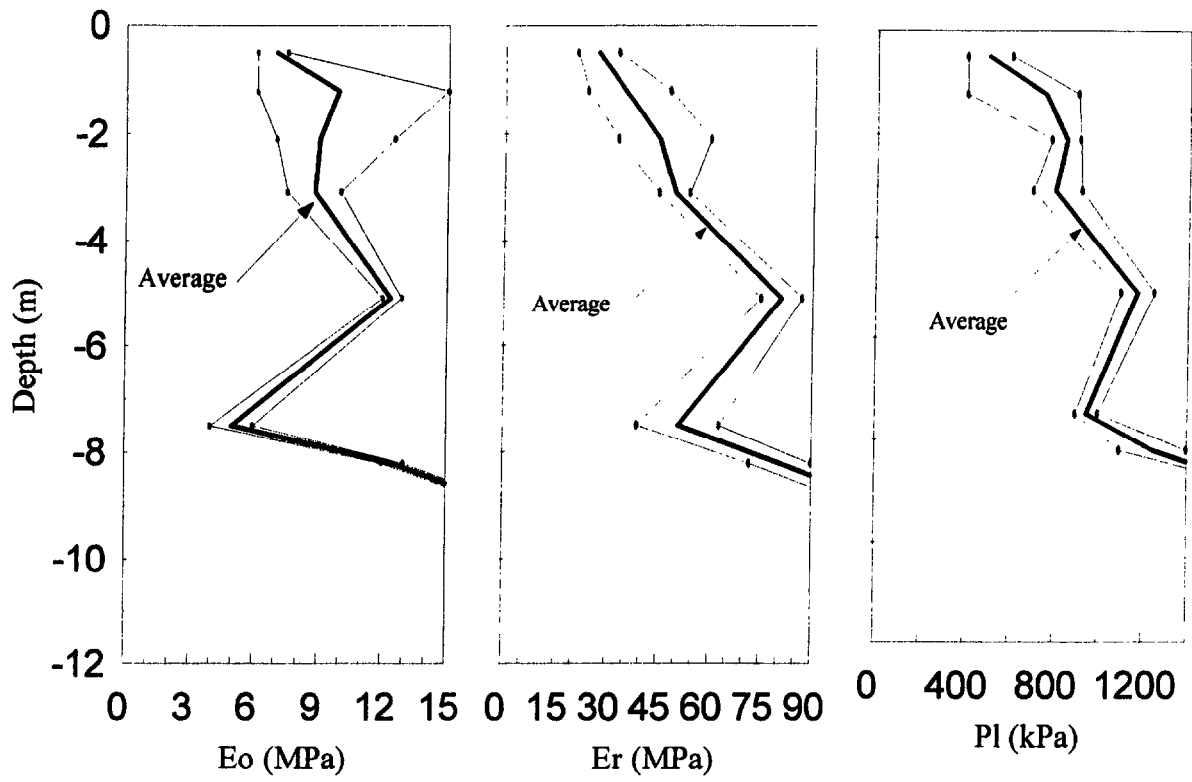


**Figure 4.9: Range of PMT Results**

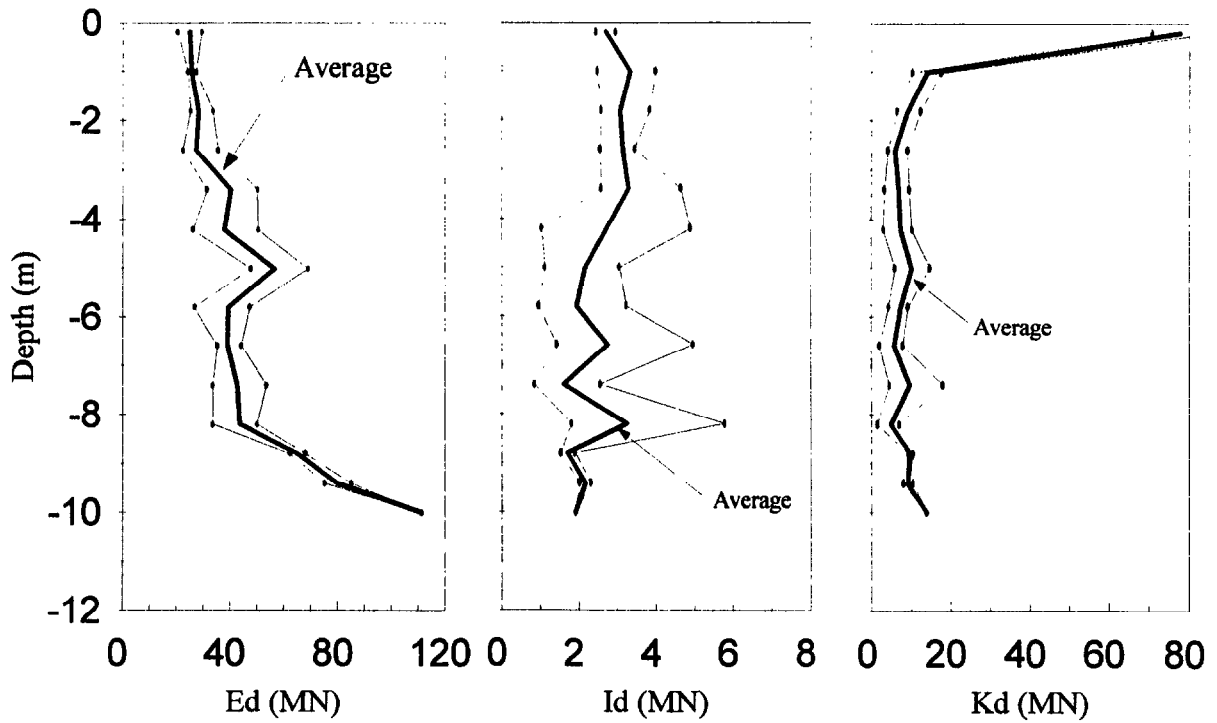


**Figure 4.10: Range of DMT Results**

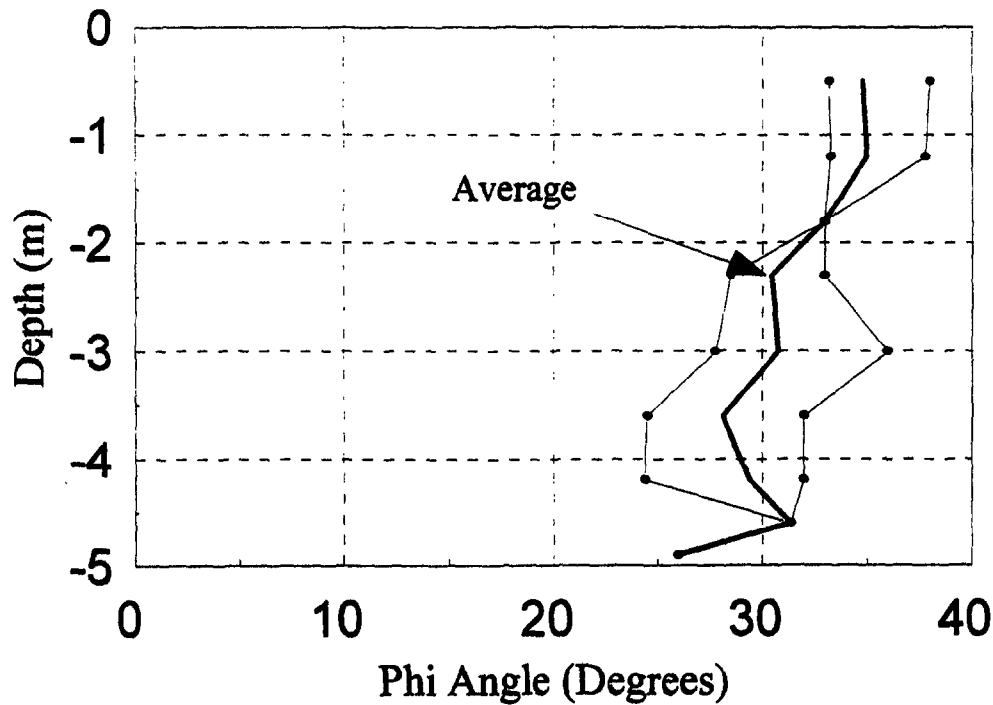


**Figure 4.11: Range of BHST Results**

the 1.5-m and 3.0-m North footings respectively. The displacement  $s$  is the displacement at a time  $t$  after the beginning of that load step while  $s_1$  is the displacement  $s$  for  $t = 1$  min. Figures 4.13 and 4.15 show creep results obtained during a 30-min hold period where a load was held and the settlement recorded at specific intervals over 30-min. Figures 4.14 and 4.16 show the same type of creep results obtained during 24-h creep tests. All data reduction procedures can be found in Gibbens and Briaud, 1995.

### 4.3.3 Inclinometer Profiles

Figures 4.17 and 4.18 show inclinometer test results for the 1.0-m and 3.0-m North footings respectively. Figure 4.17 represents an inclinometer test, performed in the North-South direction (the direction of maximum movement) at a failure load of 1.78 MN and 150 mm of settlement for the 1.0 m footing. Figure 4.18 represents three inclinometer tests, also performed in the direction of maximum movement (North-South) at failure for the 3.0 m North footing.

## Load Settlement Curve - All Footings Average 30 Minute Monotonic Curves

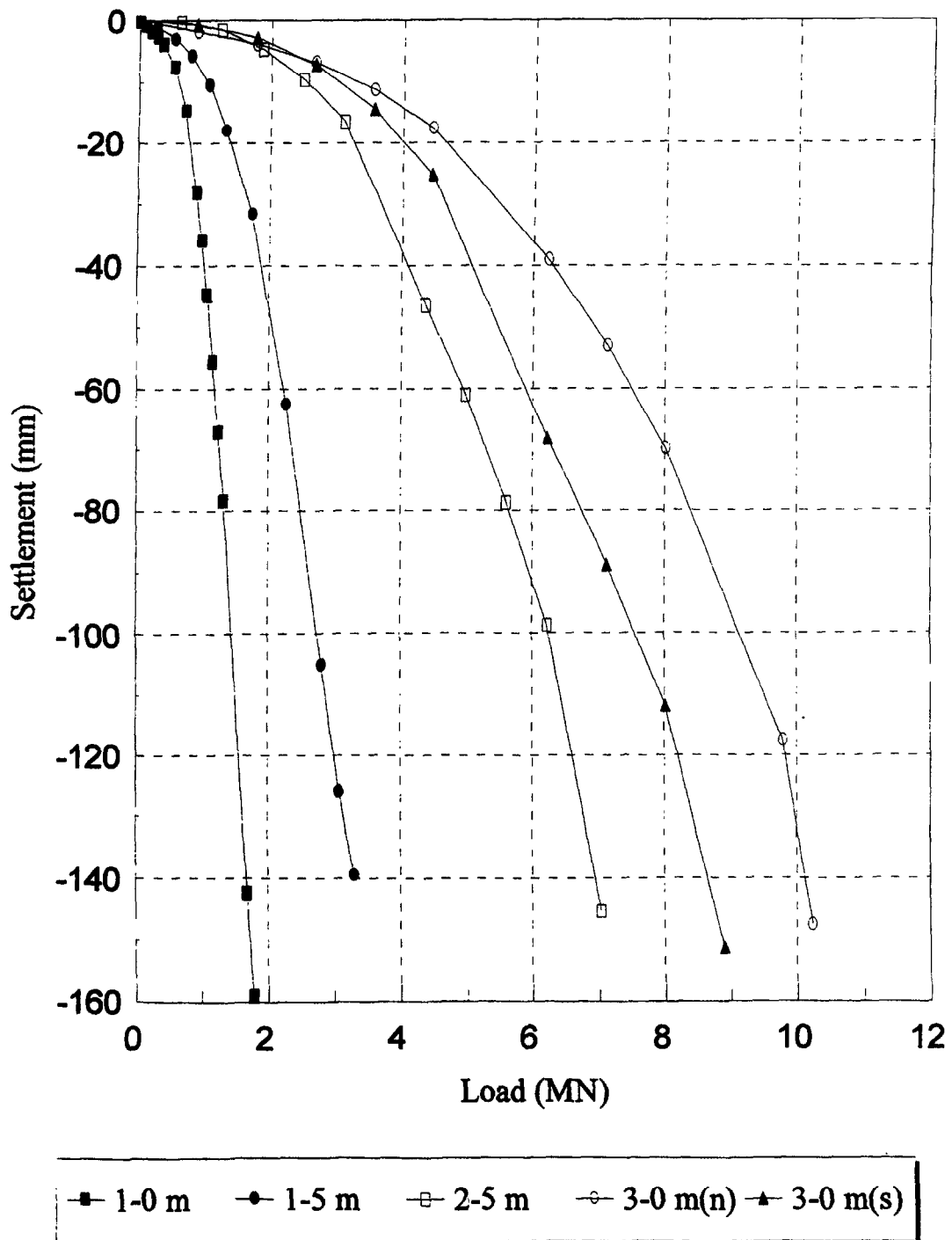


Figure 4.12: 30-Minute Monotonic Load Settlement Curves for All Footings

## Individual Creep Exponent Curves 1.5 M Footing

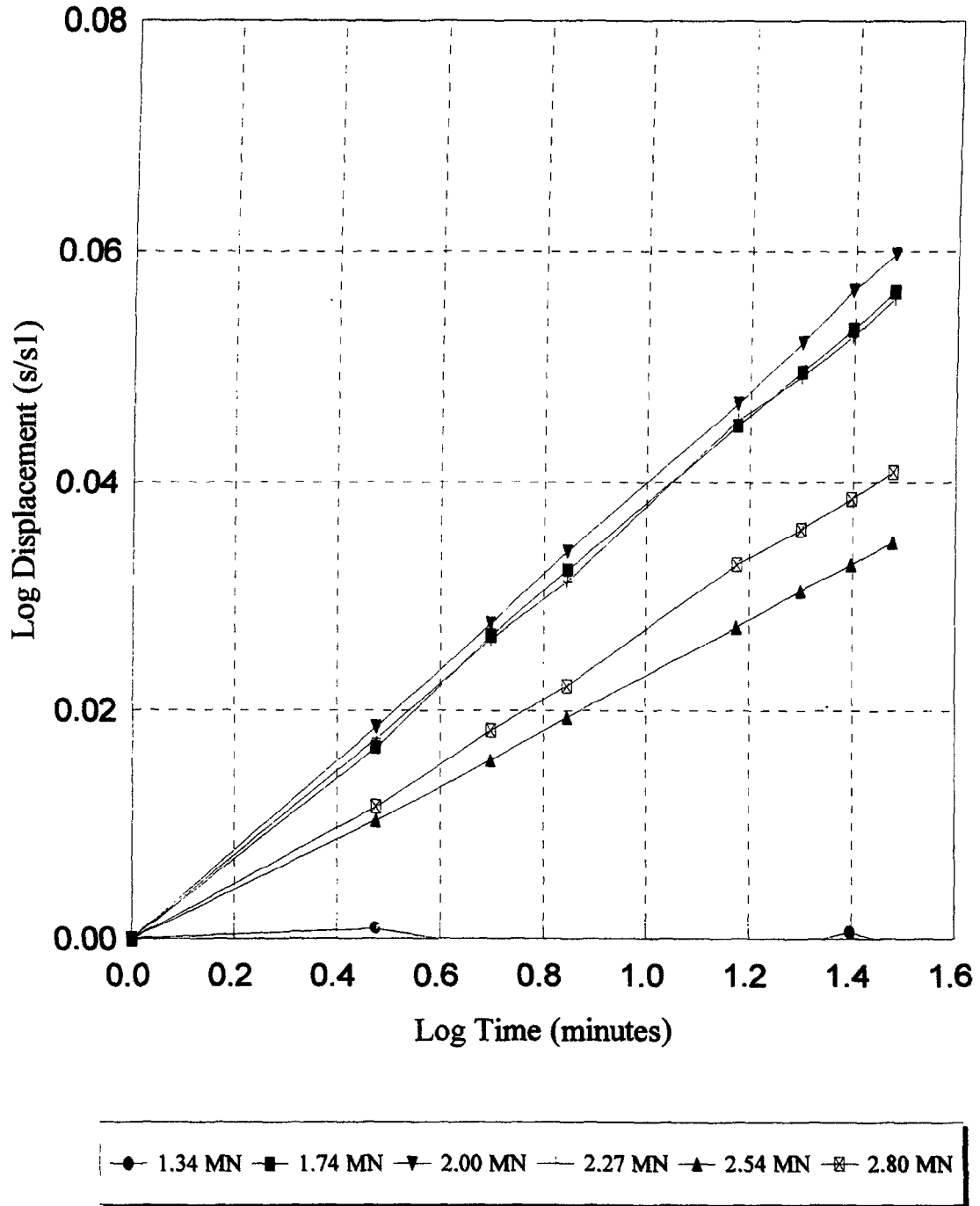


Figure 4.13: Individual Creep Exponent Curves for 1.5-m Footing, 1.34-MN - 2.80-MN

# Individual Creep Exponent Curve

## 1.5 M Footing - 24 Hour Creep Test

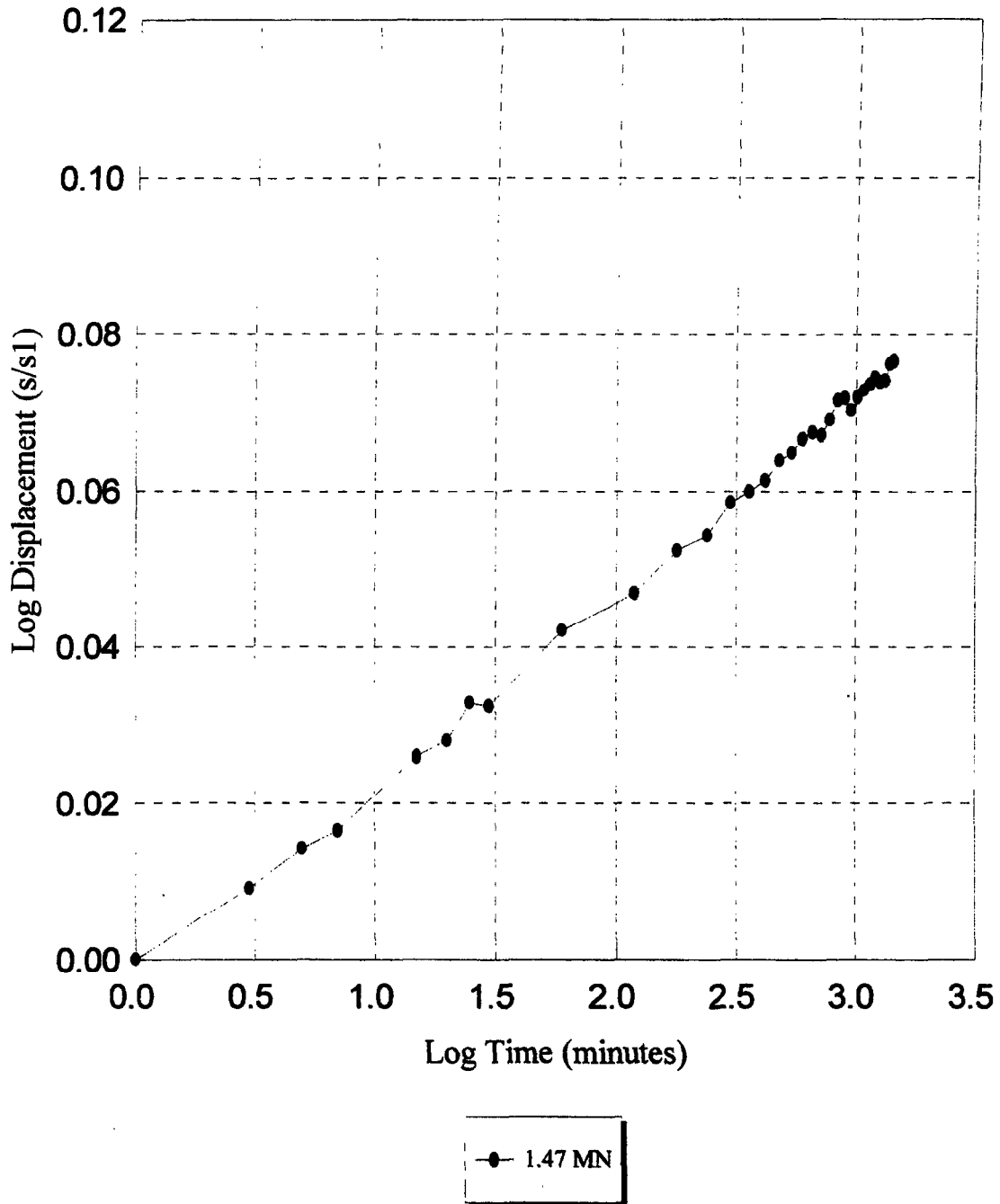


Figure 4.14: : Individual Creep Exponent Curve for 1.5-m Footing - 24-Hour Creep Test

**Individual Creep Exponent Curves**  
**3.0 M Footing**  
 NORTH

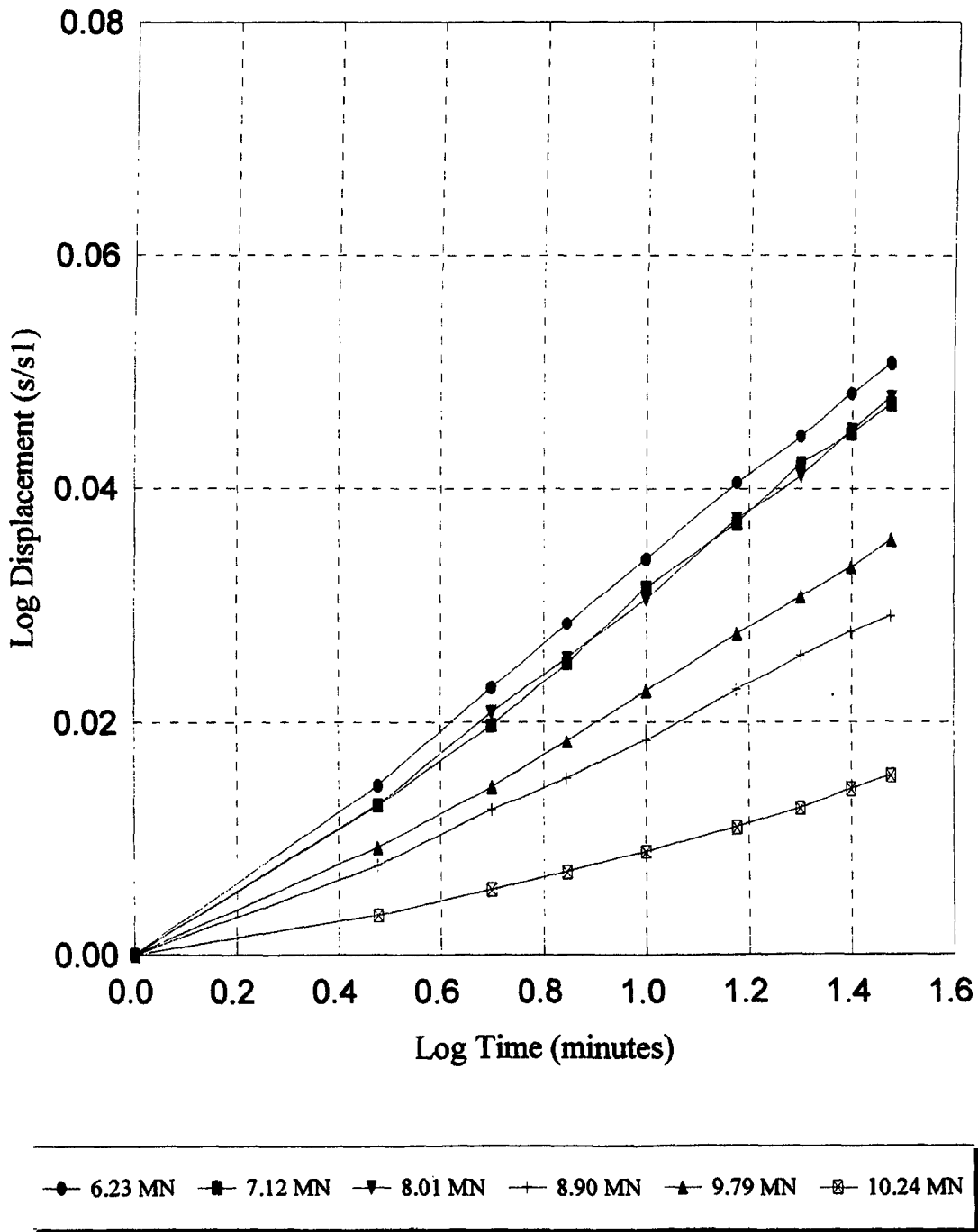
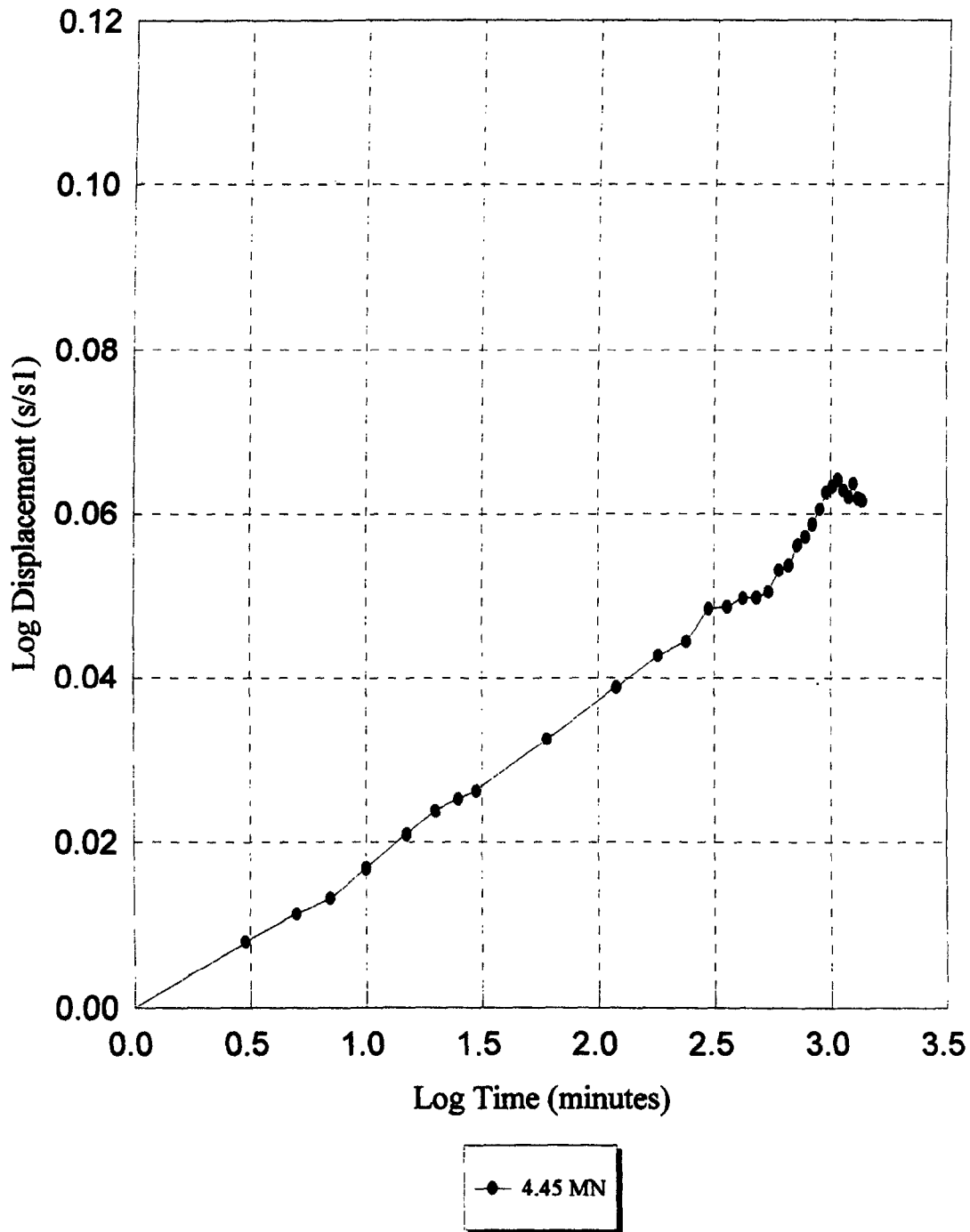


Figure 4.15: Individual Creep Exponent Curves for 3.0-m(n) Footing, 6.23-MN - 10.24-MN

**Individual Creep Exponent Curve**  
**3.0 M Footing - 24 Hour Creep Test**  
**NORTH**



**Figure 4.16: Individual Creep Exponent Curve for 3.0-m(n) Footing - 24-Hour Creep Test**

The three inclinometer curves represent three tests performed at various distances from the footing edge. All data reduction procedures can be found in Gibbens and Briaud, 1995.

#### **4.3.4 Telltale Profiles**

Figure 4.19 shows a plot of settlement versus depth below the footing bottom for the 3.0-m South footing. The results were obtained by reducing telltale data recorded during each footing load test. Each axis of Figure 4.19 is normalized in order to allow easy comparisons. The settlement  $s$  is the downward movement of the soil at a depth  $Z$  while  $s(\text{top})$  is the settlement at the top of the footing at the same load. The various curves on the graph refer to different  $s_{\text{top}}$  values expressed as percentages of  $B$  (1%, 2%, 3%, 4%, 5%). The corresponding pressures can be found in Figure 7.4. Section 7.3 shows how to obtain the strain vs. depth from this curve and gives the mean results. All data reduction procedures can be found in Gibbens and Briaud, 1995.

**1.78 MN Failure Test**  
**1.0 M Footing - spt-6 (North-South)**

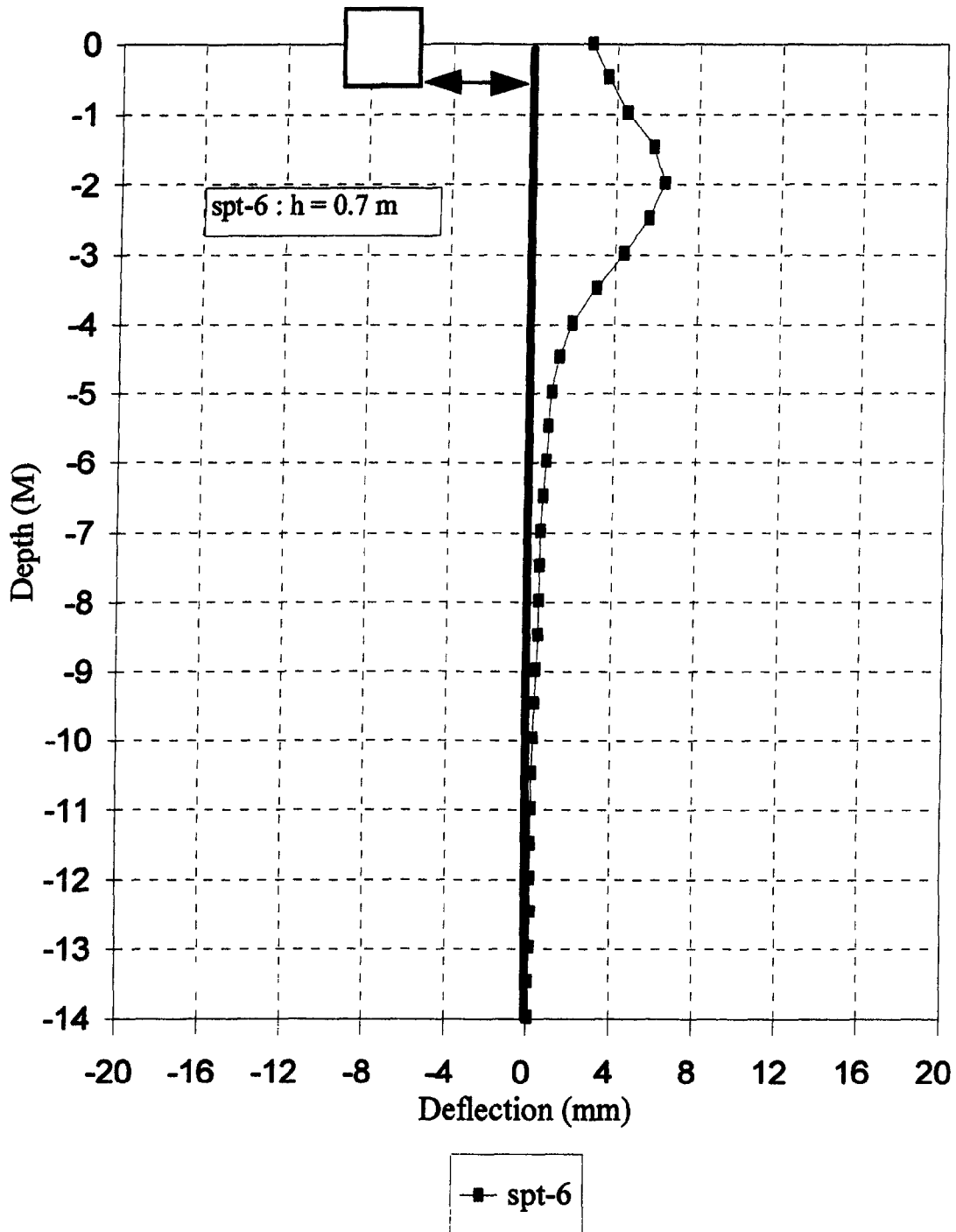


**Figure 4.17: Inclinometer Test - 1.78-MN Failure Load - N-S Direction, 1.0-M Footing**

## 8.90 MN Failure Test 3.0 M Footing - North (North-South)

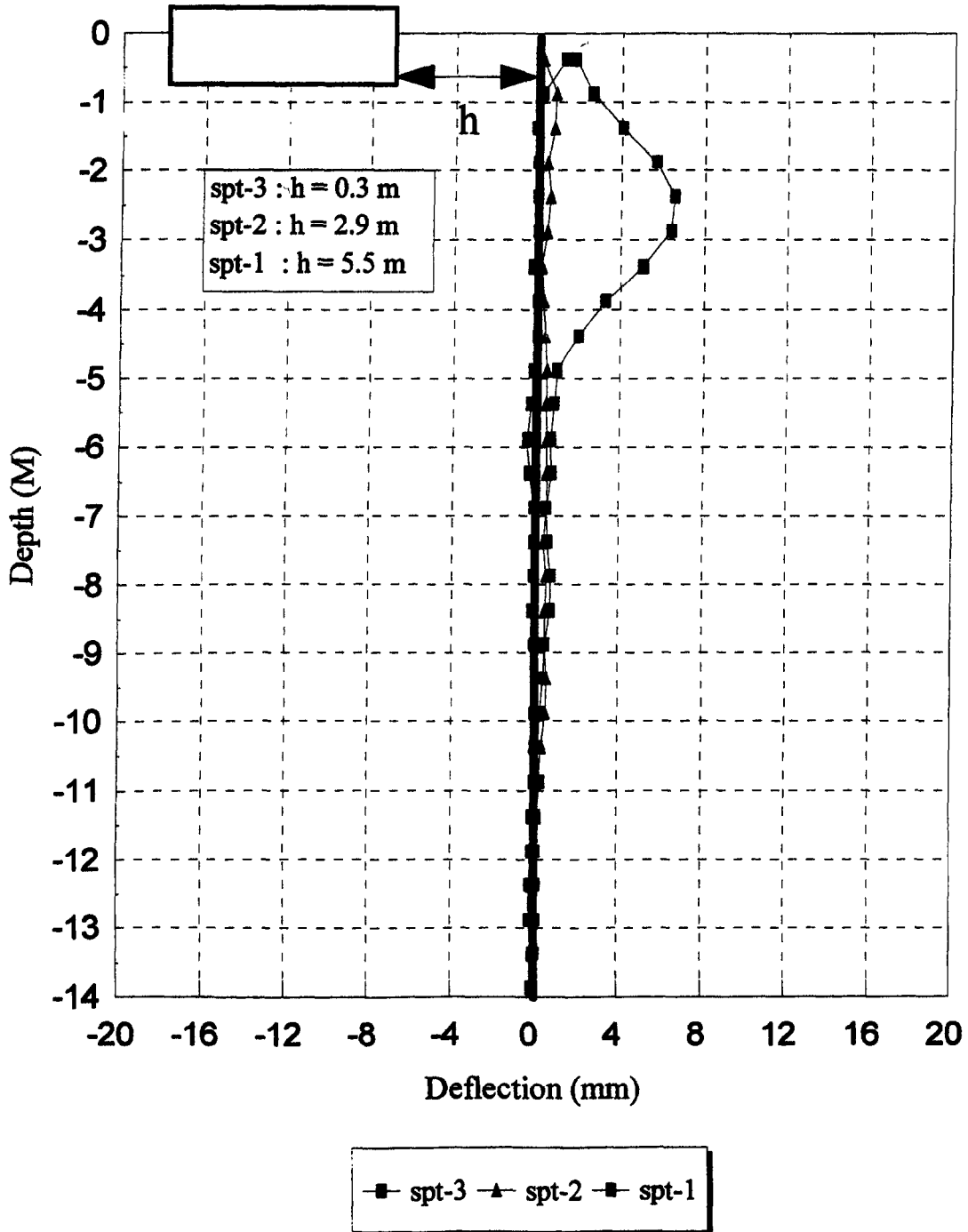


**Figure 4.18: Inclinometer Test - 8.90-MN Failure Load - N-S Direction, 3.0-m(n) Footing**

### S/S(top) versus Depth 3.0 M Footing South

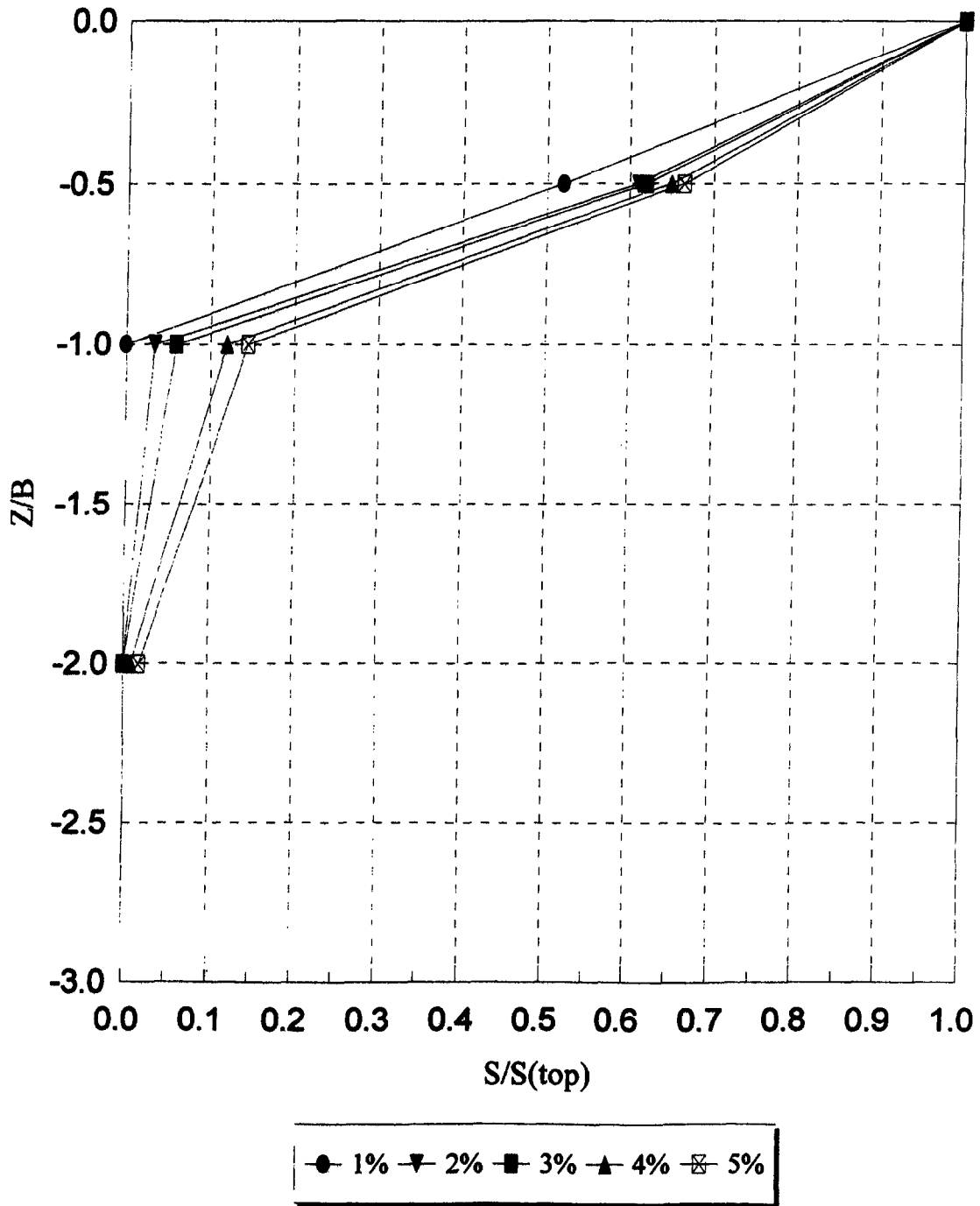


Figure 4.19: Settlement Versus Depth for 3.0-m(s) Footing With Varying Percentages of B

## **5. COMPARISON BETWEEN PREDICTED AND MEASURED RESULTS**

### **5.1 PREDICTION SYMPOSIUM EVENT USING THE 5 FOOTINGS**

This part of the project is detailed in Briaud and Gibbens, 1994.

#### **5.1.1 Introduction**

Five square spread footings ranging in size from 1-m to 3-m were load tested to 0.15-m of penetration. In parallel, a prediction event was organized. The prediction event was advertised in ASCE News and at various conferences in early 1993. A flier was distributed worldwide to the approximately 6,000 members of the ASCE Geotechnical Engineering division. About 150 requests for a prediction package were received. The 150 prediction packages were sent in July of 1993. During the following 2 months, three addendums were sent: an errata on the prediction package, an as-built set of dimensions for the footings and the time dependent modulus data from PMT tests. The prediction package and the addendums are given in Briaud and Gibbens, 1994. A total of 31 predictions were received from Israel, Australia, Japan, Canada, USA, Hongkong, Brazil, France and Italy. Of the 31 written responses obtained, 16 were from academics and 15 were from consultants.

#### **5.1.2 The Prediction Request**

The participants to the prediction event were requested to predict certain quantities obtained from each footings 30-min load-settlement curve (Figure 5.1). The first request was to predict, for each footing, the load measured in the load test at a settlement of 25-mm on the 30-min load-settlement curve. The second request was to predict, for each footing, the load measured in the load test at a settlement of 150 mm on the 30-min load-settlement curve. The third request was to predict what the creep would be for the 3- by 3-m footings between the 1- and 30-min readings at a load corresponding to a total footing settlement of 25-mm. The fourth request was to predict the total creep in the year 2014 if this load were held for 20 years.

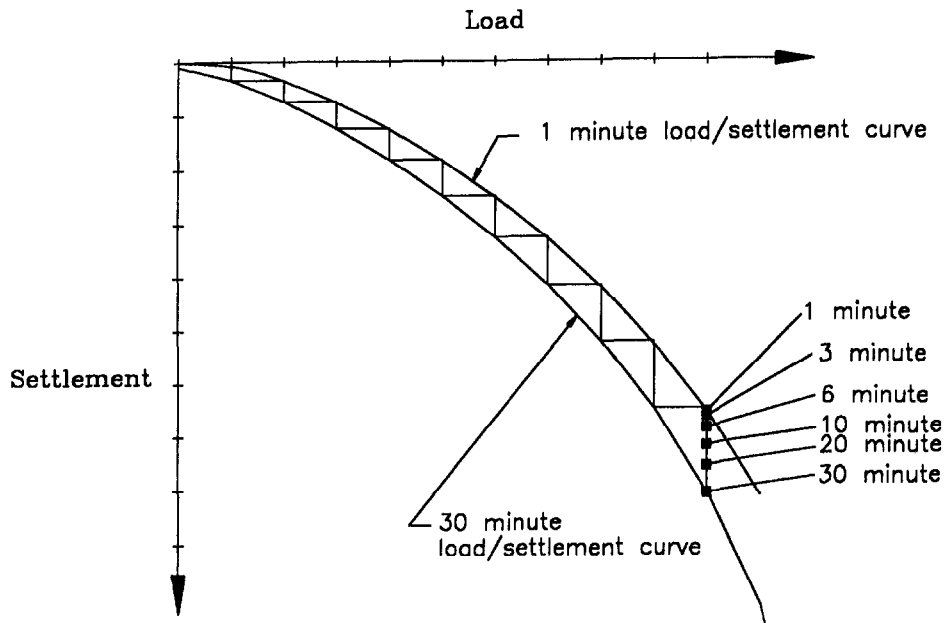


**Figure 5.1: Load-Settlement Curve**

### 5.1.3 Prediction Results and Comparisons

Tables 5.1 and 5.2 show summaries of the prediction methods and soil tests used in the 31 predictions respectively.

The predicted results (Tables 5.3 and 5.4) were compared to the measured results (Table 5.5 and Figure 4.12) by presenting a series of frequency distribution plots (Figures 5.2 through 5.11). Figures 5.2 through 5.6 give frequency of occurrence of the ratio of the predicted load at 25 mm of settlement over the measured load at 25 mm of settlement for the five footings. Figures 5.7 through 5.11 give the frequency of occurrence of the ratio of the predicted load at 150 mm of settlement over the measured load at 150 mm of settlement for the five footings.

Inspection of the  $Q_{25}$  frequency distribution plots indicates that 80% of the time the predictions were on the safe side and that this number was relatively independent of the footing scale. This is an indication that the scale effect is properly taken into account in settlement analysis.

Inspection of the  $Q_{150}$  frequency distribution plots indicates that on the average 63% of the time the predictions were on the safe side. This number however varied significantly from

**Table 5.1: Methods Used**

Method	# of Times Used
Alpan	3
Bowles	4
Buisman & DeBeer	3
Burland & Burbidge	9
Canadian Foundation Manual	1
D'Appolonia	4
DeBeer	1
Decourt	1
Finite Element Analysis	8
Hansen	1
Leonard & Frost	4
Menard & Briaud	5
Meyerhof	4
NAVFAC	4
Oweis	2
Parry	1
Peck	2
Robertson & Campanella	1
Schmertmann	18
Schultze & Sherif	3
Terzaghi & Peck	5
Vesic	6

**Table 5.2: Soil Tests Used**

Soil Tests	Frequency of Occurrence
Borehole Shear Test	0
Crosshole Wave Test	3
Cone Penetration Test	29
Dilatometer Test	14
Pressuremeter Test	16
Resonant Column Test	3
Stepped Blade Test	0
Standard Penetration Test	25
Triaxial Test	10

**Table 5.3: Prediction Results for Q<sub>25</sub> and Q<sub>150</sub> in kN**

No.	Authors	Q <sub>25</sub> 1 m	Q <sub>25</sub> 1.5 m	Q <sub>25</sub> 2.5 m	Q <sub>25</sub> 3.0 m(s)	Q <sub>25</sub> 3.0 m(n)	Q <sub>150</sub> 1 m	Q <sub>150</sub> 1.5 m	Q <sub>150</sub> 2.5 m	Q <sub>150</sub> 3.0 m(s)	Q <sub>150</sub> 3.0 m(n)	No. of Predictors within 20%
1	Wiseman	670	1300	3000	3900	3900	1120	2600	7900	11300	11300	5
2	Poulos	800	5040	2560	2790	3690	1120	11340	9680	14580	12690	1
3	Siddiquee	59	116	295	407	415	200	422	1086	1326	1502	0
4	Silvestri	448	771	1488	1929	1929	1085	2143	5060	6857	6857	0
5	Horvath	900	1450	3125	4500	4500	1650	4200	13500	23000	20000	6
6	Thomas	374	450	1786	1226	2835	457	650	2927	1633	4847	0
7	Surendra	800	2590	4020	4780	4780	800	2640	4690	13960	13960	4
8	Chang	150	320	1000	1400	2370	450	500	2600	3600	5000	0
9	Brahma	720	775	1850	1550	3025	1100	1990	9630	8450	15200	2
10	Floess	700	1500	4300	5600	6400	1000	2400	7700	11500	11600	5
11	Boone	600	1100	2400	1750	3000	760	2150	7000	10000	10000	3
12	Cooksey	550	900	2100	3750	3700	900	2000	6400	9000	9000	4
13	Scott	620	1250	2380	3000	3300	850	2400	9600	15800	15800	1
14	Townsend	404	2100	3500	5400	6080	1603	7195	12804	16620	22835	4
15	Foshee	423	564	1190	655	1838	2104	2720	5949	2641	9016	4
16	Mesri	925	1475	2775	3325	3325	-	-	-	-	-	3 of 5
17	Ariemma	1100	1165	3750	1250	5480	3965	5155	14980	5220	21575	2
18	Tand	850	1550	3000	3700	3700	960	2170	6020	8830	8740	7
19	Funegard	850	1570	3370	4470	4470	960	2170	6020	8830	8740	8
20	Deschamps	900	1800	2700	5200	5200	1500	3400	5400	10800	10800	8
21	Altaee	600	1100	1900	2300	2300	2500	4300	8000	10000	10000	3
22	Decourt	779	1295	2740	4658	4290	2360	4490	16440	27945	25740	4
23	Mayne	330	950	3350	5200	5200	395	1260	5150	8450	8450	5
24	Kuo	320	650	2000	2650	3100	420	970	3500	5400	5500	0
25	Shahrour	275	450	740	1530	1530	887	2397	3720	7560	7560	1
26	Abid	550	1000	2600	3600	3300	1600	3000	8000	12000	11500	5
27	Utah State	838	1644	3087	4808	4668	900	2119	7375	15143	13943	6
28	Gottardi	935	2008	4271	5526	5446	1093	3143	10918	17379	16587	4
29	Chua	313	540	1009	1452	1456	501	937	2413	3320	3345	0
30	Bhowmik	550	800	2000	2800	3000	1100	2500	9000	14000	15000	0
31	Diyaljee	422	788	1801	2552	2526	613	1576	5280	7293	7219	1
Mean		605	1258	2454	3150	3573	1165	2831	7291	10415	11477	5
Standard Deviation		257	899	1028	1582	1439	771	2163	3743	6063	5799	
Measured Value		850	1500	3600	4500	5200	1740	3400	7100	9000	10250	

**Table 5.4: Prediction Results for  $\Delta_s$  and S<sub>2014</sub>**

No.	Authors	$\Delta_s$ South mm	$\Delta_s$ North mm	S <sub>2014</sub> South mm	S <sub>2014</sub> North mm
1	Wiseman	13	13	36	36
2	Poulos	1	1	37	37
3	Siddiquee	-	-	-	-
4	Silvestri	1.3	1.3	31	31
5	Horvath	1	1	10	10
6	Thomas	1.5	1.5	35	35
7	Surendra	3	3	36.5	36.5
8	Chang	2.5	1.5	6	3
9	Brahma	2.8	2.4	32	31.5
10	Floess	1	1	33	33
11	Boone	2	2	32	32
12	Cooksey	1.3	1.3	30	30
13	Scott	1	1	37	37
14	Townsend	-	-	-	-
15	Foshee	-	-	37	38
16	Mesri	-	-	32	32
17	Ariemma	21	20.5	102	105
18	Tand	2.8	2.8	38	38
19	Funegard	2.8	2.8	32	32
20	Deschamps	1.3	1.3	30	30
21	Altaee	3	3	-	-
22	Decourt	2	2	44.3	44.3
23	Mayne	-	-	-	-
24	Kuo	16	16	27	27
25	Shahrour	-	-	-	-
26	Abid	1.5	1.5	25	25
27	Utah State	3	3	40.58	40.54
28	Gottardi	1.1	1.1	29.7	29.7
29	Chua	5.8	5.8	187.3	186.9
30	Bhowmik	1.6	1.4	35	32
31	Diyaljee	6	6	64	64
<b>Mean</b>		4	4	42	41
<b>Stndrd Deviation</b>		5	5	34	35
<b>Measured Value</b>		2.9	2.4	-	-

**Table 5.5: Measured Results**

	Footing 1 3 m North	Footing 2 3 m South	Footing 3 2.5 m	Footing 4 1.5 m	Footing 5 1.0 m
Load for 25 mm of settlement $Q_{25}$ on the 30-min load settlement curve (kN)	5200	4500	3600	1500	850
Load for 150 mm of settlement $Q_{150}$ on the 30-min load settlement curve (kN)	10250	9000	7100	3400	1740
Creep settlement between 1 and 30-min $Q_{25}$ curves, $\Delta_s$ (mm)	2.4	2.9	X	X	X
Settlement in the year 2014 under $Q_{25}$ , $\Delta_{2014}$ (mm)	?	?	X	X	X

84% for the 1-m footing to 48% for the 3-m South footing and showed a clear decreasing trend with increasing size. This is an indication that the scale effect is not properly taken into account in predicting the load corresponding to a large displacement.

Predicting the load at 150 mm of displacement created a dilemma for the participants: could this be considered enough displacement to use a bearing capacity equation or not? Most considered that the answer was “Yes.” Others used the FEM with a nonlinear model or did a non-linear extension of their settlement method.

If one considers all the answers which were within  $\pm 20\%$  of the measured loads, it is possible to count how many such answers each participant had (Table 5.3). This number would have a maximum of 10. The best results were from participants whose answers fell within the  $\pm 20\%$  range 8 times out of 10. The two participants who achieved this remarkable result used the Menard/Briaud pressuremeter method for one and an average of 15 simple methods plus the FEM for the other.

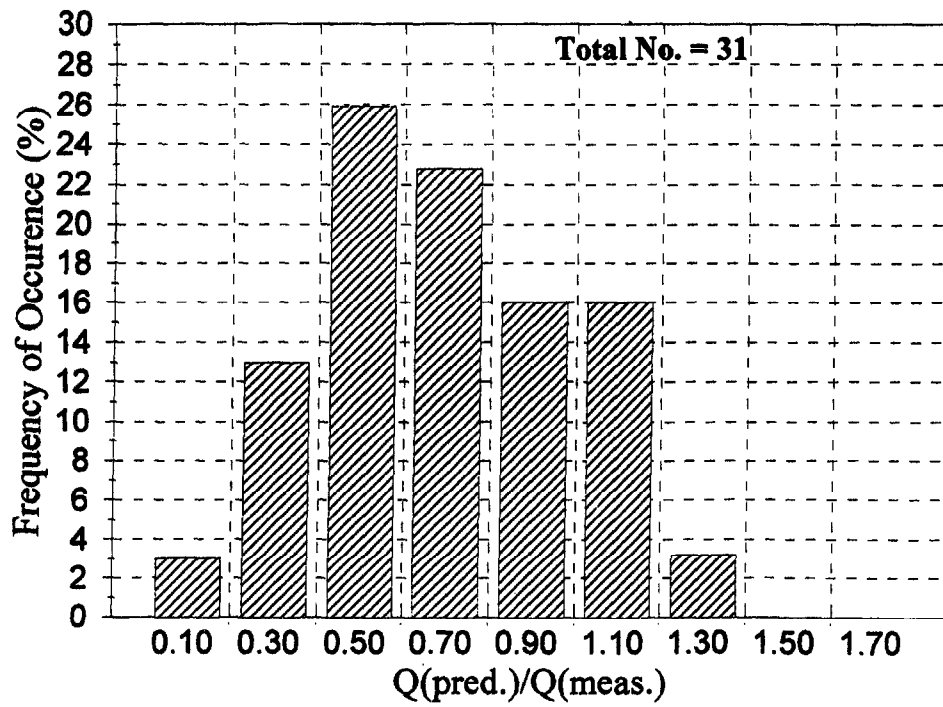


Figure 5.2: Distribution of  $Q_{pred.}/Q_{meas.}$  for 25-mm Settlement: 3-m North Footing

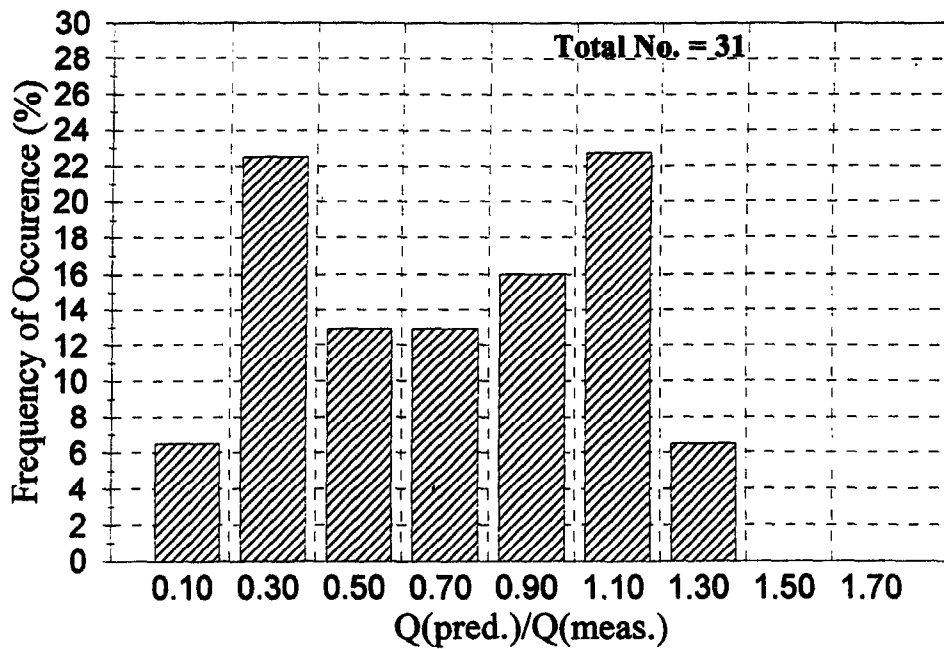


Figure 5.3: Distribution of  $Q_{pred.}/Q_{meas.}$  for 25-mm Settlement: 3-m South Footing

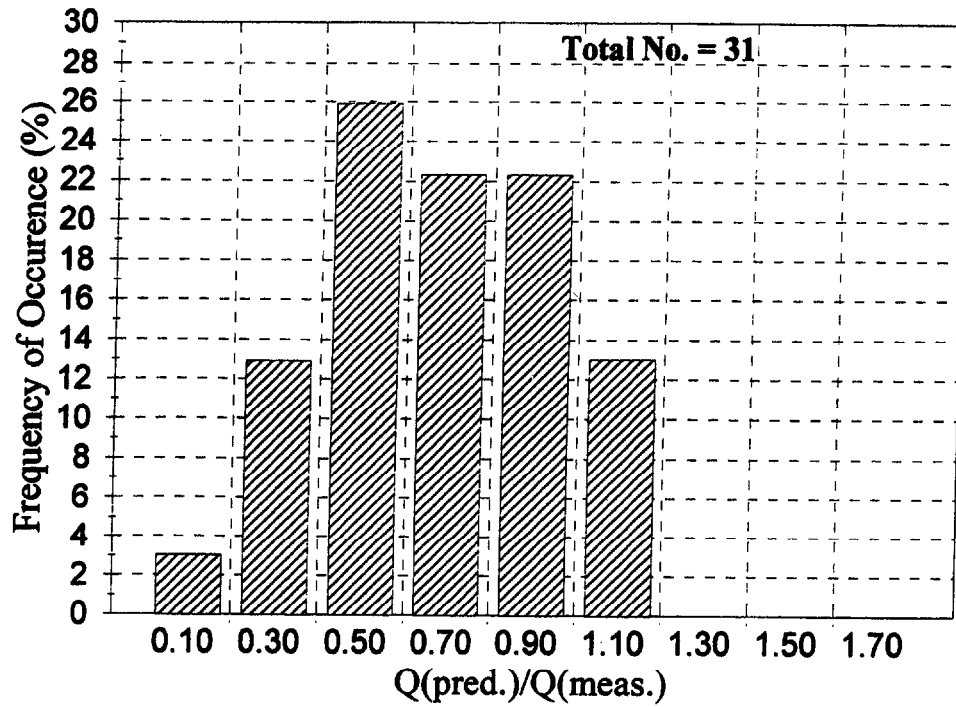


Figure 5.4 Distribution of  $Q_{pred.}/Q_{meas.}$  for 25-mm Settlement: 2.5-m Footing

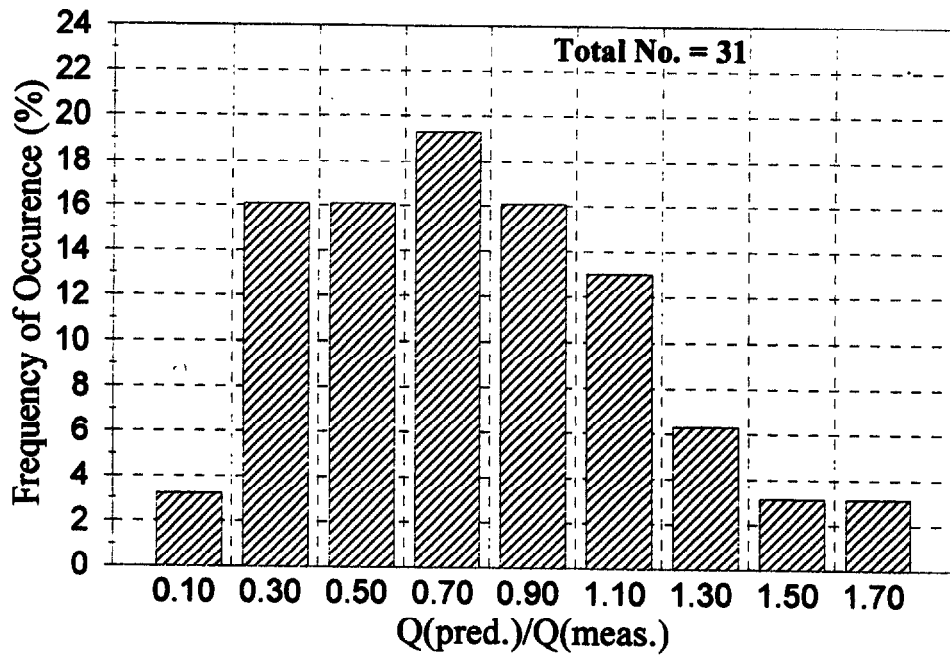


Figure 5.5 Distribution of  $Q_{pred.}/Q_{meas.}$  for 25 mm Settlement: 1.5-m Footing

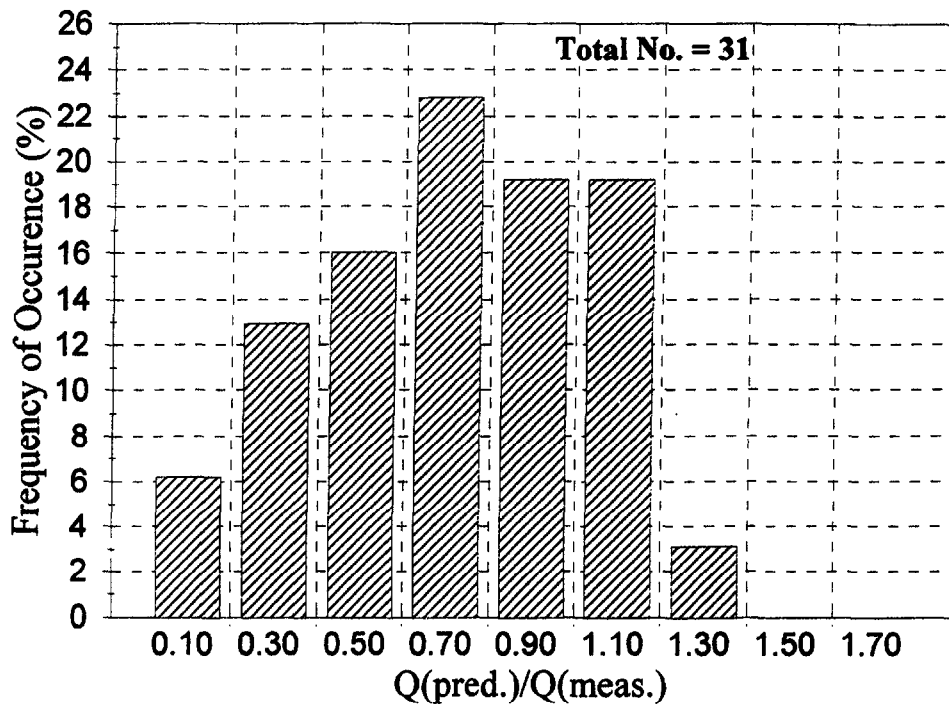


Figure 5.6 Distribution of  $Q_{pred.}/Q_{meas.}$  for 25mm Settlement: 1.0-m Footing

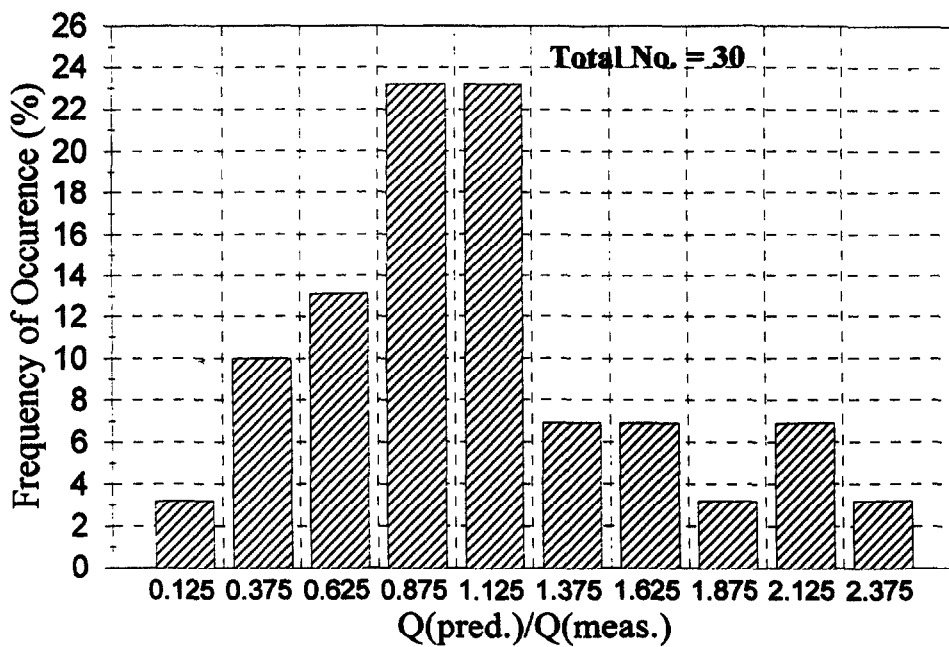


Figure 5.7: Distribution of  $Q_{pred.}/Q_{meas.}$  for 150mm Settlement: 3-m North Footing

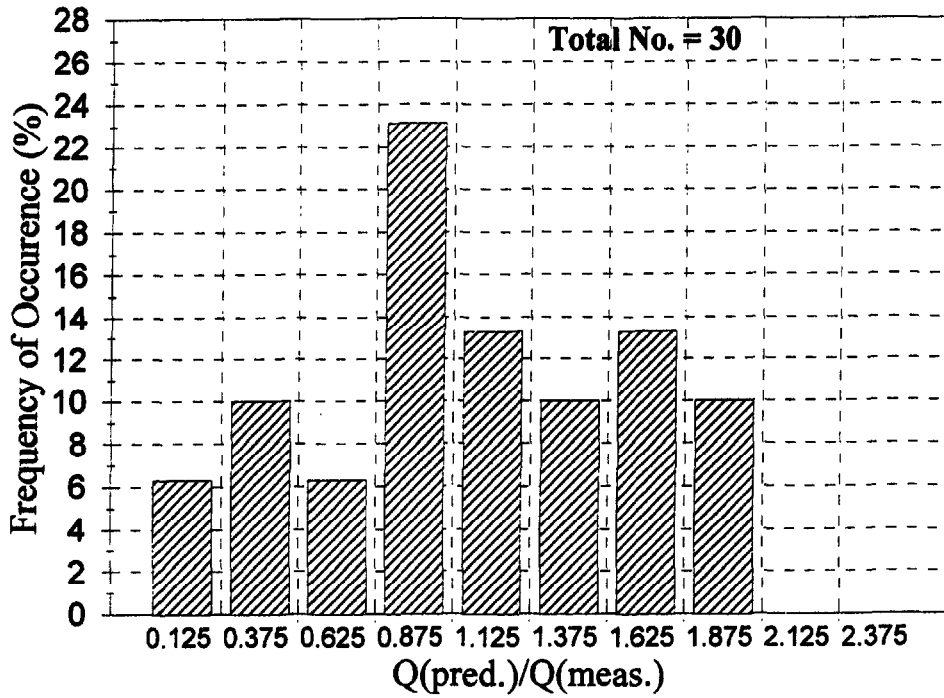


Figure 5.8 Distribution of  $Q_{pred.}/Q_{meas.}$  for 150-mm Settlement: 3-m South Footing

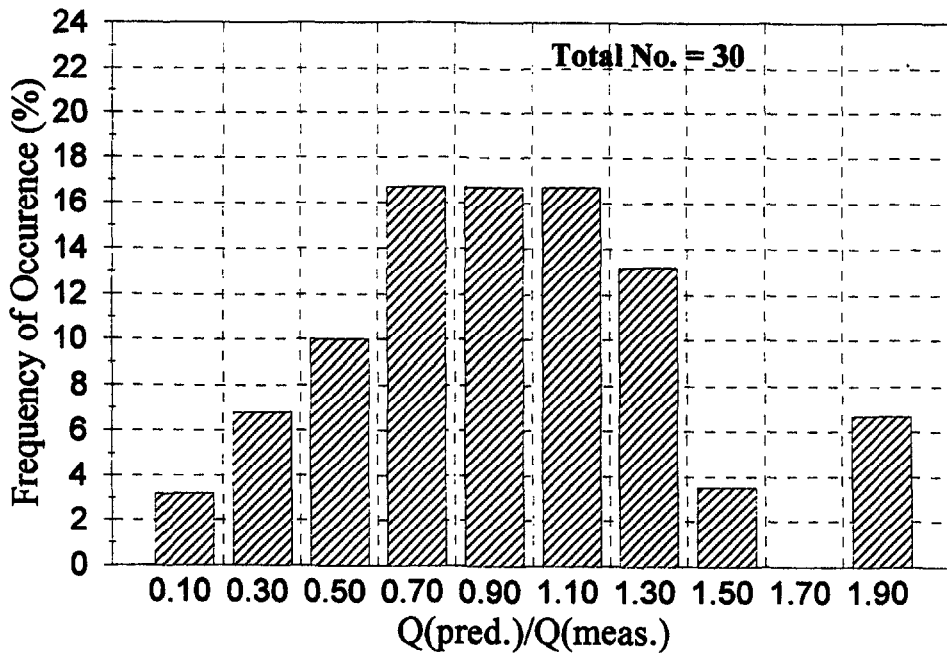


Figure 5.9: Distribution of  $Q_{pred.}/Q_{meas.}$  for 150-mm Settlement: 2.5-m Footing

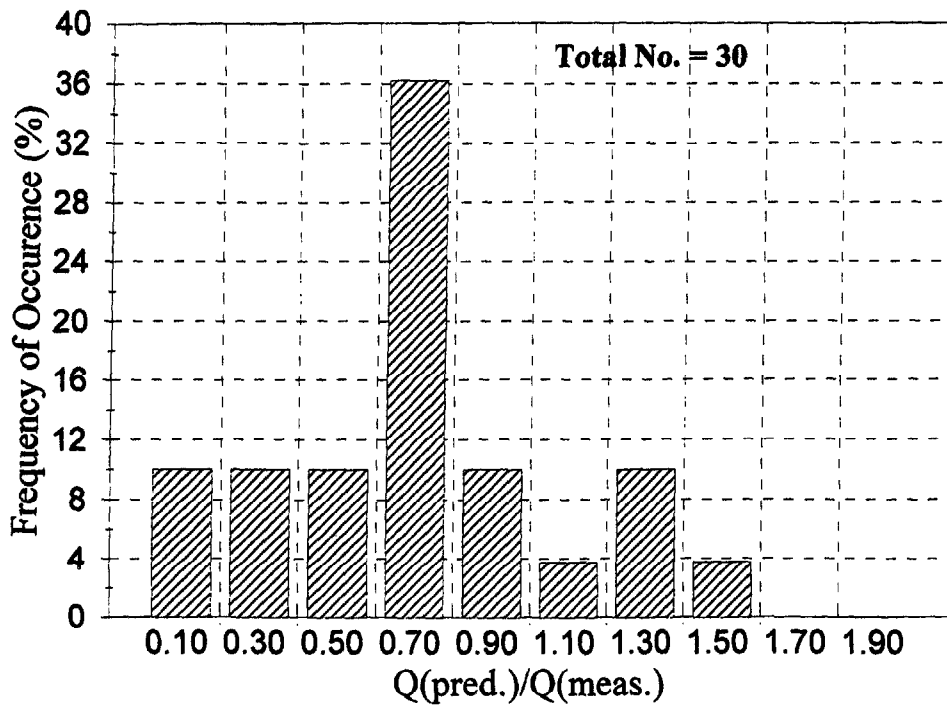


Figure 5.10: Distribution of  $Q_{pred.}/Q_{meas.}$  for 150-mm Settlement: 1.5-m Footing

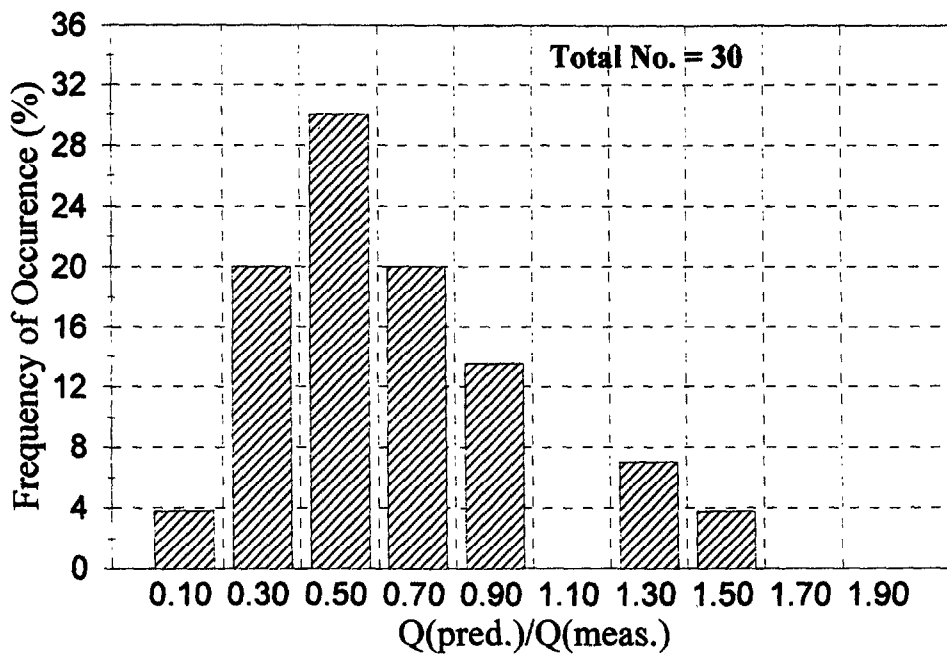


Figure 5.11: Distribution of  $Q_{pred.}/Q_{meas.}$  for 150-mm Settlement: 1.0-m Footing

An attempt was made to find out which method was the most consistently successful at predicting the loads at 25 and 150 mm. The top 10 answers for each of the loads to be predicted was studied. It was not possible to detect a clear best method. What became clear, however, is that very few participants actually used the exact procedure recommended by the authors of a method. Instead, many participants used a given method but modified it by taking into account their own experience or by using part of another method. Several participants used an average of several methods as their answer.

Reasonable predictions were obtained for  $\Delta_s$  considering the lack of directly useful data in the prediction package. Most participants used some form of Schmertmann's time factor or the time dependent pressuremeter data sent in the addendums.

The predictions for  $\Delta_{2014}$  indicate that an additional 10 mm should occur over the next 20 years. Provided funding can be secured, the plan is to place a load of 5200 kN on the 3-m North footing and 4500 kN on the 3-m South footing for the next 20 years and to organize another conference in the year 2014.

#### **5.1.4 Predicted Design Loads and Factor of Safety**

The participants predicted  $Q_{25}$  and  $Q_{150}$ . In a typical design, one uses a factor of safety of 3 on the ultimate load  $Q_u$  and uses as the design load the minimum of the load leading to 25 mm of settlement and one third of the ultimate load. For the purpose of this exercise the predicted design load for each participant was taken as:

$$Q_d = \text{MIN}\left(Q_{25}(\text{predicted}), Q_{150}(\text{predicted}) / 3\right) \quad (1)$$

These values are listed in Table 5.6. The measured load at 150 mm,  $Q_{150}$ , of settlement was taken as the measured failure load  $Q_f$  and the ratio of  $Q_f/Q_d$  was considered to be a safety factor. The values of this factor of safety are given in Table 5.7. This table shows that in only one instance the factor of safety  $Q_f/Q_d$  was less than one, and that the next worst case was 1.6. Therefore nearly all predictions lead to safe designs.

Finally the settlement that would take place under the design load was obtained. This was one by using the design load,  $Q_d$ , for each participant and reading the corresponding settlement on the measured load settlement curves (Figure 4.12). These settlement values are in Table 5.8. As can be seen, most settlements are quite acceptable. A trend is noticed where the larger the footing the higher the settlement under design load.

### **5.1.5 General Observations**

Five large spread footing load tests were performed. The square footings varied from 1 m to 3 m in width and were loaded until the settlement reached 150 mm. Participants were asked to predict the loads ( $Q_{25}$  and  $Q_{150}$ ) necessary to create 25 and 150 mm of settlement after 30 min of load application as well as the creep settlement over 30 min for the 25-mm load and the settlement by the year 2014 under the 25 mm load. A total of 31 predictions were received from 8 different countries, half from consultants and half from academics. Some observations reached from comparing the predictions and the measurements are as follows:

1. Nobody gave a complete set of answers which consistently fell within  $\pm 20\%$  of the measured values. Two participants had 80% of their answers falling within the  $\pm 20\%$  margin of error.
2. The load creating 25 mm of settlement,  $Q_{25}$ , was underestimated by 27% on the average. The predictions were 80% of the time on the safe side. The scale effect was properly predicted since this number (80%) was consistent for all sizes.
3. The load creating 150 mm of settlement,  $Q_{150}$ , was underestimated by 6% on the average. The predictions were 63% of the time on the safe side. The scale effect was not properly predicted and there was a trend towards overpredicting  $Q_{150}$  for the larger footings.

**Table 5.6: Predicted Design Loads**

No.	Authors	Q <sub>d</sub> 1 m kN	Q <sub>d</sub> 1.5 m kN	Q <sub>d</sub> 2.5 m kN	Q <sub>d</sub> 3 m(s) kN	Q <sub>d</sub> 3 m(n) kN
1	Wiseman	373	867	2633	3767	3767
2	Poulos	373	3780	2560	2790	3690
3	Siddiquee	59	116	295	407	415
4	Silvestri	362	714	1488	1929	1929
5	Horvath	550	1400	3125	4500	4500
6	Thomas	152	217	976	544	1616
7	Surendra	267	880	1563	4653	4653
8	Chang	150	167	867	1200	1667
9	Brahma	367	663	1850	1550	3025
10	Floess	333	800	2567	3833	3867
11	Boone	253	717	2333	1750	3000
12	Cooksey	300	667	2100	3000	3000
13	Scott	283	800	2380	3000	3300
14	Townsend	404	2100	3500	5400	6080
15	Foshee	423	564	1190	655	1838
16	Mesri	925	1475	2775	3325	3325
17	Ariemma	1100	1165	3750	1250	5480
18	Tand	320	723	2007	2943	2913
19	Funegard	320	723	2007	2943	2913
20	Deschamps	500	1133	1800	3600	3600
21	Altaee	600	1100	1900	2300	2300
22	Decourt	779	1295	2740	4658	4290
23	Mayne	132	420	1717	2817	2817
24	Kuo	140	323	1167	1800	1833
25	Shahrour	275	450	740	1530	1530
26	Abid	533	1000	2600	3600	3300
27	Utah State	300	706	2458	4808	4648
28	Gottardi	364	1048	3639	5526	5446
29	Chua	167	312	804	1107	1115
30	Bhowmik	367	800	2000	2800	3000
31	Diyaljee	204	525	1760	2431	2406
Mean		377	892	2042	2788	3138
Stndrd Deviation		229	682	866	1430	1338
Measured Value		580	1133	2367	3000	3417

**Table 5.7: Factors of Safety  $F = Q_f/Q_d$** 

No.	Authors	$Q_f/Q_d$ 1 m	$Q_f/Q_d$ 1.5 m	$Q_f/Q_d$ 2.5 m	$Q_f/Q_d$ 3 m(s)	$Q_f/Q_d$ 3 m(n)
1	Wiseman	4.66	3.92	2.70	2.39	2.72
2	Poulos	4.66	0.90	2.77	3.23	2.78
3	Siddiquee	29.49	29.31	24.07	22.11	24.70
4	Silvestri	4.81	4.76	4.77	4.67	5.31
5	Horvath	3.16	2.43	2.27	2.00	2.28
6	Thomas	11.42	15.69	7.28	16.53	6.34
7	Surendra	6.53	3.86	4.54	1.93	2.20
8	Chang	11.60	20.40	8.19	7.50	6.15
9	Brahma	4.75	5.13	3.84	5.81	3.39
10	Floess	5.22	4.25	2.77	2.35	2.65
11	Boone	6.87	4.74	3.04	5.14	3.42
12	Cooksey	5.80	5.10	3.38	3.00	3.42
13	Scott	6.14	4.25	2.98	3.00	3.11
14	Townsend	4.31	1.62	2.03	1.67	1.69
15	Foshee	4.11	6.03	5.97	13.74	5.58
16	Mesri	1.88	2.31	2.56	2.71	3.08
17	Ariemma	1.58	2.92	1.89	7.20	1.87
18	Tand	5.44	4.70	3.54	3.06	3.52
19	Funegard	5.44	4.70	3.54	3.06	3.52
20	Deschamps	3.48	3.00	3.94	2.50	2.85
21	Altaee	2.90	3.09	3.74	3.91	4.46
22	Decourt	2.23	2.63	2.59	1.93	2.39
23	Mayne	13.22	8.10	4.14	3.20	3.64
24	Kuo	12.43	10.52	6.09	5.00	5.59
25	Shahrour	6.33	7.56	9.59	5.88	6.70
26	Abid	3.26	3.40	2.73	2.50	3.11
27	Utah State	5.80	4.81	2.89	1.87	2.21
28	Gottardi	4.78	3.25	1.95	1.63	1.88
29	Chua	10.42	10.89	8.83	8.13	9.19
30	Bhowmik	4.75	4.25	3.55	3.21	3.42
31	Diyaljee	8.52	6.47	4.03	3.70	4.26
Mean		6.64	6.29	4.72	4.99	4.43
Stndrd Deviation		5.23	5.90	4.12	4.63	4.13
Measured Value		3	3	3	3	3

**Table 5.8: Settlement Under the Design Load,  $S_d$** 

No.	Authors	$S_d$ 1 m mm	$S_d$ 1.5 m mm	$S_d$ 2.5 m mm	$S_d$ 3 m(s) mm	$S_d$ 3 m(n) mm
1	Wiseman	3	6.5	12	16	12
2	Poulos	3	170	11	8	12
3	Siddiquee	.5	1	0	0	1
4	Silvestri	3	4	3	3	4
5	Horvath	7	21	17	25	18
6	Thomas	2	1	1	0	3
7	Surendra	2.5	7	3.5	28	19
8	Chang	2	1	1	1	20
9	Brahma	3	3.5	4.5	2	8
10	Floess	2.5	6	11	17	13
11	Boone	2.5	4.5	8	2.5	8
12	Cooksey	2.5	3.5	6	9	8
13	Scott	2.5	6	9	9	10
14	Townsend	4	55	27	47	36
15	Foshee	4.5	3	2	0	3
16	Mesri	28	24	13	12	10
17	Ariemma	48	12	33	1	30
18	Tand	2.5	4	5	9	7.5
19	Funegard	2.5	4	5	9	7.5
20	Deschamps	6	13	4	15	12
21	Altaee	10	13	4.5	5	6
22	Decourt	19	18	12.5	29	17
23	Mayne	2	2	4	8	8
24	Kuo	2	1.5	1.5	3	4
25	Shahrour	3	2	1	2	2.5
26	Abid	7.5	9	11	14	10
27	Utah State	3	4.5	9	34	20
28	Gottardi	3.5	10	29.5	50.5	29
29	Chua	1.5	1.5	0.5	1	2
30	Bhowmik	3.5	5.5	5.5	8	8.5
31	Diyaljee	2	3	4	6	6
Mean		6.1	13.5	8.4	12.1	11.5
Stndrd Deviation		9.5	30.9	8.4	13.4	8.6
Measured Value		9.5	12.0	8.5	10.0	10.5

4. A large variety of methods was used and it was not possible to identify the most accurate one because most people used published methods modified by their own experience or used a combination of methods. The most popular method was Schmertmann's method using CPT data. Of all the soil tests performed, the most used one was the CPT, then came the SPT, the PMT and the DMT.
5. The creep settlement over the 30-min load step for  $Q_{25}$  was predicted reasonably well considering the limited data available for this prediction. The average prediction for the settlement by the year 2014 under  $Q_{25}$  is 35 mm or an additional 10 mm over the next 20 years.
6. The design load  $Q_d$  for each footing and each participant was defined as  

$$Q_d = \text{MIN}(Q_{25}(\text{predicted}), Q_{150}(\text{predicted}) / 3)$$
The factor of safety  $F$  was defined as the ratio of the measured  $Q_{150}$  over  $Q_d$ . Since 31 participants predicted the behavior of 5 footings, there was a total of 155 values for the factor of safety  $F$ . Only once out of 155 was  $F$  less than 1, the next worse case was 1.6; the average was 5.4. Therefore it appears that our profession knows how to design spread footings very safely.
7. The settlement  $S_d$  under the design load  $Q_d$  was read on the measured load settlement curves at the value of the predicted design load for each footing and for each participant. The overall average was 10.3 mm which is much smaller than 25 mm. Considering the high factors of safety and the low settlement values, the design load could have been significantly higher. Therefore it appears that our profession could design spread footings more economically.

## **5.2 EVALUATION OF 18 PREDICTION METHODS USING THE 5 FOOTINGS**

This part of the project is detailed in Gibbens and Briaud, 1995.

Tables 5.9 and 5.10 list the results obtained from a study of 12 settlement and 6 bearing capacity prediction methods.

**TABLE 5.9: Tabulated Settlement Prediction Values**

	1.0 m Footing	1.5 m Footing	2.5 m Footing	3.0 m(n) Footing	3.0 m(s) Footing
<b>Predicted Load @ s=25 mm</b>	(MN)	(MN)	(MN)	(MN)	(MN)
Briaud (1992)	0.904	1.314	2.413	2.817	2.817
Burland & Burbidge (1984)	0.699	1.044	1.850	2.367	2.367
De Beer (1965)	1.140	0.803	0.617	0.597	0.597
Menard & Rousseau (1962)	0.247	0.394	0.644	1.017	1.017
Meyerhof - CPT (1965)	0.288	0.446	0.738	0.918	0.918
Meyerhof - SPT (1965)	0.195	0.416	1.000	1.413	1.413
Peck & Bazarra (1967)	1.042	1.899	4.144	5.679	5.679
Peck, Hansen & Thornburn (1974)	0.319	0.718	1.981	2.952	2.952
Schmertmann - CPT (1970)	0.455	0.734	1.475	1.953	1.953
Schmertmann - DMT (1986)	1.300	2.165	4.114	5.256	5.256
Shultze & Sherif (1973)	1.465	2.615	4.750	5.850	5.850
Terzaghi & Peck (1967)	0.287	0.529	1.244	1.476	1.476
<b>Measured Load @ s=25 mm</b>	<b>0.850</b>	<b>1.500</b>	<b>3.600</b>	<b>4.500</b>	<b>4.500</b>

**TABLE 5.10: Tabulated Bearing Capacity Prediction Values**

	1.0 m Footing	1.5 m Footing	2.5 m Footing	3.0 m(n) Footing	3.0 m(s) Footing
<b>Predicted Bearing Capacity</b>	(MPa)	(MPa)	(MPa)	(MPa)	(MPa)
Briaud-CPT (1993a)	1.394	1.287	1.389	1.513	1.513
Briaud-PMT (1992)	0.872	0.779	0.781	0.783	0.783
Hansen (1970)	0.772	0.814	0.769	0.730	0.730
Meyerhof (1951 & 1963)	0.832	0.991	1.058	1.034	1.034
Terzaghi (1943)	0.619	0.740	0.829	0.826	0.826
Vesic (1973 & 1974)	0.825	0.896	0.885	0.855	0.855
<b>Measured Pressure @ s=150 mm</b>	<b>1.740</b>	<b>1.511</b>	<b>1.136</b>	<b>1.000</b>	<b>1.139</b>

### 5.2.1 Settlement Prediction Methods

In an attempt to match the prediction results collected during the symposium, the calculations made for this study (Table 5.9) were of the load required to cause a settlement of 25 mm. Actual prediction method descriptions and calculations can be found in Gibbens and Briaud, 1995.

### **5.2.2 Bearing Capacity Methods**

In an attempt to imitate the prediction results collected during the symposium, the calculations made for this study (Table 5.10) were of the load required to cause a settlement of 150 mm. Actual prediction method descriptions and calculations can be found in Gibbens and Briaud, 1995.

### **5.2.3 Best Method**

Table 5.11 shows the ratio of the mean predicted load over the mean measured load for all settlement and bearing capacity prediction methods. On the basis of these numbers, it can be said that the best methods for settlement are the Schmertmann-DMT (1986) and the Peck and Bazarra (1967) although they are somewhat on the unconservative side. The best conservative methods are Briaud (1992) and Burland & Burbidge (1984). The best method for bearing capacity was the simple  $0.2q_c$  method from Briaud (1993a). Most other methods were 25 to 42 percent conservative.

**TABLE 5.11: Best Prediction Method Determination**

<b>SETTLEMENT</b>		<b>Mean Pred. Load / Mean Meas. Load</b>
1	Briaud (1992)	0.66
2	Burland & Burbidge (1984)	0.62
3	De Beer (1965)	0.24
4	Menard & Rousseau (1962)	0.21
5	Meyerhof- CPT (1965)	0.21
6	Meyerhof- SPT (1965)	0.28
7	Peck & Bazarra (1967)	1.19
8	Peck, Hanson & Thornburn (1974)	0.57
9	Schmetrmann- CPT (1970)	0.42
10	Schmertmann- DMT (1986)	1.16
11	Schultze & Sheriff (1973)	1.31
12	Terzaghi & Peck (1967)	0.32
<b>BEARING CAPACITY</b>		
1	Briaud- CPT (1993a)	1.08
2	Briaud- PMT (1992)	0.61
3	Hansen (1970)	0.58
4	Meyerhof (1951 & 1963)	0.76
5	Terzaghi (1943)	0.59
6	Vesic (1973 & 1974)	0.66

## 6. WAK TEST

### 6.1 PROCEDURES

This part of the project is detailed in Ballouz, Maxwell and Briaud (1995).

The Wave Activated stiffness (K) test, or WAK test, is a nondestructive impact test that was developed by Briaud and Lepert (1990). The test is useful in determining the static stiffness of the soil beneath a rigid mass, such as a spread footing. This stiffness in turn can be used to evaluate the load settlement characteristics of the footing and possibly the settlement under working loads. Such a test could serve as quality control after construction but before placing the bridge deck or even the abutment wall; it could also be used to evaluate spread footing foundations after an earthquake.

The theory is based on a simplified, linear system model of the soil-footing assembly. This model consists of a mass, a spring and a dash-pot, and is frequently used to describe the vertical vibration of soil-footing systems (Figure 6.1).

The WAK test is performed by striking a footing near its center with a rubber-tipped sledgehammer that has been instrumented with a force transducer. The impact of the hammer causes the footing and a bulb of soil beneath the footing to vibrate. The velocity of this vibration is recorded by using two geophones which are placed on diagonally opposite corners of the footing. This procedure is illustrated in Figure 6.2. More details about the set-up and data acquisition of the WAK test can be found in Maxwell and Briaud (1991), and Ballouz and Briaud (1994).

The force signal,  $F(t)$ , is the input from the hammer, and the velocity response,  $v(t)$ , is the output from the geophones, both in the time domain (Figure 6.3). The measured mobility in the frequency domain can be obtained by taking the ratio of the Fourier transformation of  $v(t)$  to the Fourier transformation of  $F(t)$ . The modulus of this ratio as a function of frequency,  $|v/F|$  versus  $\omega$ , is called mobility, or sometimes the transfer function of the soil-footing system (Figure 6.4). The mobility can also be obtained mathematically by using the theory of vibrations.

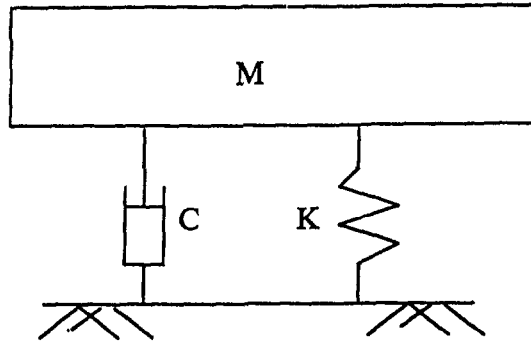


**Figure 6.1: Soil-Footing Model**

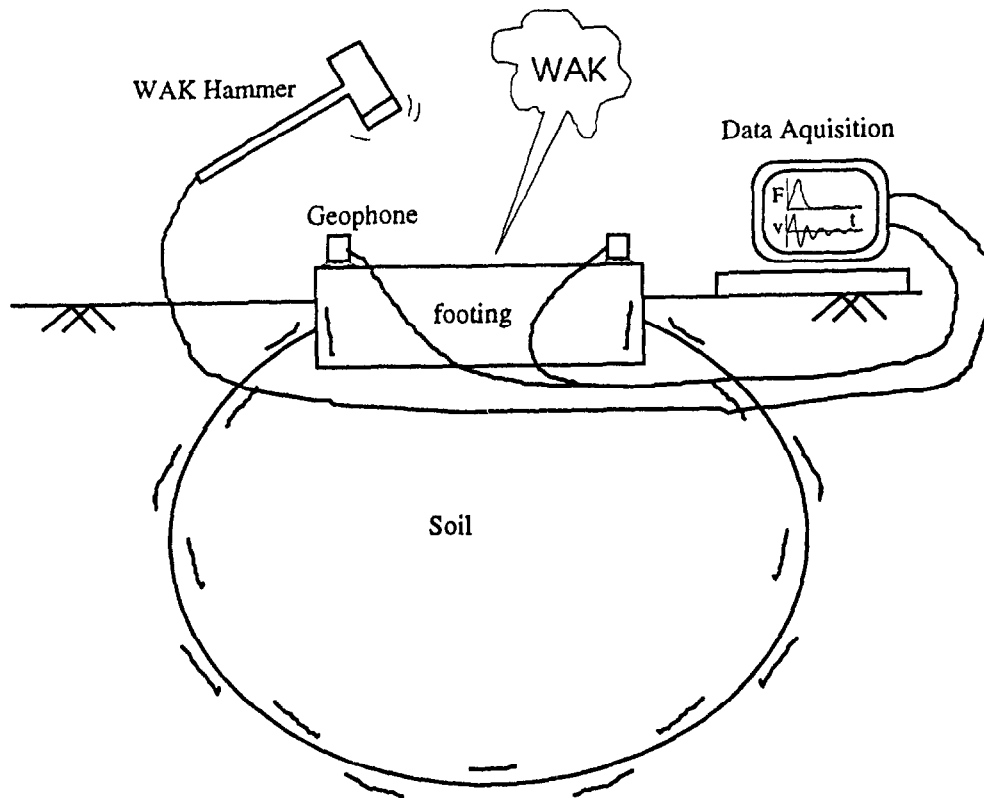


**Figure 6.2: The WAK Test**

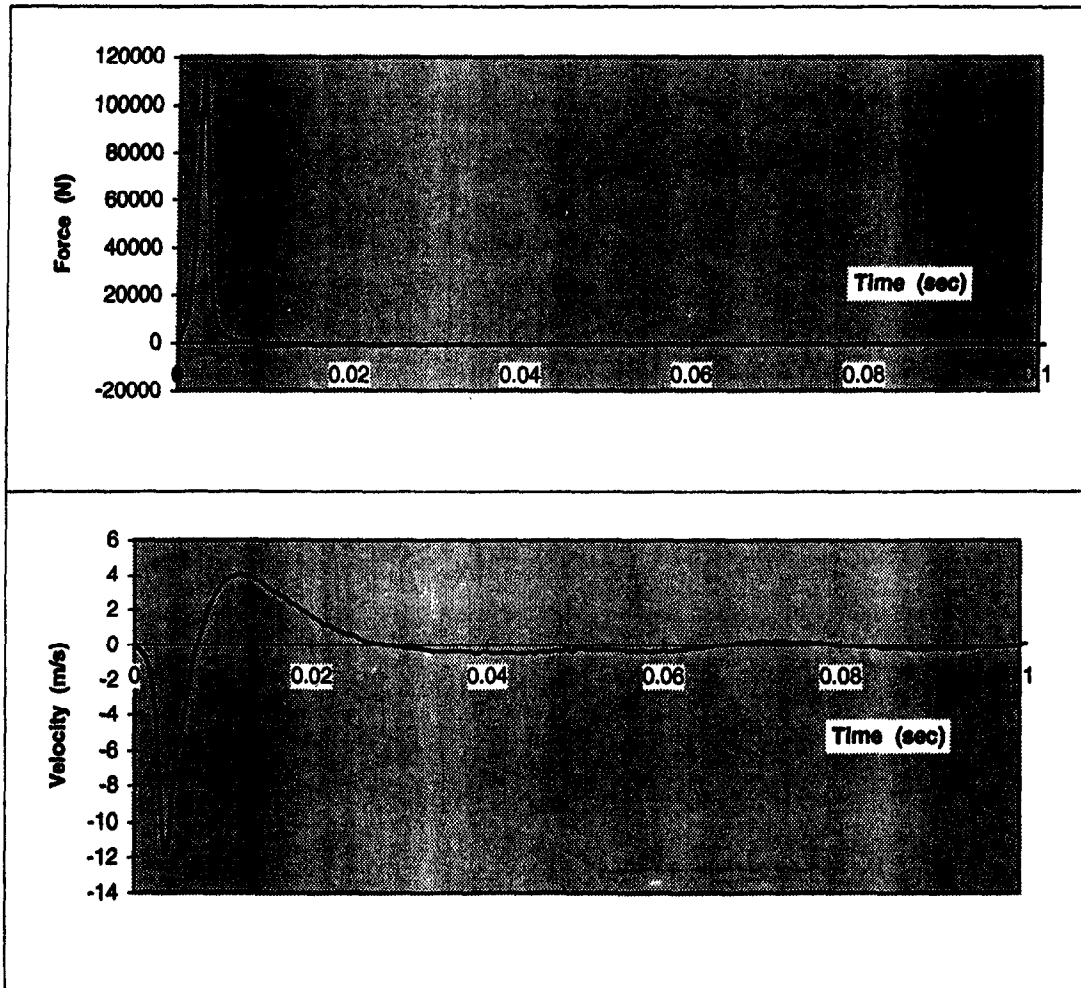


**Figure 6.3:** Sample of Time Domain Data Plot

Because of the mathematical linearity of the system, the mobility is theoretically a unique property of the soil-footing model. By curve-matching the theoretical mobility of the model with the measured mobility in the experiment, three parameters can be determined:

1. the vibrating soil-footing mass,  $M$
2. the static stiffness of the soil beneath the footing,  $K$
3. the damping,  $C$ , which describes the internal damping and energy dissipation in the soil.

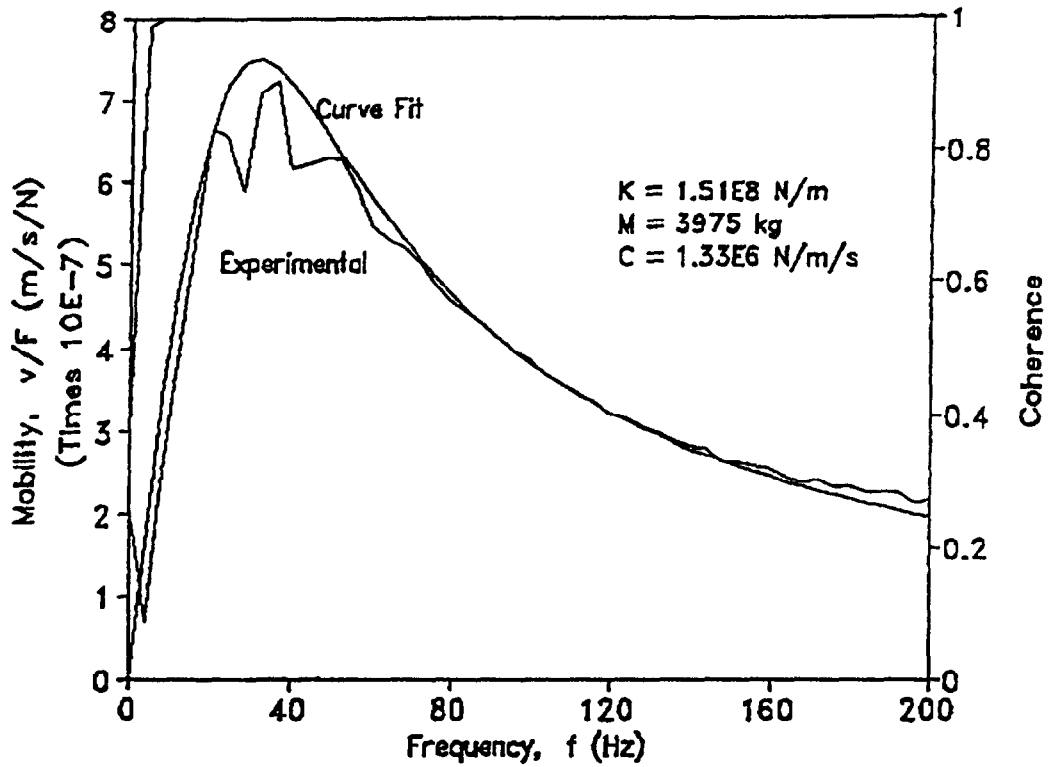


Figure 6.4: Sample of Mobility Curve: Theoretical vs. Measured

More details about the theory behind the WAK test can be found in Briaud and Lepert (1990) and Maxwell and Briaud (1991).

Actually, the static stiffness parameter  $K$  represents the slope of the initial part of the static load-settlement curve as shown in Figure 6.5. When  $K$  is predicted by the WAK test, it can be used to predict the small strain behavior of footings subjected to vertical loads.

## **6.2 DATA ANALYSIS**

Each of the five footings at the sand site was tested four times with the WAK test; two times before and two times after the load tests were conducted. The raw data files are in Ballouz, Maxwell and Briaud (1995).

The WAK test data was sent to James Maxwell in Corpus Christi who was unaware of the load test results. Static stiffness results were obtained by Maxwell using the ANAWAK computer program (Maxwell and Briaud, 1991). The ANAWAK program automatically matches the two mobility curves (experimental and theoretical) in order to identify the soil-footing parameters  $M$ ,  $K$  and  $C$ . A sample of the mobility curve match is given in Figure 6.4. The stiffness  $K$  parameter, represents the static stiffness of the soil-foundation system (Briaud and Lepert (1990), and Ballouz and Briaud, 1994). The results of the WAK tests performed at the NGES/TAMU sand site are summarized in Table 6.1.

## **6.3 COMPARISON WITH LOAD TESTS**

Five static load tests were performed as part of the research study conducted on the five spread footings. 1-0M, 1-5M, 2-5M, 3-01M and 3-03M. The load versus settlement curves for the 5 spread footings are presented on Figures 6.6 through 6.10 (Briaud and Gibbens, 1994). Stiffness predicted by the WAK tests are plotted on the measured load-settlement curves for graphical comparisons (Figures 6.6 through 6.10). The scatter between the first set of tests and the second set of tests (Table 6.1 and Figures 6.6 to 6.10) shows that the repeatability of the WAK test is quite good.

These results show that the WAK test predicted a secant stiffness which corresponds to a

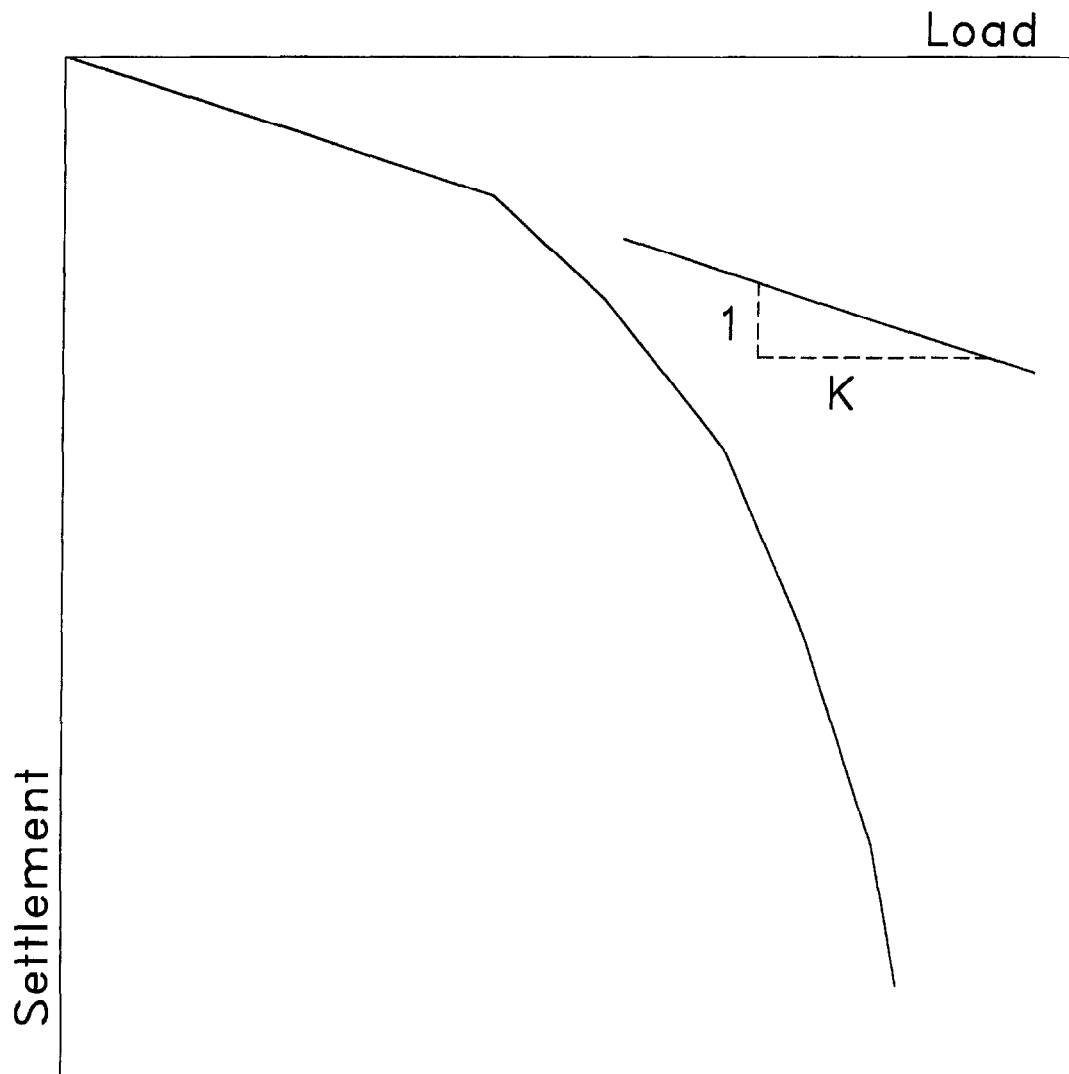


**Figure 6.5:** Typical Load-Settlement Curve

**Table 6.1: Summary of WAK Test Results**

Set Number & Test Data	File Name of WAK Data File	WAK Test Stiffness, K(N/m)	WAK Test Mass, M (N/m)
Set #1 - Before Load Test, Oct. 5, 1993	1-0M?.DAT	1.31 E8	1934
	1-5M?.DAT	1.76 E8	3994
	2-5M?.DAT	2.19 E8	10431
	3-012M?.DAT	3.29 E8	21095
	3-01M?.DAT	3.07 E8	19675
	3-03M?.DAT	3.20 E8	18950
Set #2 - Before Load Test, Oct. 14, 1993	S1-0M?.DAT	1.72 E8	324
	S1-0M?.DAT	1.55 E8	293
	S1-5M?.DAT	1.51 E8	3975
	S2-5M?.DAT	1.73 E8	10236
	S3-01M?.DAT	2.11 E8	13529
	S3-03M?.DAT	3.11 E8	17082
	S3-03HT?.DAT	1.43 E8	7823

settlement averaging about 10 mm. Therefore the WAK test stiffness  $K_{WAK}$  can be used to calculate small settlements by using:

$$s = \frac{\text{Load on Footing}}{K_{WAK}} \quad \text{for } s < 10 \text{ mm}$$

# Load Settlement Curve - 1.0 M Footing

Average 30 Minute Monotonic Curve

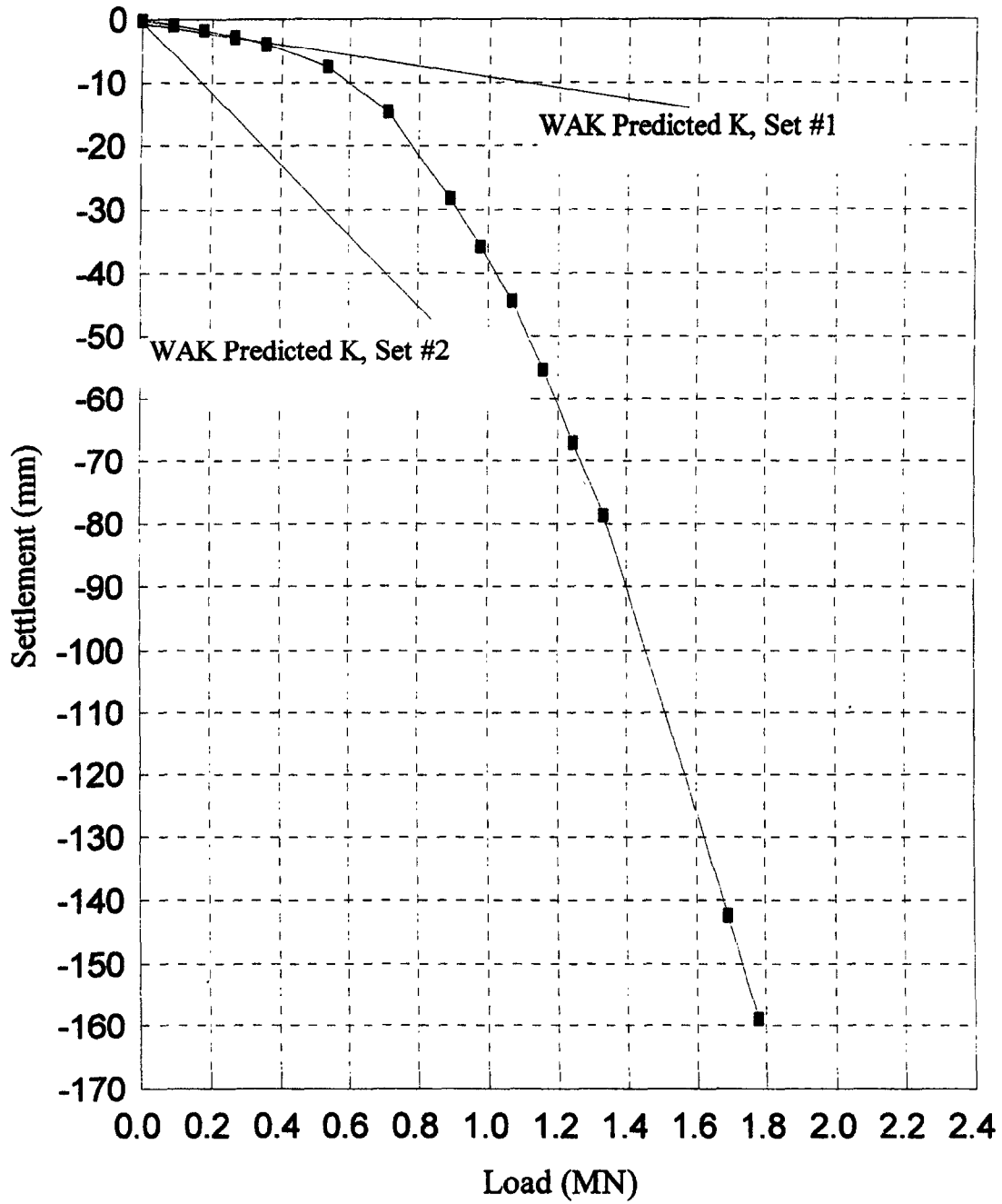


Figure 6.6: Predicted Stiffness on 1.0-m Footing Before Load Test

# Load Settlement Curve - 1.5 M Footing

## Average 30 Minute Monotonic Curve

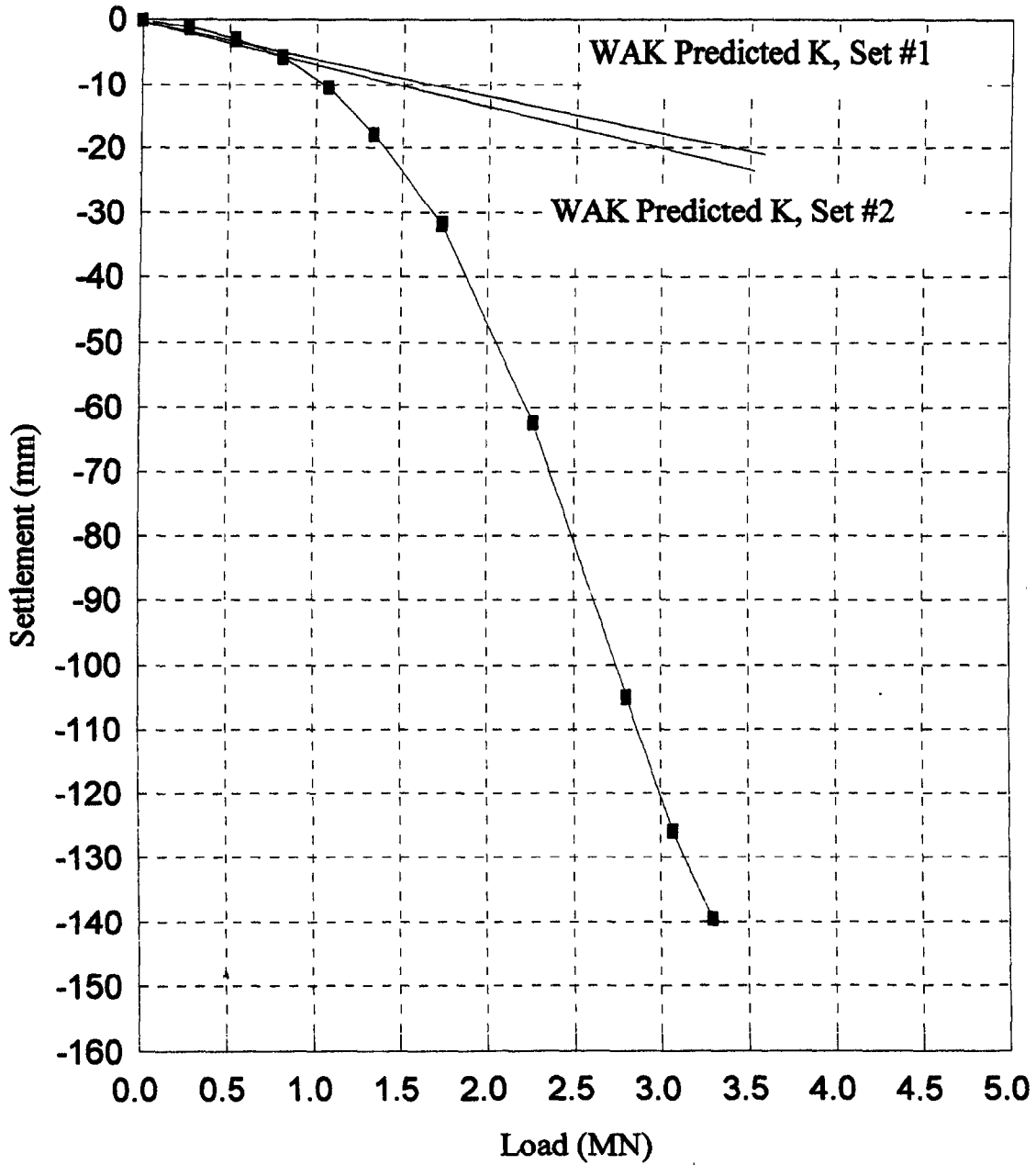


Figure 6.7: Predicted Stiffness on 1.5-m Footing Before Load Test

# Load Settlement Curve - 2.5 M Footing

## Average 30 Minute Monotonic Curve

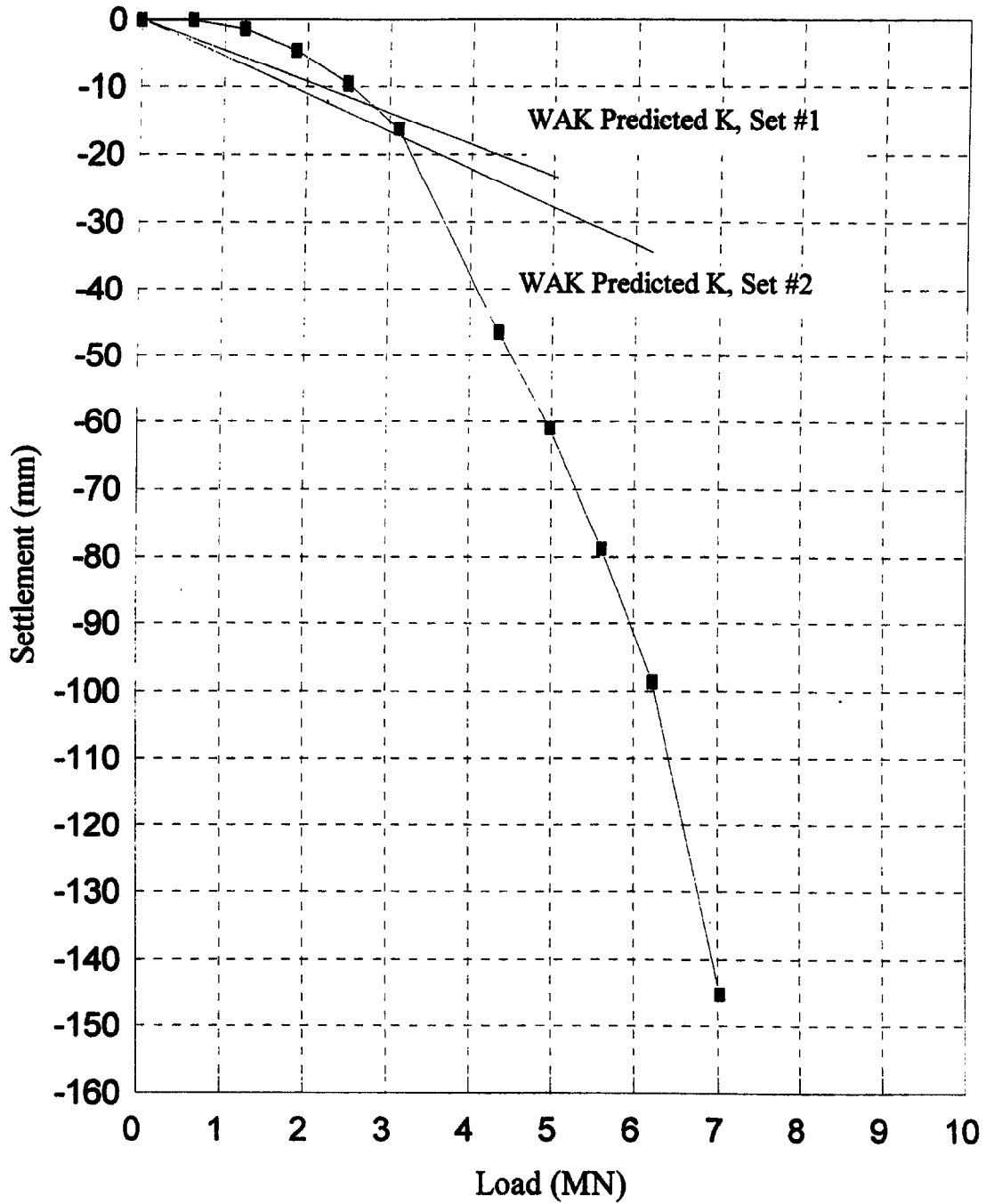


Figure 6.8: Predicted Stiffness on 2.5-m Footing Before Load Test

# Load Settlement Curve - 3.0 M Footing

## Average 30 Minute Monotonic Curve

NORTH

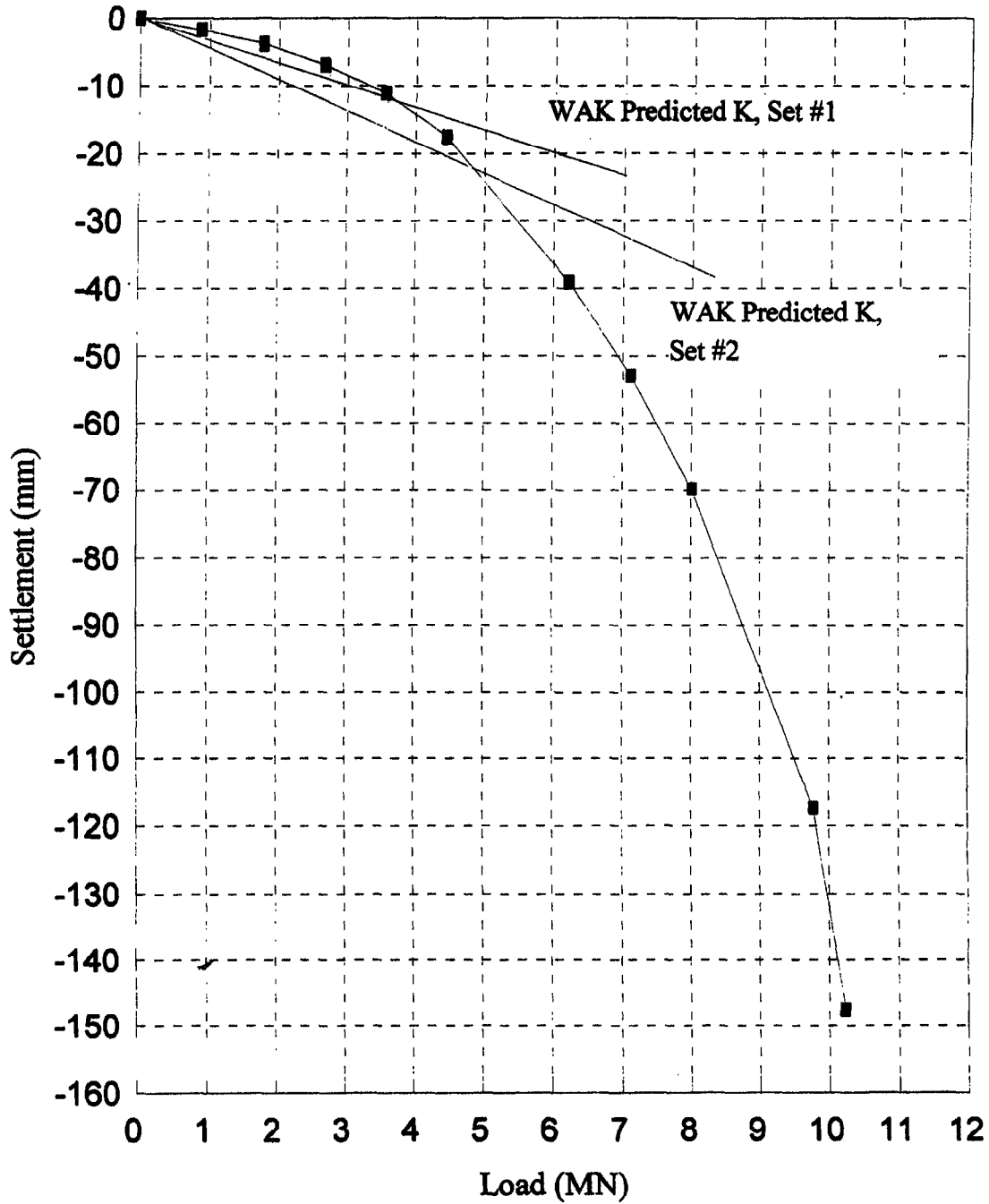


Figure 6.9: Predicted Stiffness on 3.0-m North Footing Before Load Test

# Load Settlement Curve - 3.0 M Footing

## Average 30 Minute Monotonic Curve

SOUTH

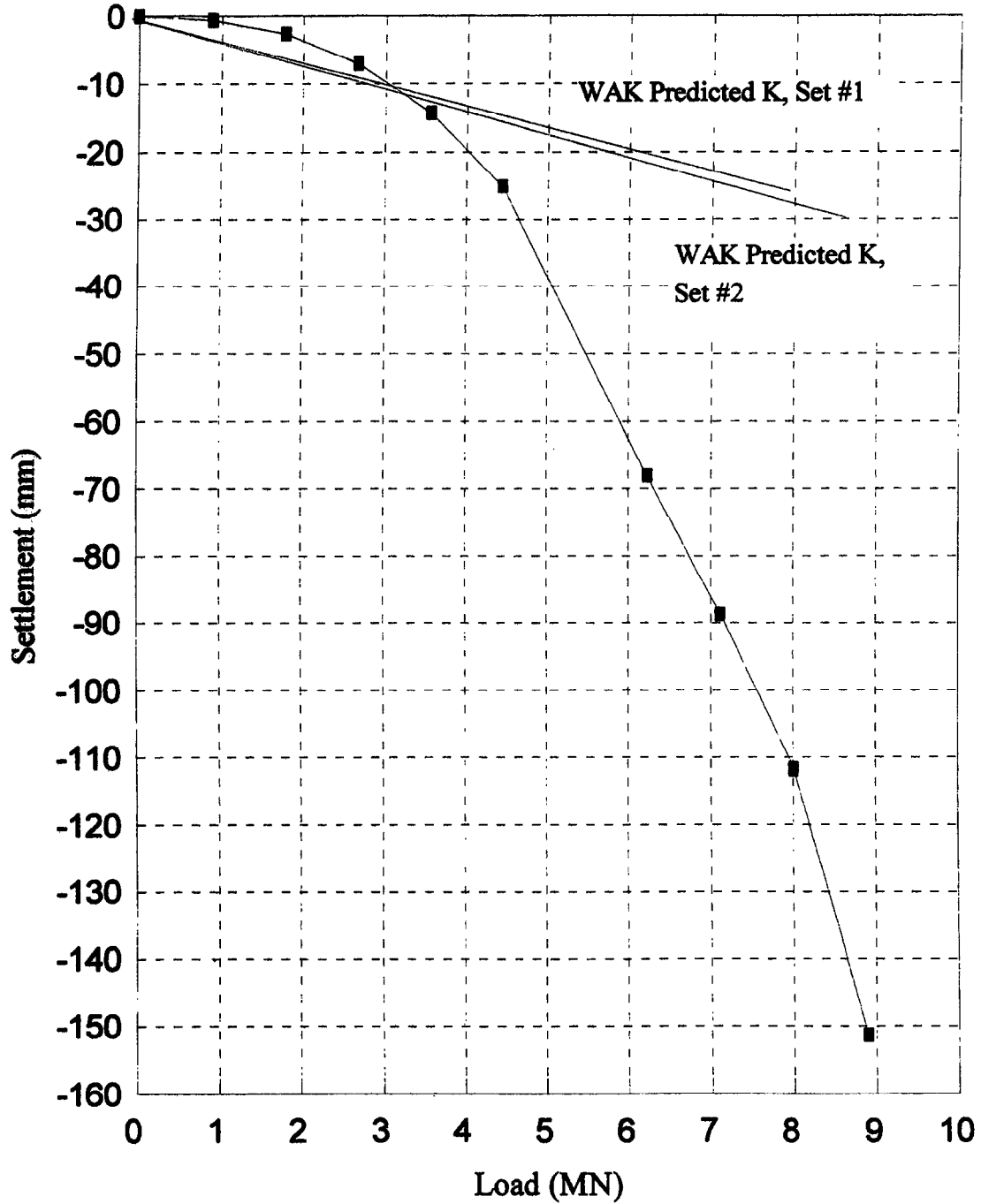


Figure 6.10: Predicted Stiffness on 3.0-m South Footing Before Load Test

## 7. ANALYSIS OF THE DATA

### 7.1 SCALE EFFECT

This part of the project is detailed in Ballouz, Maxwell and Briaud (1995).

The scale effect on bearing capacity has been acknowledged for spread footings on sand. If bearing capacity is defined as the pressure reached for a displacement of 150 mm, the scale effect is obvious (Figure 7.1); indeed the larger the footing, the smaller the pressure that can be applied before reaching a given settlement. In Figure 7.2, this is illustrated by the curve with solid dots, which shows the classical shape (Meyerhof, 1983).

Now let us imagine that one is performing a 1-m diameter and a 3-m diameter triaxial test where the top platen is a spread footing (Figure 7.3), while the confining pressure and the sand used are the same. One would expect to obtain the same stress-strain curve for both tests regardless of the scale. Therefore one would expect in either case the same stress for the same strain. However, if one was to plot the stress-displacement curves, different curves would be obtained and the stress read at the same displacement would depend on the size of the footing and would be lower for the larger footing.

This was the clue which led to comparing the bearing capacity at the same relative  $s/B$ , a measure of the average strain below the footing. If the bearing capacity is defined at a settlement over width ( $s/B$ ) ratio equal to 0.05 the scale effect disappears (Figure 7.2). In fact, if the load settlement curves are plotted as pressure vs settlement/width, the plots almost converge to a unique curve (Figure 7.4). This proves that there is no scale effect if the load tests results are plotted as "stress-strain" curves.

A literature search conducted after this finding led to a discussion by Osterberg (1947) who presented load-settlement curves for plate tests of varying diameters (0.25, 0.5, 0.75, 1 m) on clay. Osterberg shows that if the data is plotted as pressure versus settlement over diameter, the load-settlement curves for the three largest plates collapse into one curve while the load-settlement curve for the 0.25-m plate remains somewhat stiffer. Palmer (1947) also presents the

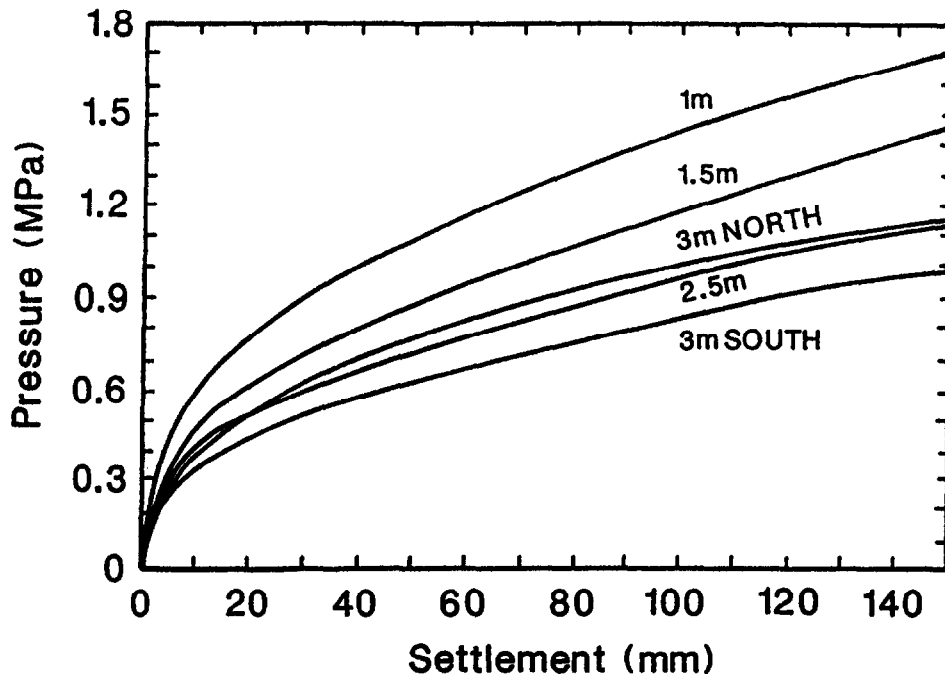


Figure 7.1: Pressure vs. Settlement Curves

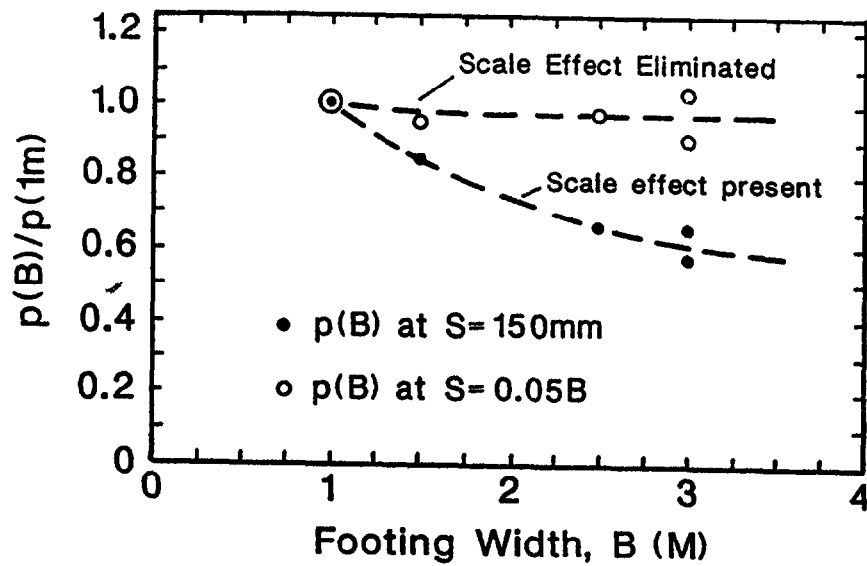
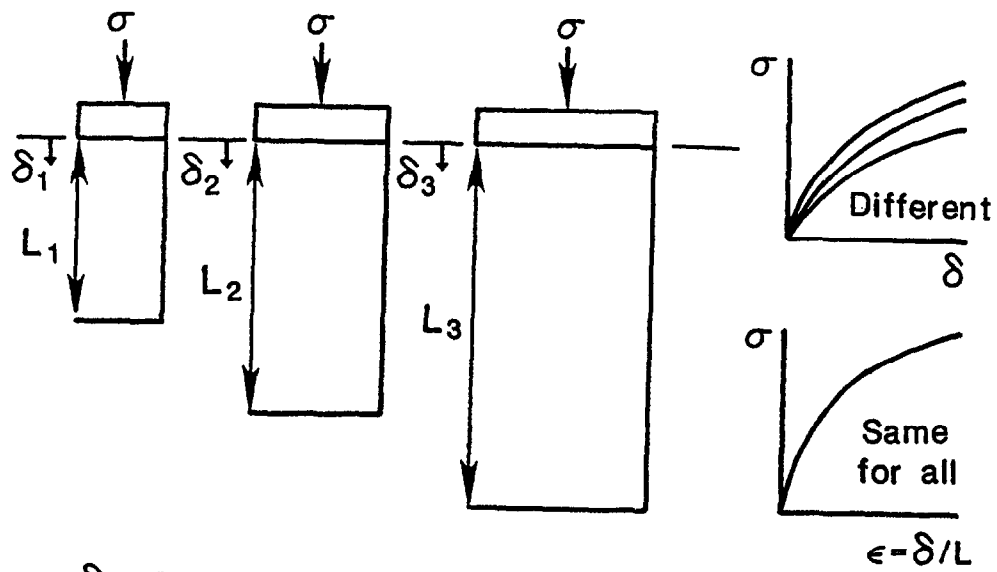


Figure 7.2: Scale Effect at Large Displacement



$\sigma$  vs  $\delta$  = Scale Effect

$\sigma$  vs  $\epsilon$  = No Scale Effect

Figure 7.3: Triaxial Test/Spread Footing Analogy

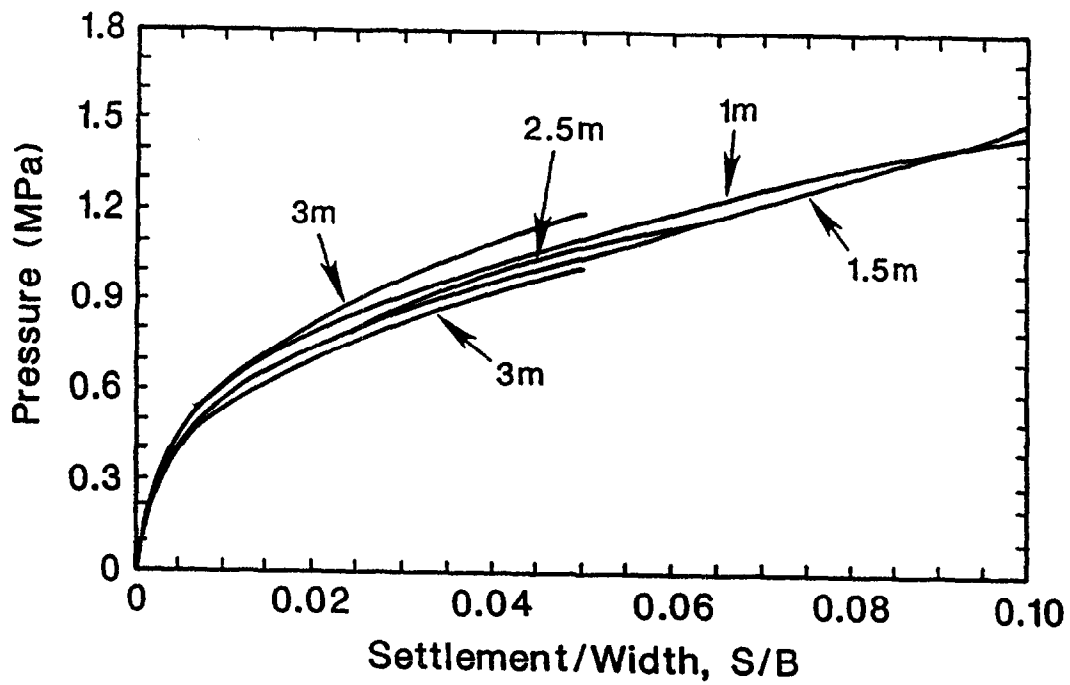


Figure 7.4: Pressure vs. Settlement/Width Curves

load-settlement curves for three plates with varying diameters (0.38, 0.61, 0.76 m) on a pavement. If those curves are plotted as pressure versus settlement over diameter, they collapse into one unique curve. Burmister (1947) goes on to propose a method to obtain the load-settlement curve for a footing from a triaxial stress-strain curve. Skempton (1951) dealing with spread footings on clay also proposed a method to obtain the load settlement curve from triaxial test results and showed, using linear elasticity, that the average vertical strain under the footing is equal to  $s/2B$ .

If the triaxial test analogy of Figure 7.3 points in the direction of the uniqueness of the  $p$  vs  $s/B$  curve, one factor points in the other direction; the depth of influence of a small footing is much shallower than the depth of influence of a large footing. Since the stiffness of a sand is dependent on the mean stress level the large footing should exhibit a somewhat stiffer  $p$  vs  $s/B$  curve than the small footing. For the footings tested, this does not seem to be a major factor.

Note that if bearing capacity is defined as the pressure for an  $s/B$  ratio of 0.1 (1.5 MPa on Figure 7.4) and if a factor of safety of 3 is applied to obtain a safe pressure (0.5 MPa), then the safe pressure corresponds to an  $s/B$  ratio equal to 0.007. For all the footings in this study, this leads to a settlement smaller than 25 mm. Therefore, for those five footings the bearing capacity criterion would control the design, not the settlement criterion. This is contrary to common belief for footings on sand but is due to the definition used for the bearing capacity ( $s/B = 0.1$ ) rather than plunging failure.

If the  $p$  vs  $s/B$  curve is unique for a given deposit then the bearing capacity  $p_u$  is independent of the footing width. For footings at the surface of a sand, the general bearing capacity equation gives:

$$P_u = \frac{1}{2} \gamma B N_\gamma \quad (1)$$

where  $\gamma$  is the unit weight and  $N_\gamma$ , a parameter depending only on the sand strength. If  $1/2\gamma B N_\gamma$  is a constant independent of  $B$ , then  $N_\gamma$ , cannot be a constant and must carry a scale effect in  $1/B$  similar to the classic trend on Figure 7.2. This major shortcoming plus the difficulty in obtaining an accurate value of the needed soil parameter  $\phi$  and the documented poor accuracy

of this method (Amar et al. 1984) lead to the recommendation that the use of this equation should be discontinued. A doubt can be cast on the above recommendation if it is argued that equation 11 gives a pressure which corresponds to plunging failure and not to  $s/B = 0.1$ , and that the load-settlement curves could diverge past  $s/B = 0.1$  (end of the experimental data) to reestablish the validity of the  $P_u$  equation described above.

By comparing the bearing capacity value  $p_u$ , read at an  $s/B$  ratio equal to 0.1 with the SPT blow count  $N$  and CPT point resistance  $q_c$ , taken as averages within the zone of influence of the footings, it appears that the following rules of thumb are reasonable for the medium dense sand at this site:

$$P_u = \frac{N}{12} \text{ with } N \text{ in blows/0.3 m and } p_u \text{ in Mpa} \quad (2)$$

$$P_u = \frac{q_c}{4} \quad (3)$$

One can also give the following approximations for the pressure  $p_a$  which leads to an  $s/B$  ratio equal to 0.01:

$$P_a = \frac{N}{36} \text{ with } N \text{ in blows/0.3-m and } P_a \text{ in Mpa} \quad (4)$$

$$P_a = \frac{q_c}{12} \quad (5)$$

Another acknowledged scale effect phenomenon exists at the settlement level. Terzaghi and Peck (1967) and NAVFAC (1982) give the following relationship:

$$k_B = k_{(0.3 \text{ m})} \left[ \frac{B + 0.3}{2B} \right]^2 \quad (6)$$

where  $k_B$  and  $k_{(0.3 \text{ m})}$  are the moduli of subgrade reaction for footings of diameter  $B$  (in meters) and  $0.3 \text{ m}$  respectively. The parameter  $k_B$  is defined as the pressure on the footing divided by the settlement of the footing under that pressure; the unit is  $\text{kN}/\text{M}^3$ . The values of  $k_B$  can be calculated for a given settlement ( $25 \text{ mm}$ ) for the five footings tested. Figure 7.5 shows that in this case there is a scale effect and that this scale effect is well represented by the function  $[(B + 0.3) / (2B)]^2$ . If however, the values of  $k_B$  are compared at the same  $s/B$  or better if a new parameter  $e$  is defined as

$$e = \frac{p}{s/B} \quad (7)$$

and if the  $e$  values are compared for the same  $s/B$ , then the scale effect disappears. In fact,  $e$  is closely related to the soil modulus,  $E$ . Indeed in elasticity:

$$e = \frac{p}{s/B} = \frac{E}{I(1-\nu^2)} \quad (8)$$

Therefore, for square footings,  $e$  is independent of  $B$  while  $k$  is dependent on  $B$ . The use of  $k$  should be discontinued because it induces an unnecessary difficulty and  $e$ , a true modulus of subgrade reaction should be used in its place because it essentially represents a soil property.

These observations and Figure 7.4 point in the direction of the uniqueness of the  $p$  vs.  $s/B$  curve for a given sand deposit. If this finding is corroborated by future research it will greatly simplify the prediction of spread footing behavior.

If one recalls the heterogeneity of the sand deposit as shown by the CPT soundings (Figure 4.8), it may be surprising to see how well behaved the pressure versus relative settlement curves are for the 5 footings (Figure 4.12). In fact the heterogeneity decreases when going from the CPT (Figure 4.8) to the SPT (Figure 4.7), to the PMT (Figure 4.9), and to the footings (Figure 4.12). This is attributed to the gradual increase in scale and in the volume of soil tested

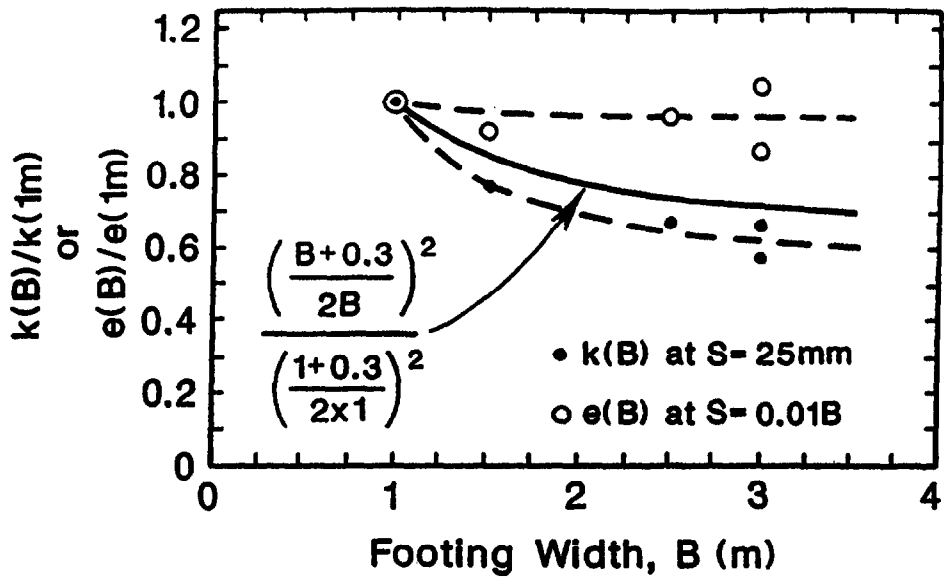


**Figure 7.5: Scale Effect on Modulus of Subgrade Reaction**

from one type of test to the next. This tends to show that a sand deposit which is apparently very heterogeneous at the scale of the CPT point (36 mm) may be quite homogeneous at the scale of a spread footing (3000 mm). The implication is that reasonably accurate predictions should be possible even for apparently heterogeneous deposits, that differential settlement between adjacent footings may not be as large as calculated on the basis of separate borings, and that the test which involves the largest soil volume has an advantage.

## 7.2 CREEP SETTLEMENT

This part of the project is detailed in Gibbens and Briaud (1995).

Section 4.3 describes the load test results including the creep curves. The model proposed by Briaud and Garland (1985) has been used for many years to predict the time dependent behavior of soils. This model is:

$$\frac{s_1}{s_2} = \left(\frac{t_1}{t_2}\right)^n \quad (9)$$

where,  $s_1$  is the settlement after a time  $t_1$ ,  $s_2$  the settlement after a time  $t_2$ , and  $n$  is the viscous exponent which is a property of the soil.

Since the time dependent problem is a creep problem in this case,  $n$  will be called the creep exponent. In order to find  $n$ , the data is plotted as  $\log \frac{s_1}{s_2}$  versus  $\log \frac{t_1}{t_2}$  and a straight line regression is performed through the points. The slope of that line is  $n$ . Typically  $n$  values for working stress levels range from 0.005 to 0.03 for sands and 0.02 to 0.08 for clays.

How well the straight line fits the data points is a measure of how appropriate the model is. As can be seen from Figures 4.13 through 4.16, the straight line fits quite well for both the 30-min long steps as well as the 24-h long steps. Therefore the first observation from those creep tests is that the Briaud-Garland model works well in describing the data up to 24 h. If it is assumed that the model is also applicable from 24 h to 50 years, the settlement at 50 years can be compared to the settlement at 24 h as follows:

$$\frac{s_{50 \text{ years}}}{s_{24 \text{ hours}}} = \left( \frac{50 \text{ years}}{24 \text{ hours}} \right)^n$$

For a value of  $n$  equal to 0.03 the ratio of  $s_{50 \text{ years}}$  to  $s_{24 \text{ hours}}$  would be 1.34 and the settlement at 50 years would be 34% larger than the settlement at 24 h. If the reference was the settlement at 1-min instead of 24 h then the above ratio would be 1.67 meaning that the settlement at 50 years would be 67% larger than the settlement at 1 min. These examples give an idea of the magnitude of the creep settlement that one can expect for footings on sands within the working stress range.

Figure 7.6 shows the variation of  $n$  with the stress level under the footing. The  $n$  values are obtained as described above and the stress level is characterized by the ratio of the load  $Q$  over the ultimate load  $Q_u$  defined as the load reached for a settlement equal to 0.1 times the footing width. Figure 7.6 corresponds to all the measurements made on one footing during that load test. As can be seen, the  $n$  values increase with  $Q/Q_u$  during the first monotonic loading.

# Creep Exponent Curve 3.0 M Footing

NORTH

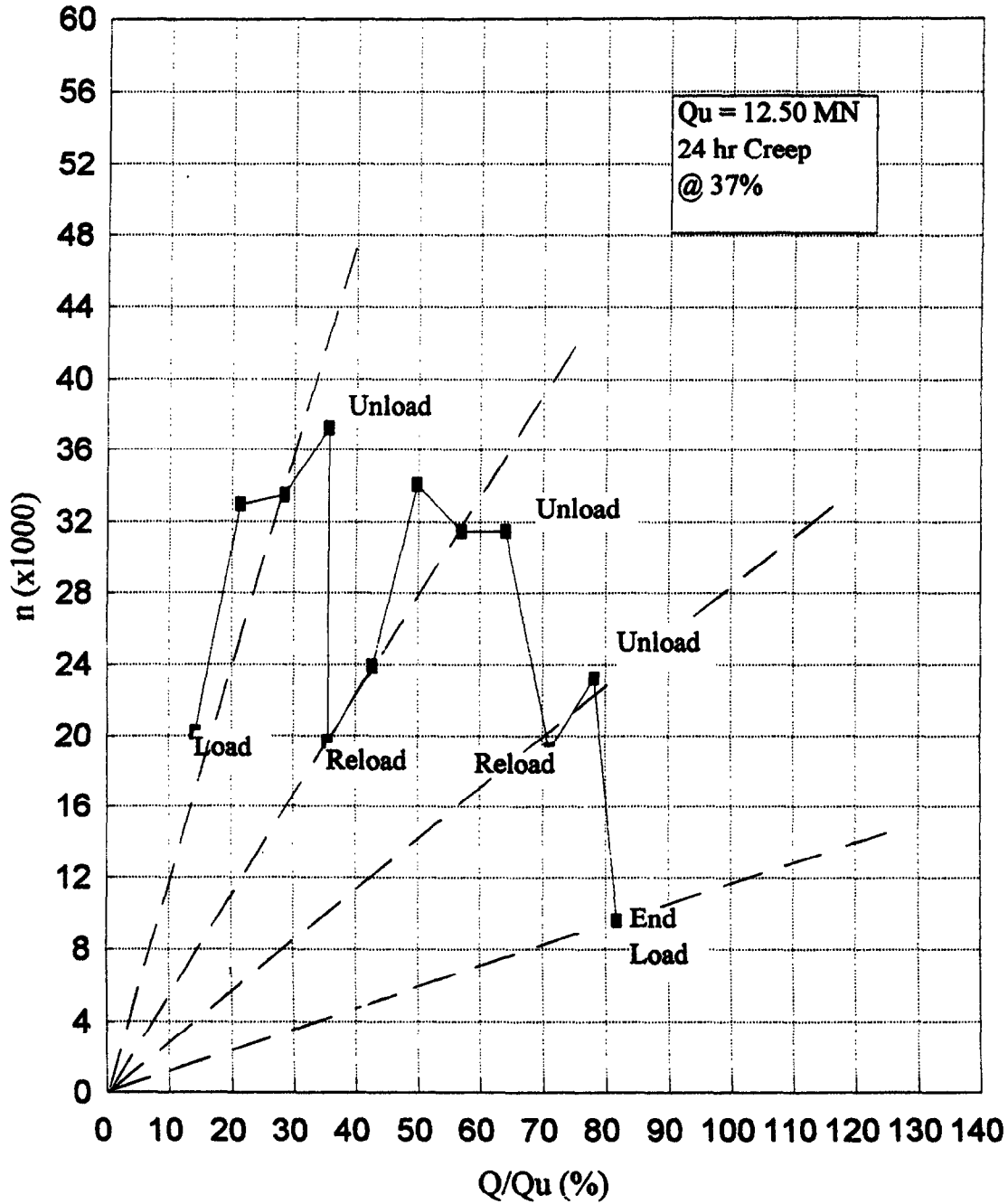


Figure 7.6: Creep Exponent Curve for 3.0-m North Footing -  $Q_u = 12.50\text{-MN}$

Then there is a sudden drop in the  $n$  value after the first unload reload cycle followed by an increase of  $n$  with  $Q/Q_u$ . This second increase however is along a different line from the first monotonic loading. This phenomenon is observed again for the third and fourth loadings. Therefore the second observation from the creep measurements is that cyclic loading influences significantly the rate and magnitude of the creep settlement. Each new cycle decreases the amount of creep settlement. This observation is based mostly on 30-min load steps and one wonders if it would hold true if the load were held for much longer periods of time.

It was also observed that if a load  $Q_1$  is held for 24 h and then the load is decreased to  $Q_2$  where it is held for a new 24 h, the creep under  $Q_2$  is very small compared to the creep under  $Q_1$ . This supports the idea that preconsolidation decreases creep settlement. It would be interesting to see if the creep settlement continues to be small when the load  $Q_2$  has been held for more than 24 h.

Overall the  $n$  values obtained from the spread footing tests ranged from 0.008 to 0.054 and averaged 0.028. Creep pressuremeter tests were performed at the site close to the footings. During those preboring tests the pressure was held for 10 min at a point on the pressuremeter curve close to the end of the straight line. Exponents  $n$  were obtained in a fashion identical to the one used for the spread footing tests. The pressuremeter exponents ranged from 0.007 to 0.025 and averaged 0.014. Therefore until further theoretical or experimental understanding of the reason for the difference between the spread footing exponents and the pressuremeter exponents it is recommended to use:

$$n_{\text{footing}} = 2n_{\text{pmt}}$$

### **7.3 STRAIN VERSUS DEPTH**

This part of the project is detailed in Gibbens and Briaud (1995).

Section 4.3 gives the results of the telltale measurements. Figure 4.19 represents the normalized settlement  $s/s_{\text{top}}$  plotted against normalized depth  $Z/B$  for the 3.0 m South footing.

The parameter  $s$  is the downward movement of a point at a depth  $Z$  in the soil. The parameter  $s_{\text{top}}$  is the settlement of the footing and  $B$  is the footing width. An  $s/s_{\text{top}}$  vs.  $Z/B$  curve is plotted for several  $s_{\text{top}}$  values calculated using varying percentages of  $B$ . The normalized plot makes it possible to show the results for all loads and all footings on the same plot and therefore to draw general conclusions.

The first observation from those plots is that the settlement of the soil at a depth of  $2B$  below the footings ranged from 0% to 10% of the settlement at the surface and averaged 3.2%. Therefore about 97% of the settlement takes place within a depth of  $2B$  below the footing and it is appropriate to use a  $2B$  depth of influence for calculating the settlement of square footings on sand. Furthermore the settlement at a depth of  $1B$  below the footing ranged from 11% to 30% of the settlement at the surface and averaged 22%. Therefore 78% of the settlement occurs within a depth of  $1B$  below the footing and therefore it is very important to obtain the compressibility properties of the soil within that zone. Similarly the settlement at a depth of  $0.5B$  ranged from 47% to 71% and averaged 64%.

The second observation relates to the use of the parameter  $s/B$  instead of  $s$  in the presentation of load test results. Since 97% of the settlement occurs within  $2B$  below the footing, the average strain in the soil within that zone is approximately  $s/2B$ . This confirms the theoretical result of Skempton (1951). It also shows that  $s/B$  is related to the average strain under the footing. Since the pressure  $p$  under the footing is related to the average vertical normal stress under the footing, the plot of  $p$  vs.  $s/B$  is directly related to the average stress versus average strain curve for the soil mass under the footing. Therefore this is a superior way of presenting the results of a spread footing load test compared to presenting a load-settlement curve.

The third observation deals with the evolution of the settlement versus depth profile as the load increases during the load test or as the footing size increases from one load test to the next. One might think for example that as the load on the footing increases the depth of influence increases or decreases. The data show that the depth of influence remains remarkably constant. Indeed no particular trend can be observed in the evolution of  $s/s_{\text{top}}$  at  $2B$  as the load increases or as the width of the footing increases.

These numbers can be used to prepare a strain versus depth profile. The strain in a layer is given by

$$\varepsilon(\text{at } z + \Delta z/2) = \frac{s(\text{at } z) - s(\text{at } z + \Delta z)}{\Delta z}$$

where  $z$  is the depth below the footing bottom to the top of the layer,  $\Delta Z$  is the thickness of the layer,  $s(\text{at } Z)$  is the settlement at the depth  $Z$ .

If,

$$s(\text{at } z) = \alpha_z s_{\text{stop}}$$

and

$$\Delta z = \beta_z B$$

where  $s_{\text{stop}}$  is the settlement of the footing then,

$$\varepsilon(\text{at } z + \Delta z/2) = \frac{(\alpha_z - \alpha_{(z + \Delta z)}) s_{\text{stop}}}{\beta_z B}$$

or,

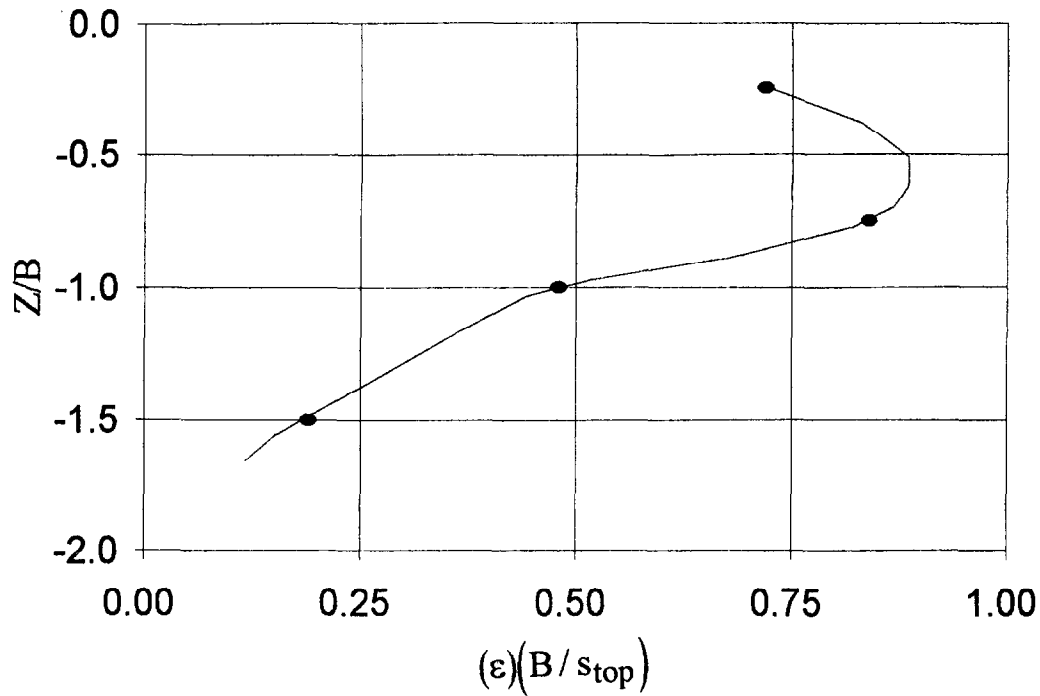
$$\varepsilon(\text{at } z + \Delta z/2) = \frac{(\alpha_z - \alpha_{(z + \Delta z)}) \frac{s_{\text{stop}}}{B}}{\beta_z}$$

Figure 7.7 is a plot of  $\varepsilon(\text{at } z + \Delta z/2) \left( \frac{B}{s_{\text{stop}}} \right)$  versus  $\frac{z}{B}$ . For example for  $Z = 0$  and  $\Delta Z = 0.5B$ ,

the values of  $\alpha_z$  and  $\alpha_{(z + \Delta z)}$  are obtained from the results mentioned in the previous

paragraph. In this case  $\alpha_{(z=0)} = 1$  and  $\alpha_{(z=0.5B)} = 0.64$ , therefore  $\varepsilon(\text{at } 0.25B) \frac{B}{s_{\text{stop}}} = 0.72$ .

Figure 7.7 shows a natural decrease in strain with depth except close to the bottom of the footing



**Figure 7.7:** Lateral Strain Versus Vertical Strain

paragraph. In this case  $\alpha_{(z=0)} = 1$  and  $\alpha_{(z=0.5B)} = 0.64$ , therefore  $\epsilon_{(at\ 0.25B)} \frac{B}{s_{top}} = 0.72$ .

Figure 7.7 shows a natural decrease in strain with depth except close to the bottom of the footing where the strain decreases due to the lateral confinement brought about by the roughness of the footing.

#### 7.4 SOIL MASS DEFORMATION

This part of the project is detailed in Gibbens and Briaud (1995).

Section 4.3 describes the results of the inclinometer measurements. Figures 4.17 and 4.18 represent the lateral deflections of the casing as a function of depth.

The first observation is the general shape of those curves which indicate a lateral bulging of the soil reaching a maximum at a depth which ranged from  $0.4B$  to  $1.25B$  and averaged  $0.73B$ . Note that this depth of maximum lateral strain corresponds quite well to the depth of maximum

the deformation pattern in the soil mass under the footing corresponds quite well to a cylindrical cavity expansion. This observation is not consistent with the assumption of a single shear slip surface analysis which is the basis of the classical bearing capacity equation.

The second observation deals with the magnitude of the horizontal displacement at the edge of the footing compared to the magnitude of the vertical displacement of the footing. Figure 7.8 shows the relationship between the ratio  $\delta_{h(\max)}/\delta_v$  as a function of  $H/B$ . The parameter  $\delta_v$  is the settlement of the footing under a given load  $Q$ ,  $\delta_{h(\max)}$  is the maximum horizontal movement measured by the inclinometer under the same load  $Q$ ,  $H$  is the distance between the inclinometer casing and the footing edge and  $B$  is the footing width. Figure 7.8 indicates that at the footing edge the maximum horizontal movement is of the order of 15% of the footing settlement and that the horizontal zone of influence extends to about  $1.8B$  on each side of the footing. This means that settlement beams should be at least  $5B$  long to provide a good measurement of the absolute footing settlement.

The third observation deals with the volume change in the soil. Indeed the inclinometer results make it possible to estimate the volume change of the soil mass below the footing. Figure

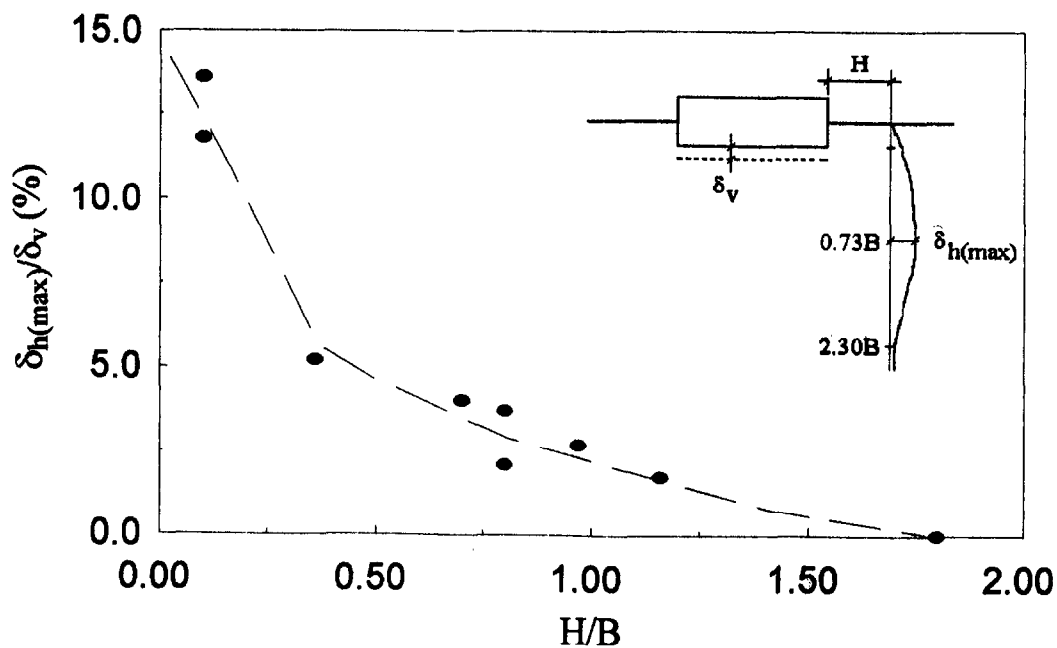


**Figure 7.8:** Comparison of the Horizontal and Vertical Soil Movement

7.9 is a schematic of the soil mass influenced by the footing. The change in volume imposed by the penetration of the footing is (ABCD on Figure 7.9):

$$\Delta V_{\text{footing}} = \delta_v B^2$$

The change in volume of the soil mass corresponding to the  $B^2$  area and to the depth of influence  $2.33B$  can be estimated as follows. The initial volume is (CEFD on Figure 7.9):

$$(B^2)(2.33B) = 2.33B^3$$

The deformed volume is approximated by:

$$\left( \frac{\delta h(\text{max})}{2}(2) + B \right)^2 (2.33B)$$

This assumes that the deformed volume CIEFND on Figure 7.9 can be approximated by GOPH where JK is equal to  $\frac{1}{2}IK$  with  $IK = \delta h(\text{max})$ . Note also that the profile DNF is an approximation of the shape of the inclinometer profiles such as the one of Figure 4.17. From Figure 7.8, the value of  $\delta h(\text{max})$  at the edge of the footing is taken as  $0.15\delta_v$ . Therefore the volume change of the soil mass CEFD (Figure 7.9) is:

$$\Delta V_{\text{soil}} = \left( \frac{0.15\delta_v}{2}(2) + B \right)^2 (2.33B) - 2.33B^3$$

or,

$$\Delta V_{\text{soil}} = 2.33B \left( (0.15\delta_v + B)^2 - B^2 \right)$$

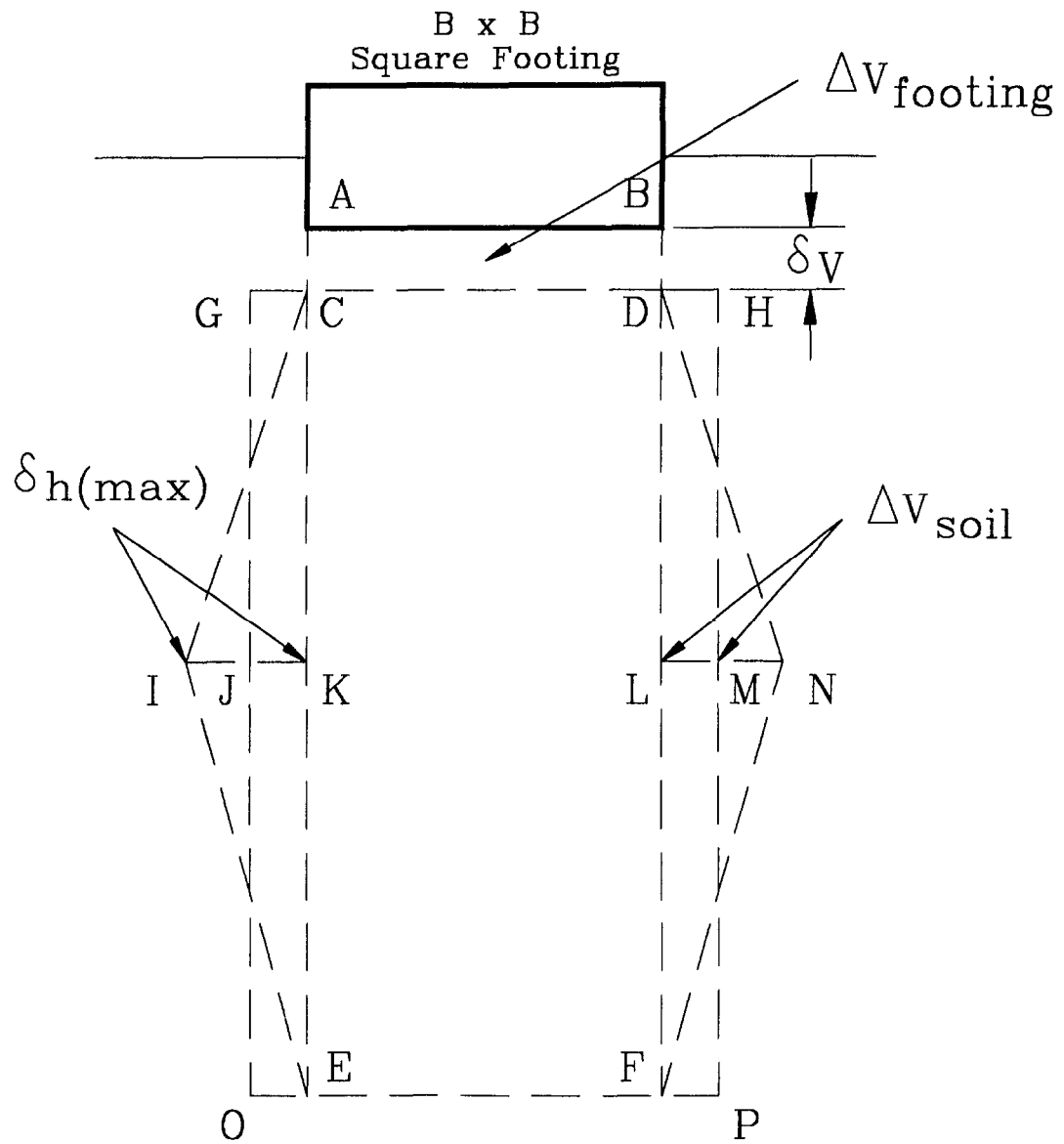


**Figure 7.9:** Schematic of the Volume Change Under the Footing

Since  $0.15\delta_v$  is very small compared to  $B$ ,  $(0.15\delta_v + B)^2$  is approximated by  $[B^2 + 2(0.15\delta_v B)]$  then,

$$\Delta V_{\text{soil}} = 2.33B(0.3\delta_v B)$$

and the ratio  $\frac{\Delta V_{\text{soil}}}{\Delta V_{\text{footing}}}$  is:

$$\frac{\Delta V_{\text{soil}}}{\Delta V_{\text{footing}}} = \frac{(2.33)0.3\delta_v B^2}{\delta_v B^2} = 0.7$$

Therefore the change in soil volume is smaller than the change of volume imposed by the footing and the soil compresses during the load test. While a number of approximations were used to calculate the ratio  $\Delta V_{\text{soil}}/\Delta V_{\text{footing}}$  the result tends to show that there is no dilation and instead compression of the sand during loading.

## **8. NEW LOAD SETTLEMENT CURVE METHOD**

### **8.1 THE IDEA**

This part of the project is detailed in Jeanjean and Briaud (1994).

The idea is to develop a method to predict the complete load settlement curve for spread footings. For piles subjected to axial monotonic loading this problem was solved by Seed and Reese (1957) and led to the t-z curve concept for axially loaded piles. The idea is to do for spread footings what was done for piles a long time ago.

There are several approaches to solving a geotechnical problem. One is the fundamental approach where the soil is modeled by discrete elements and the continuum behavior is theoretically assembled: this is the case of the finite element method. One is the empirical approach where a correlation is used between a test result and the parameter to be predicted: this is the case of Peck et al.'s method (1974) for predicting the pressure corresponding to 25 mm of settlement for footings on sand on the basis of SPT blow counts. Another method which fits possibly between those two approaches is the approach by analogy where the soil test which is performed closely resembles the loading imposed on the soil by the foundation and where the remaining difference is bridged by using theoretically and experimentally based corrections: this is the case of the cone penetrometer method used to predict the axial capacity of a pile or the pressuremeter method used to predict the behavior of a horizontally loaded pile.

In the long run the fundamental approach will be the method of choice. At present however, the complexity of the modeling process and the inability to assess the many required parameters reliably and economically prevent this approach from being a routine design approach. The method by analogy was chosen to develop the new load settlement curve method.

## 8.2 DEVELOPMENT OF THE METHOD

The inclinometer measurements shown in section 7.4 indicate that the penetration of a footing into a sand deposit can be considered as a cavity expansion phenomenon. Therefore a cavity expansion test would make sense for the approach by analogy. Since the complete load settlement curve is desired, this cavity expansion test should give a complete pressure-deformation curve. This led to the choice of the pressuremeter test (PMT) for the method by analogy. The concept is then to perform pressuremeter tests within the zone of influence of the spread footing, generate an average PMT curve by using an influence factor distribution for a weighted average of the individual curves, and transform the average PMT curve into a spread footing curve by using a correction factor obtained from theoretical and experimental considerations.

It is recommended that pressuremeter tests be performed at 0.5B, 1B and 2B below the footing level where B is the footing width. Each test leads to a pressure  $p$  versus relative increase in probe radius  $\Delta R_p/R_p$  as shown on Figure 8.1 where  $R_p$  is the radius of the deflated probe and  $\Delta R_p$  the increase in probe radius. Each curve is then adjusted for the size of the borehole (Figure 8.1) by extending the straight line part of the PMT curve to  $P = 0$ , shifting the vertical axis to that new origin and calculating the relative increase in cavity radius ( $\Delta R_c/R_c$ ) as:

$$\frac{\Delta R_c}{R_c} = \frac{\frac{\Delta R_p}{R_p} - \left[ \frac{\Delta R_p}{R_p} \right]_c}{1 + \left[ \frac{\Delta R_p}{R_p} \right]_c} \quad (1)$$

where  $R_c$  is the initial radius of the borehole (cavity),  $\Delta R_c$  the increase in cavity radius, and  $(\Delta R_p/R_p)_c$  the value of the relative increase in probe radius corresponding to the initial radius of the cavity.

The corrected curves ( $p$  vs  $\Delta R_c/R_c$ ) obtained at the testing depths below the footing are

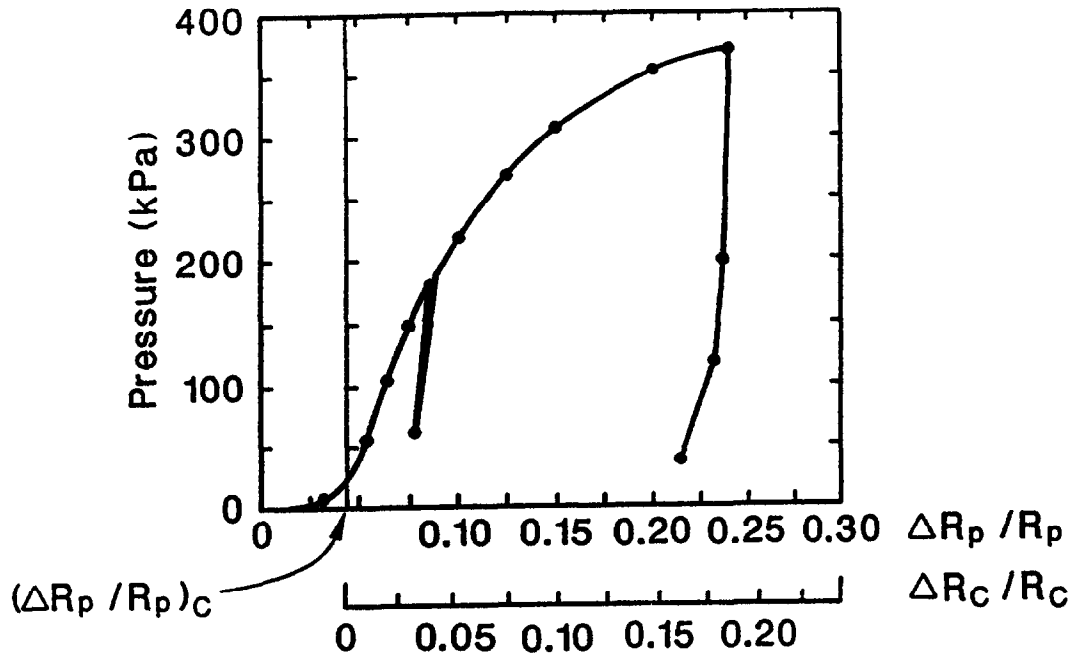


Figure 8.1: Pressuremeter Curve (PMT 1, z = 0.6-m)

then averaged into a single curve called the average PMT curve on the basis of a stress influence factor  $I$  similar to the one proposed by Schmertmann (1970). This factor is defined as:

$$I = \frac{\Delta\sigma_1 - \Delta\sigma_3}{\Delta p} \quad (2)$$

where  $\Delta\sigma_1$  and  $\Delta\sigma_3$  are the increase in major and minor principal stress respectively at a depth  $z$  below the footing when the footing is loaded with a pressure  $\Delta p$ . A three dimensional non-linear finite element simulation was performed. The results are shown on Figure 8.2. These profiles appear to be relatively independent of the pressure level on the footing and of the sand density. Therefore, a unique simplified diagram is used (Figure 8.3).

For any value of  $\Delta R_c/R_c$ , the pressures  $p_i$  for each of the pressuremeter curves within the depth of influence are averaged as follows to give the pressure  $p$  on the average PMT curve

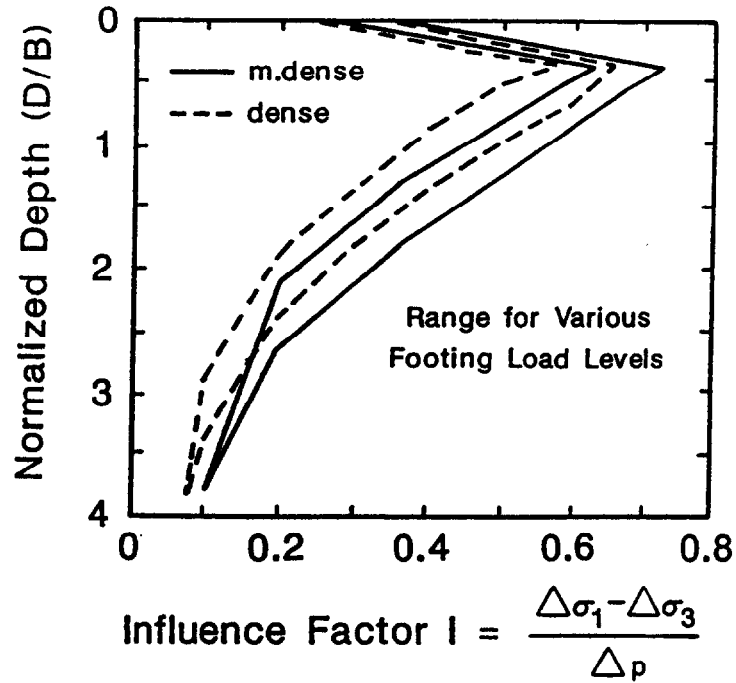


**Figure 8.2:** Influence Factor Distribution with Depth

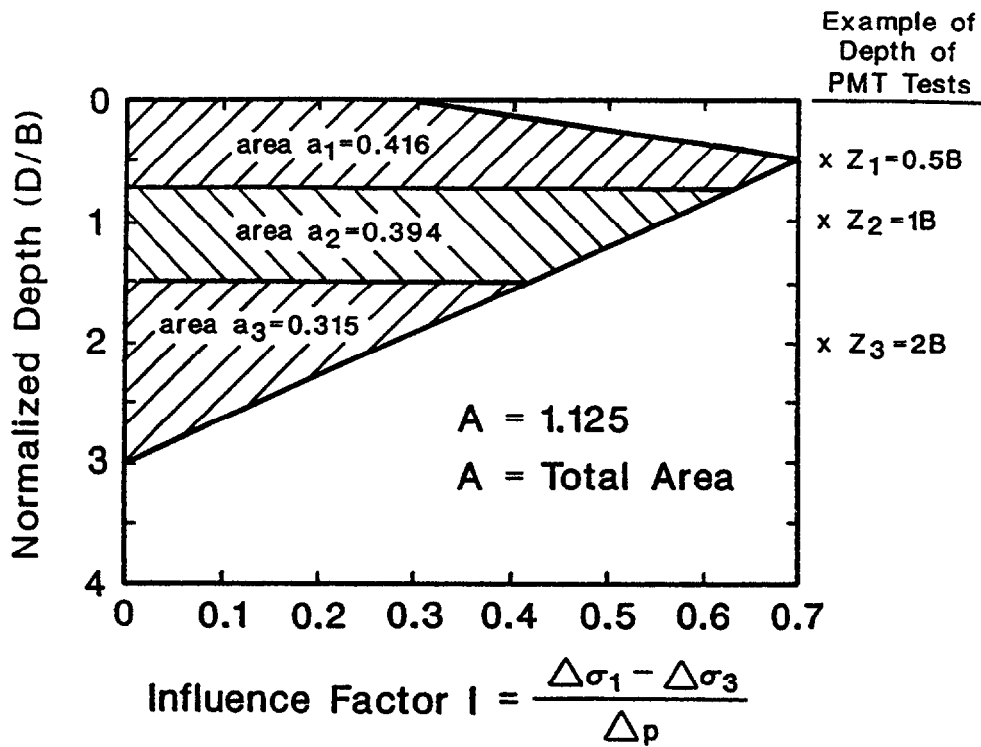


**Figure 8.3:** Recommended Influence Factor Distribution, and Example of the Determination of the  $a_i$  Factors

corresponding to this  $\Delta R_c/R_c$ :

$$p = \frac{1}{A} \sum p_i a_i \quad (3)$$

where  $a_i$  is the tributary area under the influence diagram for the PMT test at depth  $z_i$ ; and  $A$  is the total area under the diagram ( $A = 1.125$ ). In order to obtain the  $a_i$  values, the depths at which the PMT tests were performed are identified, then boundaries are established at mid-height between two consecutive PMT test depths, and  $a_i$  values are calculated as the areas between the boundaries (Figure 8.3). This process leads to the average PMT curve for that footing (Figures 8.4 and 8.5).

In order to transform the average PMT curve into the footing curve, the following was considered. First, the PMT limit pressure which is found at  $\Delta R_c/R_c = 42\%$  is generally associated with the bearing capacity of the footing  $p_u$  defined here as the footing pressure reached at a settlement over width ratio ( $s/B$ ) equal to 10%. In order for those two points to match, the  $\Delta R_c/R_c$  axis is transformed into a  $(\Delta R_c/4.2R_c)$  axis. Second, a three dimensional nonlinear finite element simulation of the footing and of PMT tests at 0.5B, 1B and 2B was performed for two sand densities ( $D_r = 55\%$  and 95%). For the pressuremeter tests, both the preboring and selfboring tests were simulated. The mesh was first validated against the elastic theory, then the geostatic stresses were turned on in the whole mass. For the selfboring test the geostatic stresses which would have existed against the borehole wall had the borehole not been drilled were applied against the borehole wall (this step was bypassed for the simulation of the preboring test). Then the pressure exerted by the pressuremeter probe was applied in increments on the borehole wall. This allowed to generate the PMT curves as  $p$  versus  $(\Delta R_c/4.2R_c)$  mentioned above at the depths 0.5B, 1B, and 2B below the 3- by 3-m footing. The weighted average of these three curves was determined using the influence factor process described earlier. The weighted average PMT curves for both pressuremeter types are shown on Figures 8.4 and 8.5 together with the 3- by 3-m

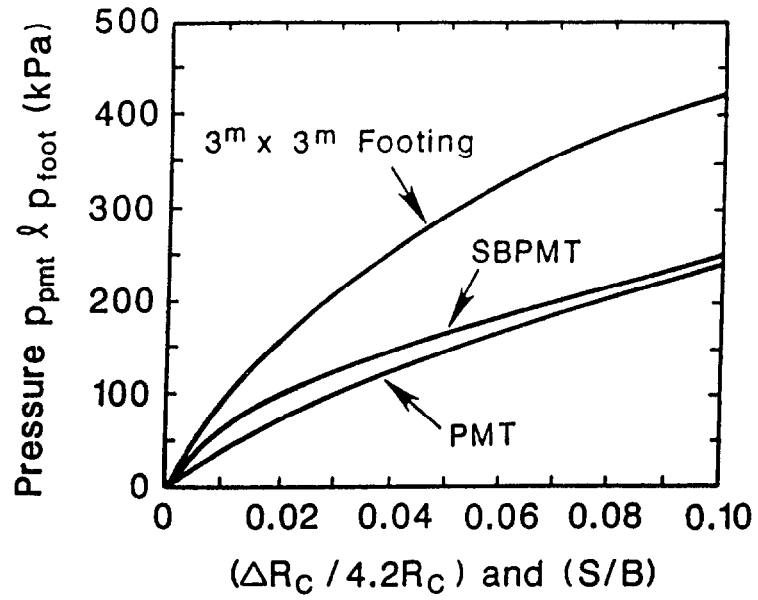


Figure 8.4: FEM Results for the Medium Dense Sand

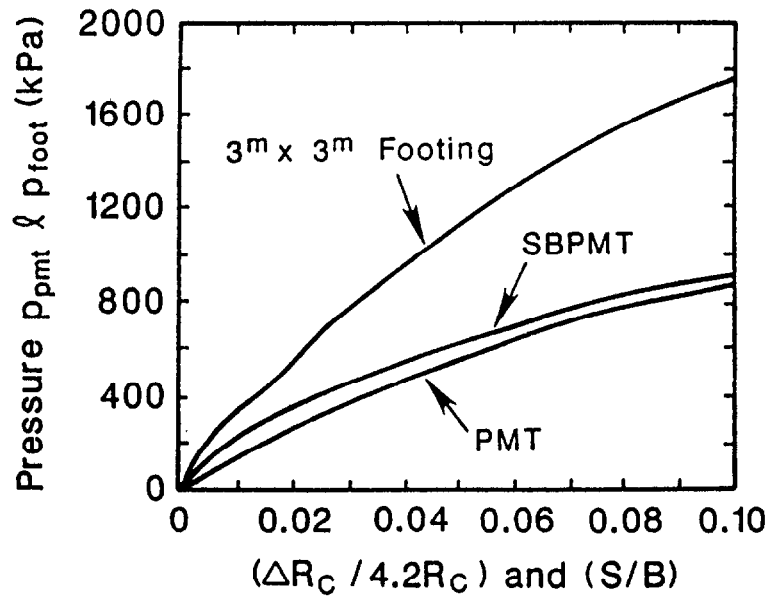


Figure 8.5: FEM Results for the Dense Sand

footing pressure versus relative settlement curve. These curves allowed to develop the transformation function  $\Gamma$  to go from the weighted average PMT curve to the footing pressure vs. relative settlement curve.

The transformation is performed by using the function  $\Gamma$  as follows for each point on the average PMT curve:

$$\frac{s}{B} = \frac{\Delta R_c}{4.2R_c} \quad (4)$$

$$p_{\text{footing}} = \Gamma(p_{\text{pmt}}) \quad (5)$$

where  $s$  is the footing settlement,  $B$  the footing width,  $(\Delta R_c/R_c)$  and  $p_{\text{pmt}}$  correspond to a point on the average PMT curve,  $p_{\text{footing}}$  is the pressure on the footing corresponding to  $s/B$ , and  $\Gamma$  the transformation function which depends on  $s/B$ . The function  $\Gamma$  was obtained from the finite element simulation by taking the ratio of  $p_{\text{footing}}/p_{\text{pmt}}$  for a given  $s/B$  (Figures 8.4 and 8.5). The results are shown on Figure 8.6 for the preboring pressuremeter and for the medium dense and dense sand.

At the limit pressure where  $(\Delta R_c/4.2R_c)$  and  $s/B$  are equal to 0.1, it is known from footing load tests (Briaud 1992) that for sand, the  $\Gamma$  factor is about 1.4 as shown on Figure 8.6 for relative embedments ( $D/B$ ) between 0.25 and 0.75. Indeed in this case the  $\Gamma$  factor is the bearing capacity factor  $k$  used in the design of spread footings based on pressuremeter data. This is lower than the FEM  $\Gamma$  value which is about 2. Furthermore, the results of the full-scale load tests allowed to generate the experimental  $\Gamma$  values shown on Figure 8.6 for the 3 m footing and the 1-m footing. The FEM results, the full-scale tests performed in this study, and the previous experimental data at  $s/B = 0.1$  led to the choice of a recommended conservative function  $\Gamma$  (solid line on Figure 8.6).

In order to predict the settlement as a function of time for a given pressure, the model

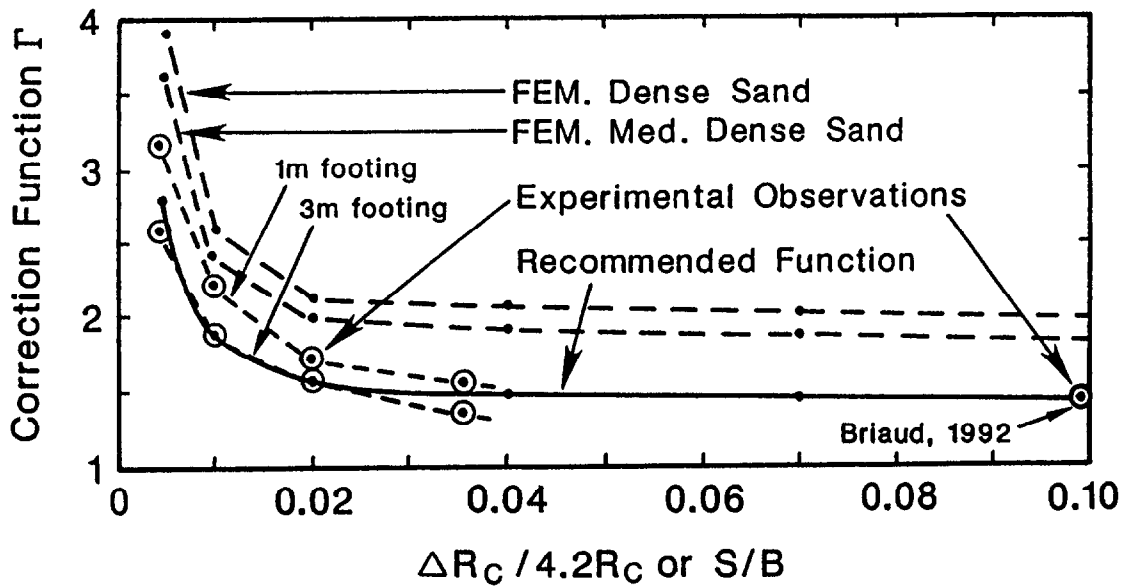


Figure 8.6: The Correction Function  $\Gamma$  (s/B)

proposed by Briaud (1992) is used.

$$s_t = s(1 \text{ min}) \left[ \frac{t}{1 \text{ min}} \right]^{n(\text{footing})} \quad (6)$$

where  $s_t$  is the settlement after a time  $t$  in minutes,  $s(1 \text{ min})$  is the settlement predicted by the proposed method, and  $n_{\text{footing}}$  is related to the value of  $n_{\text{pmt}}$  obtained from a creep step towards the end of the linear phase in the pressuremeter test; the pressure is held constant and the relative increase in radius is recorded as a function of time (Briaud 1992). The modulus is then plotted as shown on Figure 8.7 and the values of the time exponent  $n_{\text{pmt}}$  are given by the slopes of those lines. The relationship between  $n_{\text{footing}}$  and  $n_{\text{pmt}}$  is given by the results of section 7.2:

$$n_{\text{footing}} = 2n_{\text{pmt}}$$

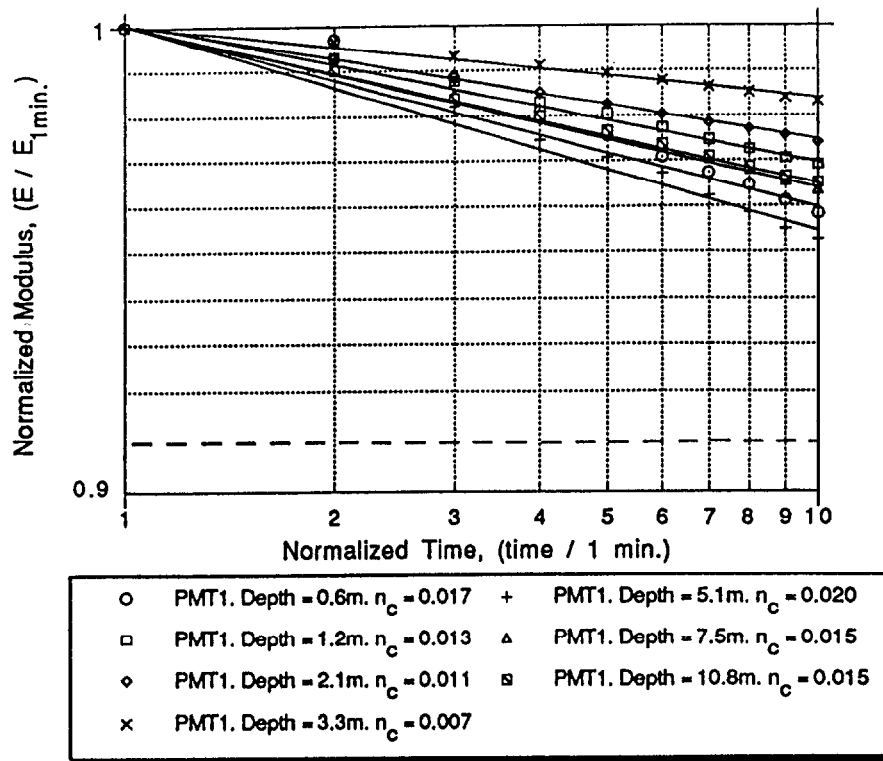


Figure 8.7: Pressuremeter Modulus as a Function of Time

### 8.3 STEP BY STEP PROCEDURE

1. Estimate the required width  $B$  of the footing.
2. Perform preboring, pressuremeter tests at  $0.5B$ ,  $1B$  and  $2B$  below the footing base. This method is based on the use of the TEXAM pressuremeter. During those tests expand the probe as much as possible.
3. Correct the PMT curves to pressure on the cavity wall  $p$  versus relative increase of the cavity radius  $(\Delta R_c/R_c)$  by making use of Eq. (1).
4. Select the PMT curves relevant to the problem within the  $3B$  depth of influence and generate a profile of curves for the footing location.
5. For this footing the PMT curves are averaged according to the influence factor distribution (Figure 8.3, Eq. (3) and Figure 8.8). This leads to the weighted average PMT curve for this footing giving  $p_{pmt}$  vs  $(\Delta R_c/R_c)$ .

6. The weighted average PMT curve is then transformed into the footing curve  $p_{\text{foot}}$  vs  $s/B$  by using Eqs. (4) and (5). The function  $\Gamma$  recommended on Figure 8.6 is the one used for the prediction.
7. The time rate of settlement is then estimated by using the power law model proposed in Eq. (6).

As an example, the step by step procedure was followed for the 1-m and 3-m footings listed at the site. Figure 8.1 is an example of the TEXAM PMT tests performed and of the results obtained after step 3. More details about steps 1, 2 and 3 can be found in Briaud (1992). Figure 8.8 is the average PMT curve obtained after steps 4 and 5. Figure 8.9 shows the transformation from the weighted average PMT curve to this footing load settlement curve. Figure 8.10 is a comparison between the predicted and the measured load settlement curves for the 1-m and 3-m footings.

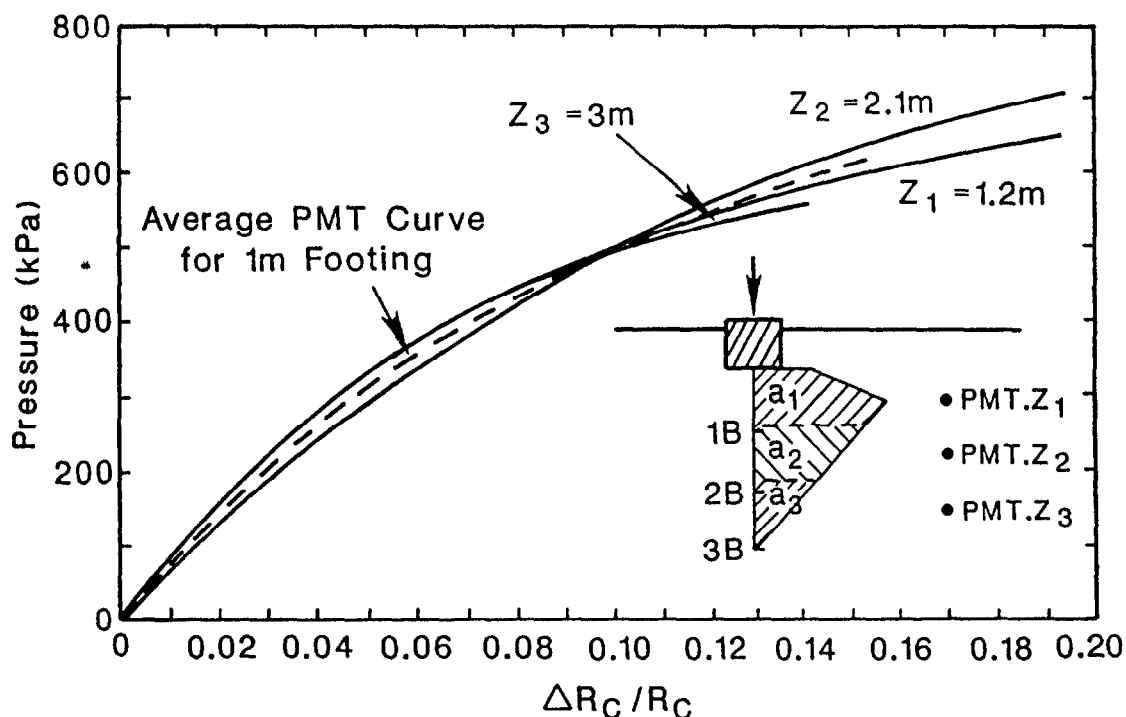


**Figure 8.8:** Generating the Average PMT Curve for a Footing

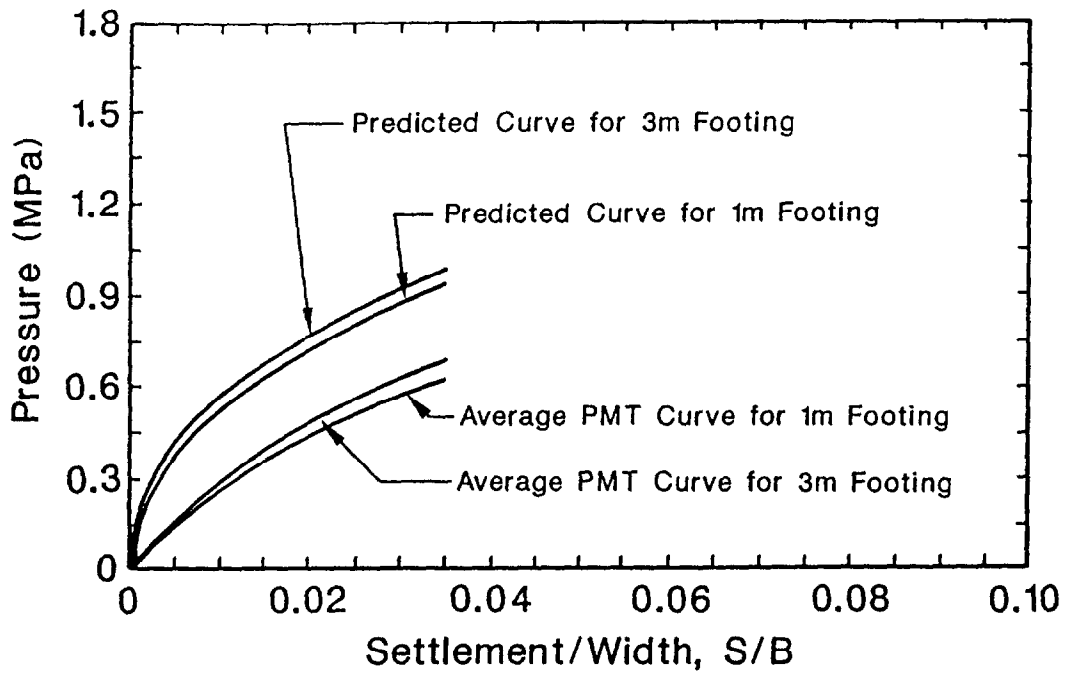


**Figure 8.9:** Predicted Footing Response by Proposed PMT Method

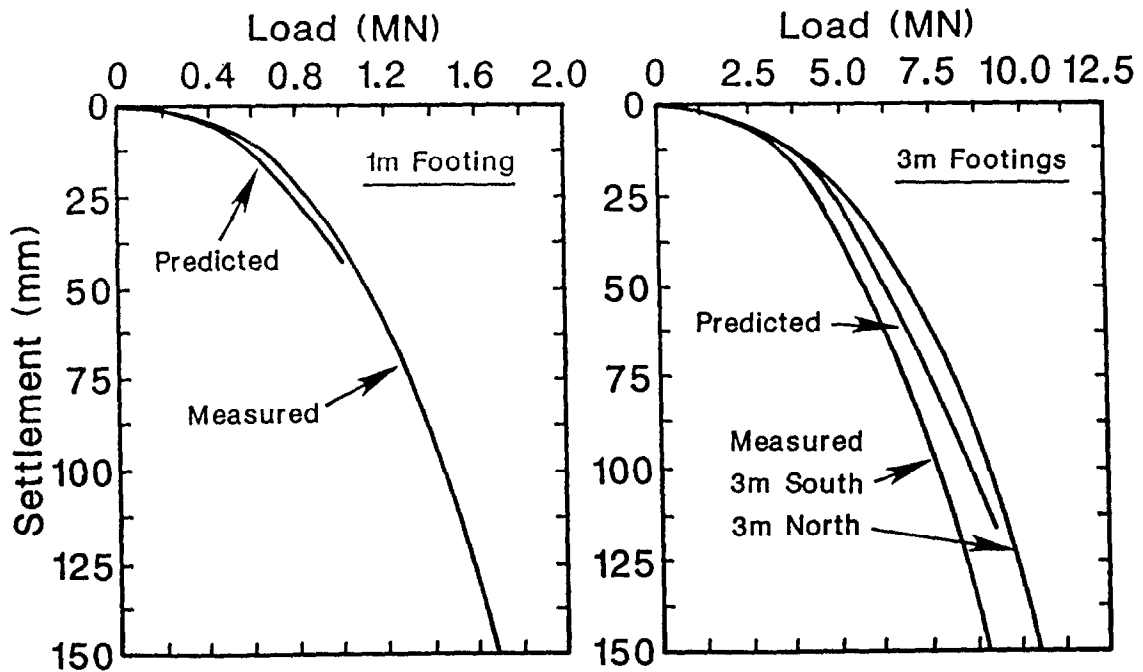


**Figure 8.10:** Measured Versus PMT Predicted Load Settlement Curves

## 9. CONCLUSIONS

The following outlines the conclusions which were drawn from the 5 tasks described in this report:

1. A spread footing data base has been developed. This data base comes in the form of an IBM PC compatible computer program called SHALDB. The program is in two parts: an organized set of data files follows the DBASE format and a program to manipulate these data written in Visual Basic. SHALDB version no. 4 is the version prepared as an outcome of this project. Version nos. 1 to 3 were also developed at Texas A&M University from which version no. 4 is available. SHALDB contains at the present time 77 case histories where the behavior of spread footings is documented. Some of the case histories are of the load test type where a complete load settlement curve was recorded; some of the case histories are of the performance monitoring type where the settlement versus time was recorded for the given structural load. With the program one can retrieve the data, inspect it, create a sub data base satisfying chosen criteria, compare the measurements with predictions and so on.
2. Load tests were performed on five square footings ranging in size from 1 m to 3 m. They were all embedded 0.76 m. The load settlement curve was recorded for all footings which were pushed up to 150 mm of penetration. During the tests the deformation of the soil at depth in the vertical direction was measured with telltales at 0.5B, 1B and 2B depths. At the same time the deformation of the soil at depth in the horizontal direction was measured with inclinometers at various distances from the footing edge. One of the major lessons learned from the instrumentation is that settlement beams for large footing tests may be unreliable and that the best way to measure settlement is to place a telltale through the footing near its center and anchored at a depth of 4B. A very inexpensive telltale system was developed.

3. A very successful prediction event was organized. A total of 31 predictions were received from 8 different countries, half from consultants, half from academics. The load creating 25 mm of settlement  $Q_{25}$  was under estimated by 27% on the average. The predictions were 80% of the time on the safe side. The load creating 150 mm of settlement  $Q_{150}$  was underestimated by 6% on the average. The predictions were 63% of the time on the safe side. The scale effect was not properly predicted and there was a trend towards overpredicting  $Q_{150}$  for the larger footings. The most used methods were based on the CPT, SPT and PMT in that order. The average true factor of safety was 5.4. Therefore it appears that our profession knows how to design spread footings very safely but could design them more economically.
4. An independant set of predictions were performed on the 5 load tested footings using 12 settlement calculation methods and 6 bearing capacity calculation methods. The best settlement methods were the Schmertmann DMT (1986) and the Peck & Bazarra (1967) although they are somewhat on the unconservative side. The best conservative methods are Briaud (1992) and Burland & Burbidge (1984). The best method for bearing capacity was the simple  $0.2q_c$  method from Briaud (1993a). Most other methods were 25 to 42 percent conservative.
5. WAK tests were performed on the five footings before load testing them. This sledgehammer impact test allowed to obtain the static stiffness of the soil-footing assembly. The stiffness predicted by the WAK test was compared to the stiffness measured at small displacements in the load tests. The comparison shows that the WAK test predicted a secant stiffness which corresponds to a settlement averaging about 10 mm.
6. The medium dense sand had a mean SPT blow count of 20 blows/0.3 m, a mean CPT  $q_c$  of 7 MPa, a mean PMT limit pressure and modulus of 800 kPa and 8 MPa respectively, a mean friction angle of  $32^\circ$ , and a mean cross hole shear wave velocity of 270 m/s. In this sand the loads necessary to reach 150 mm of penetration were 1740 kN, 3400 kN, 7100 kN, and 9625 kN for the 1 m, 1.5 m, 2.5 m and 3 m footings respectively. In this sand the load necessary to reach 25 mm of penetration were 850 kN, 1500 kN, 3600 kN, and 4850 kN for the 1 m, 1.5 m, 2.5 m and 3 m footings respectively.

7. The scale effect was studied. It was found that for the five footings tested there was no scale effect; indeed when plotting the load-settlement curves as pressure vs. settlement over width curves, all such curves vanish to one curve and the scale effect disappears. This is explained by the uniqueness of the soil stress strain curve. Since the general bearing capacity equation shows a definite scale effect, the use of this equation is not recommended. The pressure  $p_u$  corresponding to an  $s/B$  ratio equal to 0.1 can be estimated as follows:

$$p_u = \frac{N}{12} \quad \text{with } N \text{ in blows/0.3 m and } p_u \text{ in MPa} \quad (1)$$

$$p_u = \frac{q_c}{4} \quad (2)$$

The pressure  $p_a$  corresponding to an  $s/B$  ratio equal to 0.01 allowable pressure can be estimated as follows:

$$p_a = \frac{N}{36} \quad \text{with } N \text{ in blows/0.3 m and } p_a \text{ in MPa} \quad (3)$$

$$p_a = \frac{q_c}{12} \quad (4)$$

Another finding related to scale was that a sand deposit which is apparently very heterogeneous at the scale of an in situ test (say maybe 50 mm) may be quite homogeneous at the scale of a spread footing (say maybe 3000 mm).

8. The creep settlement was studied. It was found that the power law model proposed by Briaud and Garland fit the data very well:

$$\frac{s_t}{s_{t_0}} = \left( \frac{t}{t_0} \right)^n \quad (5)$$

where  $s_t$  and  $s_{t_0}$  are the settlements of the footing after a time  $t$  and  $t_0$  respectively. The exponent  $n$  was found to vary from 0.01 to 0.05. For  $n = 0.03$  the settlement at 50 years would be 1.67 times larger than the settlement at 1 min. Therefore the creep settlement in sand cannot be neglected but is not very large. The value of  $n$  for the footings increased with the load level and decreased with unload-reload cycles and was, on the average, equal to 2 times the  $n$  value obtained from the pressuremeter test:

$$n_{\text{footing}} = 2n_{\text{pressuremeter}} \quad (6)$$

9. The soil movement at depth in the vertical direction was studied. For footing settlements between 1 to 5 percent of  $B$  It was found that on the average 36% of the top settlement occurs between 0 and  $0.5B$  below the footing, 42% between  $0.5B$  and  $1B$ , 19% between  $1B$  and  $2B$ , and 3% below  $2B$ . Therefore  $2B$  seems to be a reasonable depth of influence for such footings. The strain vs. depth profile obtained from the telltales shows a natural decrease in strain with depth except close to the bottom of the footing where the strain increases due to the lateral confinement brought about by the roughness of the footing.
10. The soil movement at depth in the horizontal direction was studied. It was found that the general shape of the inclinometer curves is a lateral bulging of the soil with a maximum at a depth below the bottom of the footing averaging  $0.73B$  and a bottom at a depth below the bottom of the footing averaging  $2.33B$ . The maximum horizontal movement at the edge of the footing is of the order of 15% of the footing settlement and the horizontal zone of influence extends to about  $1.8B$  beyond the edge on each side of the footing. Approximate calculations indicate that the soil mass under the footing does not dilate but instead compresses for this medium dense sand.
11. A new method for predicting the behavior of spread footings on sand was developed. It is drastically different from existing methods in that it gives a prediction of the complete load settlement curve. Because the deformation pattern under the footing resembles the expansion of a cavity, the pressuremeter test was chosen as the basis for the method. The pressuremeter curve is simply transformed point by point to obtain the footing curve as follows:

$$p_{\text{footing}} = \Gamma(p_{\text{pressuremeter}}) \quad (7)$$

$$\frac{s}{B} = \frac{\Delta R_c}{4.2R_c} \quad (8)$$

where  $p_{\text{footing}}$  is the footing pressure,  $p_{\text{pressuremeter}}$  is the pressuremeter pressure,  $\Gamma$  is the transfer function recommended on the basis of the load test data and finite element analysis,  $s$  is the footing settlement corresponding to  $p_{\text{footing}}$ ,  $B$  is the footing width and  $\Delta R_c/R_c$  is the relative increase in cavity radius on the pressuremeter curve at a pressure equal to  $p_{\text{pressuremeter}}$ .



**APPENDIX A: Soil Data**

BORING LOG		
PROJECT: PERFORMANCE OF FOOTINGS ON SAND		BORING NO: SPT-1
CLIENT: FEDERAL HIGHWAY ADMINISTRATION		LOCATION: SAND SITE
DATE: 4/5/93	PROJECT NO: 146604	BORING TYPE: 121 mm BIT
DRILLER: GUSTAVUS	SOIL TECHNICIAN: GIBBENS	GROUND ELEV:
Depth in Meters	Blows Per 150mm/150mm/150mm	<input type="checkbox"/> Shelby Tube Sample <input type="checkbox"/> X-Penetration Sample <input type="checkbox"/> J-Jar <input type="checkbox"/> /-No Recovery <input type="checkbox"/> \-Disturbed sample from cuttings <input type="checkbox"/> ∇-Water encountered while drilling <input type="checkbox"/> √-Open-hole water level <input type="checkbox"/> B/F-Blows per foot, ASTM D 1586 Penetration Test <input type="checkbox"/> Pen.(tsf)-Field estimate of compressive strength
DESCRIPTION OF STRATUM		
	4/5/6	NO SAMPLING
	7/9/14	NO SAMPLING
- 1.5 -	13/18/12	NO SAMPLING
	6/10/11	NO SAMPLING
- 3.0 -	8/10/13	NO SAMPLING
	11/14/14	NO SAMPLING
- 4.5 -		
- 6.0 -	9/15/19	NO SAMPLING
	8/8/9	NO SAMPLING
- 7.5 -		
- 9.0 -	4/5/8	NO SAMPLING
	10/20/34	NO SAMPLING
- 10.5 -		
- 12.0 -	19/29/47	NO SAMPLING
	14/19/21	NO SAMPLING
- 13.5 -		
- 15.0 -	15/22/31	NO SAMPLING
Bottom @ 15.2 m		

Figure A1: SPT-1

BORING LOG		
PROJECT: PERFORMANCE OF FOOTINGS ON SAND		BORING NO: SPT-2
CLIENT: FEDERAL HIGHWAY ADMINISTRATION		LOCATION: SAND SITE
DATE: 4/6/93	PROJECT NO: 146604	BORING TYPE: 121 mm Bit
DRILLER: GUSTAVUS	SOIL TECHNICIAN: GIBBENS	GROUND ELEV:
Depth in Meters	Blows Per 150mm/150mm/150mm	<input type="checkbox"/> Shelby Tube Sample <input type="checkbox"/> X-Penetration Sample <input type="checkbox"/> J-Jar <input type="checkbox"/> /-No Recovery <input type="checkbox"/> \-Disturbed sample from cuttings <input type="checkbox"/> V-Water encountered while drilling <input type="checkbox"/> v-Open-hole water level <input type="checkbox"/> B/F-Blows per foot, ASTM D 1586 Penetration Test <input type="checkbox"/> Pen.(tsf)-Field estimate of compressive strength
DESCRIPTION OF STRATUM		
	4/5/7	Tan Silty Fine Sand
	7/10/13	Tan Silty Fine Sand
- 1.5 -	8/8/10	Tan Silty Fine Sand
	6/9/9	Tan Silty Fine Sand
- 3.0 -	4/8/8	Tan Silty Fine Sand
	10/10/9	Tan Sand
- 4.5 -	7/9/8	Tan Sand w/Gravel
	7/10/11	Tan Sandy Clay
- 6.0 -		
	5/6/8	Tan Sandy Clay
- 7.5 -		
	6/8/13	Tan Silty Fine Sand
- 9.0 -		
	11/24/39	Dark Gray Clay
- 10.5 -		
	11/16/24	Dark Gray Clay
- 12.0 -		
	14/17/22	Dark Gray Clay
- 13.5 -		
	18/25/32	Dark Gray Clay
- 15.0 -		
Bottom @ 15.2 m		

Figure A2: SPT-2

BORING LOG		
PROJECT: PERFORMANCE OF FOOTINGS ON SAND		BORING NO: SPT-3
CLIENT: FEDERAL HIGHWAY ADMINISTRATION		LOCATION: SAND SITE
DATE: 4/21/93	PROJECT NO: 14G604	BORING TYPE: 121 mm BIT
DRILLER: GUSTAVUS	SOIL TECHNICIAN: GIBBENS	GROUND ELEV:
Depth in Meters	Blows Per 150mm/150mm/150mm	■ Shelby Tube Sample    X-Penetration Sample    J-Jar    /-No Recovery \-Disturbed sample from cuttings    V-Water encountered while drilling v-Open-hole water level    B/F-Blows per foot, ASTM D 1586 Penetration Test Pen.(tsf)-Field estimate of compressive strength
DESCRIPTION OF STRATUM		
	5/5/8	Tan Silty Fine Sand
	4/8/10	Tan Silty Fine Sand
1.5	6/11/14	Tan Silty Fine Sand
	6/9/8	Tan Silty Fine Sand
	6/8/10	Tan Silty Fine Sand
3.0		
	4/9/10	Tan Sand
4.5		
	6/12/14	Tan Sand w/Gravel
	7/11/11	Tan Sandy Clay w/Gravel
6.0		
	6/9/10	Tan Sandy Clay w/Gravel
7.5		
	3/5/5	102 mm of Tan Silty Fine Sand becomes Tan Clay w/Gravel
9.0		
	11/20/24	26 mm of Clayey Gravel becomes Dark Gray Clay
10.5		
	43/48/51	Dark Gray Clay
12.0		
	14/18/28	Dark Gray Clay
13.5		
	13/15/21	Dark Gray Clay
15.0		
Bottom @ 15.2 m		

Figure A3: SPT-3

BORING LOG		
PROJECT: PERFORMANCE OF FOOTINGS ON SAND		BORING NO: SPT-4
CLIENT: FEDERAL HIGHWAY ADMINISTRATION		LOCATION: SAND SITE
DATE: 4/16/93	PROJECT NO: 146604	BORING TYPE: 121 mm BIT
DRILLER: GUSTAVUS	SOIL TECHNICIAN: GIBBENS	GROUND ELEV:
Depth in Meters	Blows Per 150mm/150mm/150mm	<input type="checkbox"/> Shelby Tube Sample <input type="checkbox"/> X-Penetration Sample <input type="checkbox"/> J-Jar <input type="checkbox"/> /-No Recovery <input type="checkbox"/> \-Disturbed sample from cuttings <input type="checkbox"/> V-Water encountered while drilling <input type="checkbox"/> v-Open-hole water level <input type="checkbox"/> B/F-Blows per foot, ASTM D 1586 Penetration Test <input type="checkbox"/> Pen.(tsf)-Field estimate of compressive strength
DESCRIPTION OF STRATUM		
	3/4/7	Tan Silty Fine Sand
	5/8/7	Tan Silty Fine Sand
- 1.5 -	5/8/10	Tan Silty Fine Sand
	5/8/9	Tan Silty Fine Sand
	5/8/8	Tan Silty Fine Sand
- 3.0 -	6/8/7	Tan Sand
- 4.5 -	8/7/7	Tan Silty Fine Sand
	6/8/9	Tan Silty Fine Sand
- 6.0 -		
	8/8/8	Gravel
- 7.5 -		
	5/9/11	Tan Sandy Clay
- 9.0 -		
	11/23/27	76 mm of Tan Sandy Clay becomes Dark Gray Clay
- 10.5 -		
	21/31/39	Dark Gray Clay w/Gravel
- 12.0 -		
	14/21/32	Dark Gray Clay
- 13.5 -		
	17/23/37	Dark Gray Clay
- 15.0 -		
		Bottom @ 15.2 m

Figure A4: SPT-4

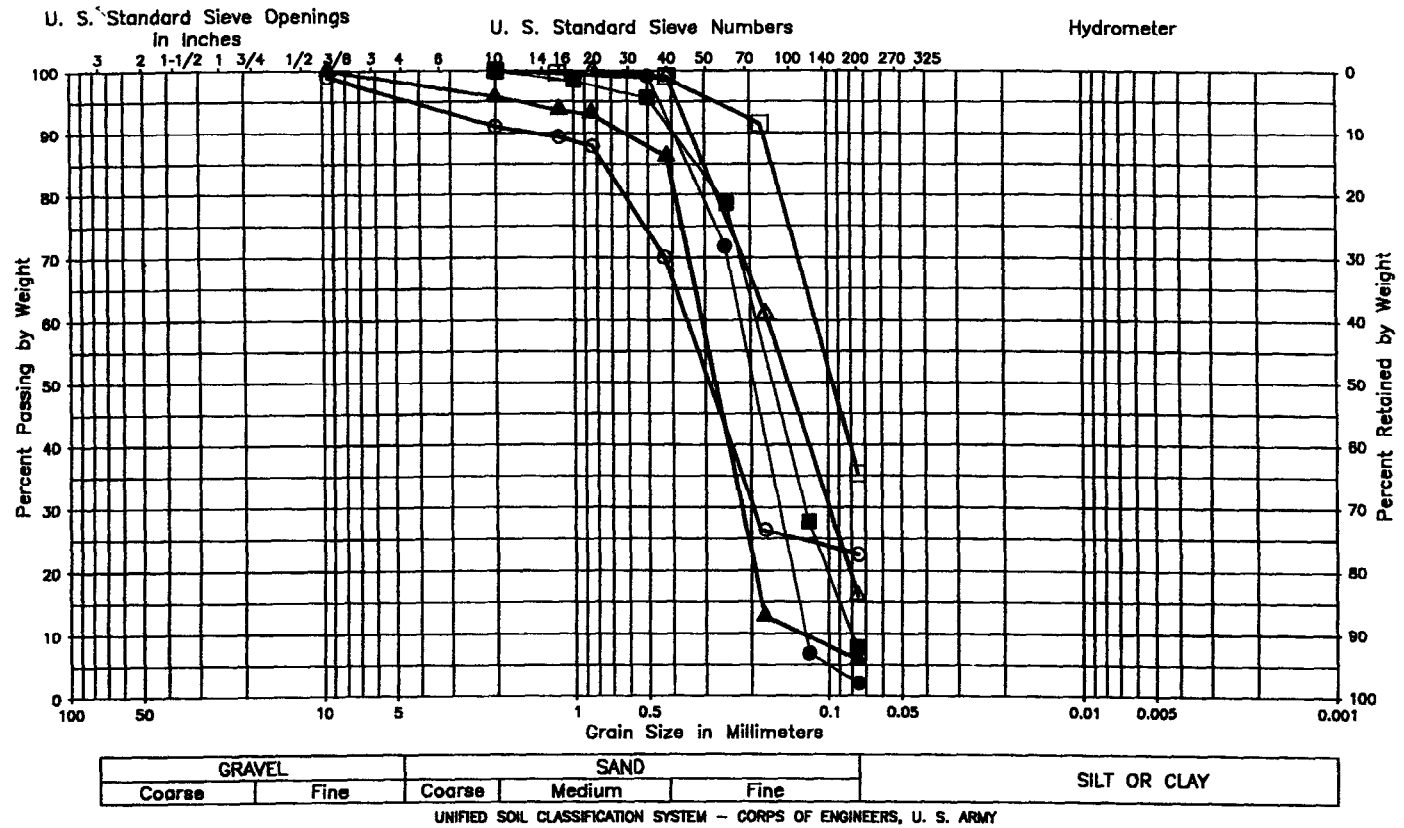
BORING LOG		
PROJECT: PERFORMANCE OF FOOTINGS ON SAND		BORING NO: SPT-5
CLIENT: FEDERAL HIGHWAY ADMINISTRATION		LOCATION: SAND SITE
DATE: 4/13/93	PROJECT NO: 14G604	BORING TYPE: 121 mm BIT
DRILLER: GUSTAVUS	SOIL TECHNICIAN: GIBBENS	GROUND ELEV:
Depth in Meters	Blows Per 150mm/150mm/150mm	■ Shelby Tube Sample    X-Penetration Sample    J-Jar    /-No Recovery \-Disturbed sample from cuttings    V-Water encountered while drilling v-Open-hole water level    B/F-Blows per foot, ASTM D 1586 Penetration Test Pen.(tsf)-Field estimate of compressive strength
DESCRIPTION OF STRATUM		
	4/5/6	Tan Silty Fine Sand
	5/7/8	Tan Silty Fine Sand
1.5	6/10/10	Tan Silty Fine Sand
	4/8/11	Tan Silty Fine Sand
	4/7/9	Tan Silty Fine Sand
3.0	4/7/9	Tan Silty Fine Sand
4.5	8/12/15	Tan Silty Sand w/Gravel Pockets
	6/7/11	Tan Sandy Clay w/Gravel
6.0		
	4/9/7	Tan Sand
7.5		
	4/12/13	102 mm of Tan Sandy Clay w/Gravel becomes Gray Clayey Sand
9.0		
	12/33/31	51 mm of Fine Sand w/Gravel becomes Dark Gray Clay
10.5		
	11/17/21	Dark Gray Clay
12.0		
	10/14/22	Dark Gray Clay
13.5		
	11/12/27	Dark Gray Clay
15.0		
Bottom @ 15.2 m		

Figure A5: SPT-5

BORING LOG		
PROJECT: PERFORMANCE OF FOOTINGS ON SAND		BORING NO: SPT-6
CLIENT: FEDERAL HIGHWAY ADMINISTRATION		LOCATION: SAND SITE
DATE: 4/21/93	PROJECT NO: 14G604	BORING TYPE: 121 mm BIT
DRILLER: GUSTAVUS	SOIL TECHNICIAN: GIBBENS	GROUND ELEV:
Depth in Meters	Blows Per 150mm/150mm/150mm	<input type="checkbox"/> Shelby Tube Sample <input type="checkbox"/> X-Penetration Sample <input type="checkbox"/> J-Jar <input type="checkbox"/> /-No Recovery <input type="checkbox"/> \-Disturbed sample from cuttings <input type="checkbox"/> V-Water encountered while drilling <input type="checkbox"/> v-Open-hole water level    B/F-Blows per foot, ASTM D 1586 Penetration Test <input type="checkbox"/> Pen.(tsf)-Field estimate of compressive strength
DESCRIPTION OF STRATUM		
	6/6/7	Tan Silty Fine Sand
	6/8/11	Tan Silty Fine Sand
- 1.5 -	5/9/9	Tan Silty Fine Sand
	4/7/6	Tan Silty Fine Sand
	4/7/7	Tan Sand
- 3.0 -		
	11/11/15	Tan Sand
- 4.5 -	5/9/14	Tan Sand w/Gravel
- 6.0 -	5/9/11	Gravel w/Sand
	7/13/15	Tan Sand w/Traces of Gravel
- 9.0 -	3/4/4	No Recovery
- 10.5 -	9/20/29	76 mm of Clayey Gravel becomes Dark Gray Clay
- 12.0 -	12/20/31	Dark Gray Clay
- 13.5 -	16/18/35	Dark Gray Clay
- 15.0 -	17/21/33	Dark Gray Clay
		Bottom @ 15.2 m

Figure A6: SPT-6

### MECHANICAL ANALYSIS CHART



BORING NO.: SPT-2  
 DEPTH:   1.4m-1.8m  
  3.5m-4.0m  
  4.6m-5.0m  
  8.7m-9.1m

BORING NO.: HAND AUGERED HOLE  
 DEPTH:   0.1 m  
  2.5 m

TEXAS A&M RESEARCH PROJECT  
 RIVERSIDE CAMPUS

MAY 28, 1993

**Figure A7: Grain Size Distribution**

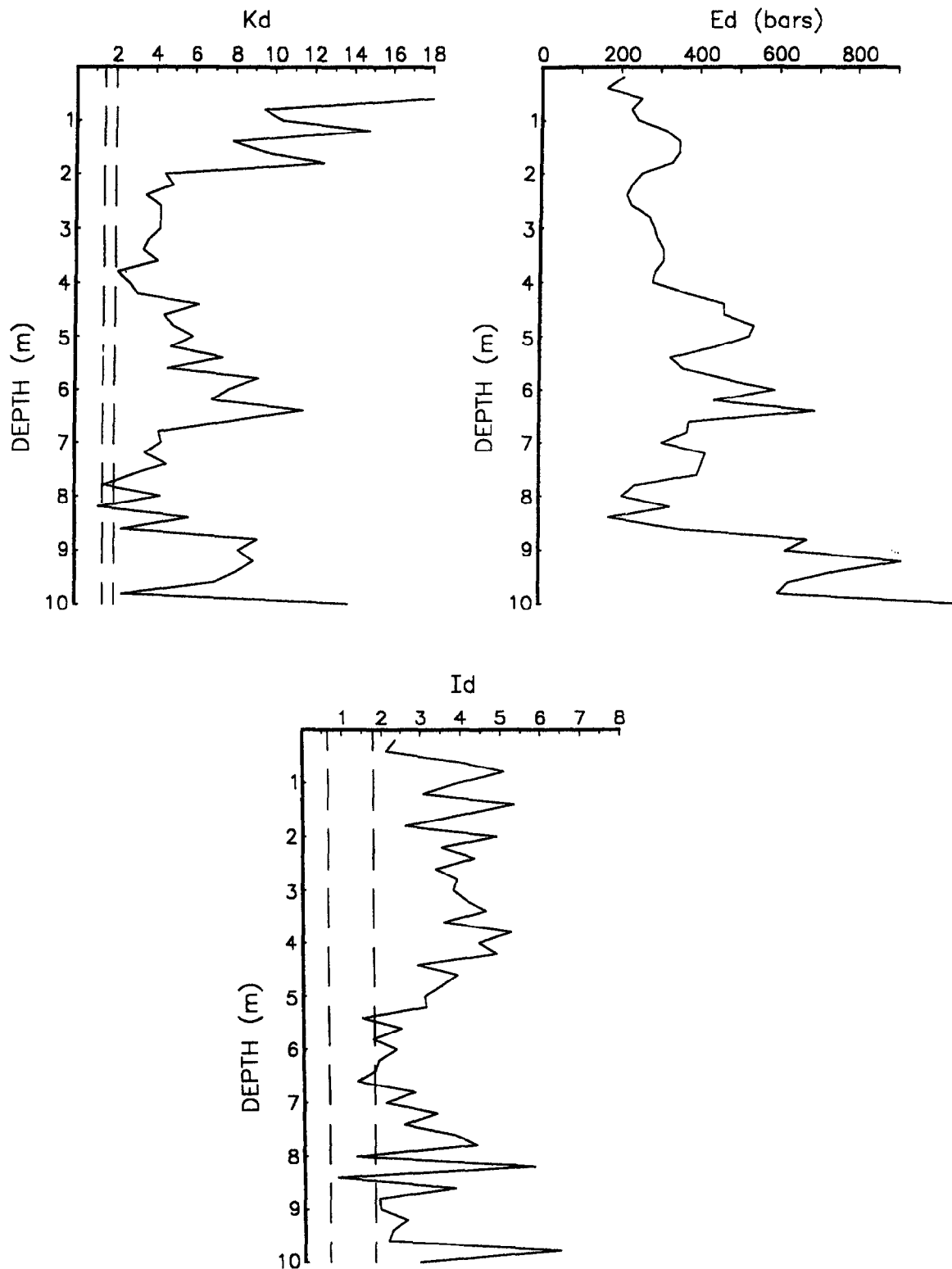


**Figure A8: DMT-1 Test Results w/o Axial Thrust Measurements**

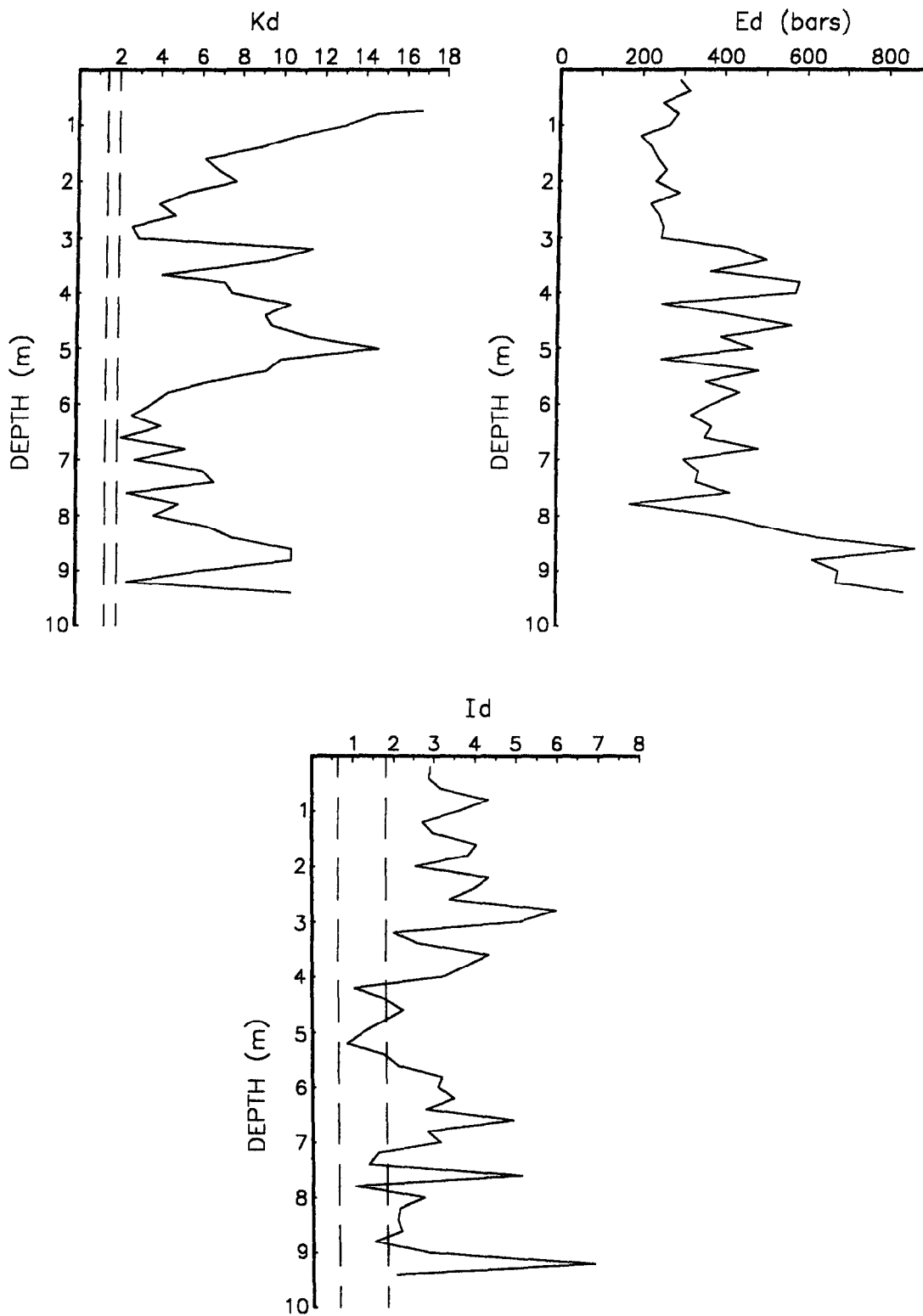


**Figure A9: DMT-2 Test Results w/o Axial Thrust Measurements**

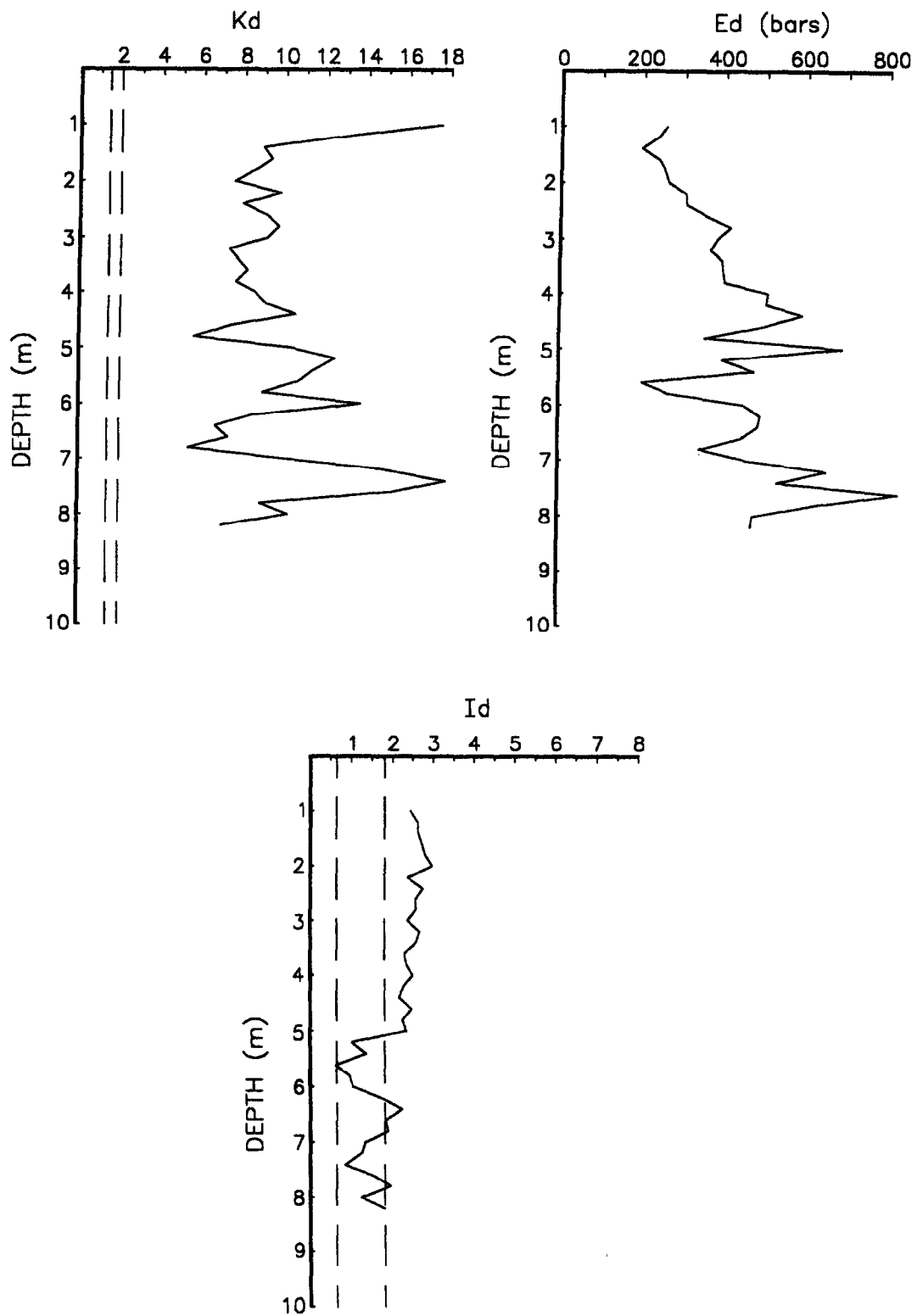


**Figure A10: DMT-3 Test Results w/ Axial Thrust Measurements**

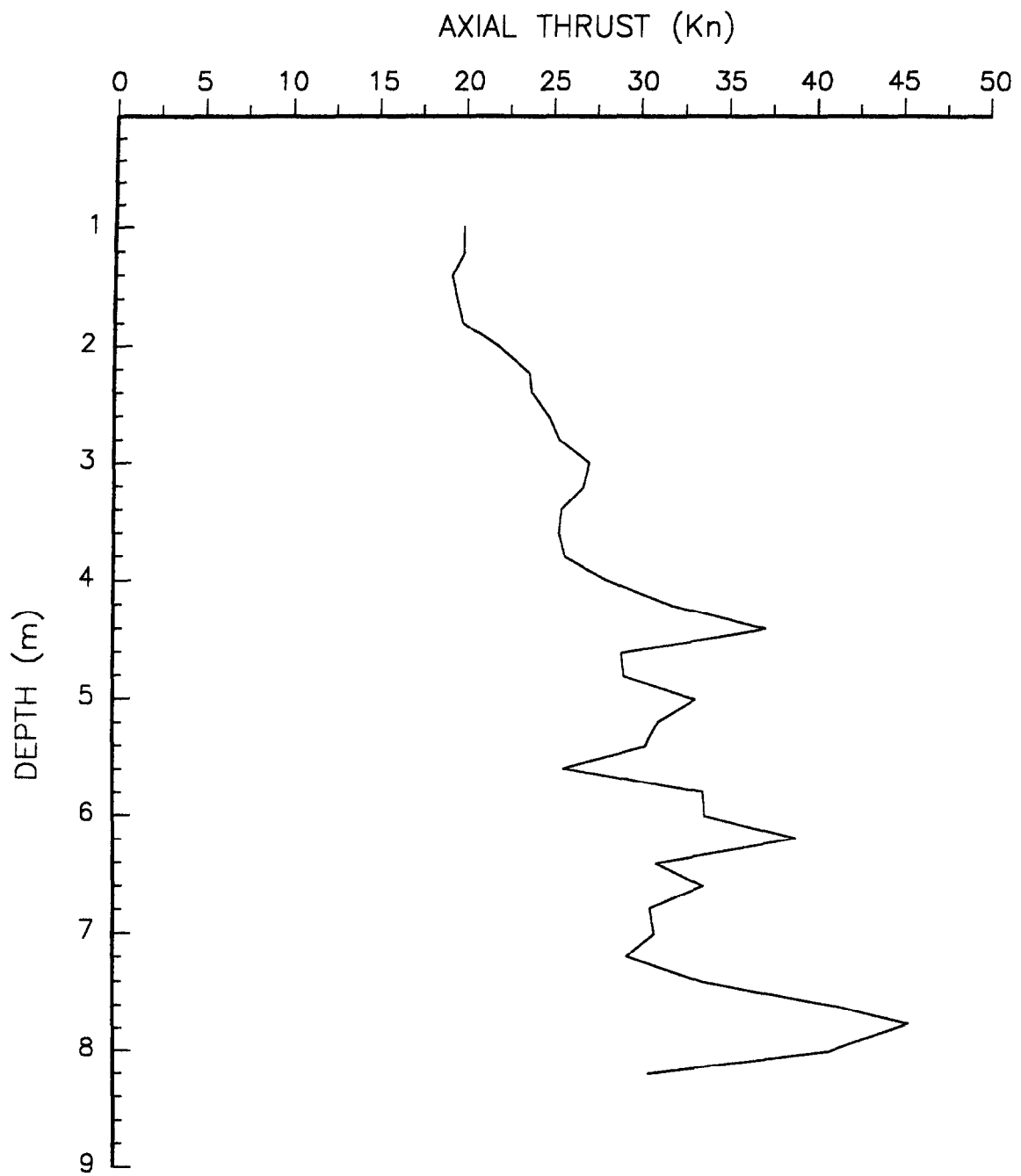


**Figure A11: Axial Thrust Versus Depth for DMT-3**

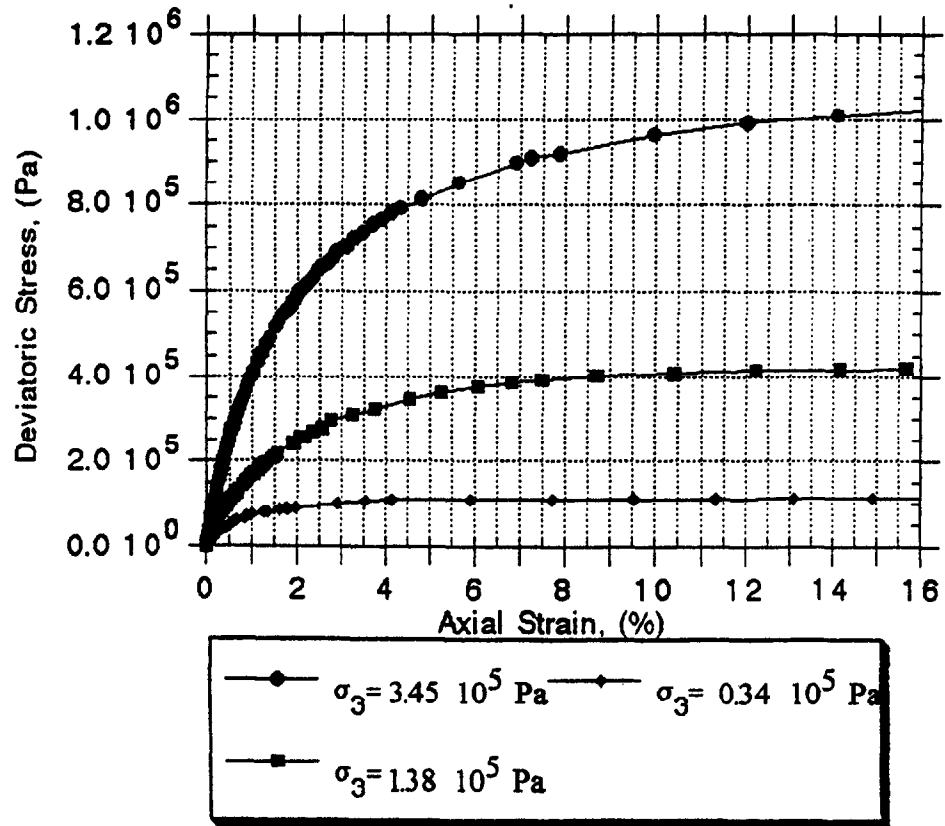


Figure A12: Stress Strain Curve for 0.6-m Sample

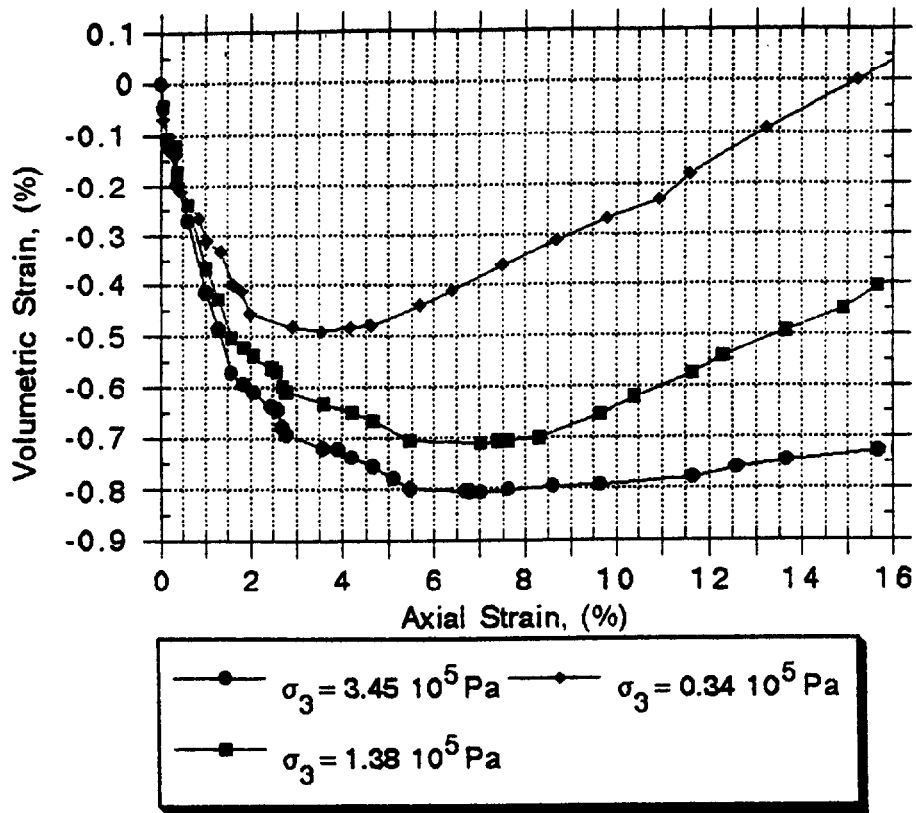
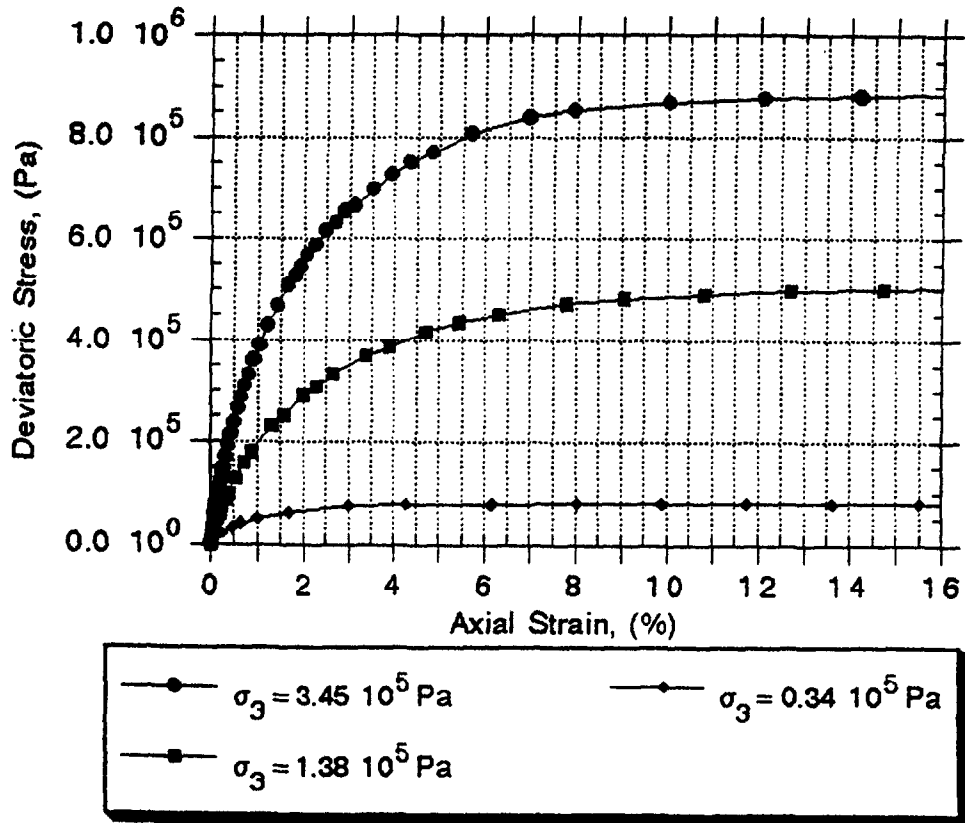
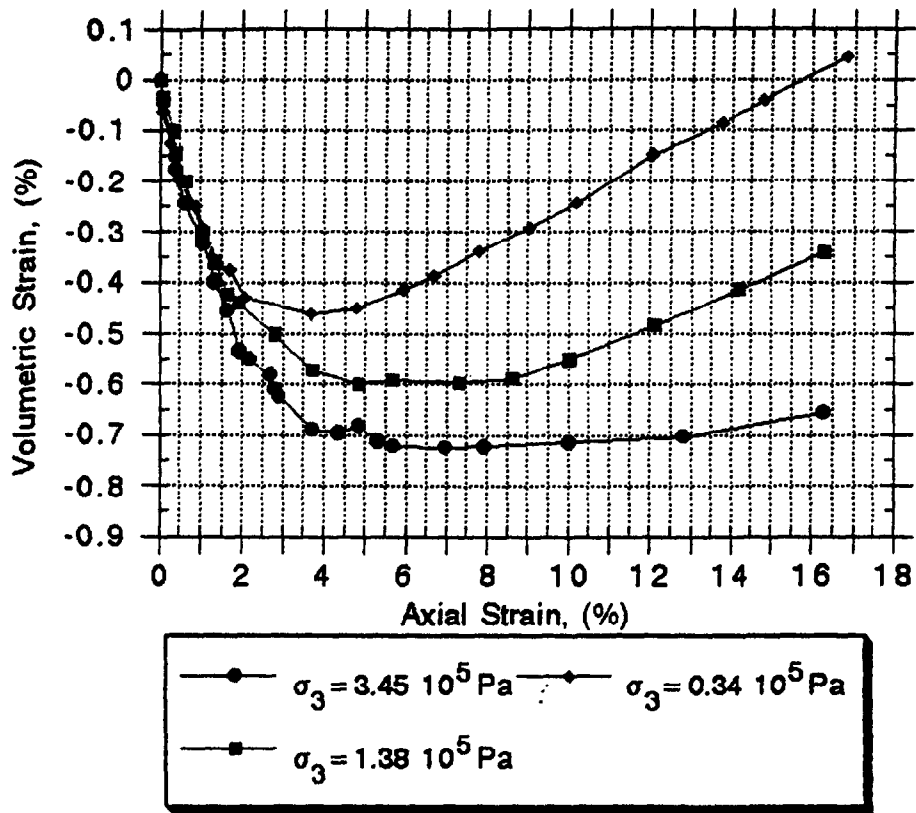


Figure A13: Volume Change Curve for 0.6-m Sample



**Figure A14:** Stress Strain Curve for 3.0-m Sample



**Figure A15:** Volume Change Curve for 3.0-m Sample

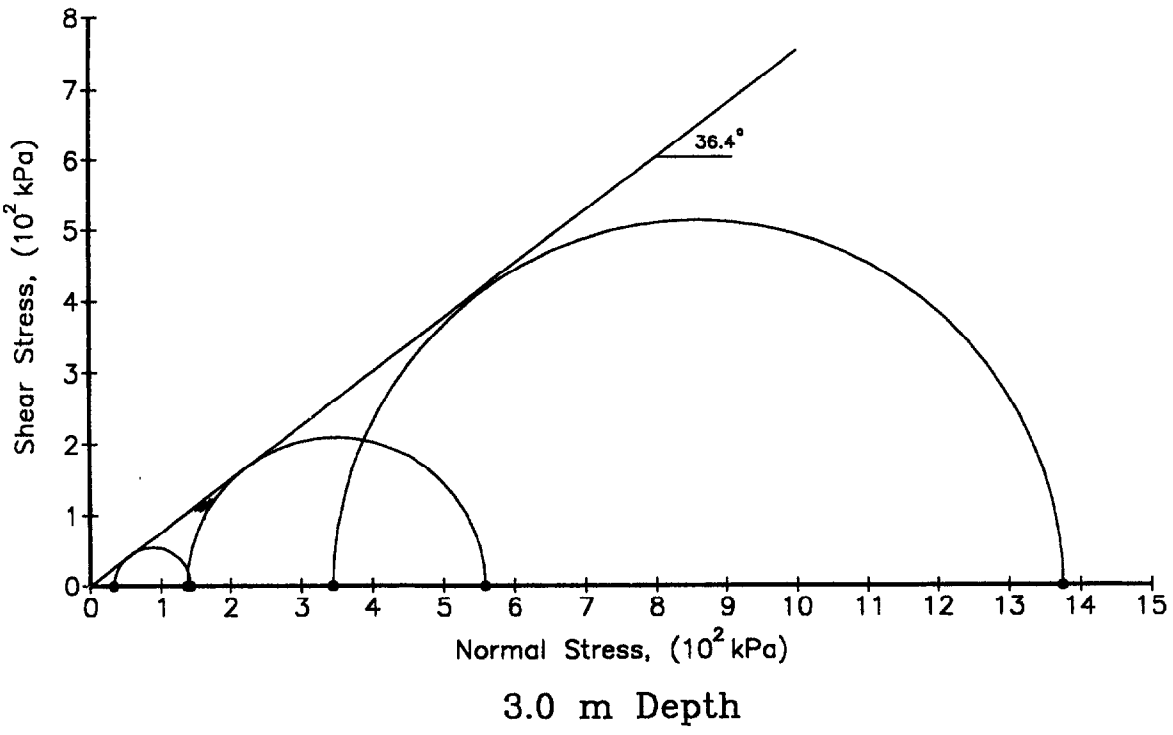
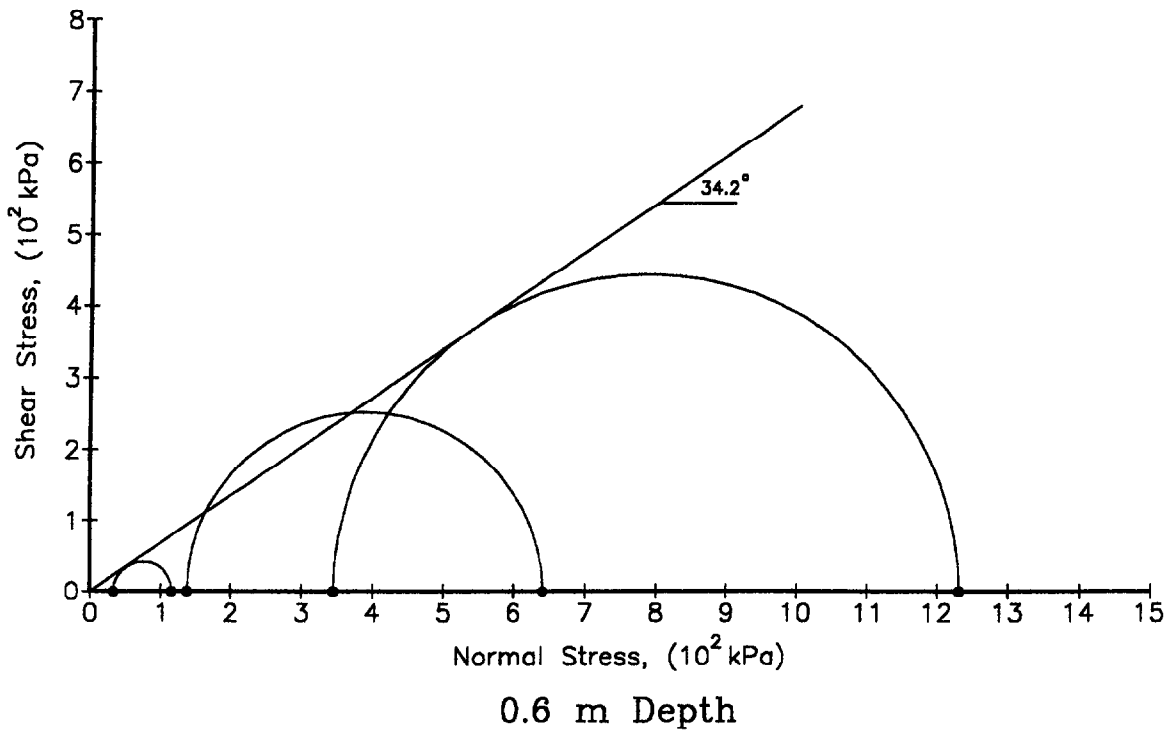


**Figure A16: Mohr's Circles From Triaxial Test**

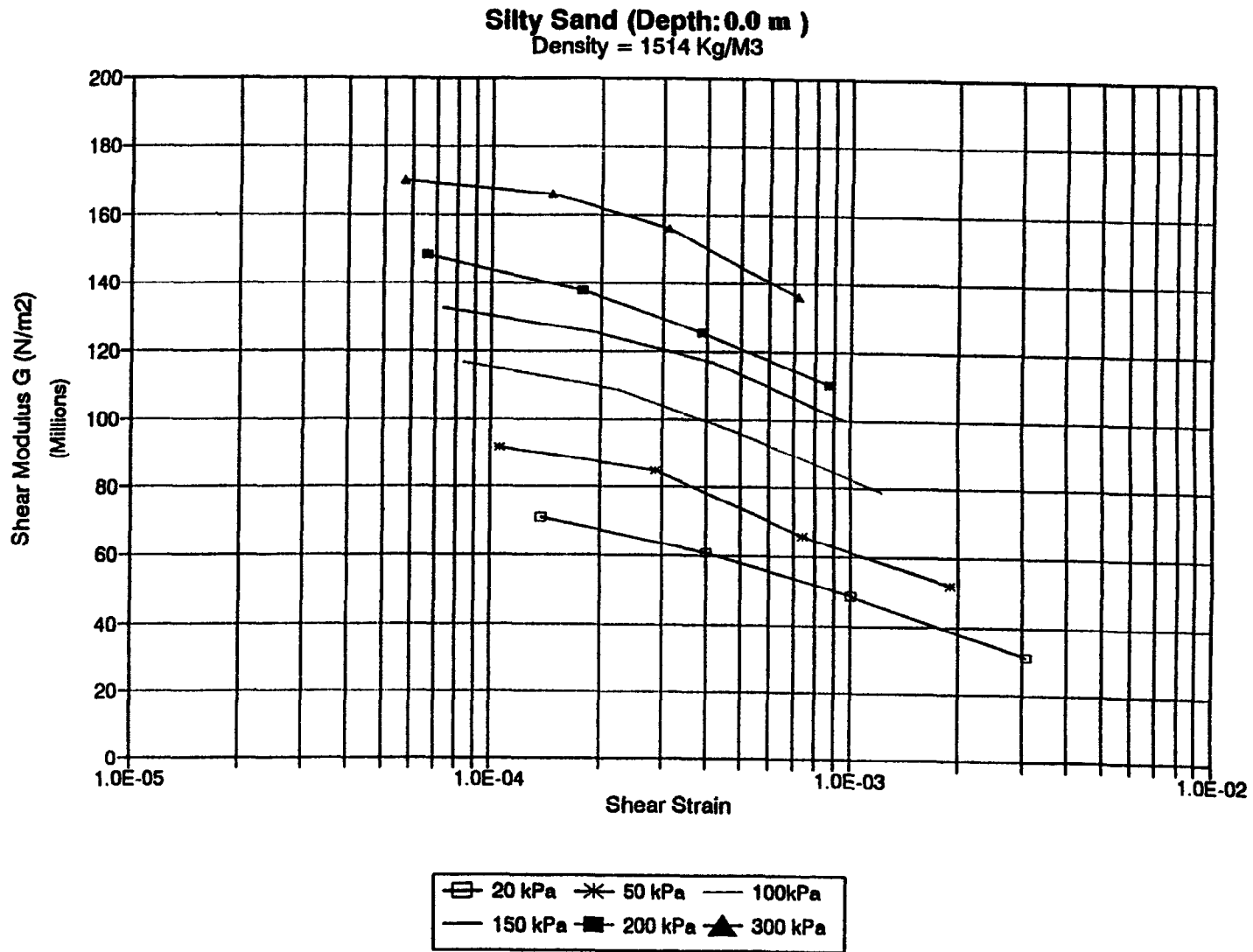
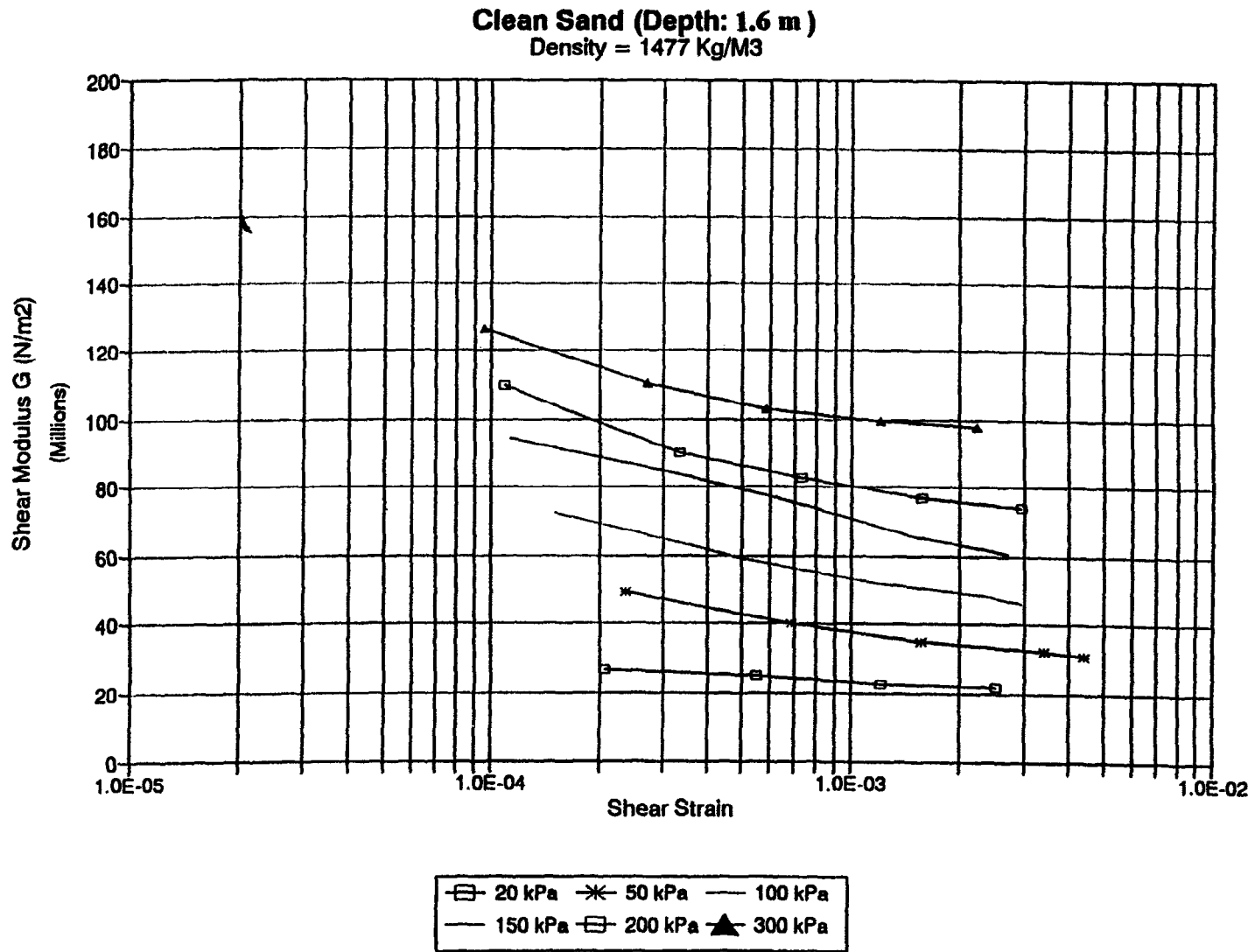


**Figure A17: Resonant Column Test Results @ 0.0 m**



**Clean Sand (Depth: 3.3 m)**  
 Density = 1480 Kg/M3

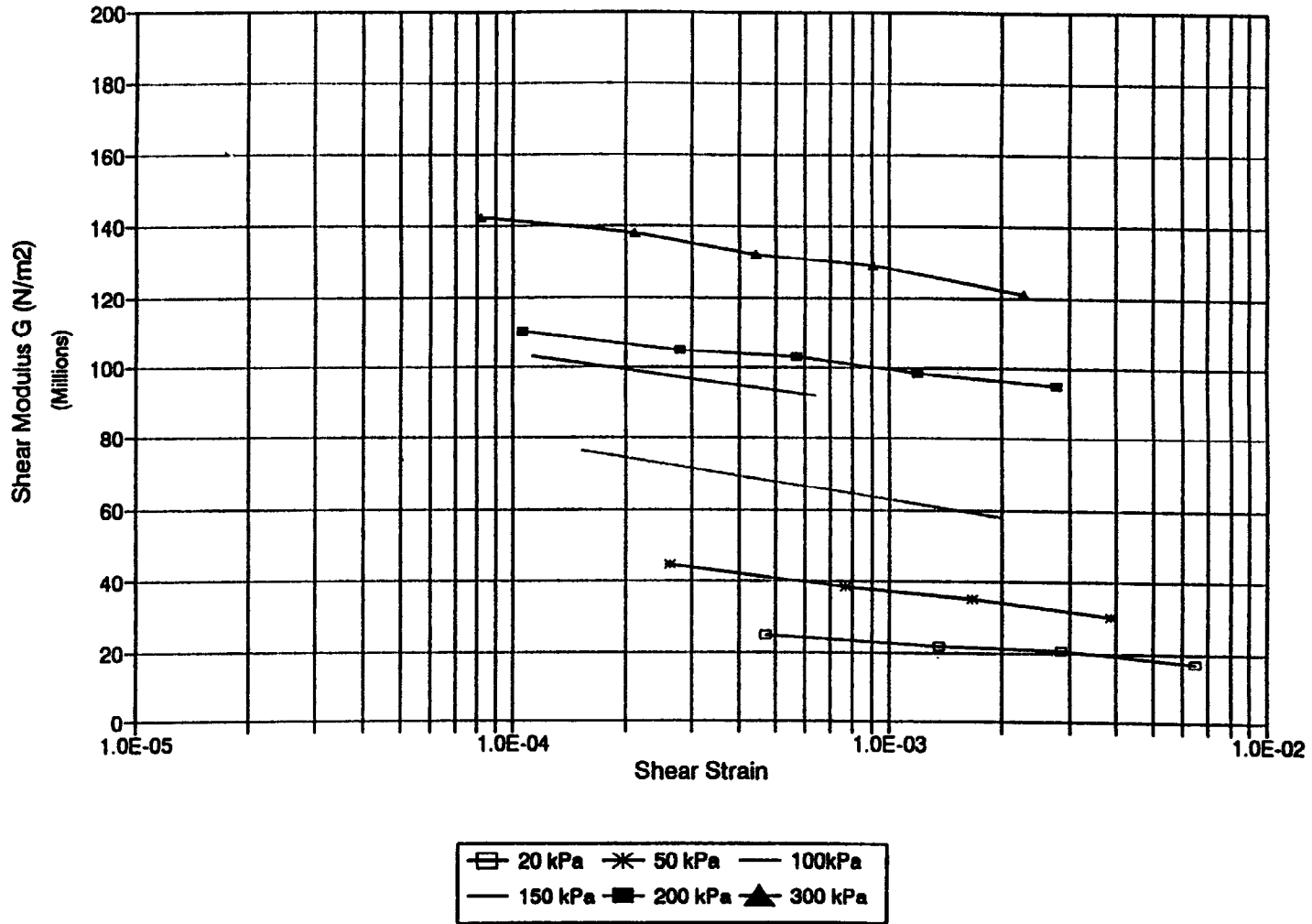


**Figure A19: Resonant Column Test Results @ 3.3 m**

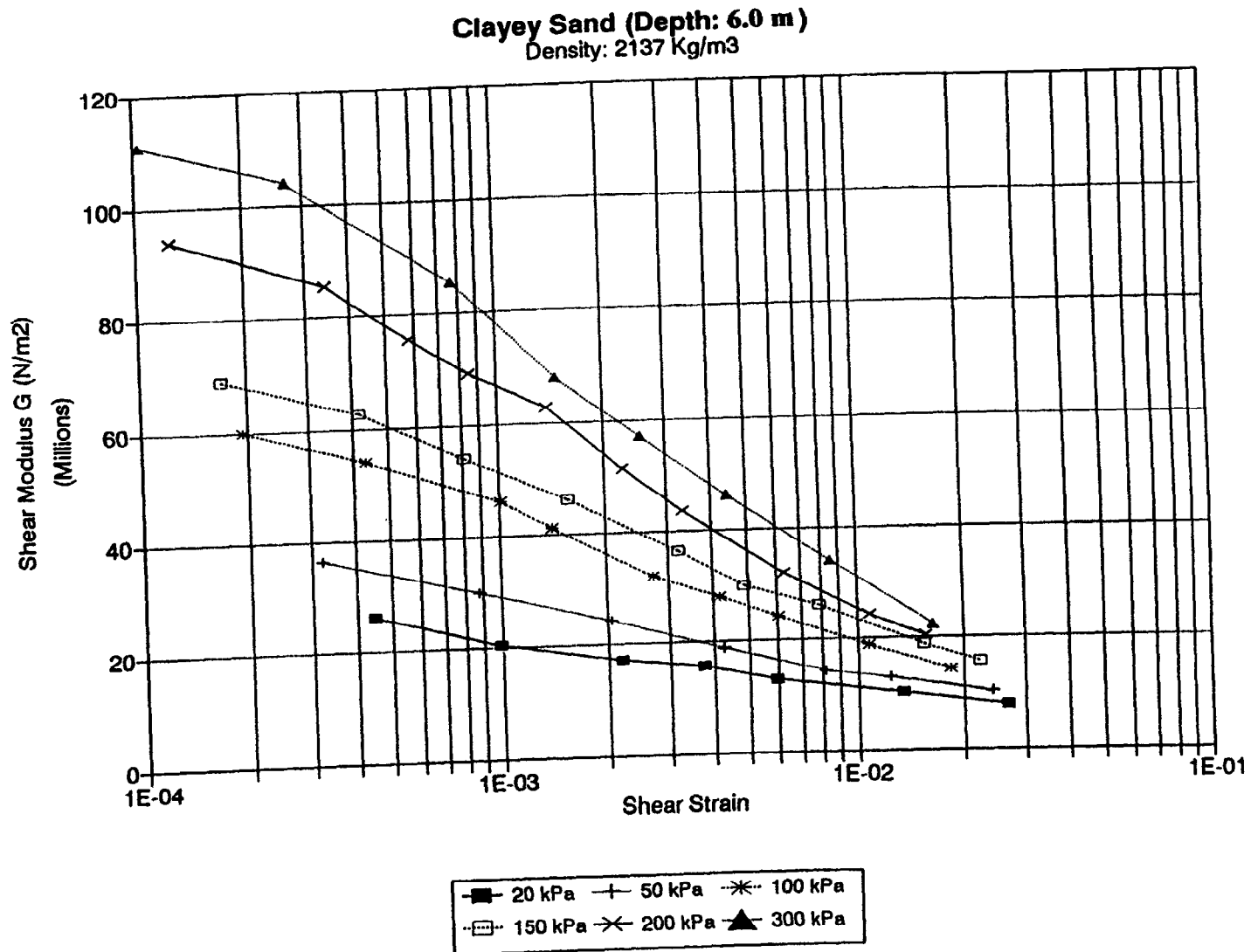


**Figure A20: Resonant Column Test Results @ 6.0 m**

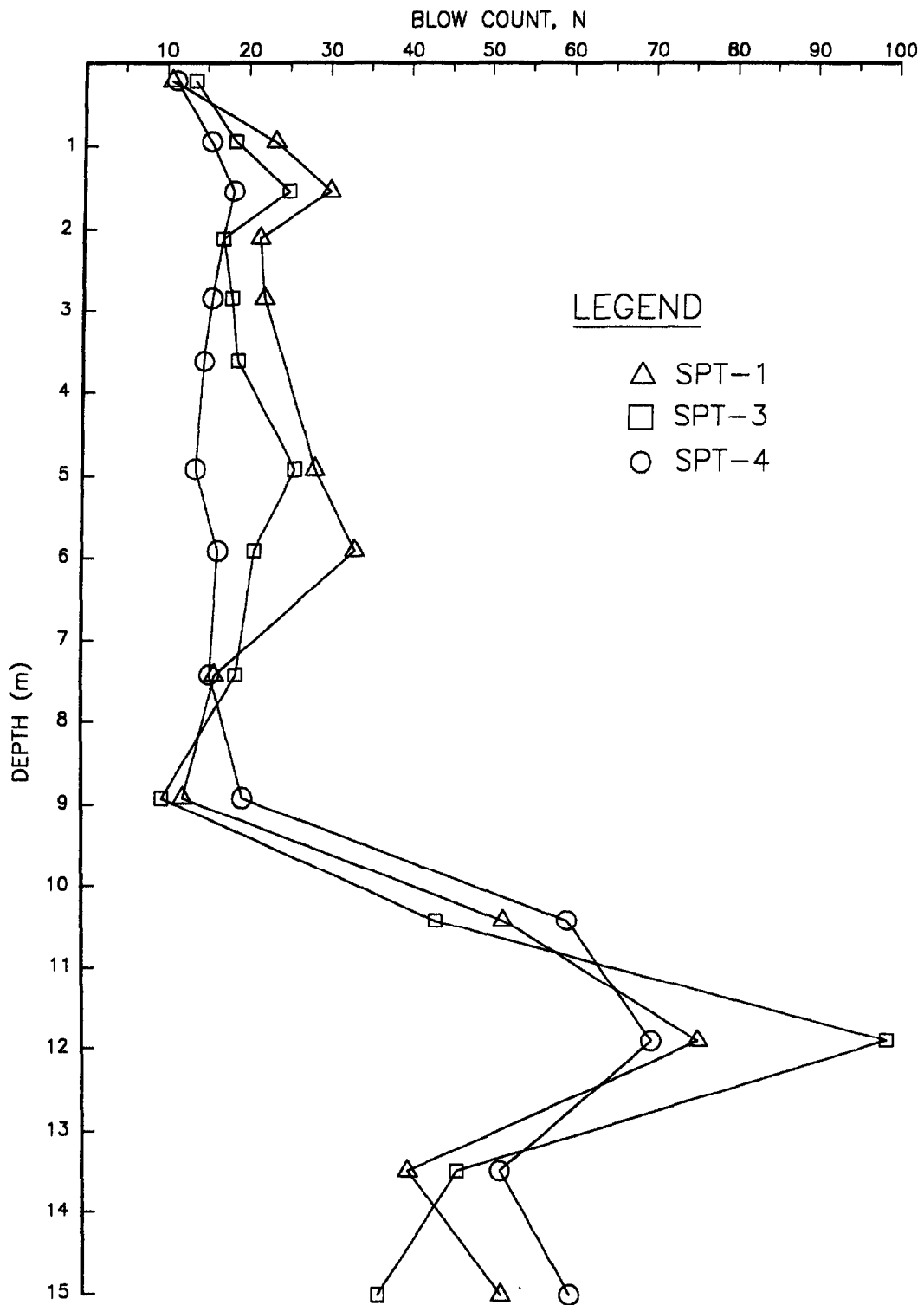


**Figure A21: Graph of Blow Counts N Versus Depth for SPT 1, 3 & 4**

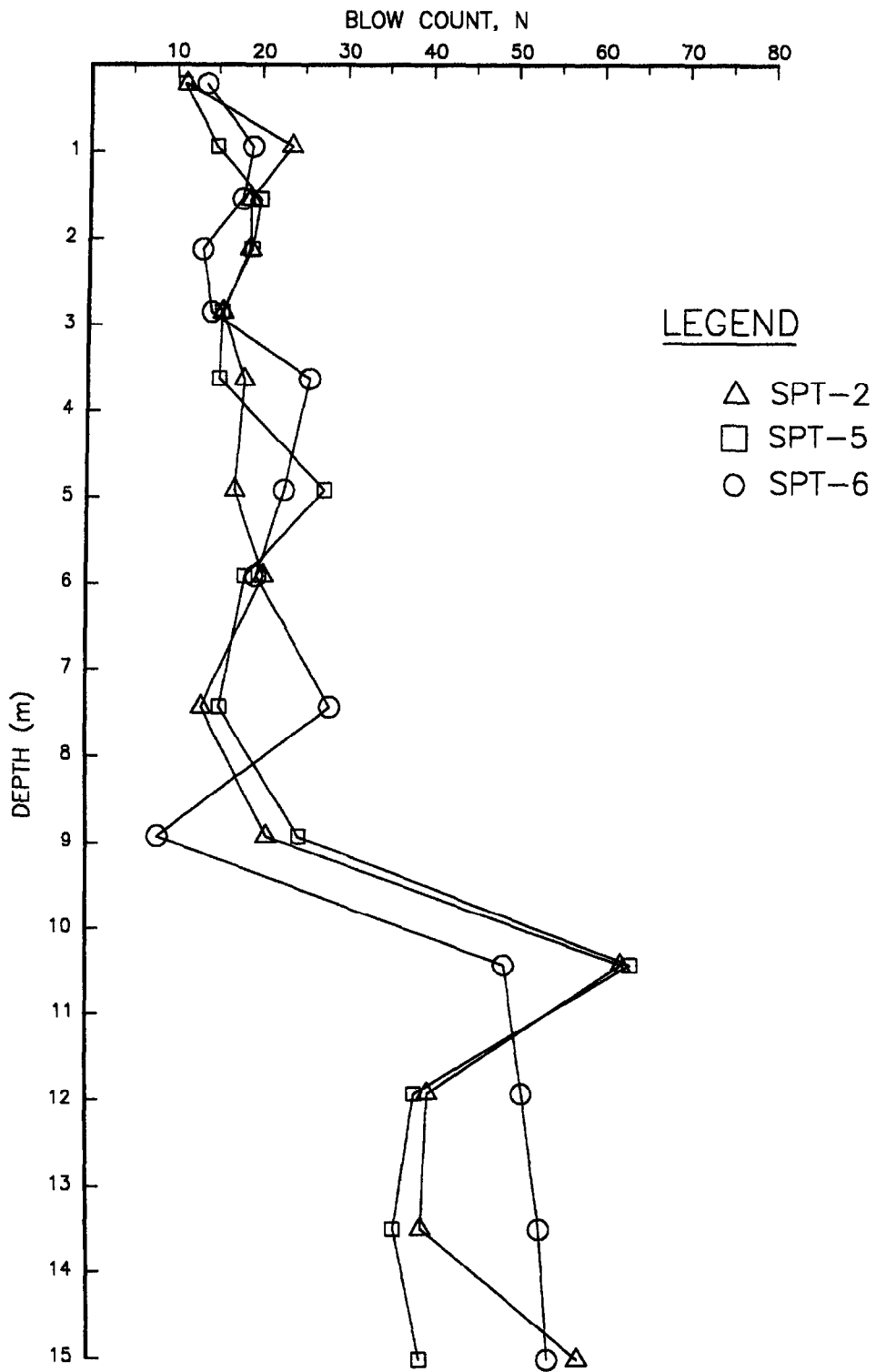


**Figure A22: Graph of Blow Counts N Versus Depth for SPT 2, 5 & 6**

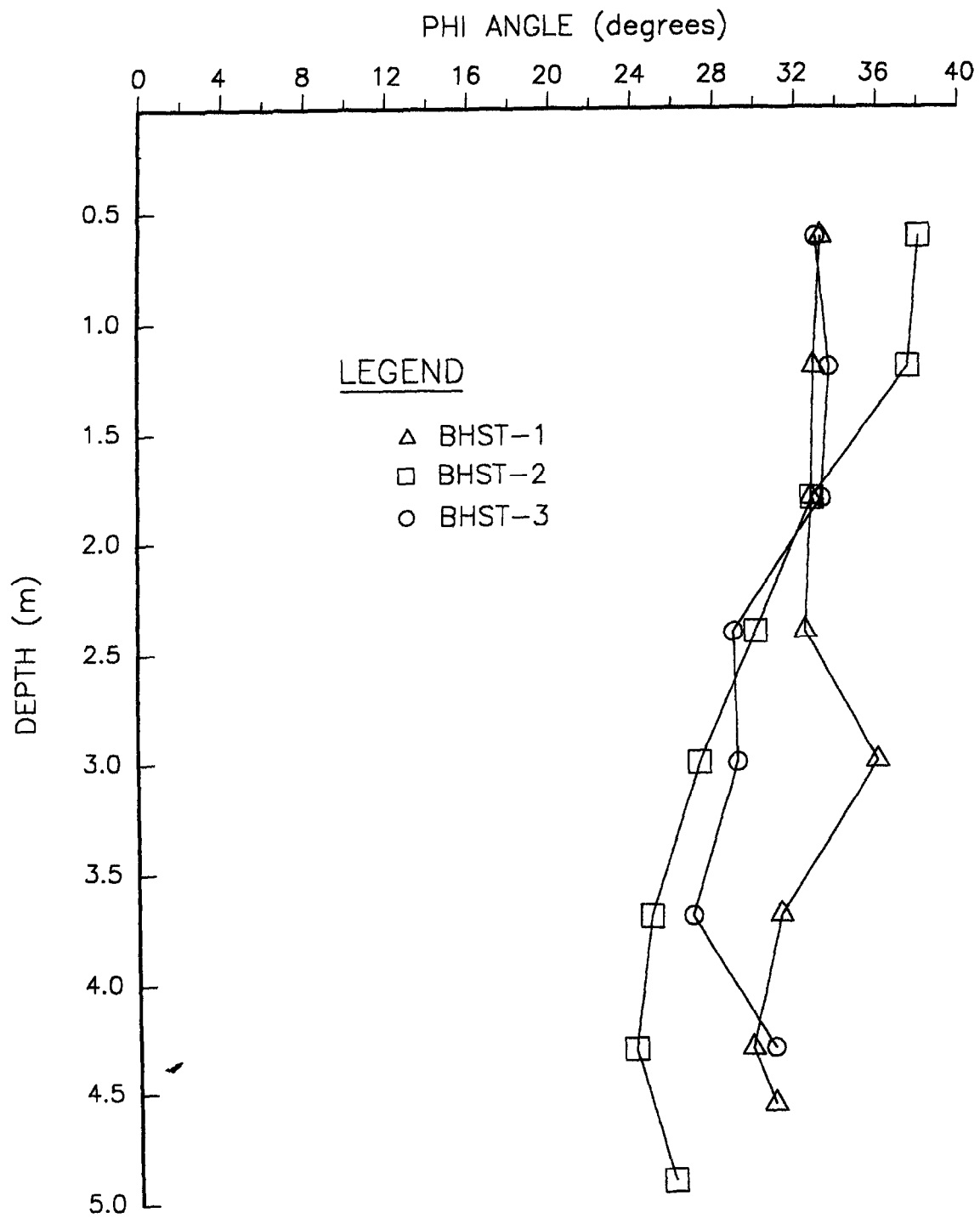


**Figure A23: Graph of  $\phi$  Versus Depth From Borehole Shear Results**

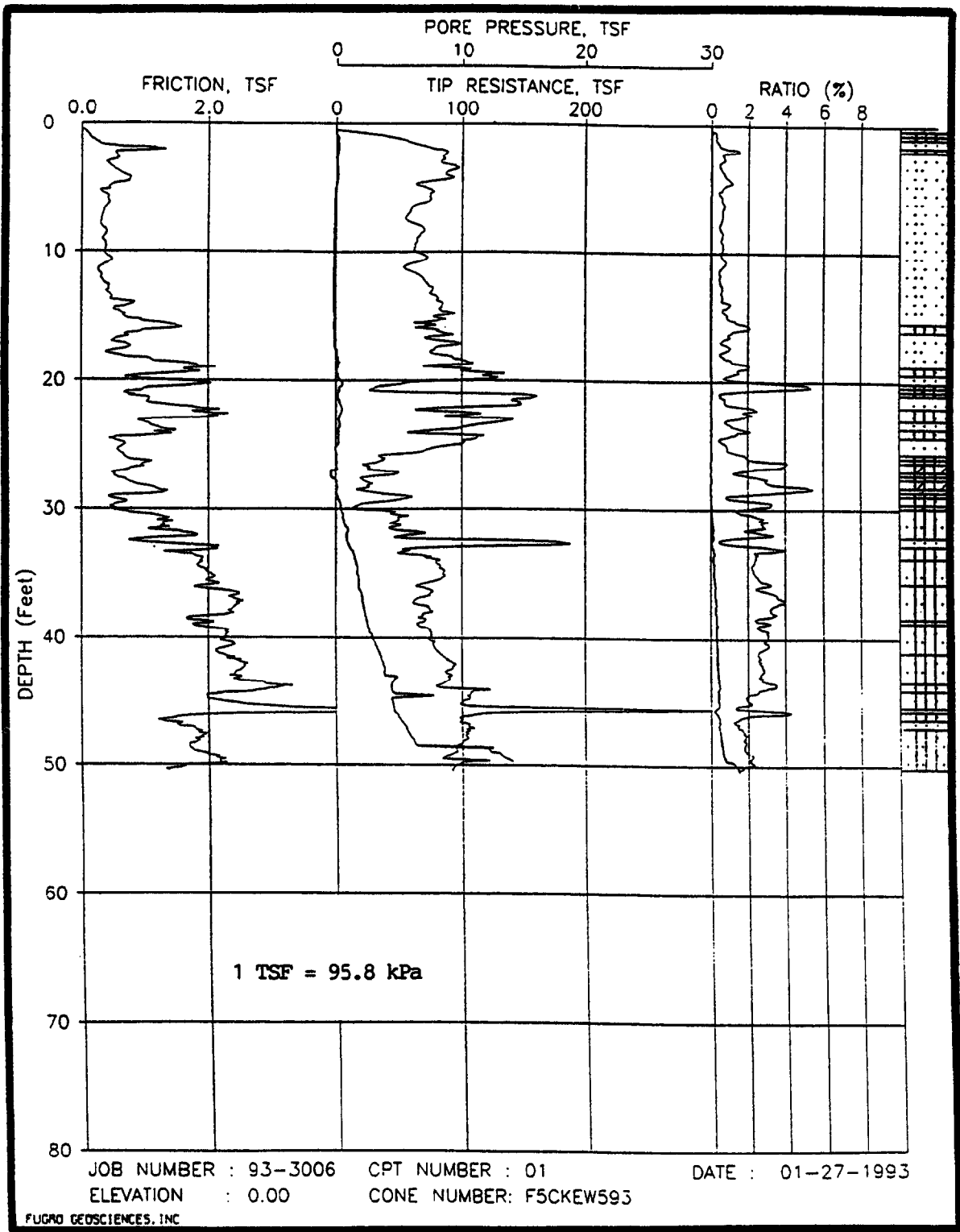


**Figure A24: Cone Penetrometer Test Results for CPT 1**

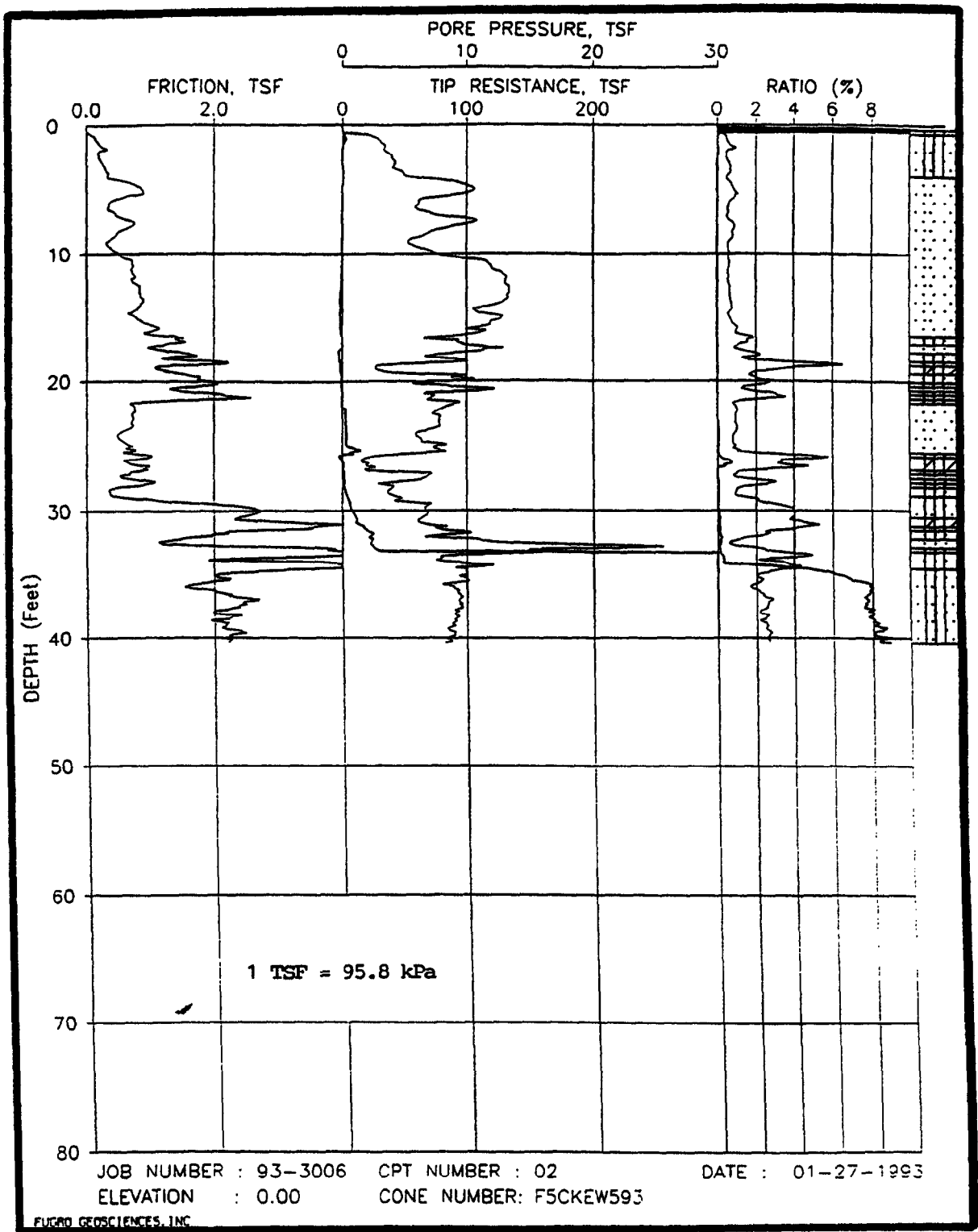


**Figure A25: Cone Penetrometer Test Results for CPT 2**

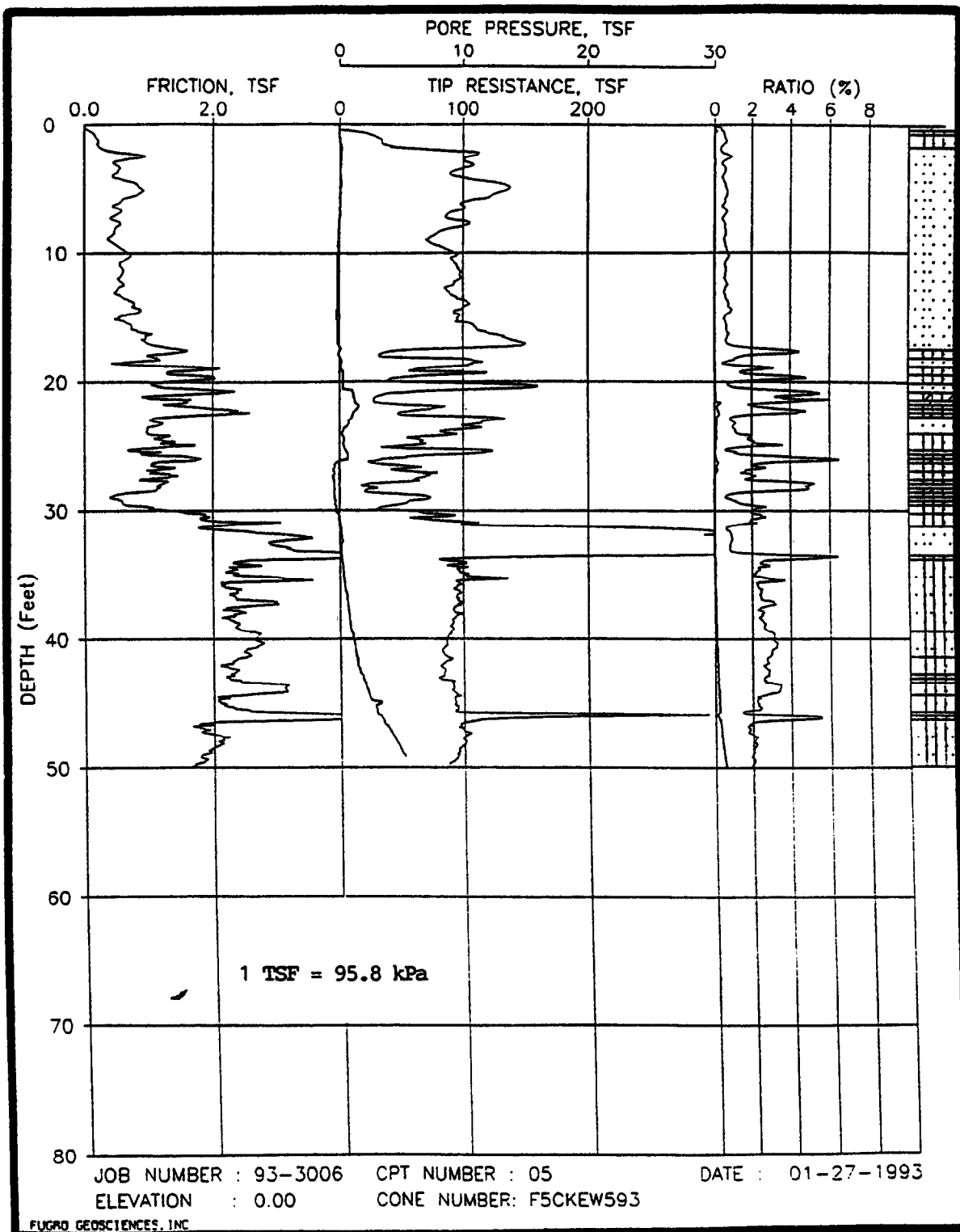


**Figure A26: Cone Penetrometer Test Results for CPT 5**

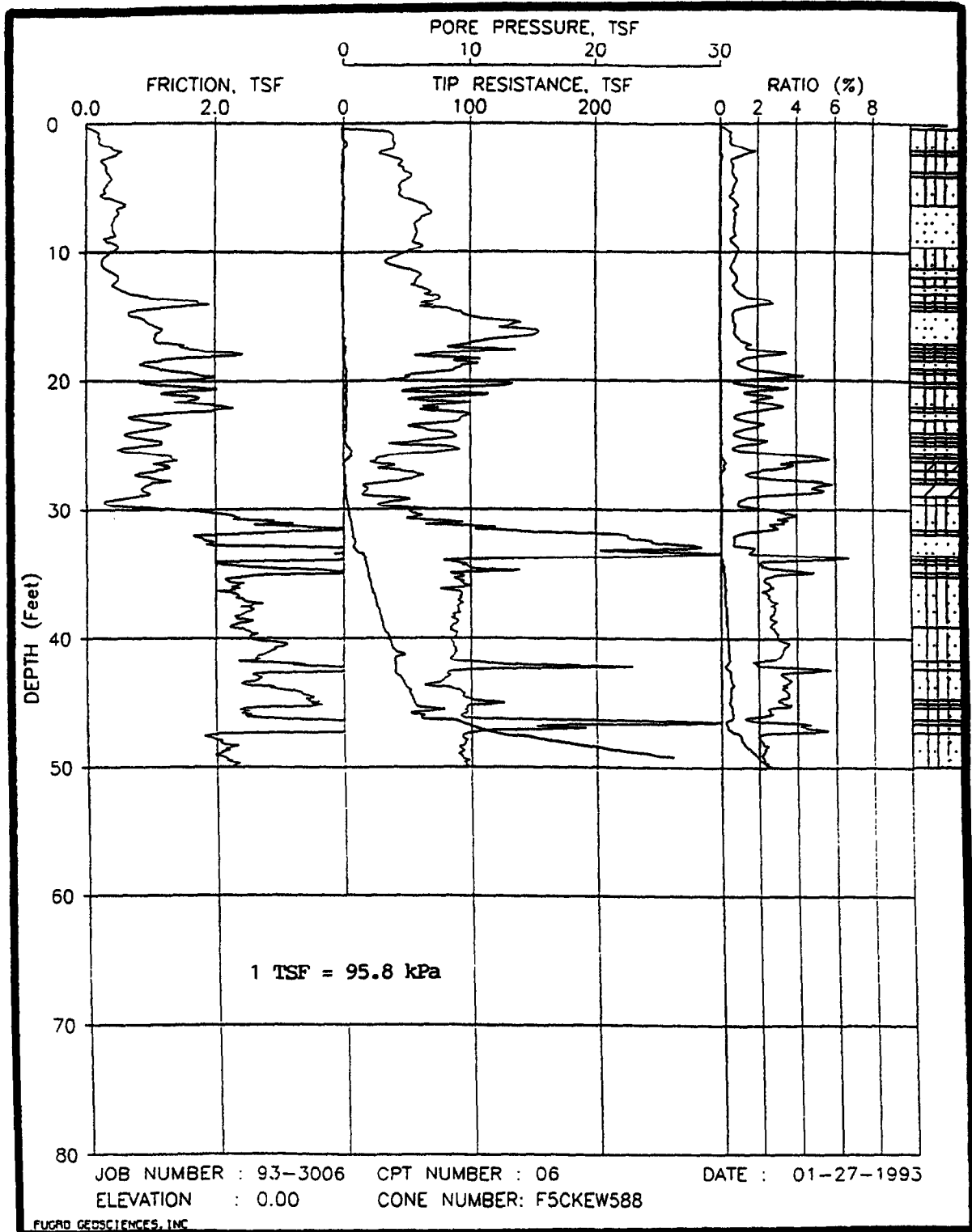


**Figure A27: Cone Penetrometer Test Results for CPT 6**

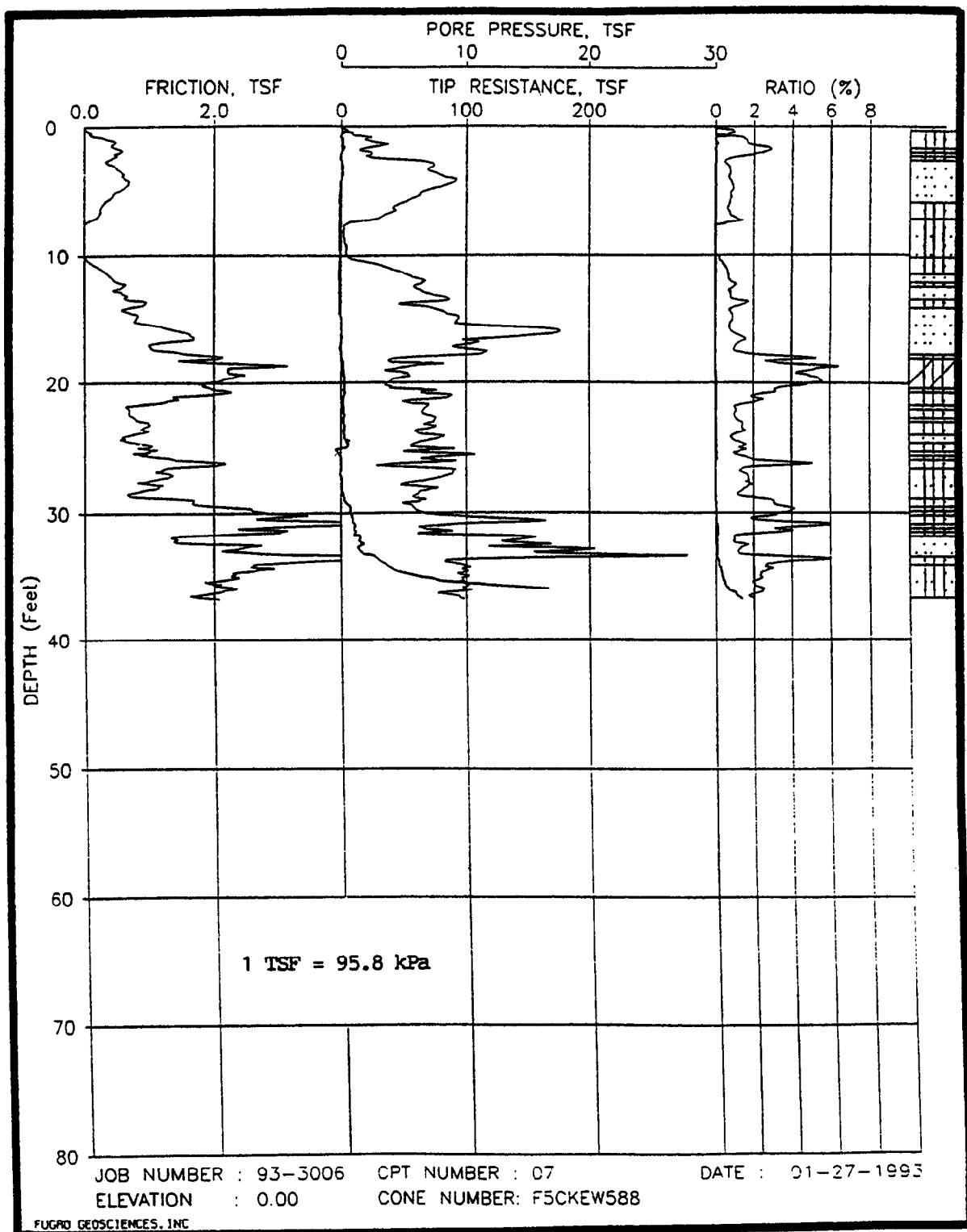


**Figure A28: Cone Penetrometer Test Results for CPT 7**

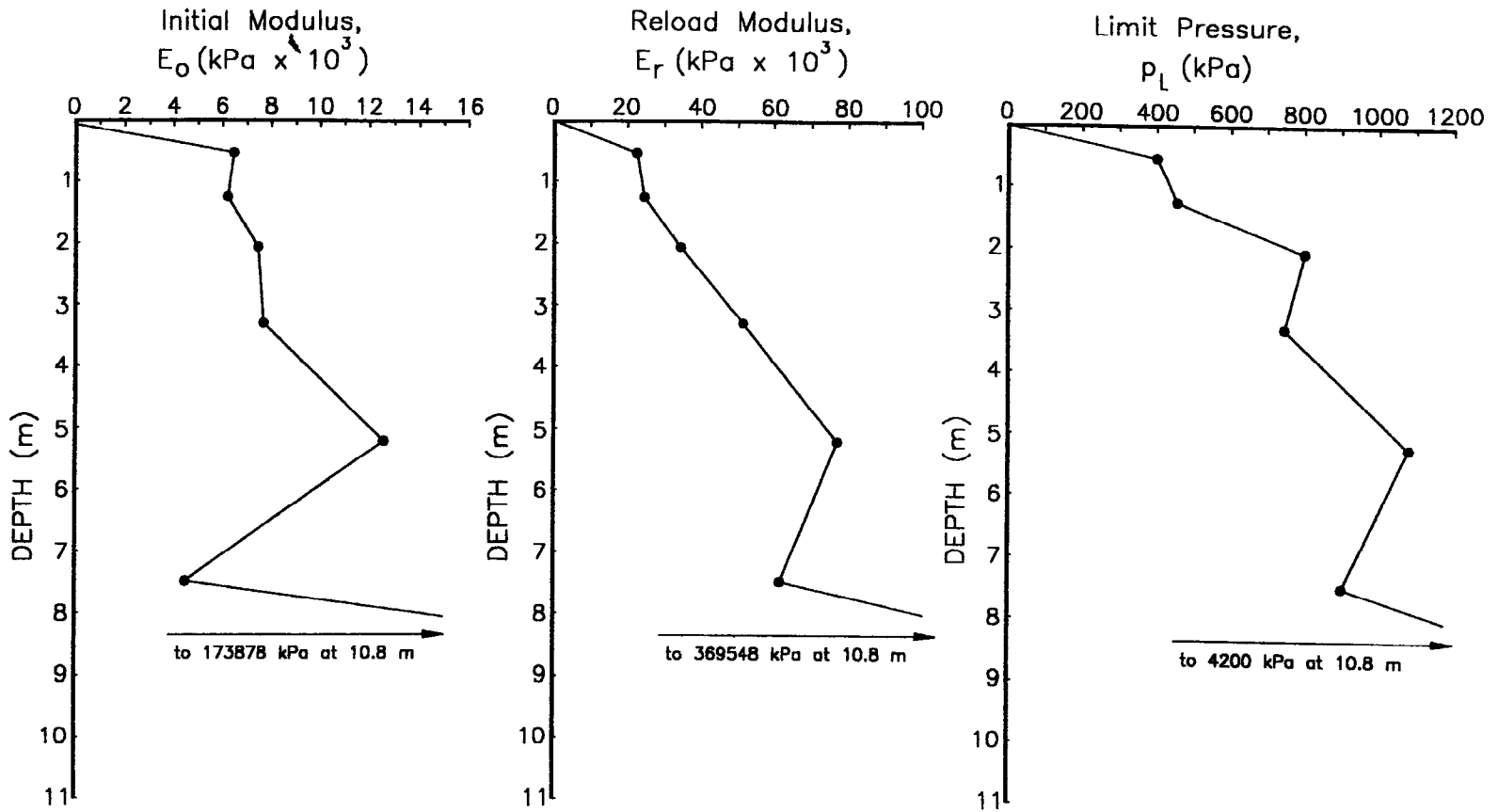


Figure A29: Pressuremeter Test Results for PMT-1

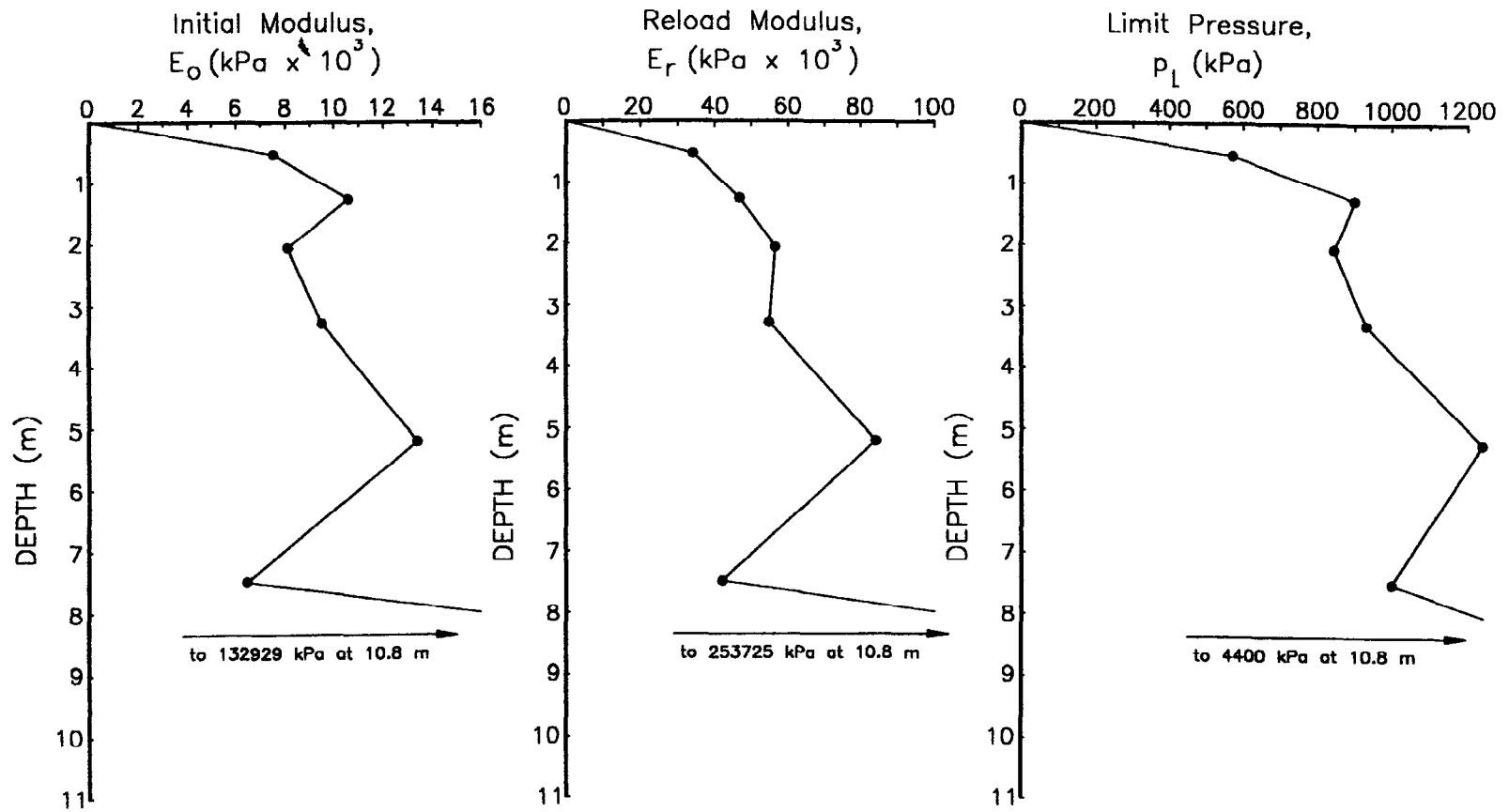


Figure A30: Pressuremeter Test Results for PMT-2

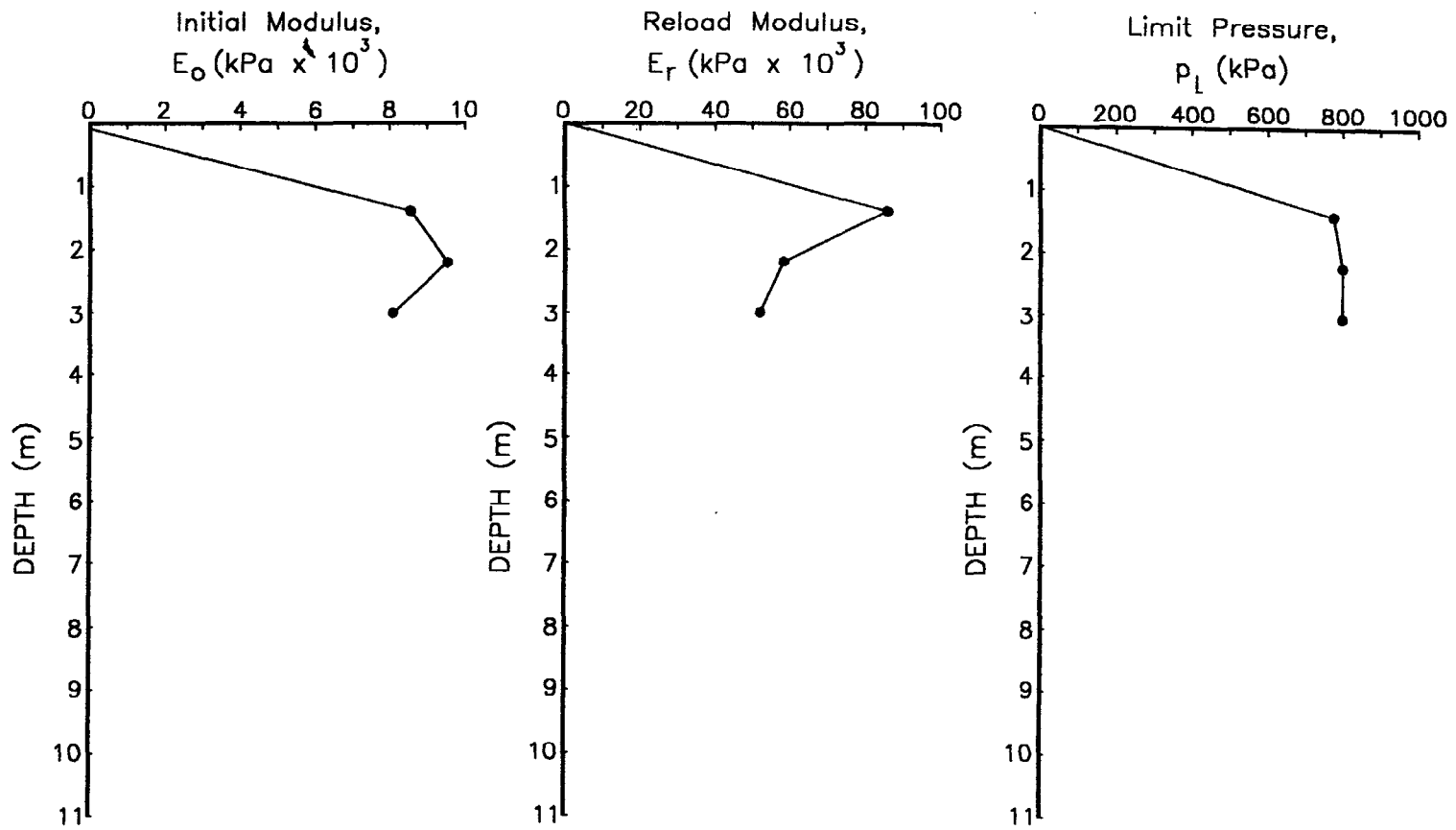
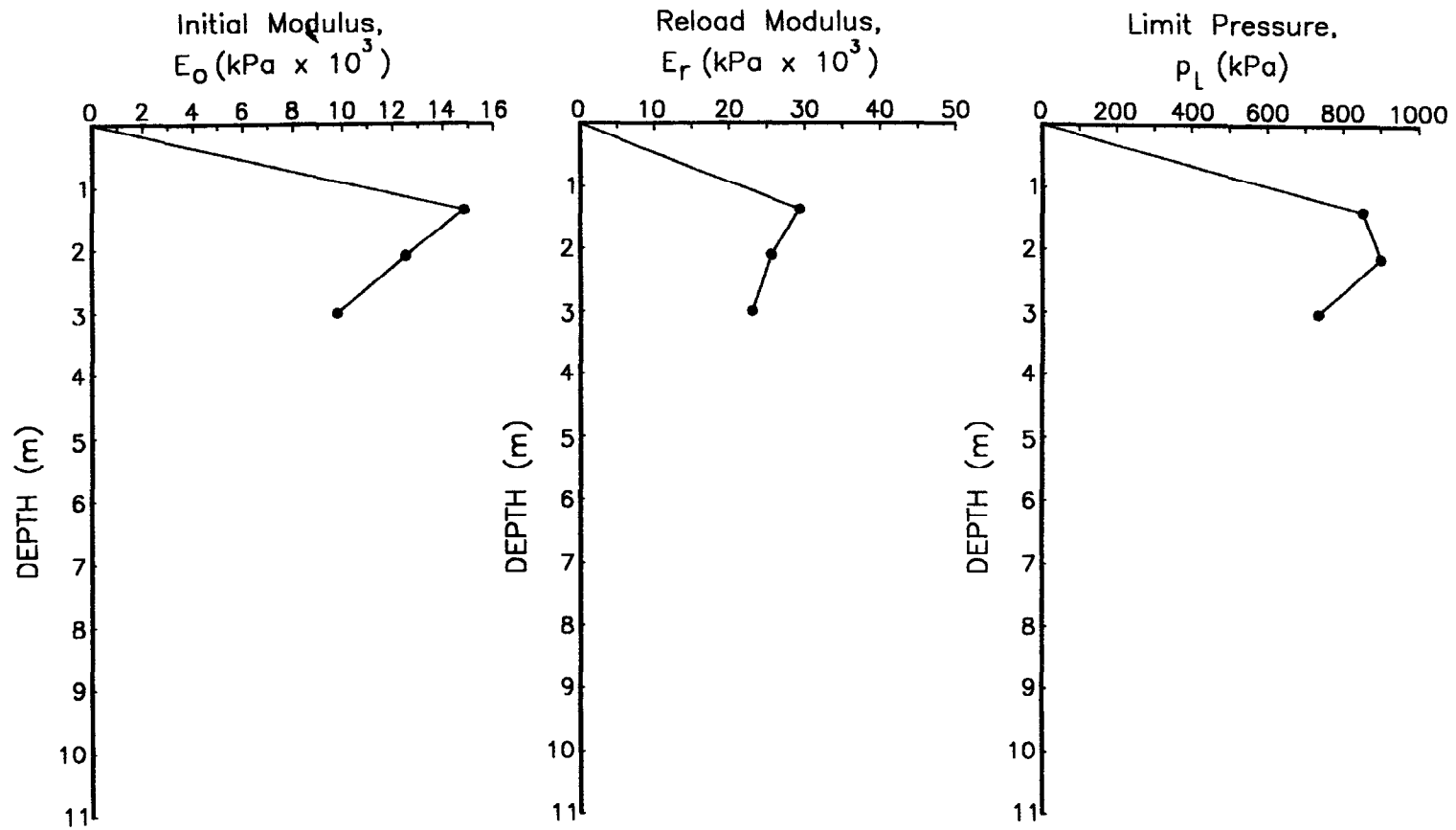


Figure A31: Pressuremeter Test Results for PMT-3



**Figure A32: Pressuremeter Test Results for PMT-4**

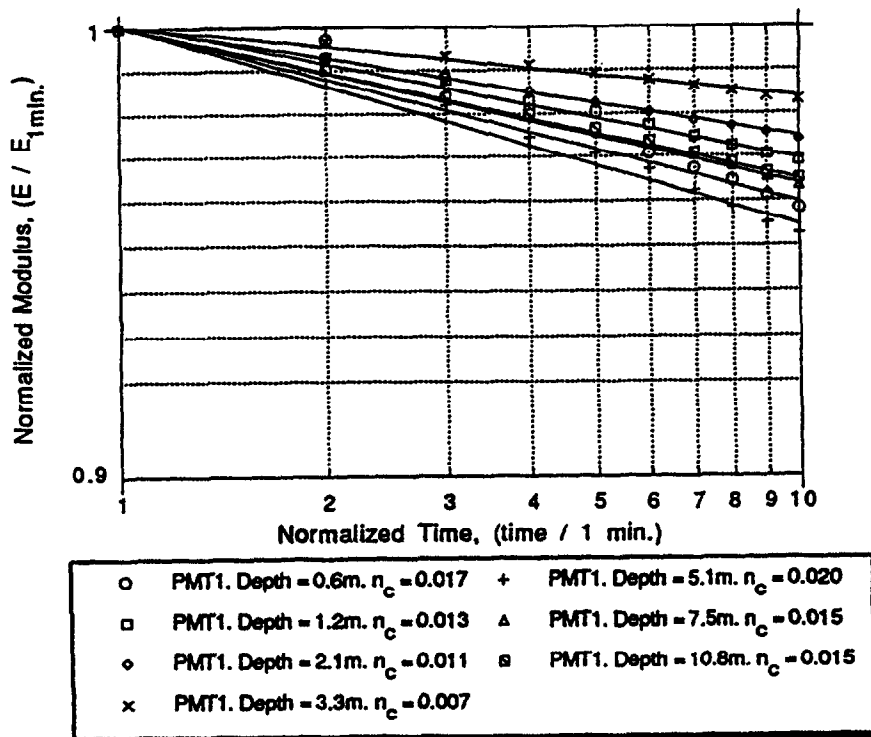


Figure A33: Determination of the Creep Exponent for PMT-1

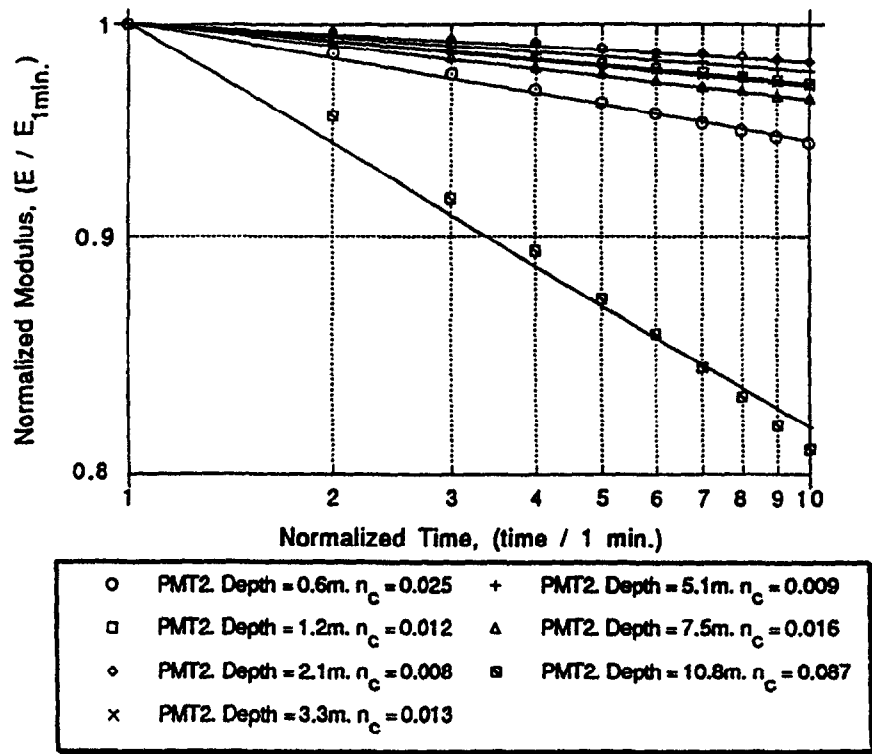


Figure A34: Determination of the Creep Exponent for PMT-2

**Table A1: Stepped Blade Test Results**

Depth (m)	CELL PRESSURE (kPa)			
	Cell-1	Cell-2	Cell-3	Cell-4
0.76	69	62	18	35
1.5	104	86	93	80
2.2	93	38	62	86
3.0	93	69	76	90
3.8	76	55	49	66
4.6	76	36	NR	73
5.3	80	35	35	45
6.1	80	73	76	40

**Table A2: Cross-Hole Test Results**

North-South direction between holes cht-2 and cht-1 (Figure 3),  
nominal surface spacing = 2.415 m

Depth (m)	Time Difference (ms)	Corrected Separation (m)	Shear Wave Velocity (m/s)	Shear Modulus (MPa)
2	10	2.398	240	104
4	8	2.397	300	162
6	8.5	2.391	281	142
8	12	2.383	199	71
10	10	2.380	238	102

East-West direction between holes cht-2 and cht-5 (Figure 3),  
nominal surface spacing = 1.924 m

Depth (m)	Time Difference (ms)	Corrected Separation (m)	Shear Wave Velocity (m/s)	Shear Modulus (MPa)
2	9.5	1.918	202	73
4	9	1.902	211	80
6	9	1.887	210	79
8	11	1.865	170	52
10	8	1.839	230	95

**Table A3: Summary of Field Results for SPT Energy Measurements**

Test Penetration D	Average Rod Top Force	Average Ram Impact Velocity	Average Ram Kinetic Energy	Average Maximum Transferred Energy (FV)	Average System Efficiency	Average Transferred Energy (FF)	Corrected Transferred Energy (ASTM D4633-86)	Average System Efficiency (FF)	Operating Speed	SPT Blow Count
Rod Length R	(kN)	(m/s)	(kN-m)	(kN-m)	%	(kN-m)	(kN-m)	%	(bpm)	bl/150 mm
D=0.8-1.2 R=2.4	74.3	3.0	0.28	0.24	51	0.07	0.117	23?	48	7/10/13
D=1.4-1.8 R=2.4	76.1	2.9	0.27	0.22	45	0.15	0.26	54	48	8/8/10
D=2.0-2.4 R=4.0	70.8	3.0	0.28	0.23	48	0.15	0.26	54	49	6/9/9
D=2.6-3.0 R=4.0	71.6	3.0	0.28	0.26	54	0.16	0.22	46	47	4/8/8
D=3.5-4.0 R=5.5	66.8	2.8	0.26	0.18	38	0.19	0.22	46	50	10/10/9
D=4.6-5.0 R=5.5	71.6	3.0	0.28	0.23	49	0.20	0.23	49	48	7/9/8
D=5.6-6.1 R=7.0	76.5	3.0	0.27	0.23	48	0.23	0.26	53	50	7/10/11
D=7.2-7.6 R=8.5	71.2	2.9	0.26	0.26	54	0.23	0.24	51	47	5/6/8
D=8.7-9.1 R=10.1	73.9	3.0	0.28	0.23	49	0.24	0.24	51	48	6/8/13
D=10.2-10.7 R=11.6	70.3	2.7	0.24	0.23	49	0.26	0.26	54	50	11/24/39
D=11.7-12.2 R=13.1	77.0	2.8	0.24	0.24	51	0.28	0.28	60	48	11/16/24
D=13.3-13.7 R=14.6	76.1	2.9	0.27	0.28	59	0.28	0.28	60	46	14/17/22
D=14.8-15.2 R=16.2	75.7	2.8	0.24	0.24	51	0.27	0.27	57	50	18/25/32
							E(avg) = 0.25	e(avg) = 53		

**Table A4: Physical Properties**

Property	Sand 0.6 m	Sand 3.0 m
Specific Gravity	2.64	2.66
Minimum Void Ratio	0.65	0.62
Maximum Void Ratio	0.94	0.91
Maximum Dry Unit Weight (kN/m <sup>3</sup> )	15.70	16.10
Minimum Dry Unit Weight (kN/m <sup>3</sup> )	13.35	13.66
Liquid Limit	N/P	N/P
Plastic Limit	-	-
USCS Classification	SP	SP-SM
Natural Void Ratio ?	0.78	0.75
Dry Unit Weight ? (kN/m <sup>3</sup> )	14.55	14.91
Natural Moisture Content (%)	5.0	5.0
Natural Unit Weight ? (kN/m <sup>3</sup> )	15.28	15.65

**Table A5: Moisture Content with Depth for SPT 2 & 3**

BORING NO.	DEPTH IN METERS	MOISTURE CONTENT (%)	BORING NO.	DEPTH IN METERS	MOISTURE CONTENT (%)
SPT-2	0-0.46	14.3	SPT-3	0-0.46	11.9
	0.76-1.2	13.0		0.76-1.2	12.1
	1.4-1.8	17.2		1.4-1.8	15.5
	2.0-2.4	19.2		2.0-2.4	18.3
	2.6-3.0	21.8		2.6-3.0	21.5
	3.5-4.0	16.3		3.5-4.0	21.1
	4.7-5.2	16.6		4.7-5.2	19.2
	5.6-6.1	27.7		5.6-6.1	25.4
	7.2-7.6	29.2		7.2-7.6	29.3
	8.7-9.1	27.4		8.7-9.1	23.0
	10.2-10.7	27.0		10.2-10.7	30.9
	11.7-12.2	27.5		11.7-12.2	34.0
	13.3-13.7	27.2		13.3-13.7	21.9
	14.8-15.2	22.1		14.8-15.2	25.8

**Table A6: Moisture Content with Depth for SPT 4 & 5**

BORING NO.	DEPTH IN METERS	MOISTURE CONTENT (%)	BORING NO.	DEPTH IN METERS	MOISTURE CONTENT (%)
SPT-4	0-0.46	16.8	SPT-5	0-0.46	14.4
	0.76-1.2	11.6		0.76-1.2	13.0
	1.4-1.8	11.8		1.4-1.8	14.0
	2.0-2.4	14.1		2.0-2.4	20.5
	2.6-3.0	19.0		2.6-3.0	17.6
	3.5-4.0	20.9		3.5-4.0	16.6
	4.7-5.2	20.7		4.7-5.2	16.6
	5.6-6.1			5.6-6.1	19.4
	7.2-7.6	33.5		7.2-7.6	29.7
	8.7-9.1	20.9		8.7-9.1	29.6
	10.2-10.7	32.6		10.2-10.7	26.7
	11.7-12.2	36.7		11.7-12.2	29.3
	13.3-13.7	28.5		13.3-13.7	32.1
	14.8-15.2	21.7		14.8-15.2	25.1

**Table A7: Moisture Content with Depth for SPT 6**

BORING NO.	DEPTH IN METERS	MOISTURE CONTENT (%)
SPT-6	0-0.46	15.9
	0.76-1.2	12.4
	1.4-1.8	11.1
	2.0-2.4	20.5
	2.6-3.0	18.9
	3.5-4.0	18.3
	4.7-5.2	18.7
	5.6-6.1	12.2
	7.2-7.6	31.2
	8.7-9.1	-
	10.2-10.7	28.6
	11.7-12.2	29.0
	13.3-13.7	30.7
	14.8-15.2	23.4

## **APPENDIX B: Load-Settlement Curves**

# Load Settlement Curve - 1.0 M Footing

## Average Total History Curve

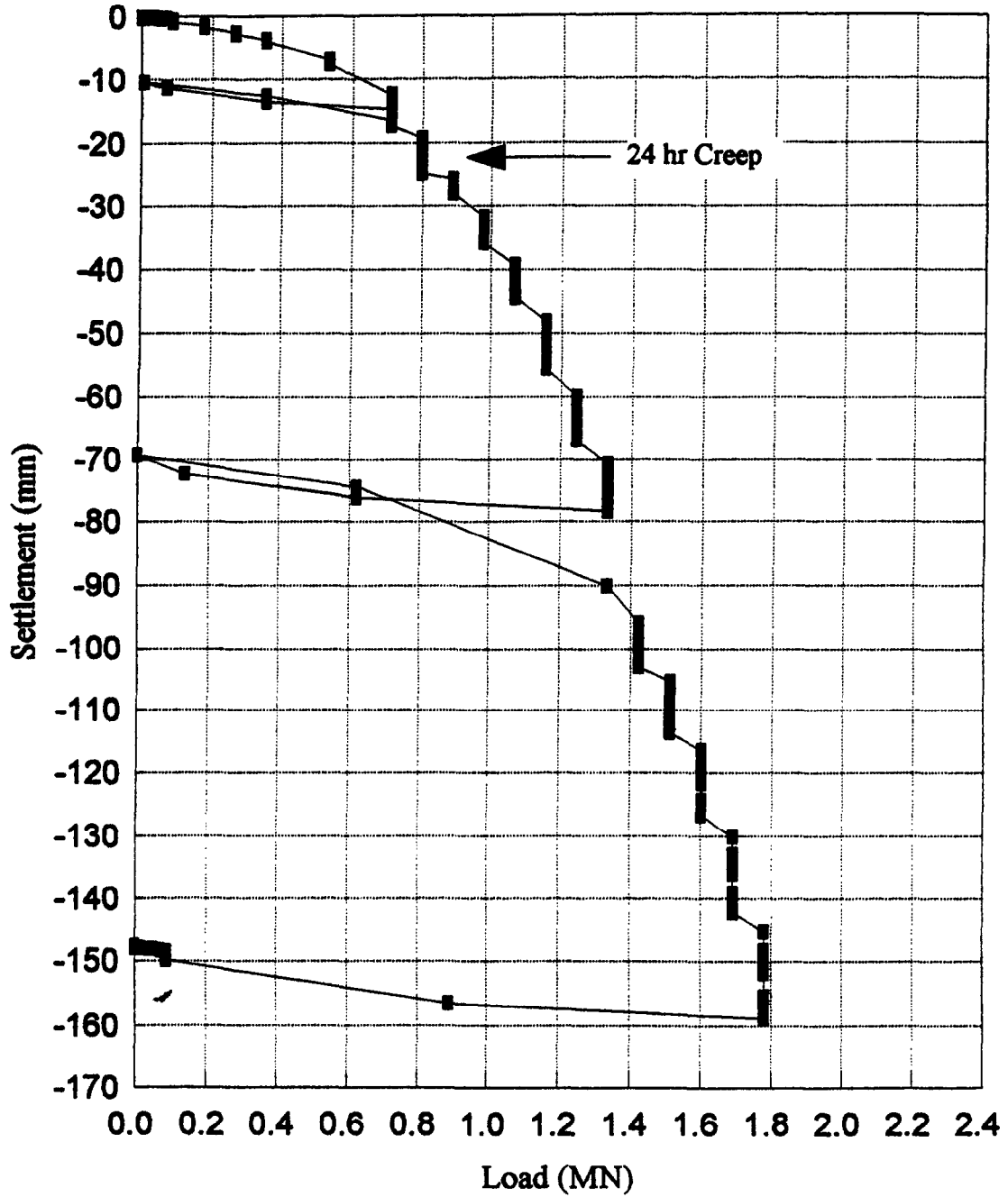


Figure B1: Load Settlement Curve for 1.0-m Footing - Total History

# Load Settlement Curve - 1.0 M Footing Average 30 Minute Curve

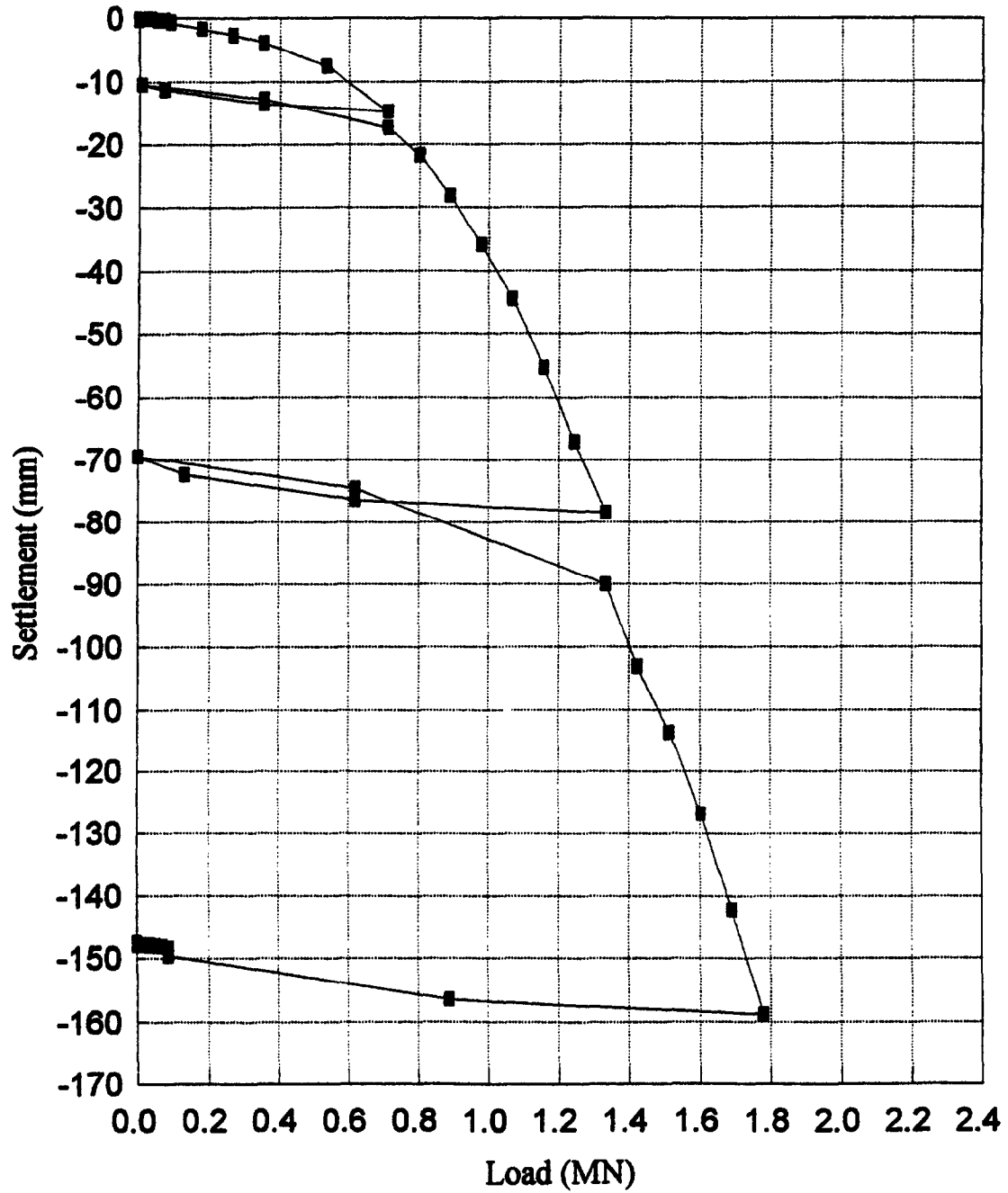


Figure B2: Load Settlement Curve for 1.0-m Footing - Avg. 30-min Curve

# Load Settlement Curve - 1.5 M Footing Average Total History Curve

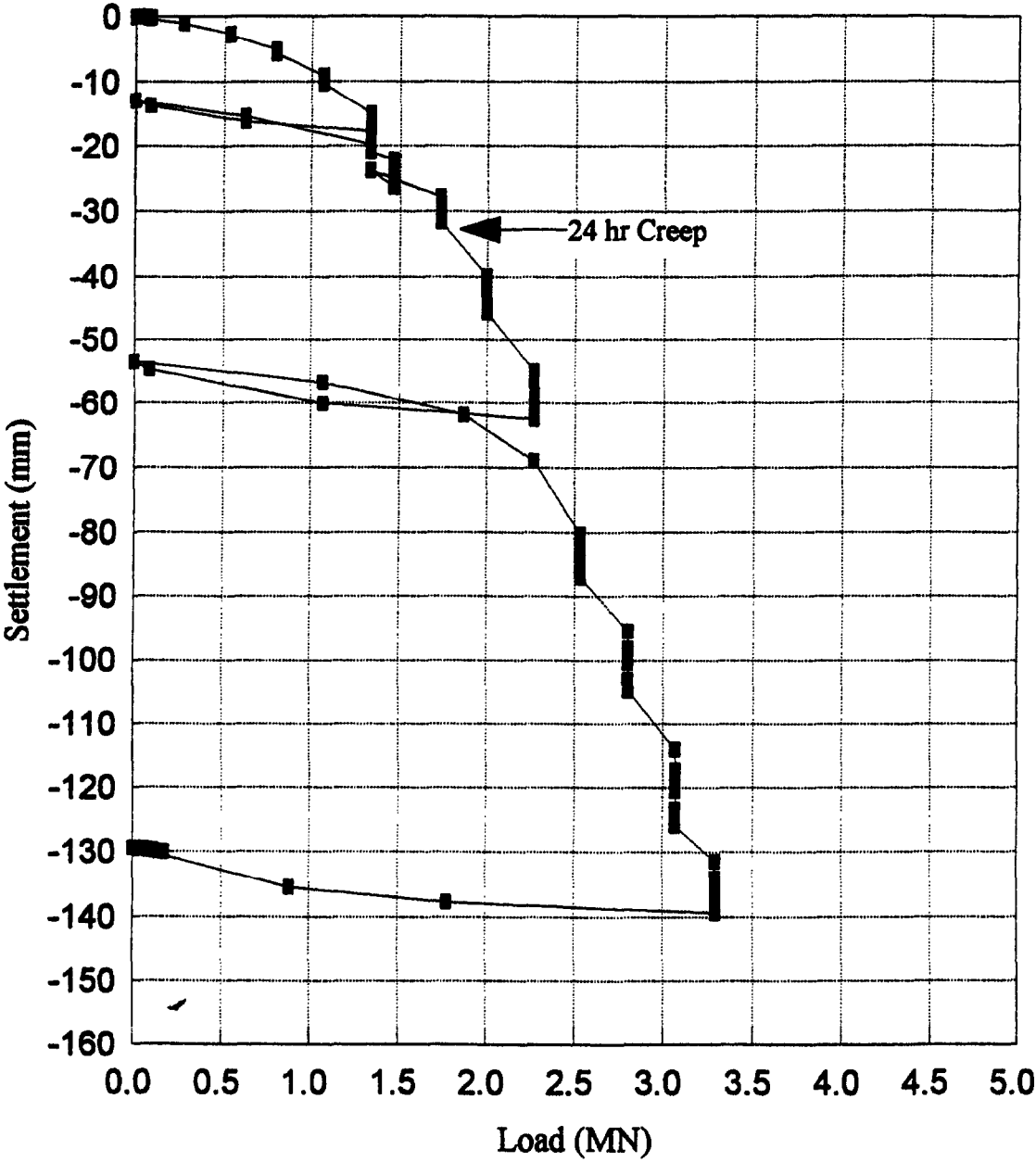


Figure B3: Load Settlement Curve for 1.5-m Footing - Total History

## Load Settlement Curve - 1.5 M Footing Average 30 Minute Curve

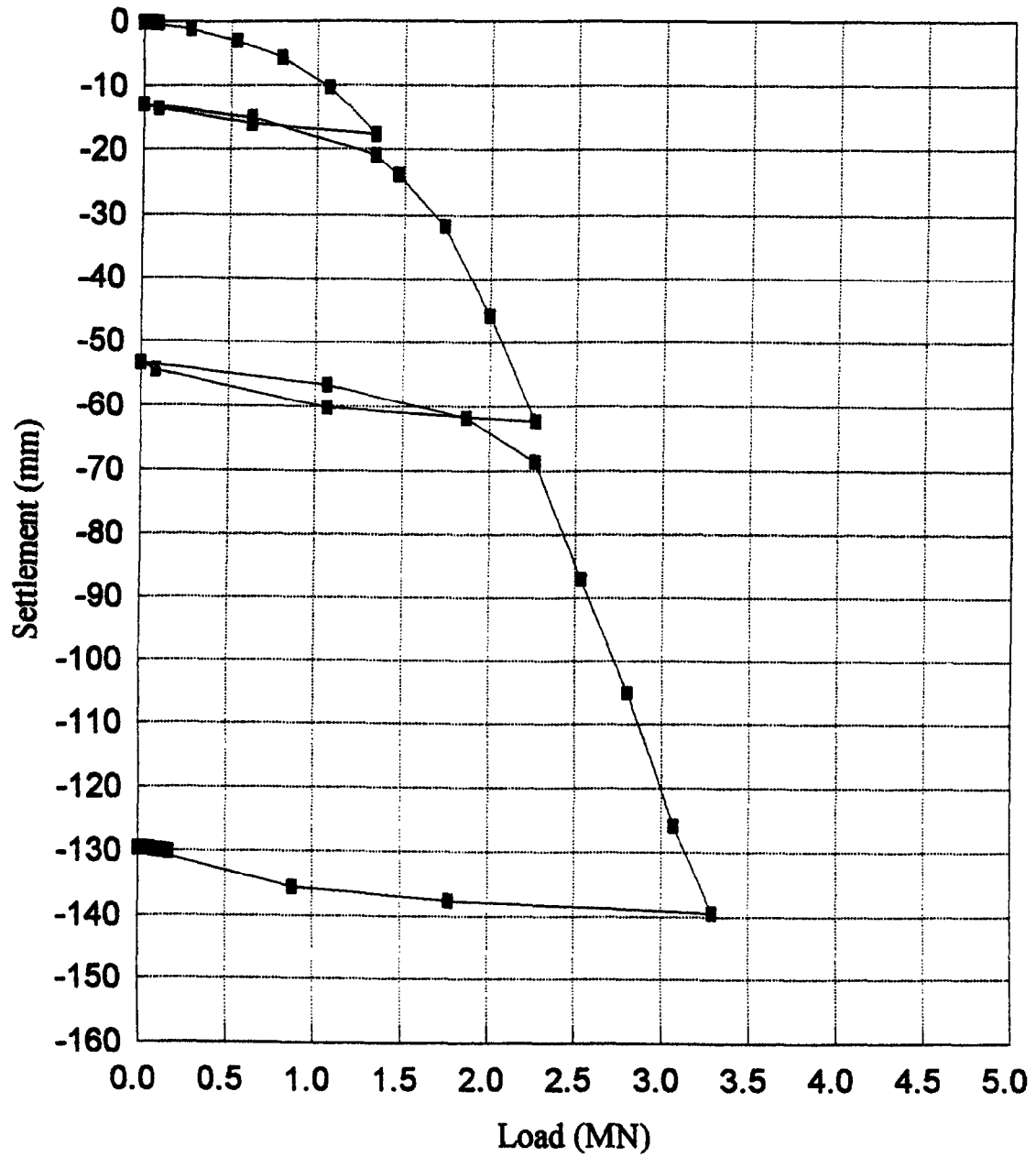
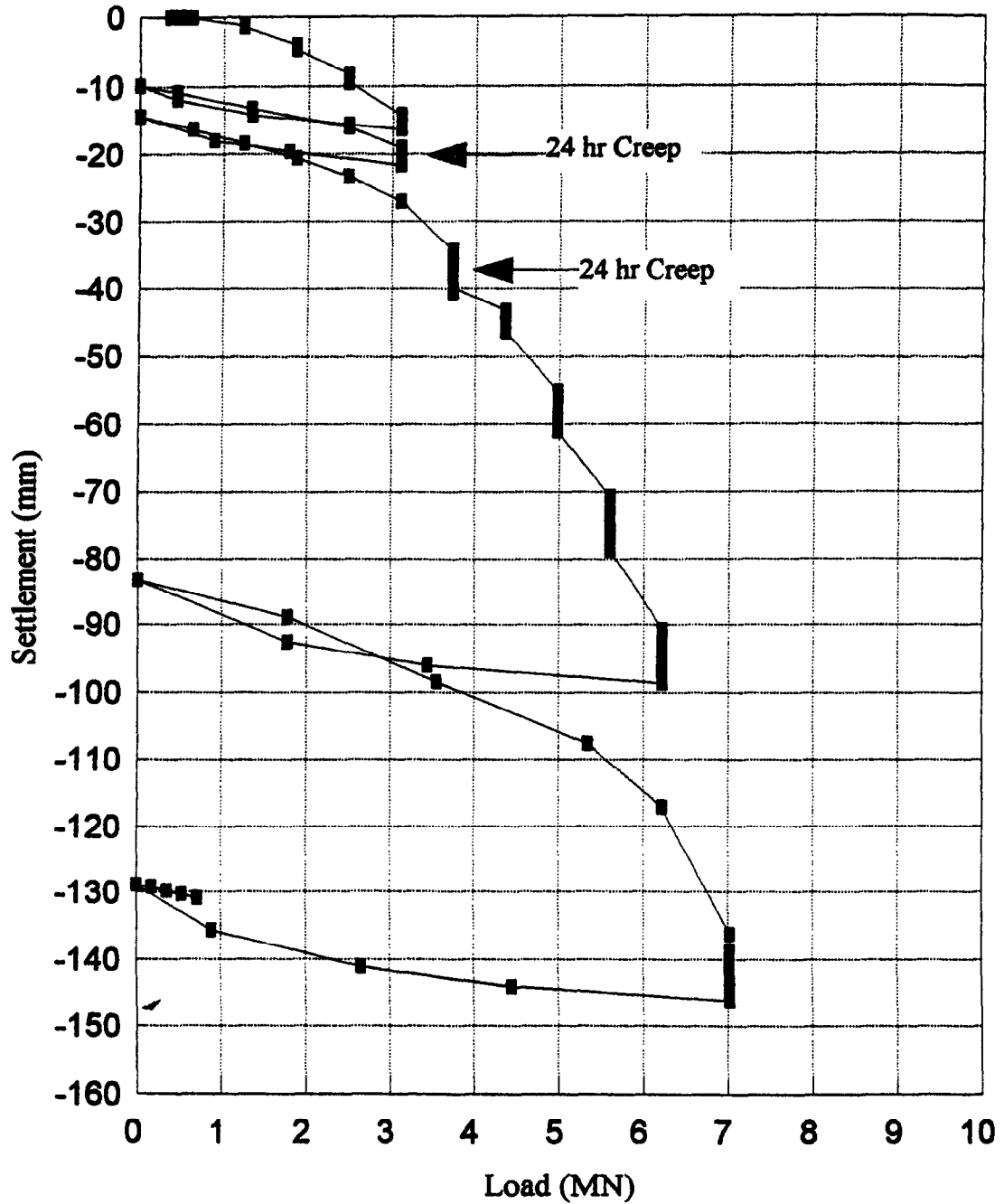


Figure B4: Load Settlement Curve for 1.5-m Footing - Avg. 30-Minute Curve

## Load Settlement Curve - 2.5 M Footing Average Total History Curve



**Figure B5:** Load Settlement Curve for 2.5-m Footing - Total History

# Load Settlement Curve - 2.5 M Footing Average 30 Minute Curve

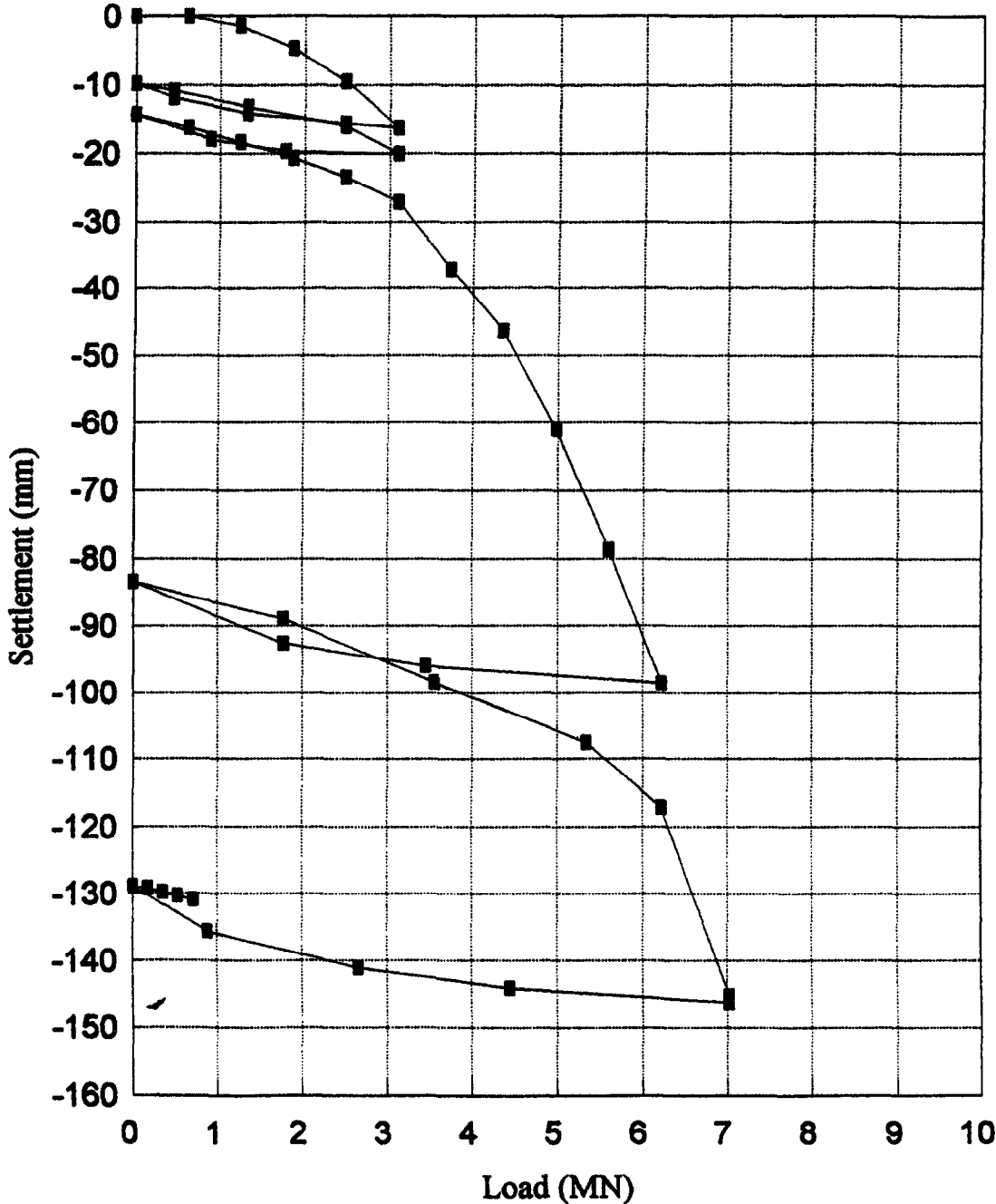
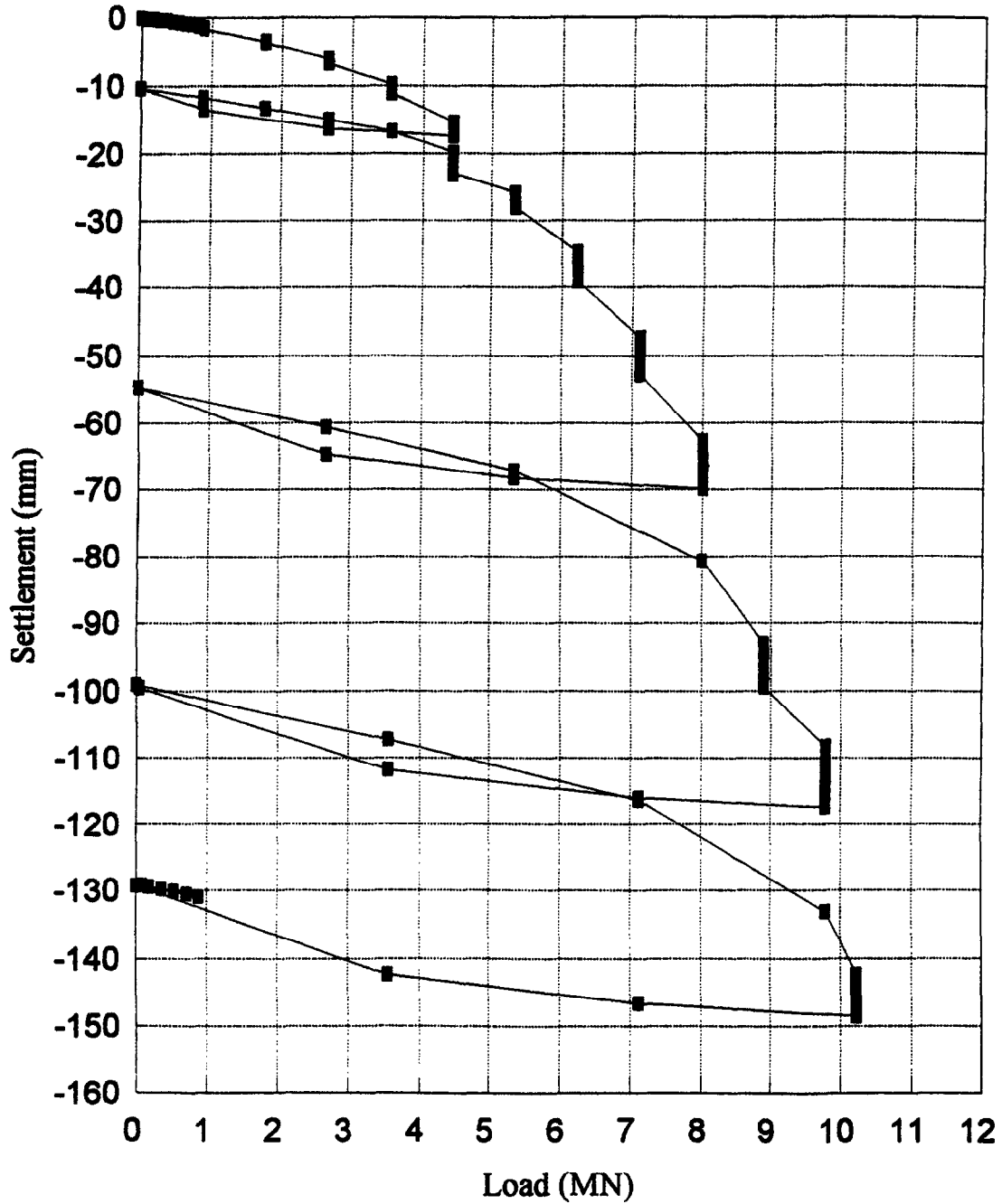


Figure B6: Load Settlement Curve for 2.5-m Footing - Avg. 30-Minute Curve

# Load Settlement Curve - 3.0 M Footing

## Average Total History Curve

NORTH



**Figure B7:** Load Settlement Curve for 3.0-m(n) Footing - Total History

# Load Settlement Curve - 3.0 M Footing

## Average 30 Minute Curve

NORTH

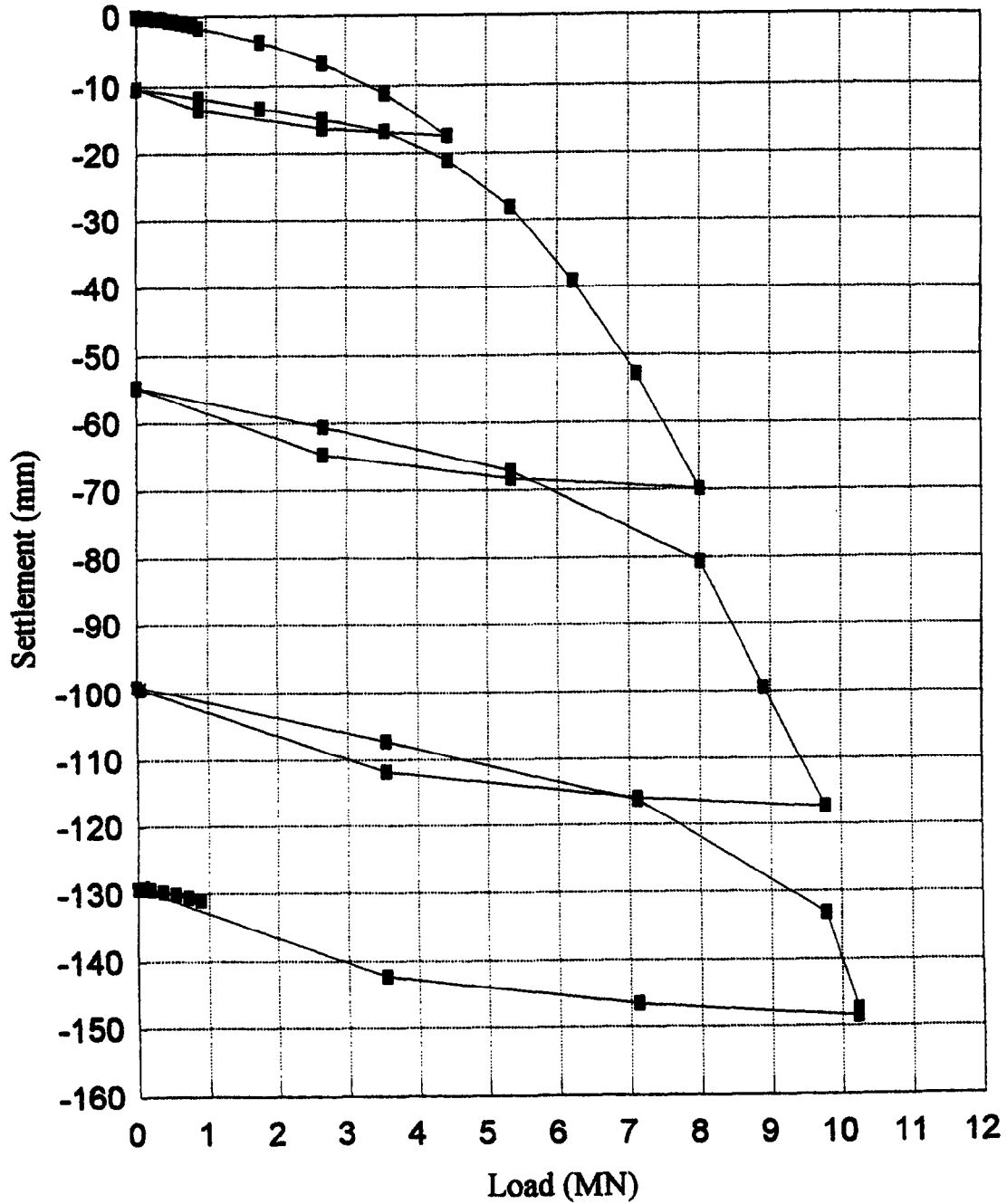
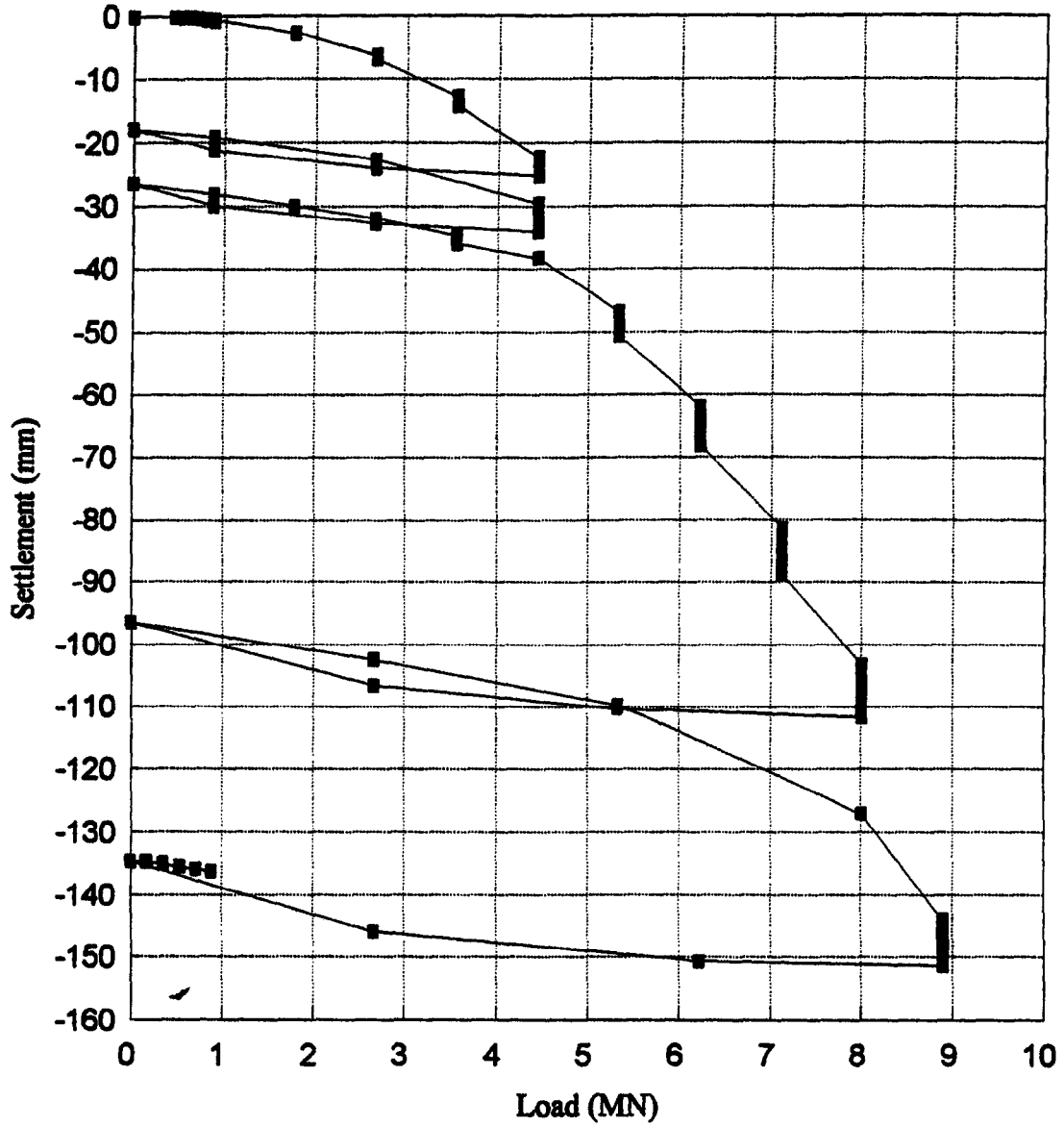


Figure B8: Load Settlement for 3.0-m(n) Footing - Avg. 30 Minute Curve

**Load Settlement Curve - 3.0 M Footing**  
**Average Total History Curve**

SOUTH



**Figure B9: Load Settlement Curve for 3.0-m(s) Footing - Total History**

# Load Settlement Curve - 3.0 M Footing

## Average 30 Minute Curve

SOUTH

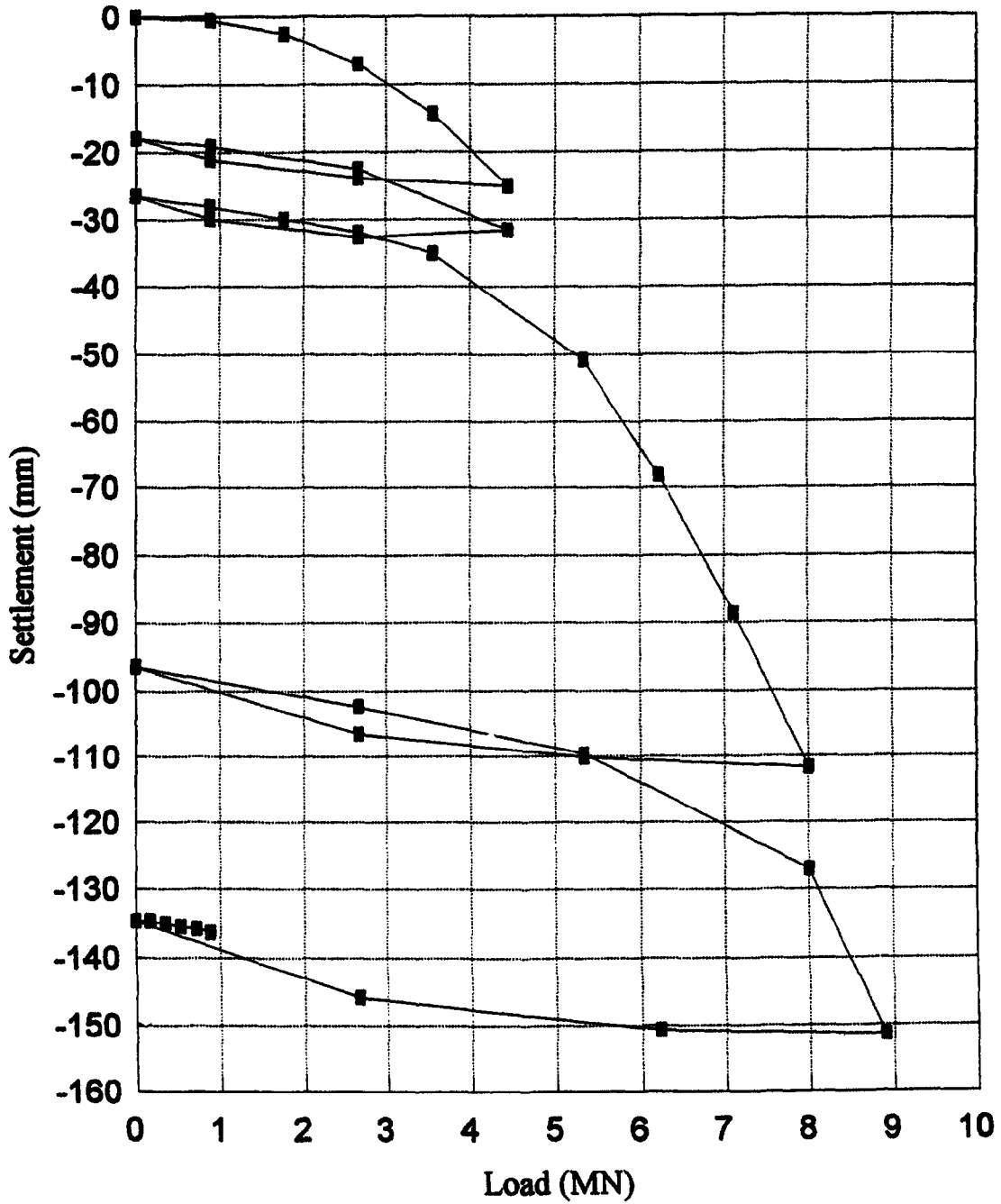
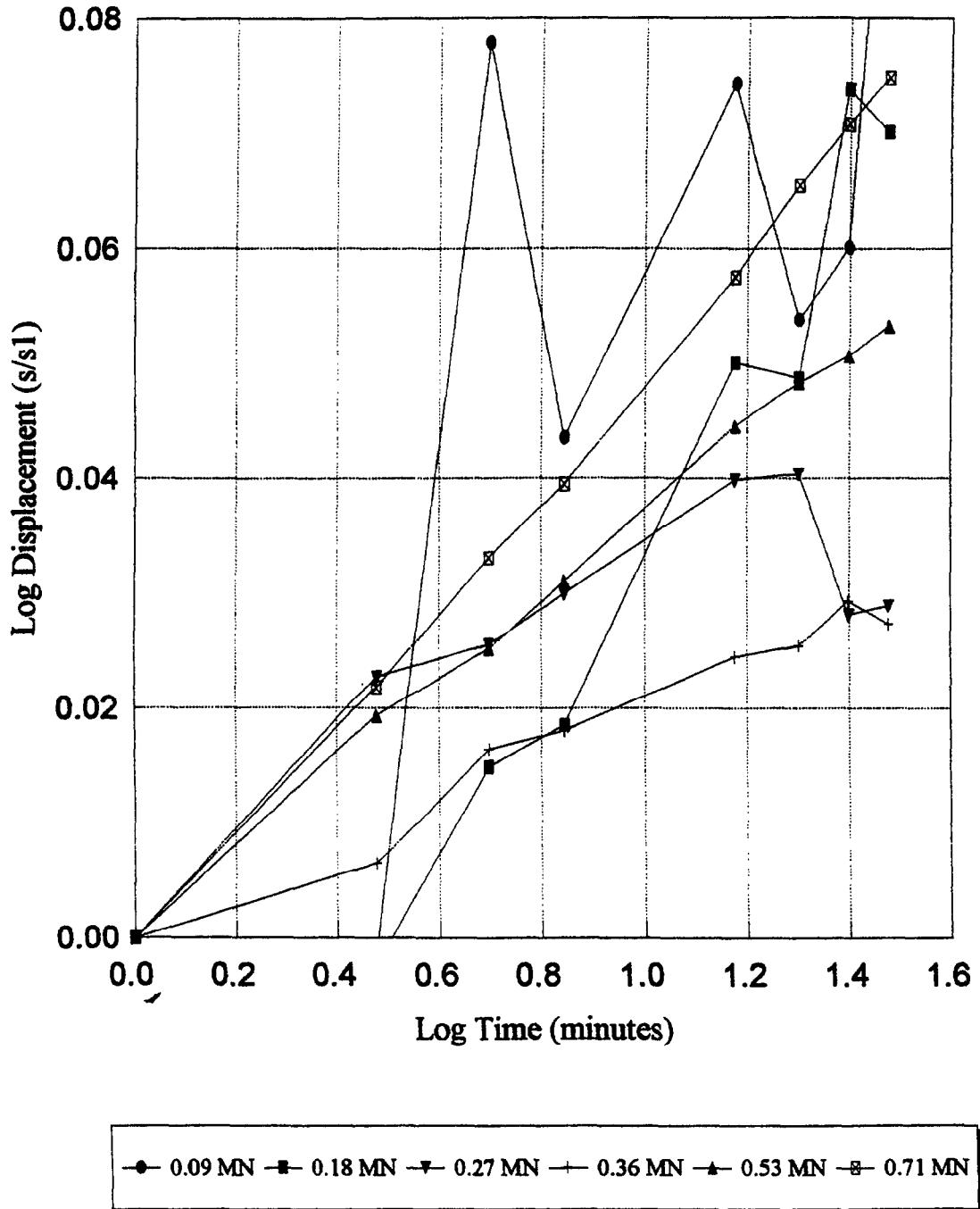


Figure B10: Load Settlement Curve for 3.0-m(s) Footing - Avg. 30-Minute Curve

## **APPENDIX C: Creep Curves**

# Individual Creep Exponent Curves 1.0 M Footing



**Figure C1:** Individual Creep Exponent Curves for 1.0-m Footing, 0.09 MN - 0.71 MN

# Individual Creep Exponent Curves 1.0 M Footing

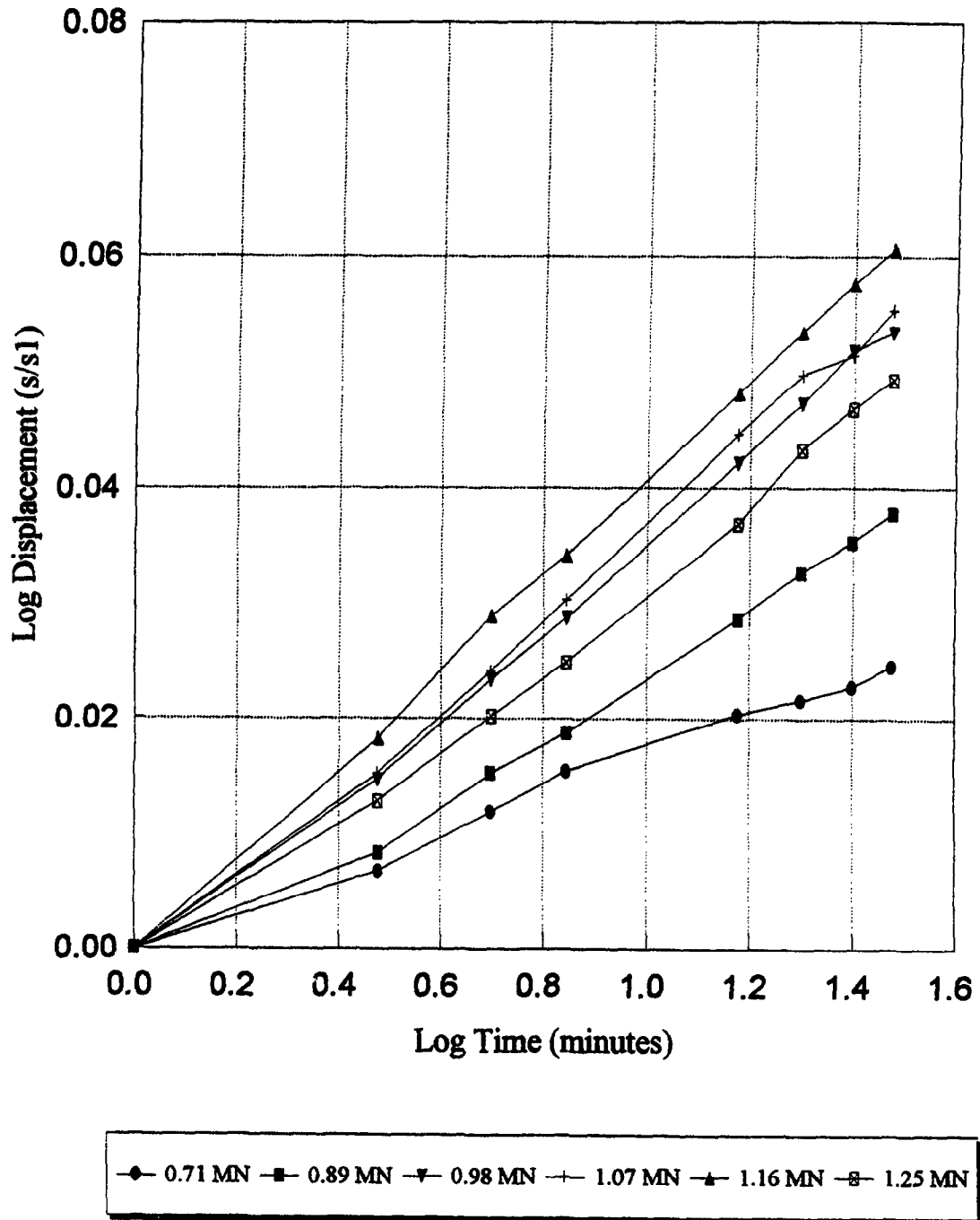


Figure C2: Individual Creep Exponent Curves for 1.0-m Footing, 0.71 MN - 1.25 MN

# Individual Creep Exponent Curves 1.0 M Footing

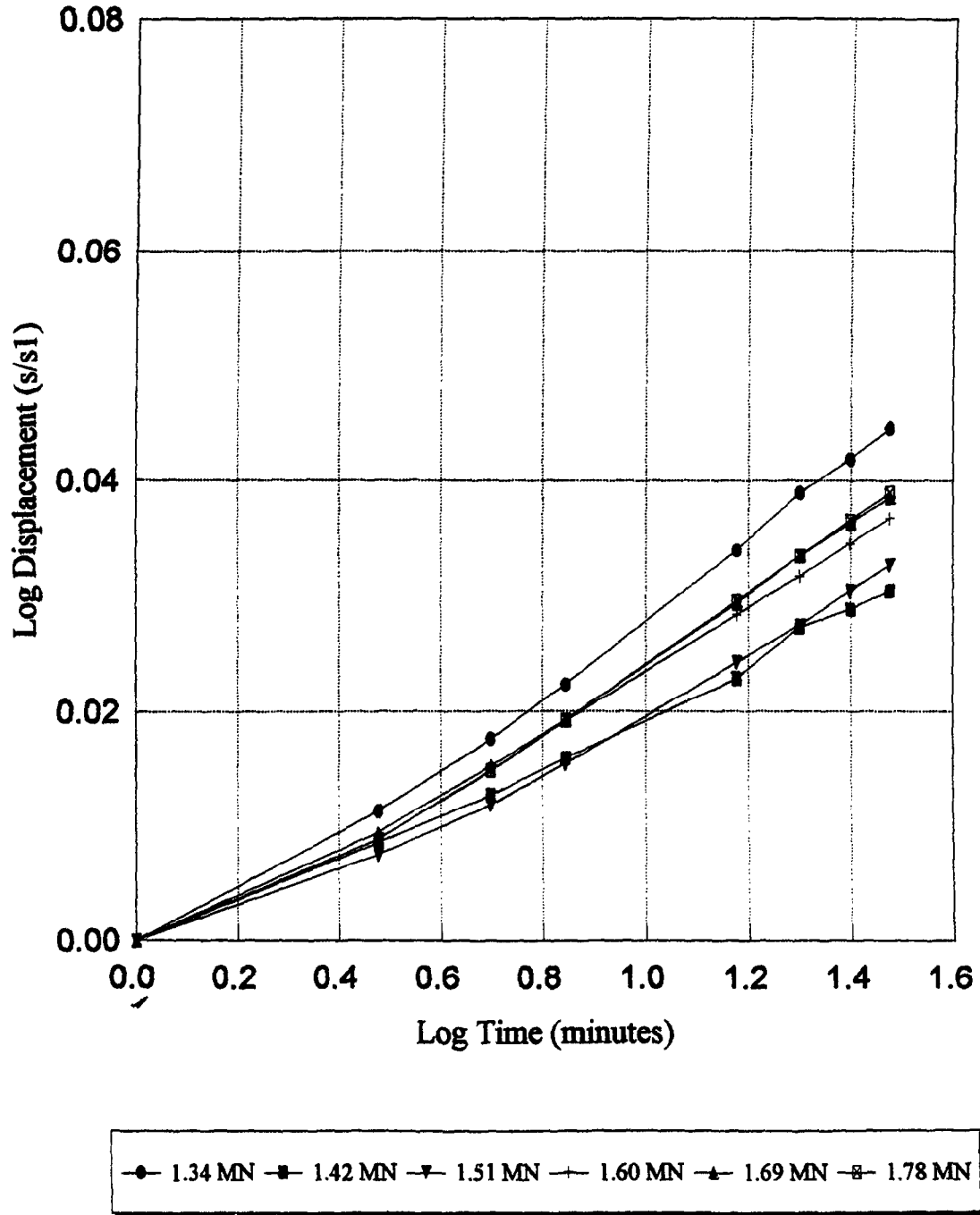


Figure C3: Individual Creep Exponent Curves for 1.0-m Footing, 1.34 MN - 1.78 MN

# Individual Creep Exponent Curve

## 1.0 M Footing - 24 Hour Creep Test

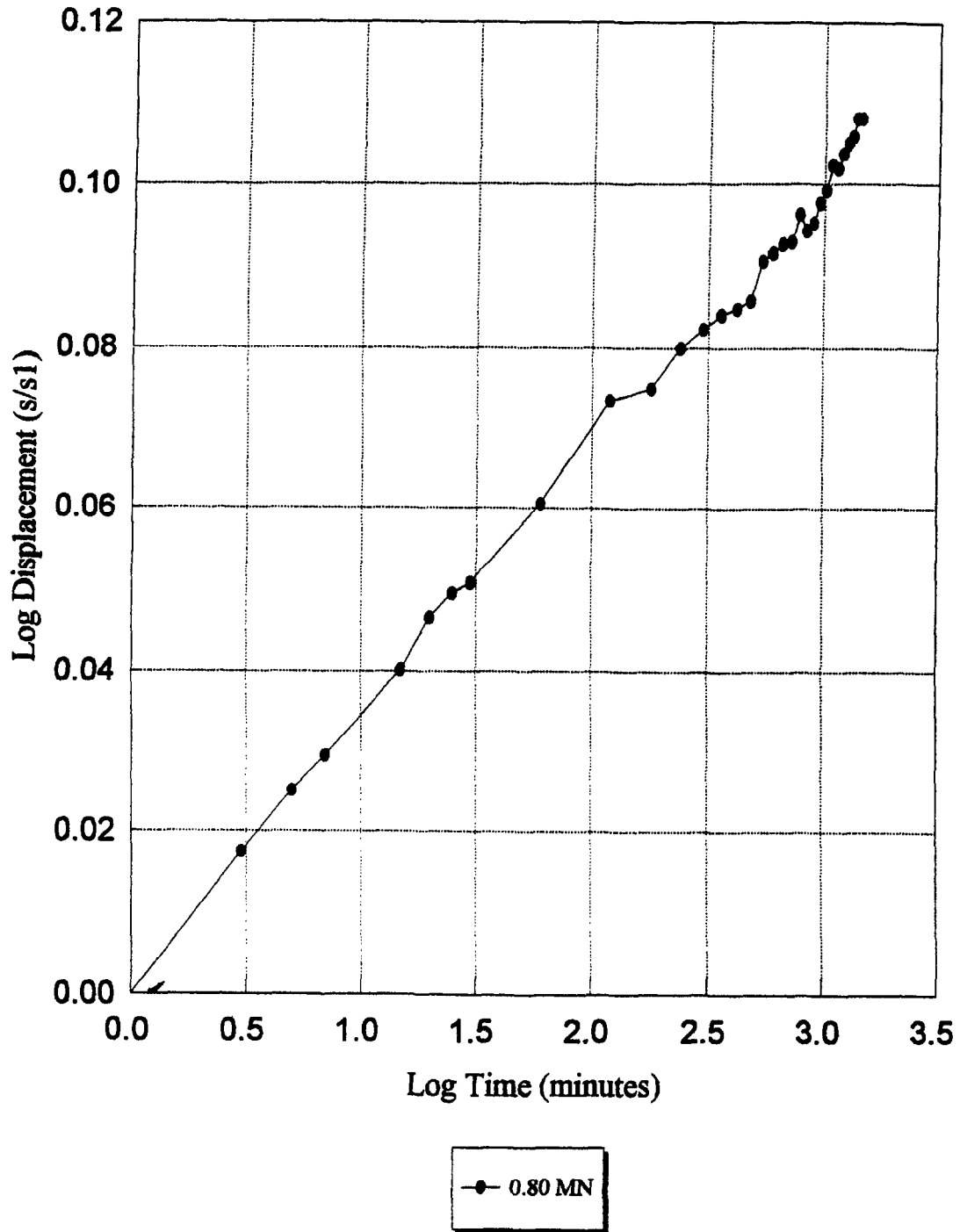
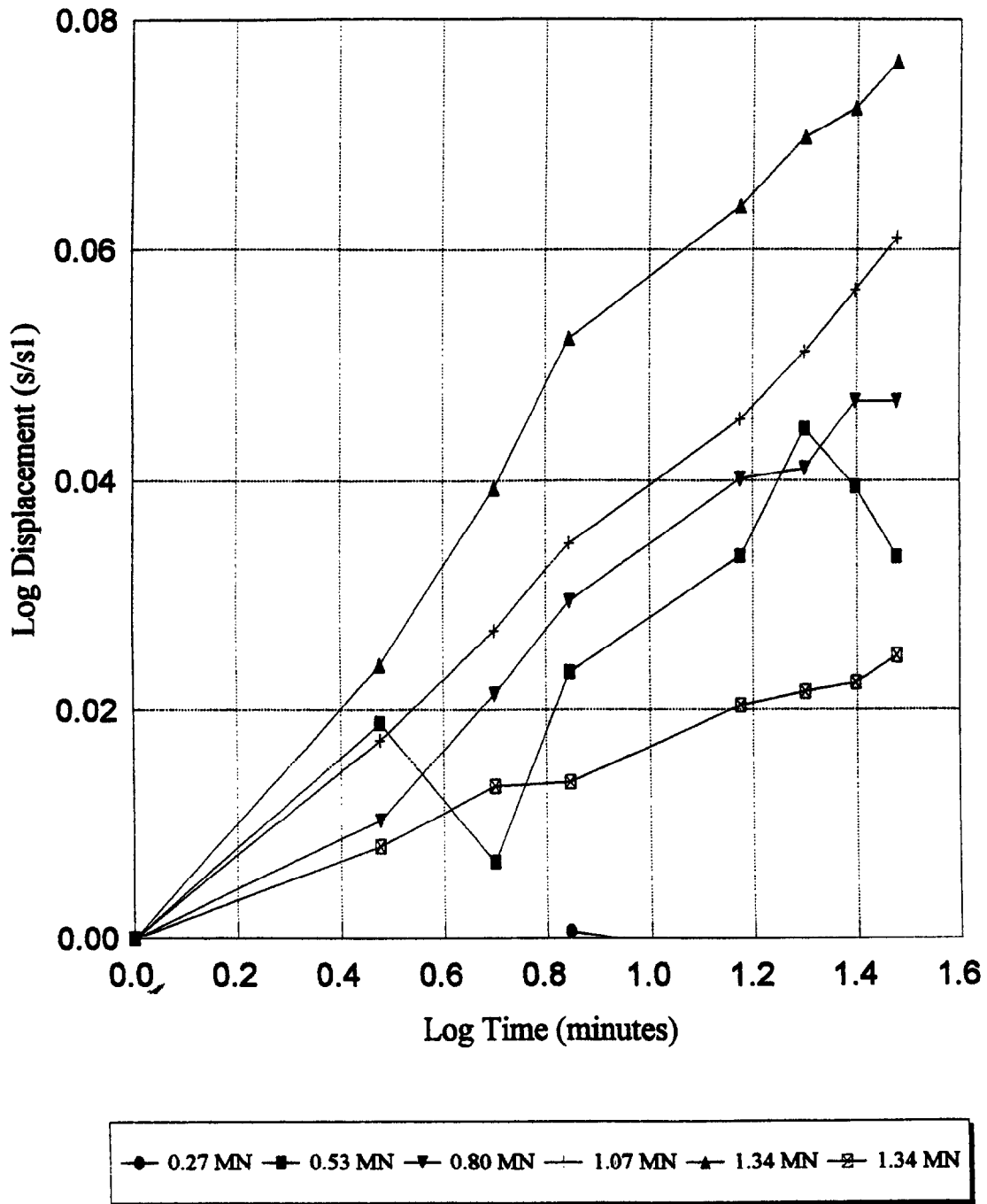


Figure C4: Individual Creep Exponent Curve for 1.0-m Footing -24-Hour Creep Test

## Individual Creep Exponent Curves 1.5 M Footing



**Figure C5:** Individual Creep Exponent Curves for 1.5-m Footing, 0.27 MN - 1.34 MN

# Individual Creep Exponent Curves 1.5 M Footing

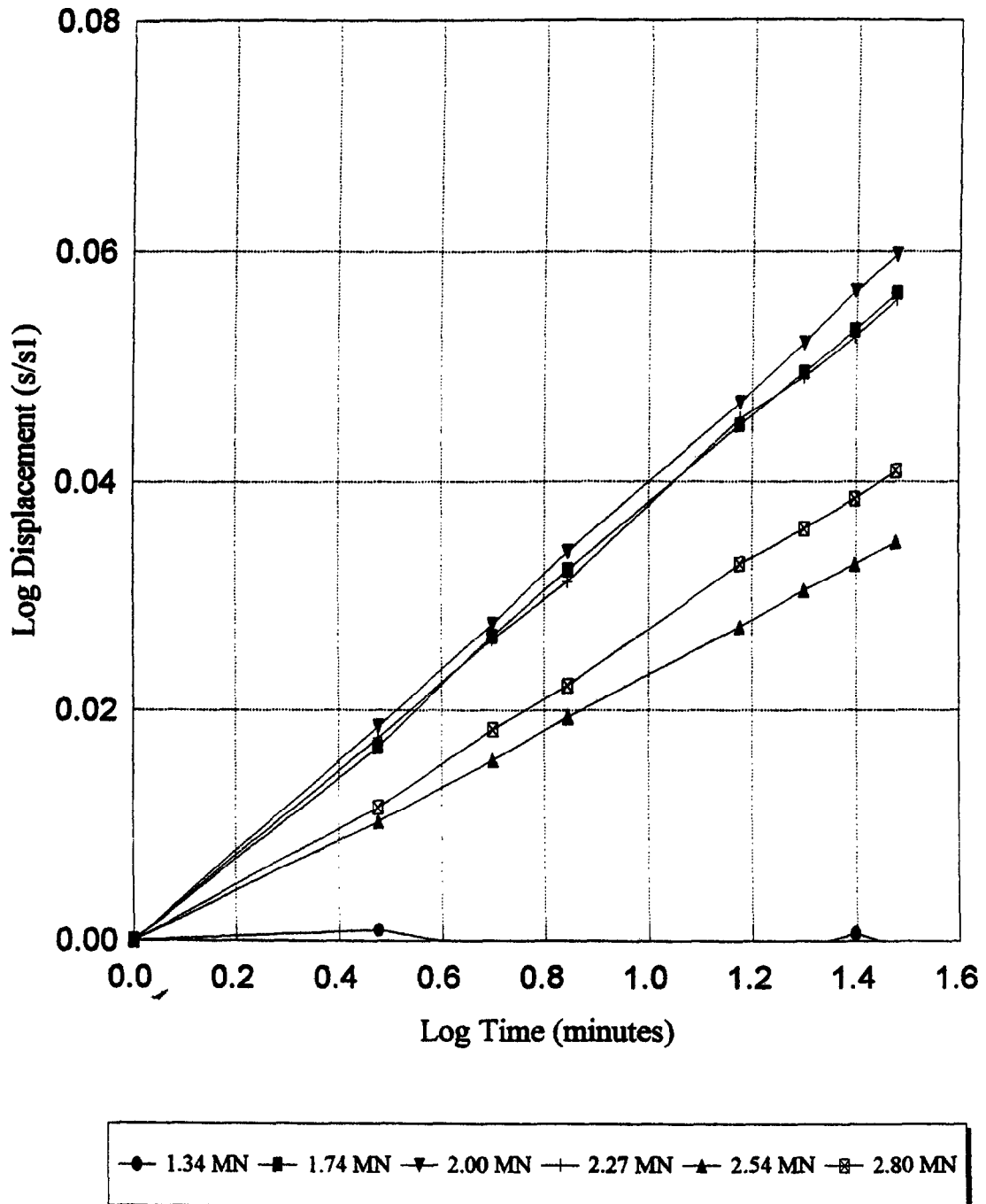


Figure C6: Individual Creep Exponent Curves for 1.5-m Footing, 1.34 MN - 2.80 MN

# Individual Creep Exponent Curves 1.5 M Footing

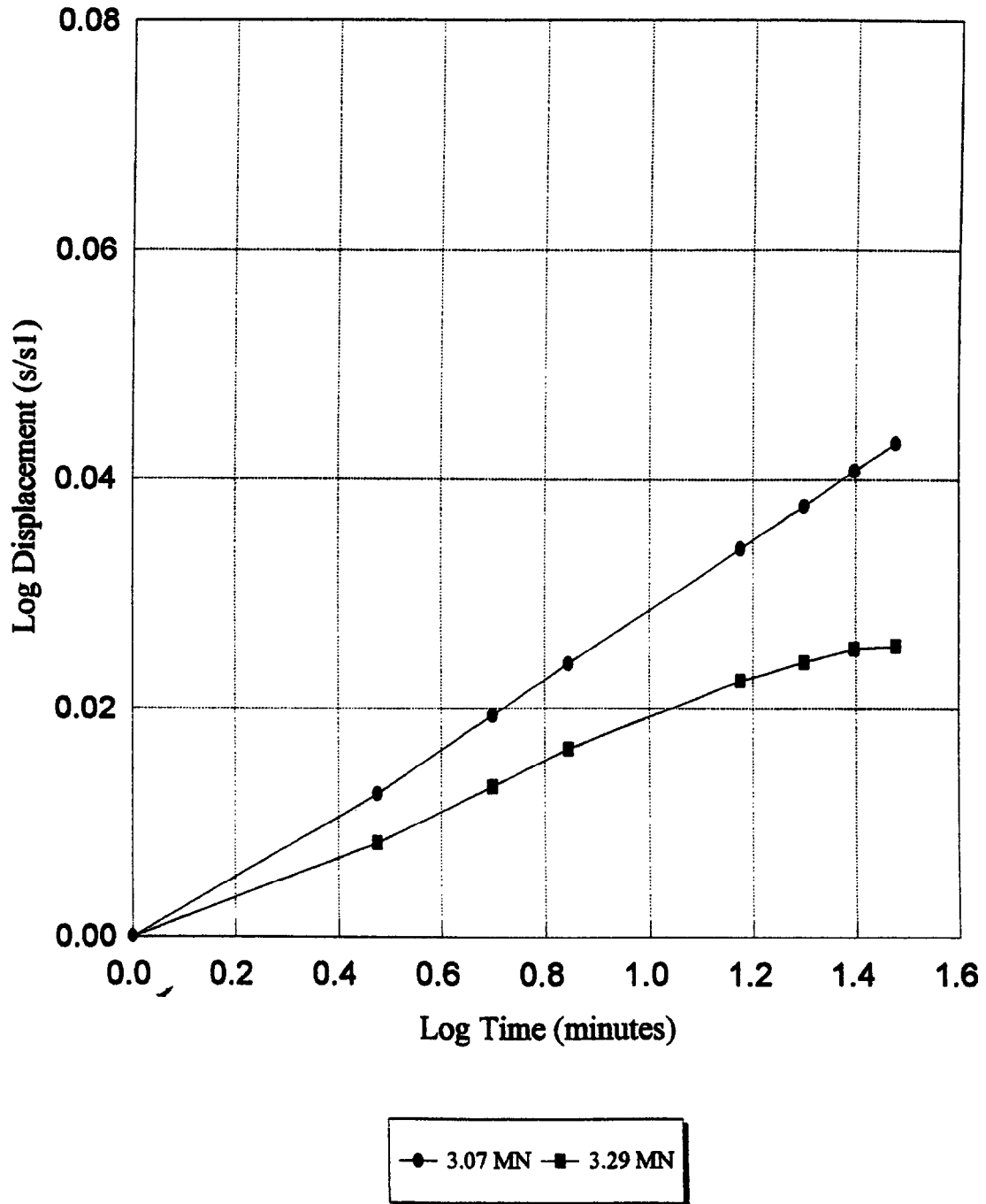


Figure C7: Individual Creep Exponent Curves for 1.5-m Footing, 3.07 MN - 3.29 MN

# Individual Creep Exponent Curve

## 1.5 M Footing - 24 Hour Creep Test

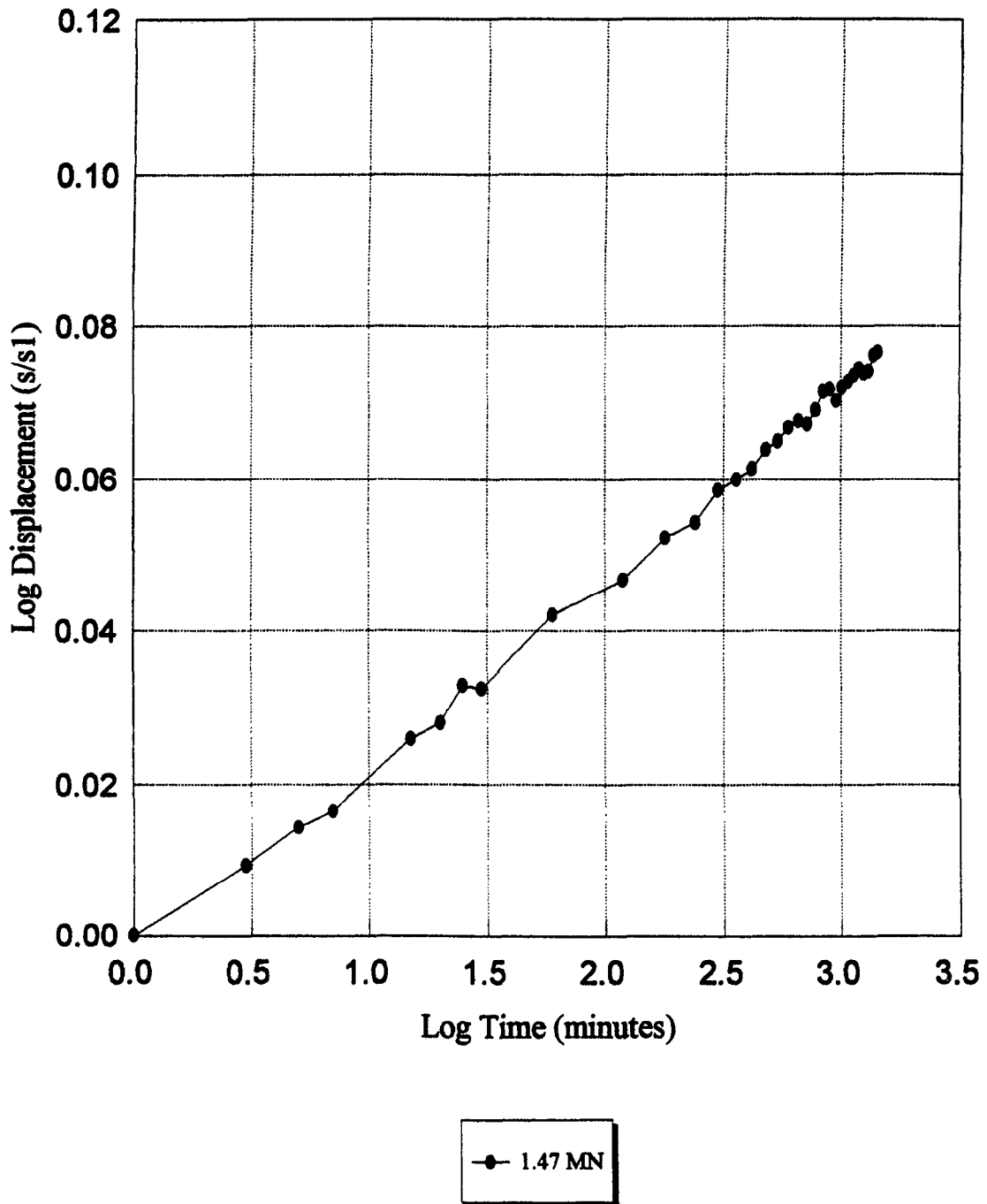


Figure C8: Individual Creep Exponent Curve for 1.5-m Footing - 24 Hour Creep Test

# Individual Creep Exponent Curves 2.5 M Footing

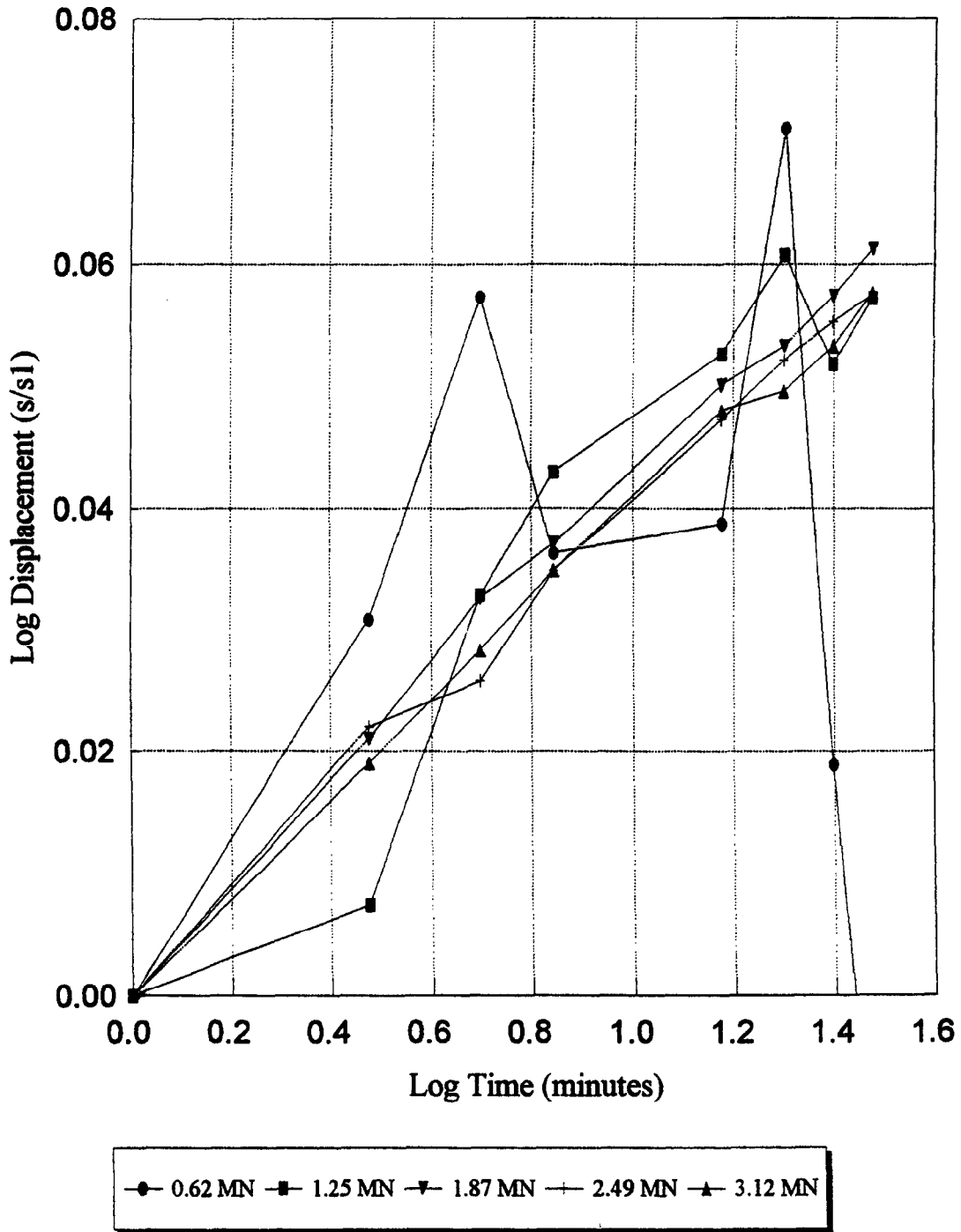


Figure C9: Individual Creep Exponent Curves for 2.5-m Footing, 0.62 MN - 3.12 MN

# Individual Creep Exponent Curves 2.5 M Footing

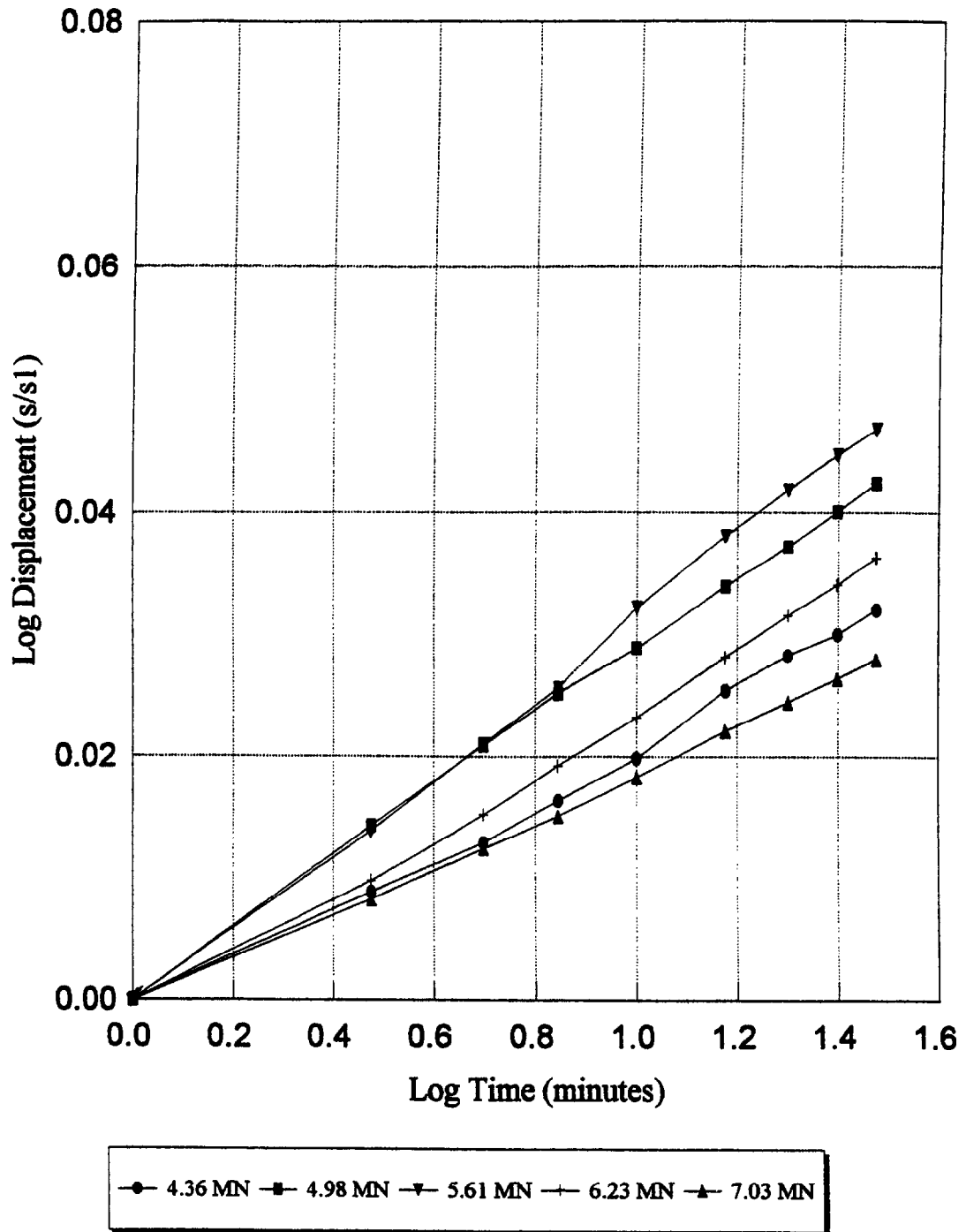


Figure C10: Individual Creep Exponent Curves for 2.5-m Footing, 4.36 MN - 7.03 MN

# Individual Creep Exponent Curves 2.5 M Footing - 24 Hour Creep Tests

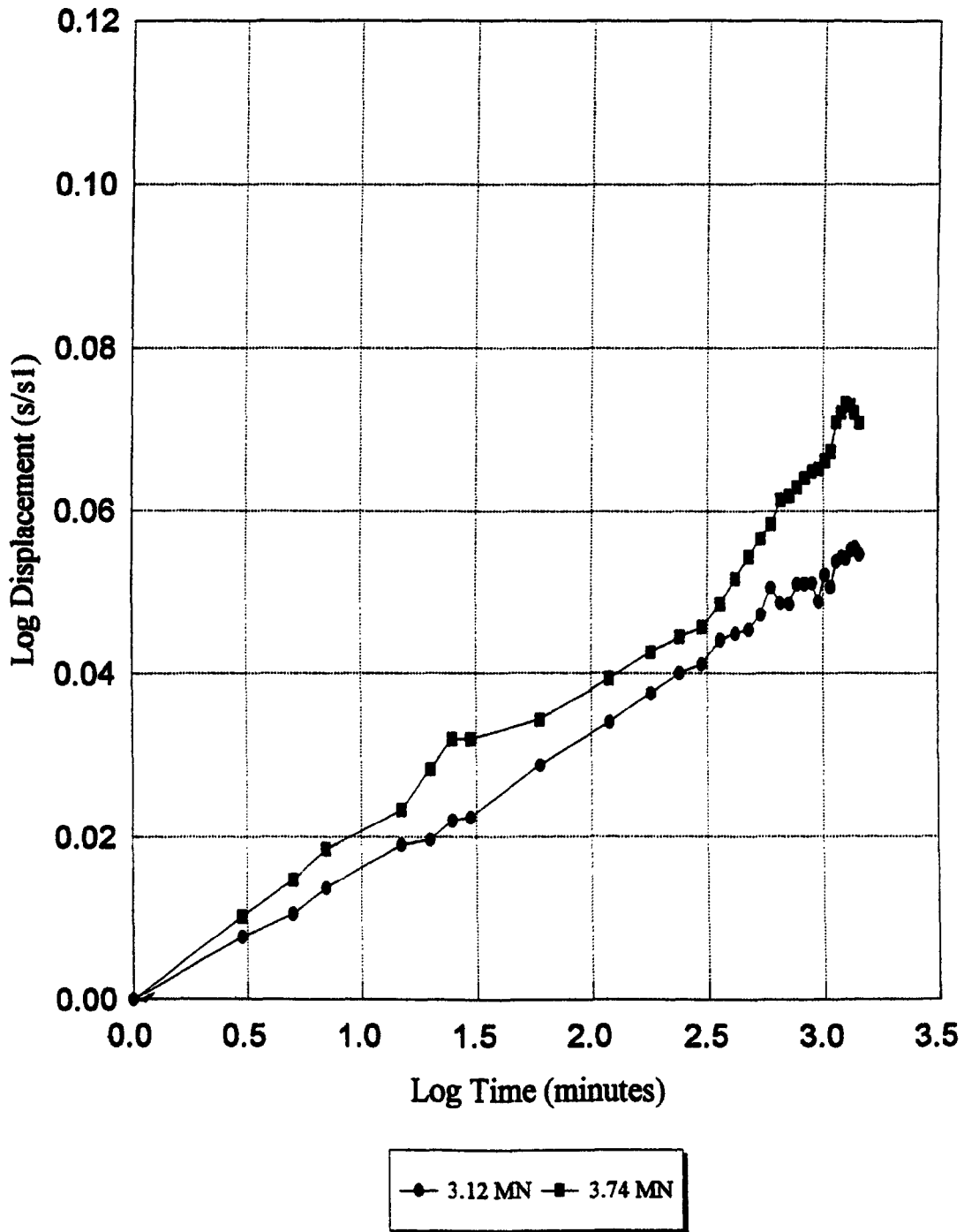
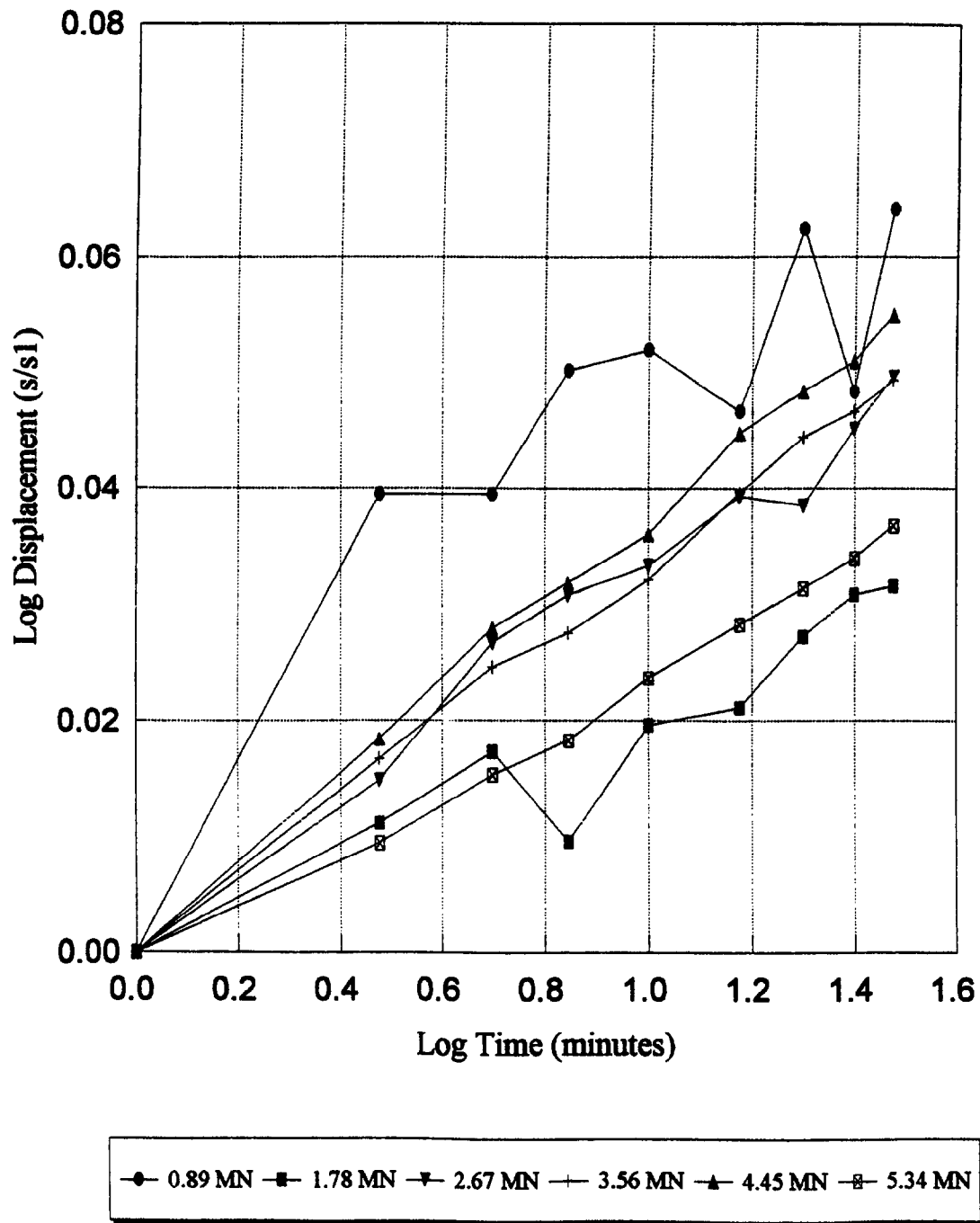


Figure C11: Individual Creep Exponent Curves for 2.5-m Footing - 24 Hour Creep Tests

# Individual Creep Exponent Curves 3.0 M Footing

NORTH



**Figure C12:** Individual Creep Exponent Curves for 3.0-m(n) Footing, 0.89 MN - 5.34 MN

# Individual Creep Exponent Curves 3.0 M Footing

NORTH

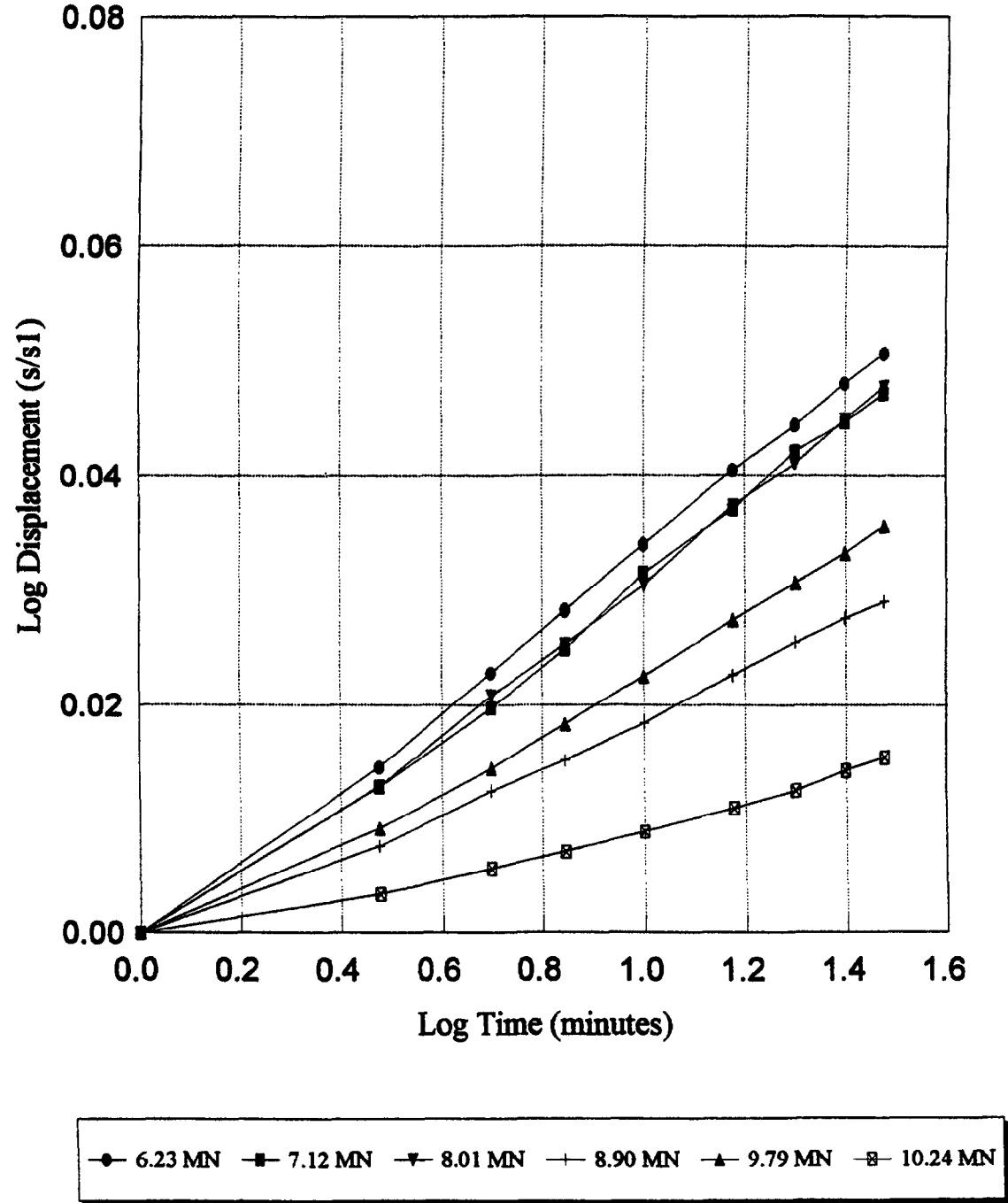


**Figure C13:** Individual Creep Exponent Curves for 3.0-m(n) Footing, 6.23 MN - 10.24 MN

# Individual Creep Exponent Curve 3.0 M Footing - 24 Hour Creep Test

NORTH

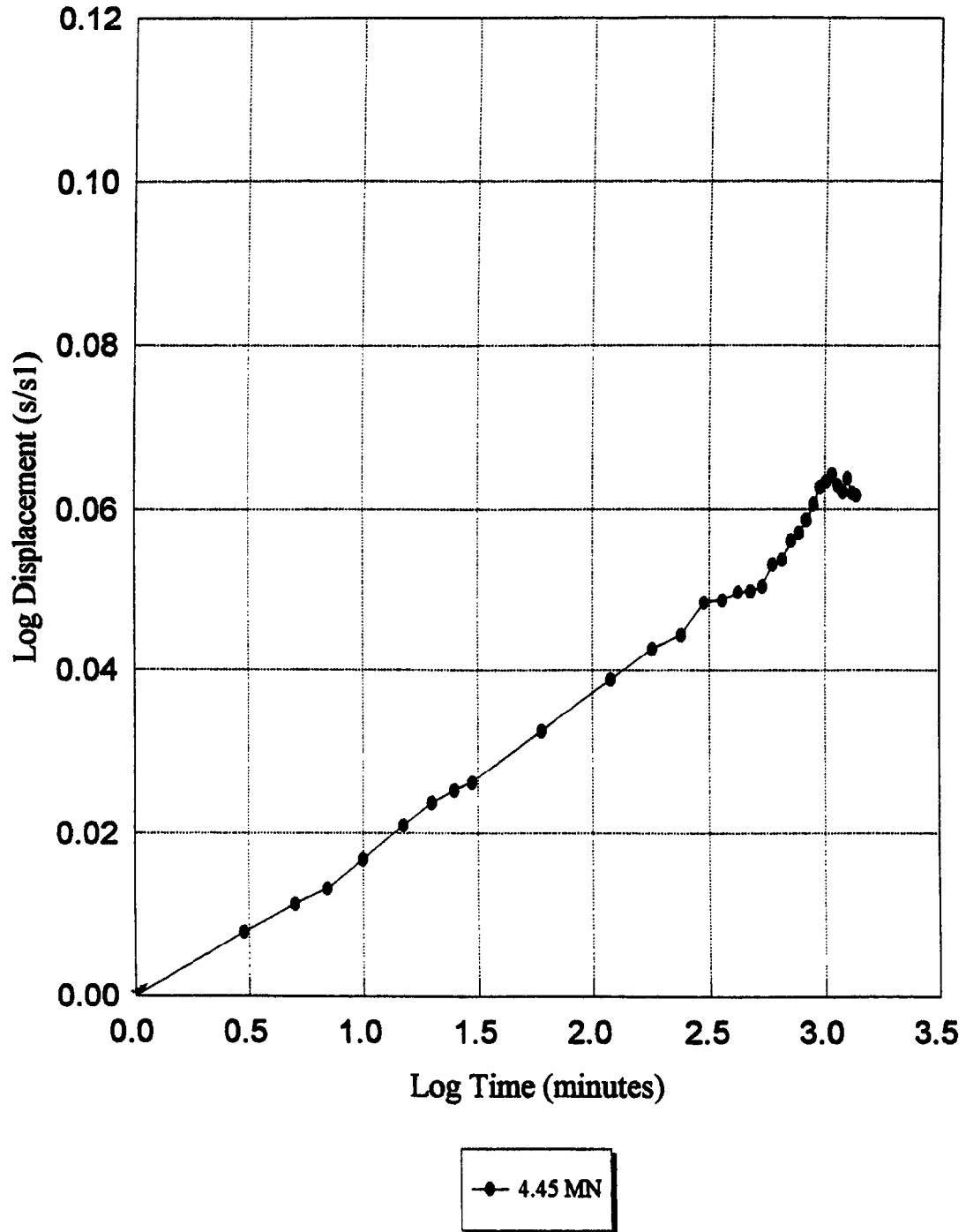


Figure C14: Individual Creep Exponent Curve for 3.0-m(n) Footing -24-Hour Creep Test

# Individual Creep Exponent Curves 3.0 M Footing

SOUTH

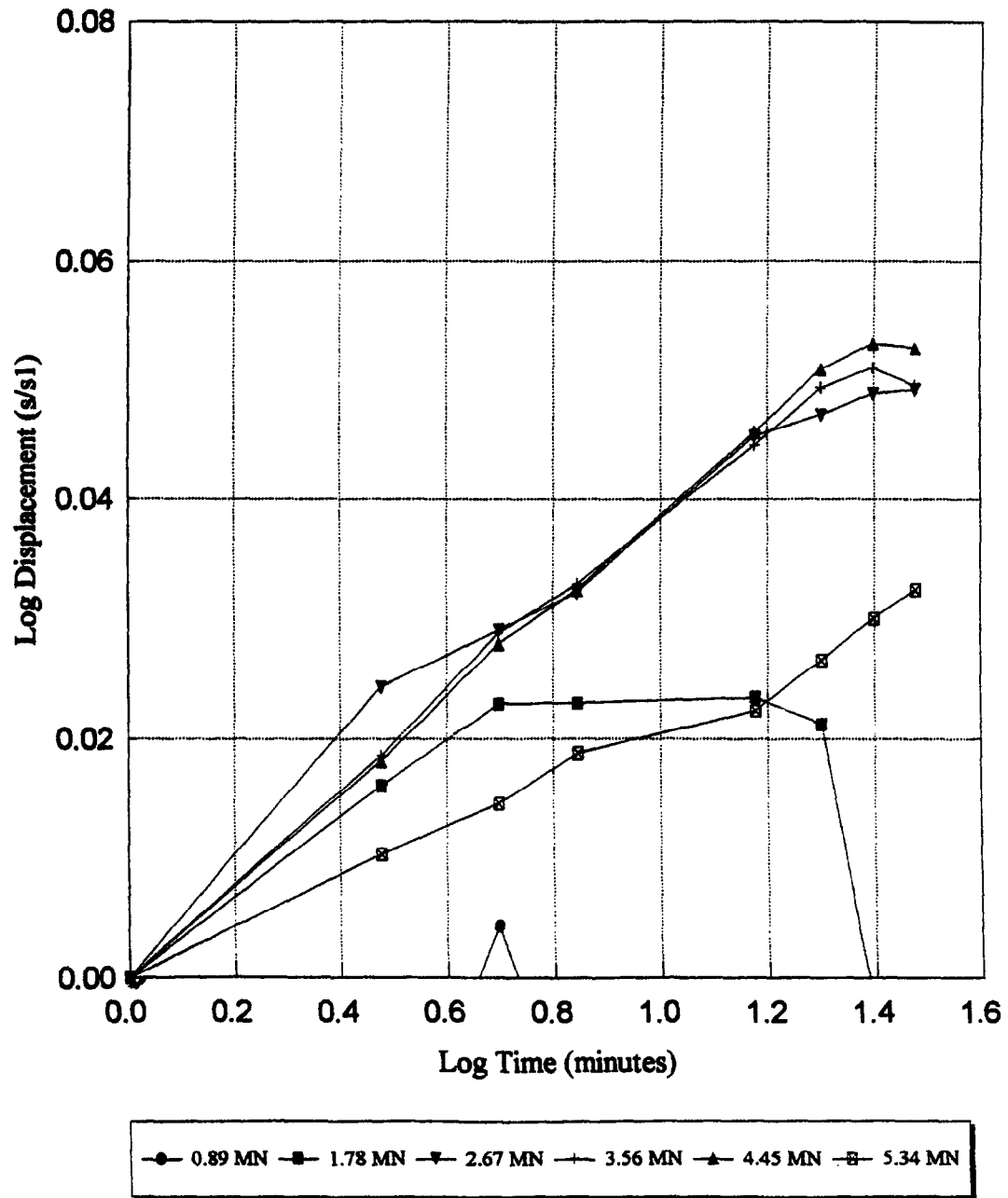


Figure C15: Individual Creep Exponent Curves for 3.0-m(s) Footing, 0.89 MN - 5.34 MN

# Individual Creep Exponent Curves 3.0 M Footing

SOUTH

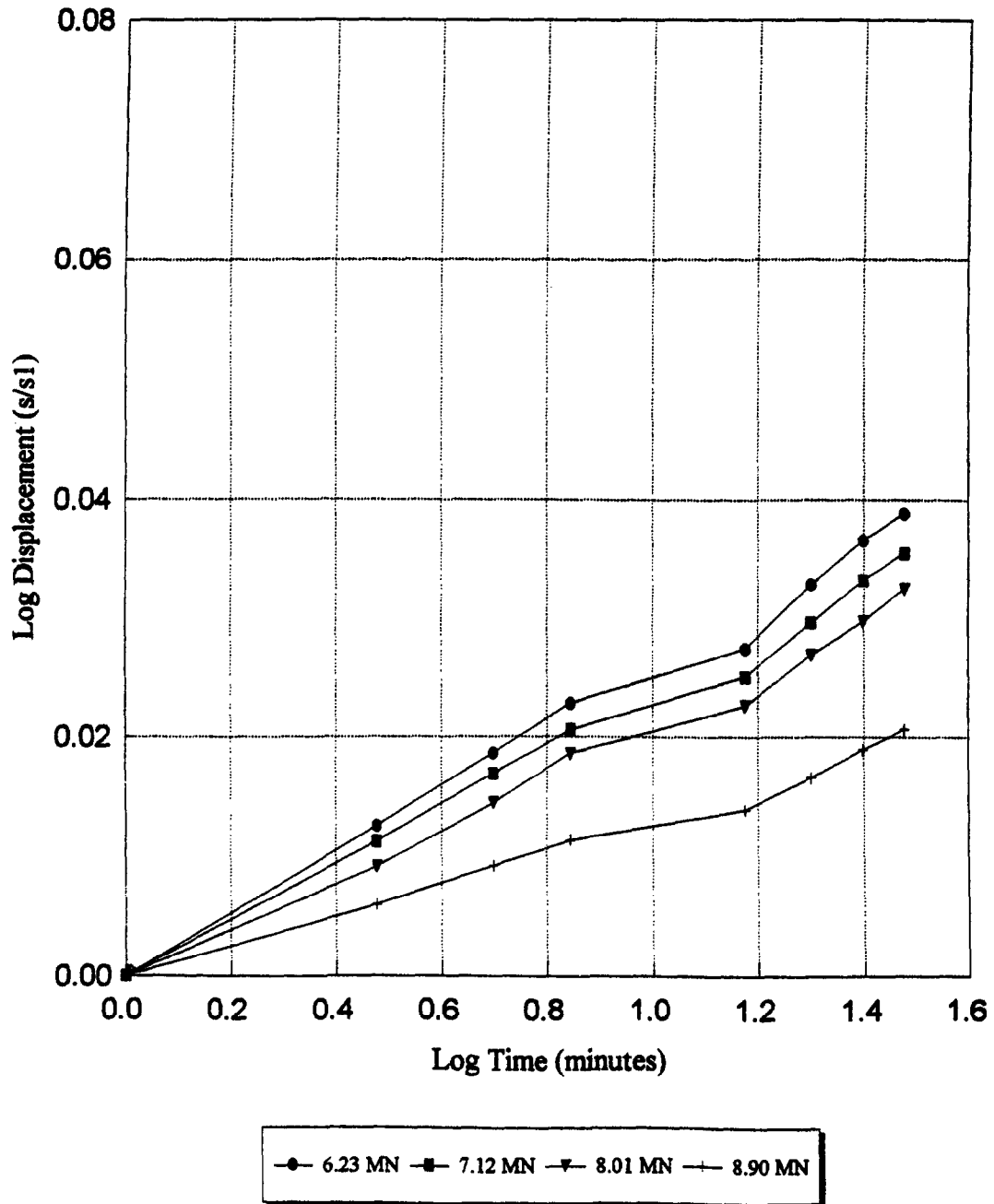


Figure C16: Individual Creep Exponent Curves for 3.0-m(s) Footing, 6.23 MN - 8.90 MN

# Individual Creep Exponent Curves 3.0 M Footing - 24 Hour Creep Tests

SOUTH

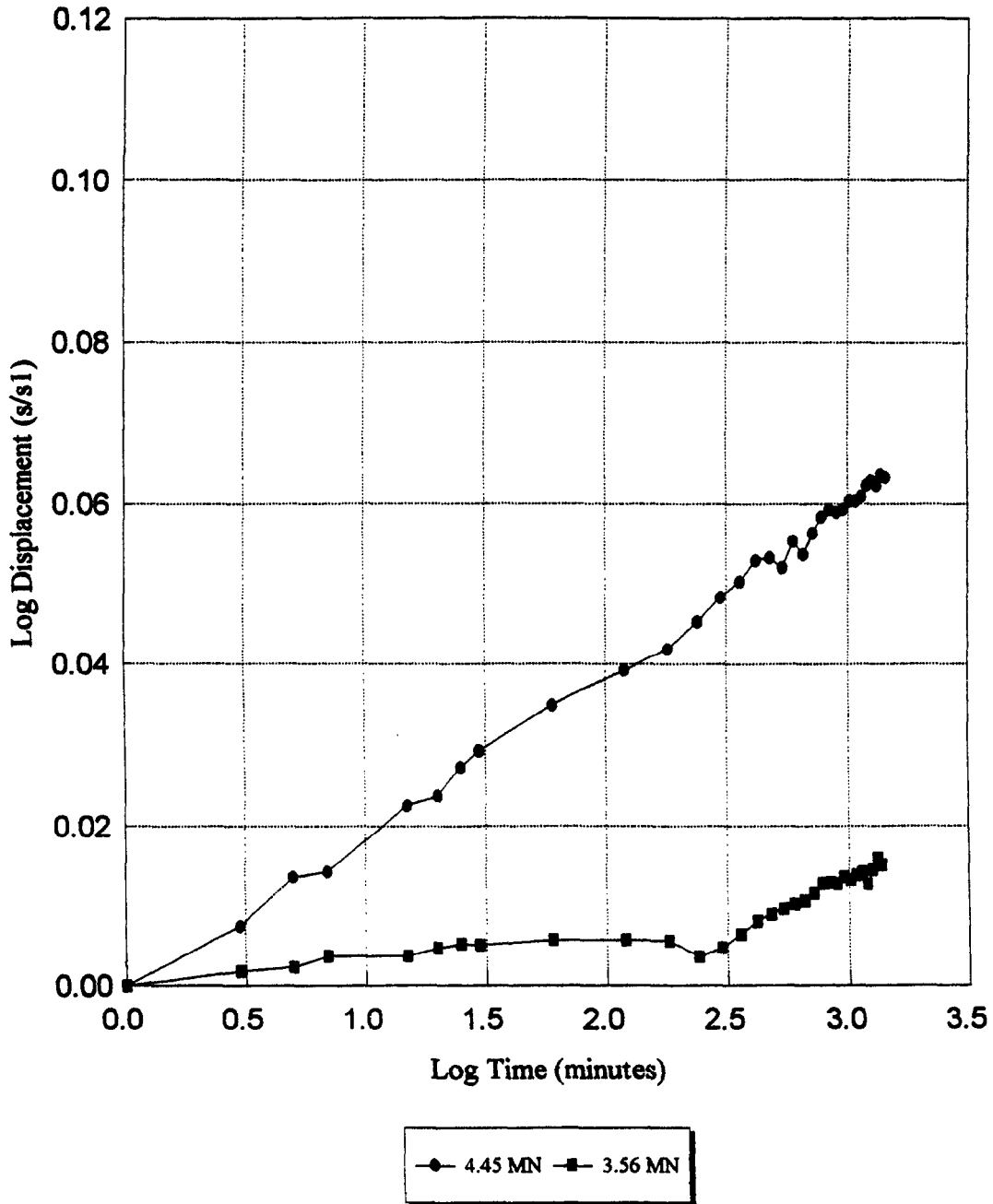
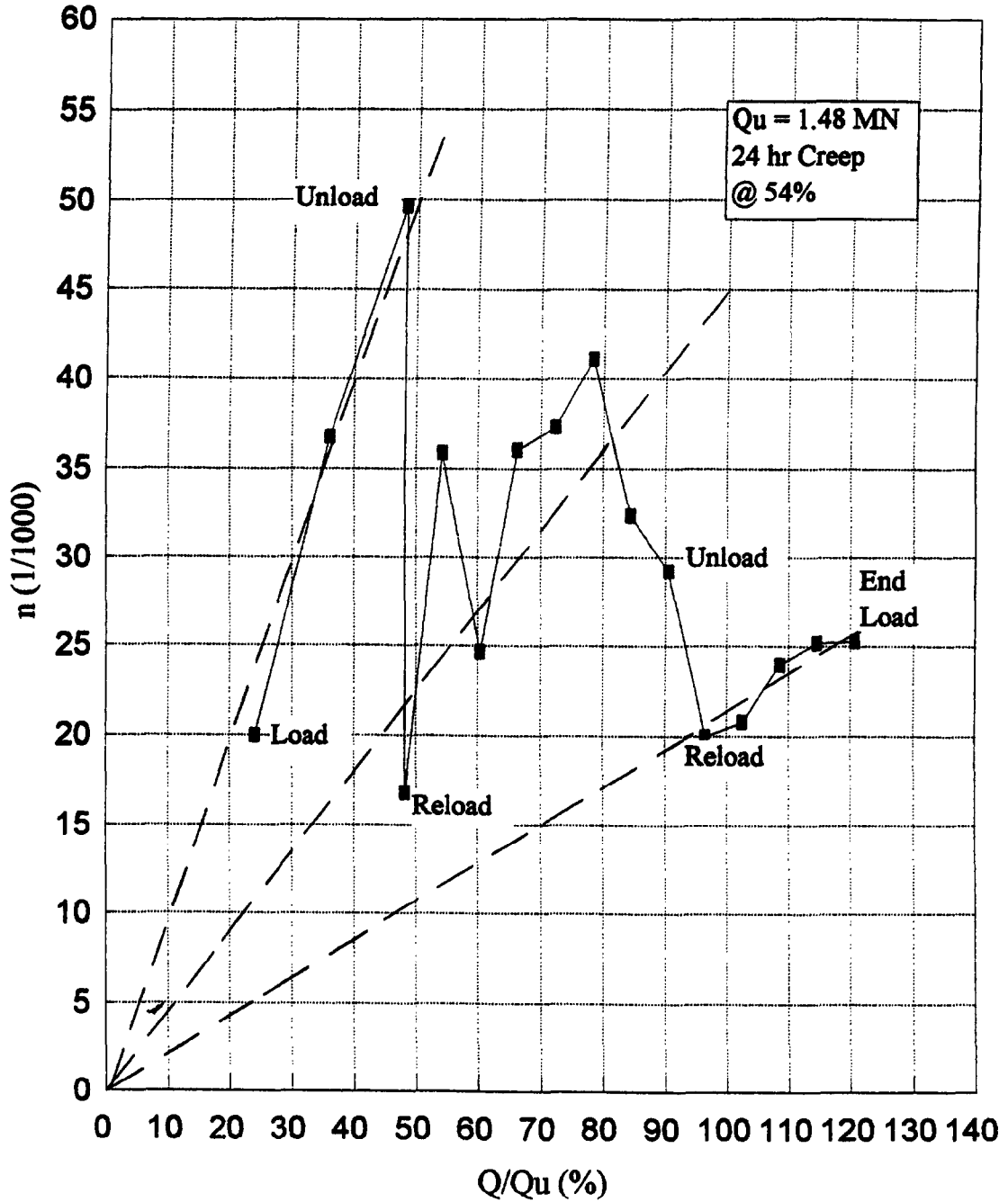


Figure C17: Individual Creep Exponent Curves for 3.0-m(s) Footing - 24-Hour Creep Tests

# Creep Exponent Curve 1.0 M Footing



**Figure C18:** Creep Exponent Curve for 1.0-m Footing -  $Q_u = 1.48 \text{ MN}$

# Creep Exponent Curve 1.5 M Footing

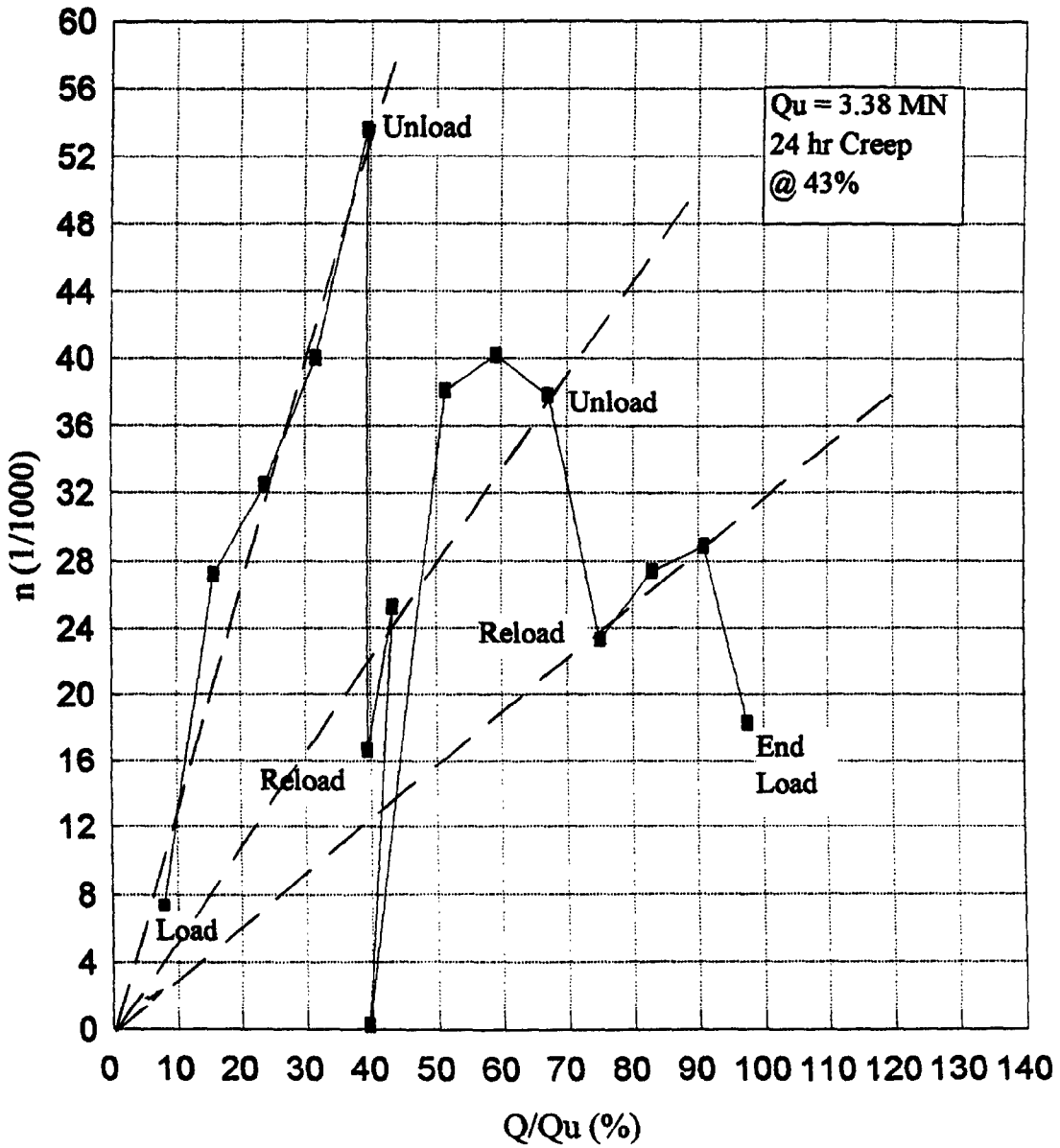


**Figure C19:** Creep Exponent Curve for 1.5-m Footing -  $Q_u = 3.38 \text{ MN}$

# Creep Exponent Curve 2.5 M Footing

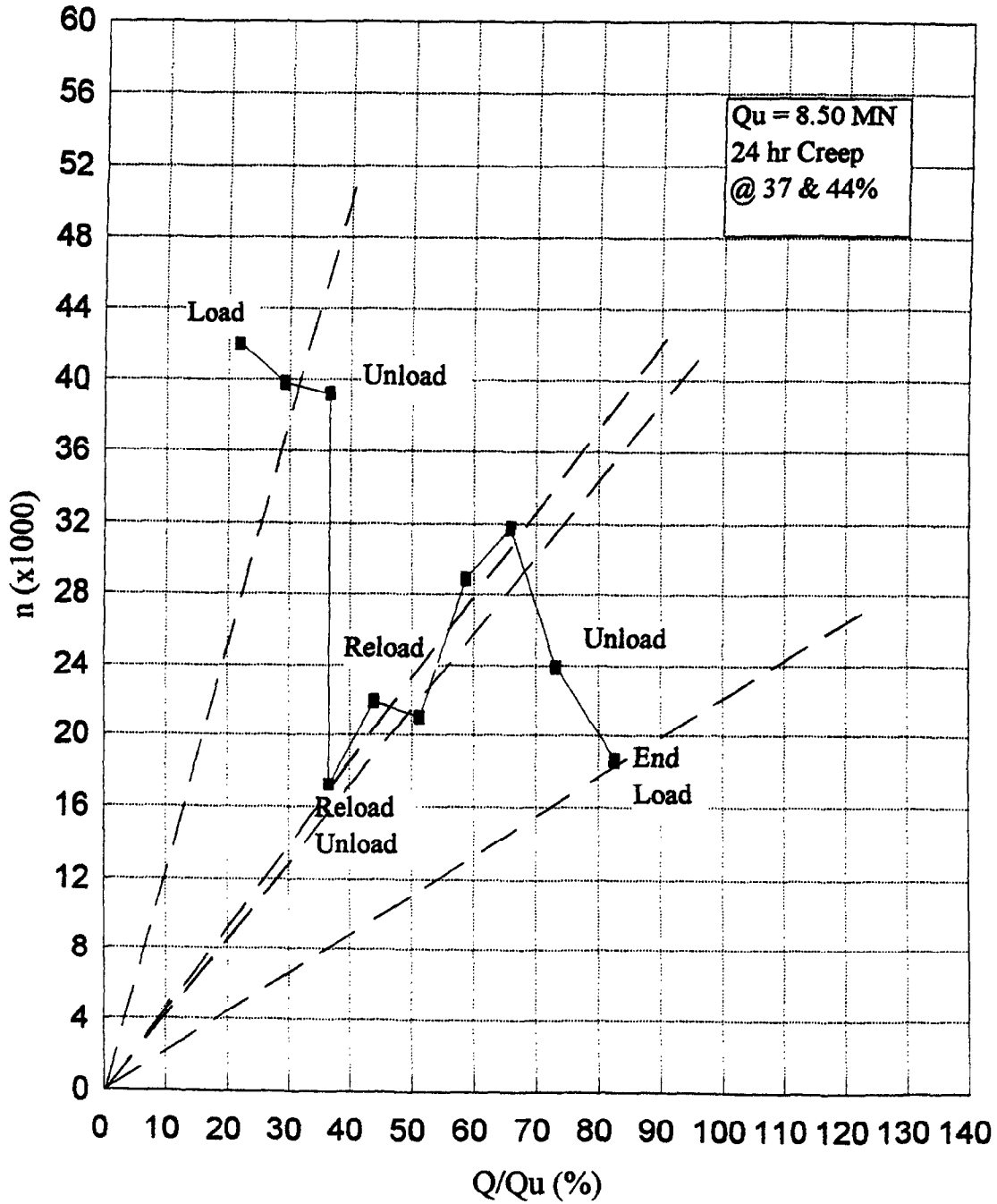


**Figure C20:** Creep Exponent Curve for 2.5-m Footing -  $Q_u = 8.50 \text{ MN}$

# Creep Exponent Curve 3.0 M Footing

NORTH

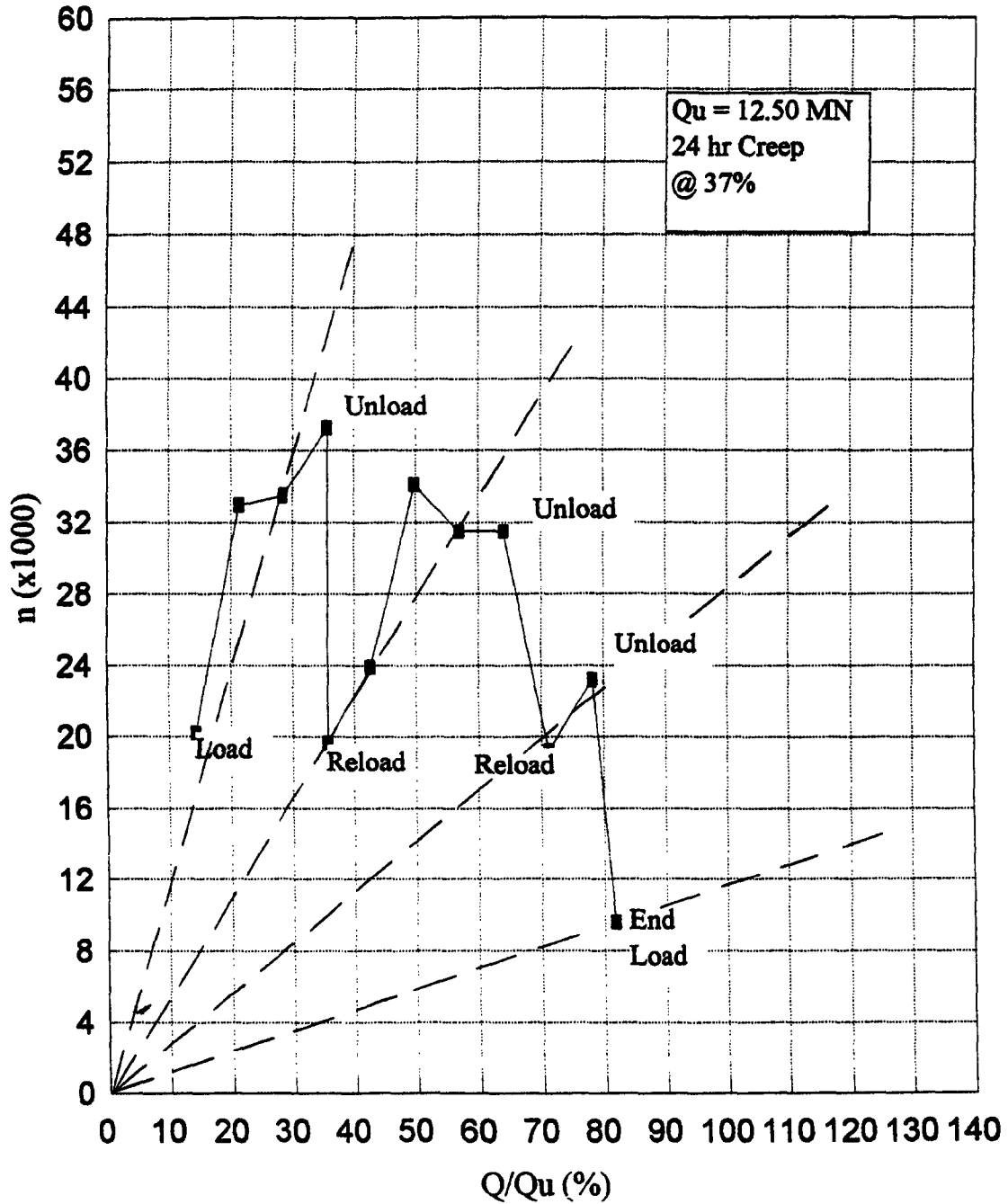


**Figure C21:** Creep Exponent Curve for 3.0-m(n) Footing -  $Q_u = 12.50$  MN

# Creep Exponent Curve 3.0 M Footing

SOUTH

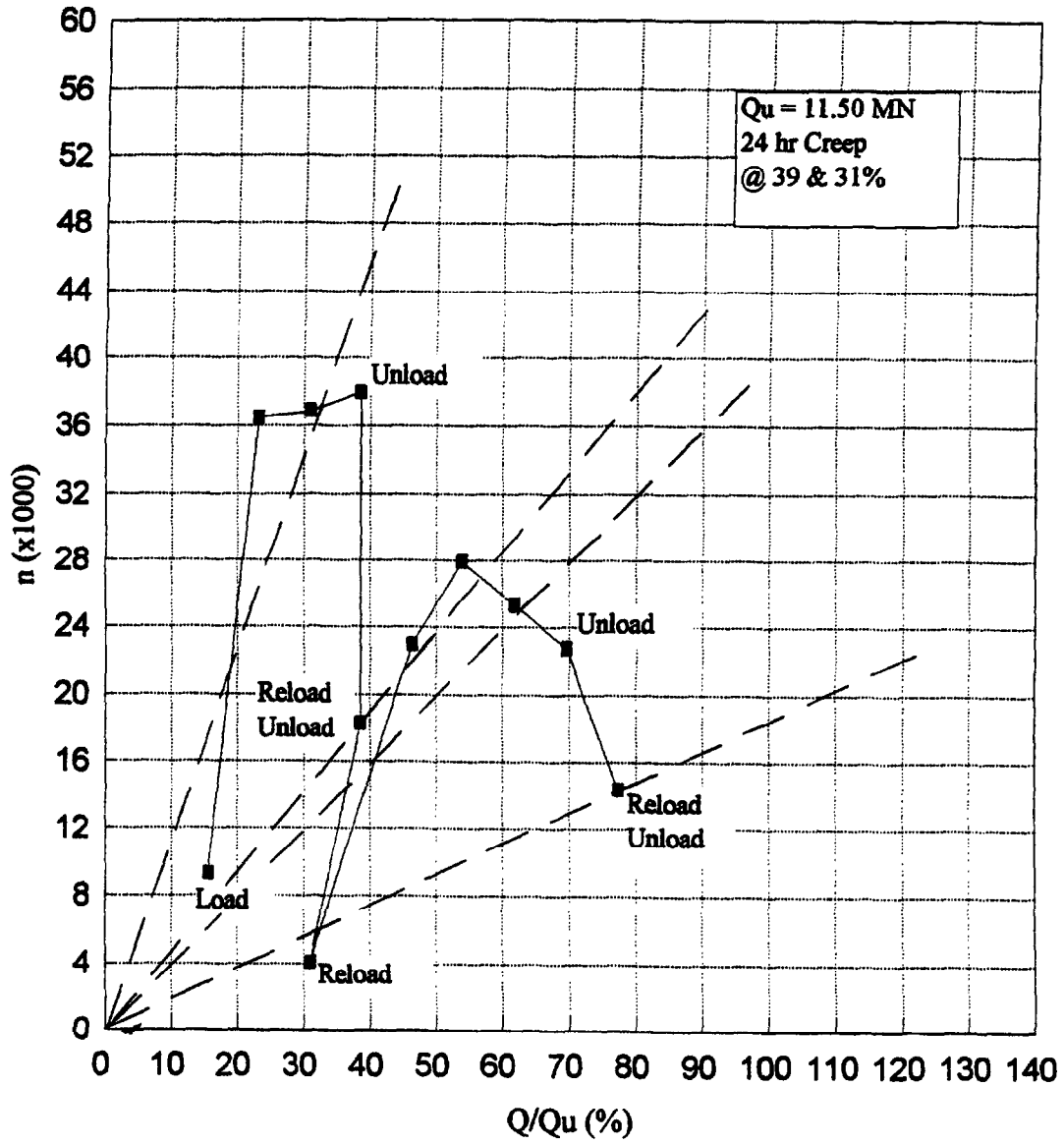


**Figure C22:** Creep Exponent Curve for 3.0-m(s) Footing -  $Q_u = 11.50 \text{ MN}$

## **APPENDIX D: Inclinator Curves**

# 1.78 MN Failure Test

## 1.0 M Footing - spt-6 (North-South)

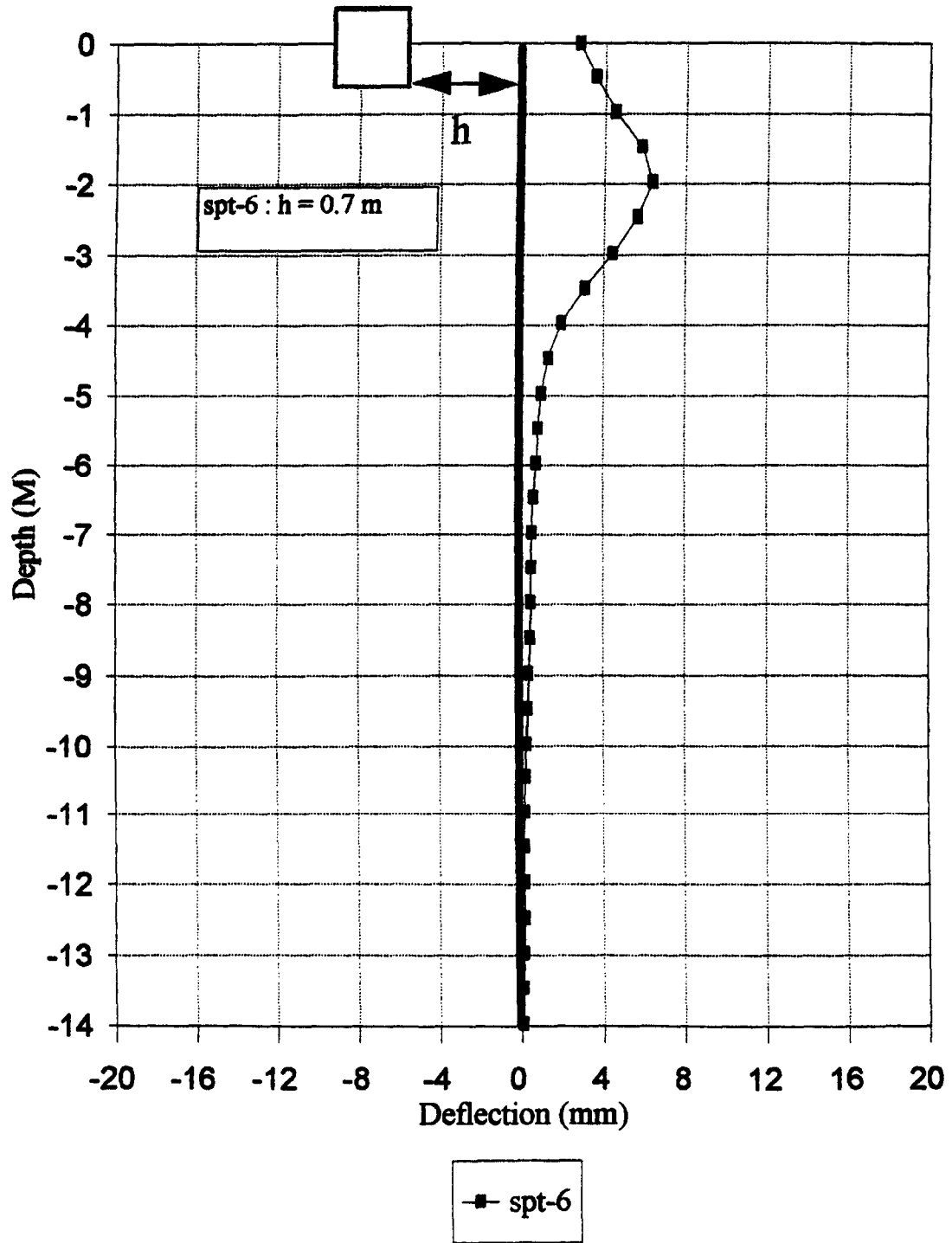


Figure D1: Inclinometer Test - 1.78-MN Failure Load - N-S Direction, 1.0 M Footing

# 1.47 MN Creep & 3.29 MN Failure Tests 1.5 M Footing - spt-4 (North-South)

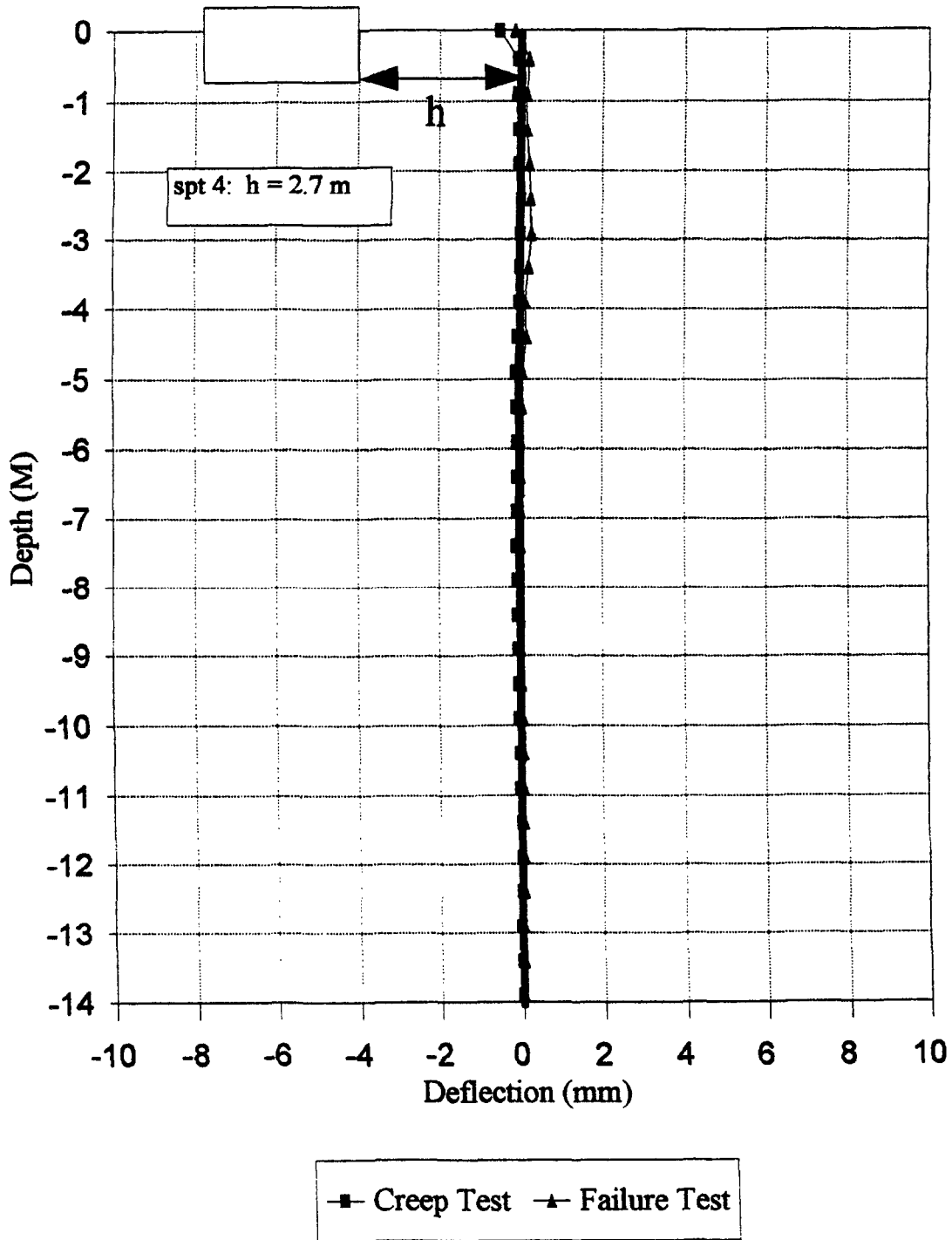


Figure D2: Inclinometer Test - 1.47 & 3.29-MN Loads - N-S Direction, 1.5 M Footing

# 1.47 MN Creep & 3.29 MN Failure Tests

## 1.5 M Footing - spt-4 (East-West)

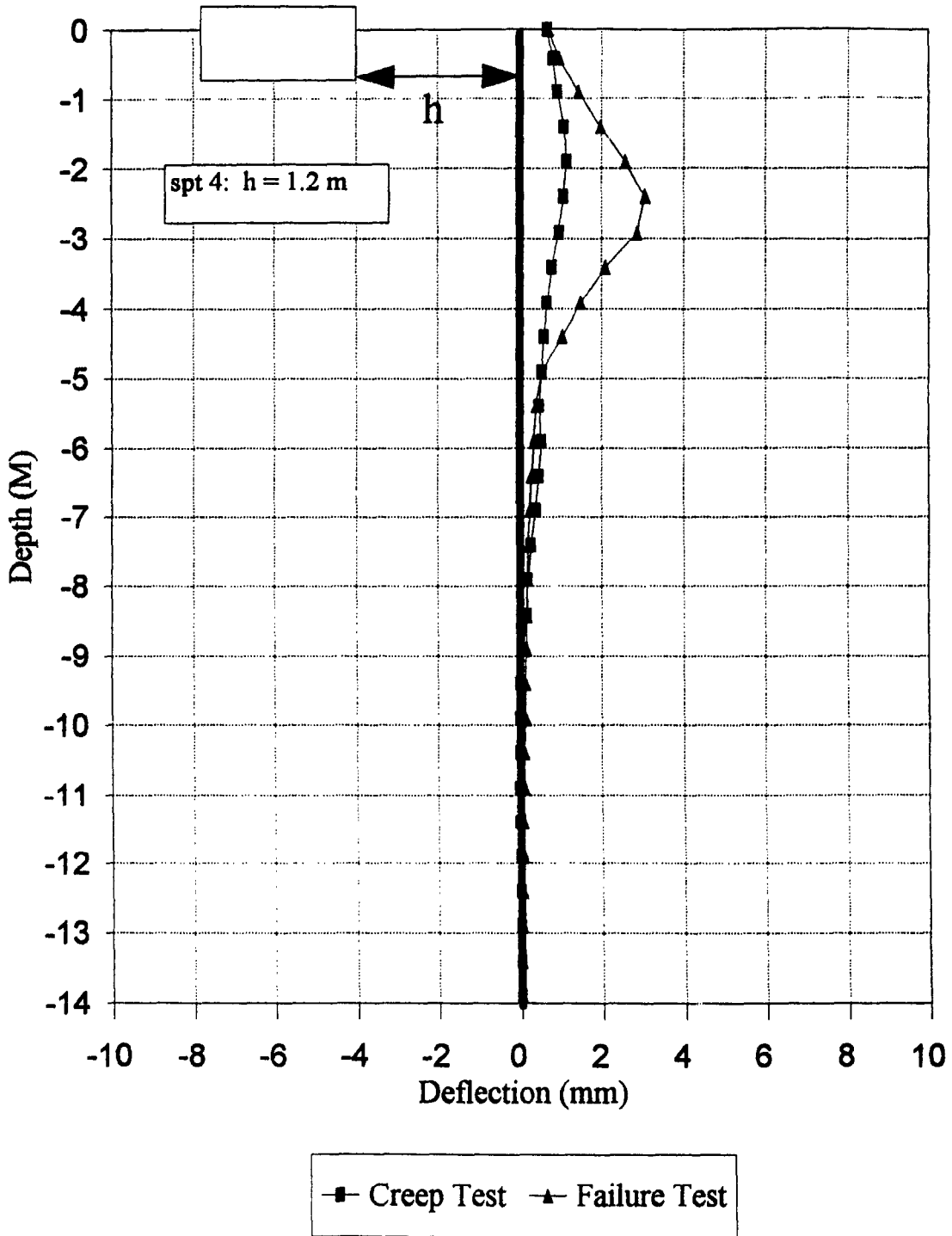


Figure D3: Inclinometer Test - 1.47 & 3.29-MN Loads - E-W Direction, 1.5-m Footing

### 3.12 MN Creep Test 2.5 M Footing (North-South)

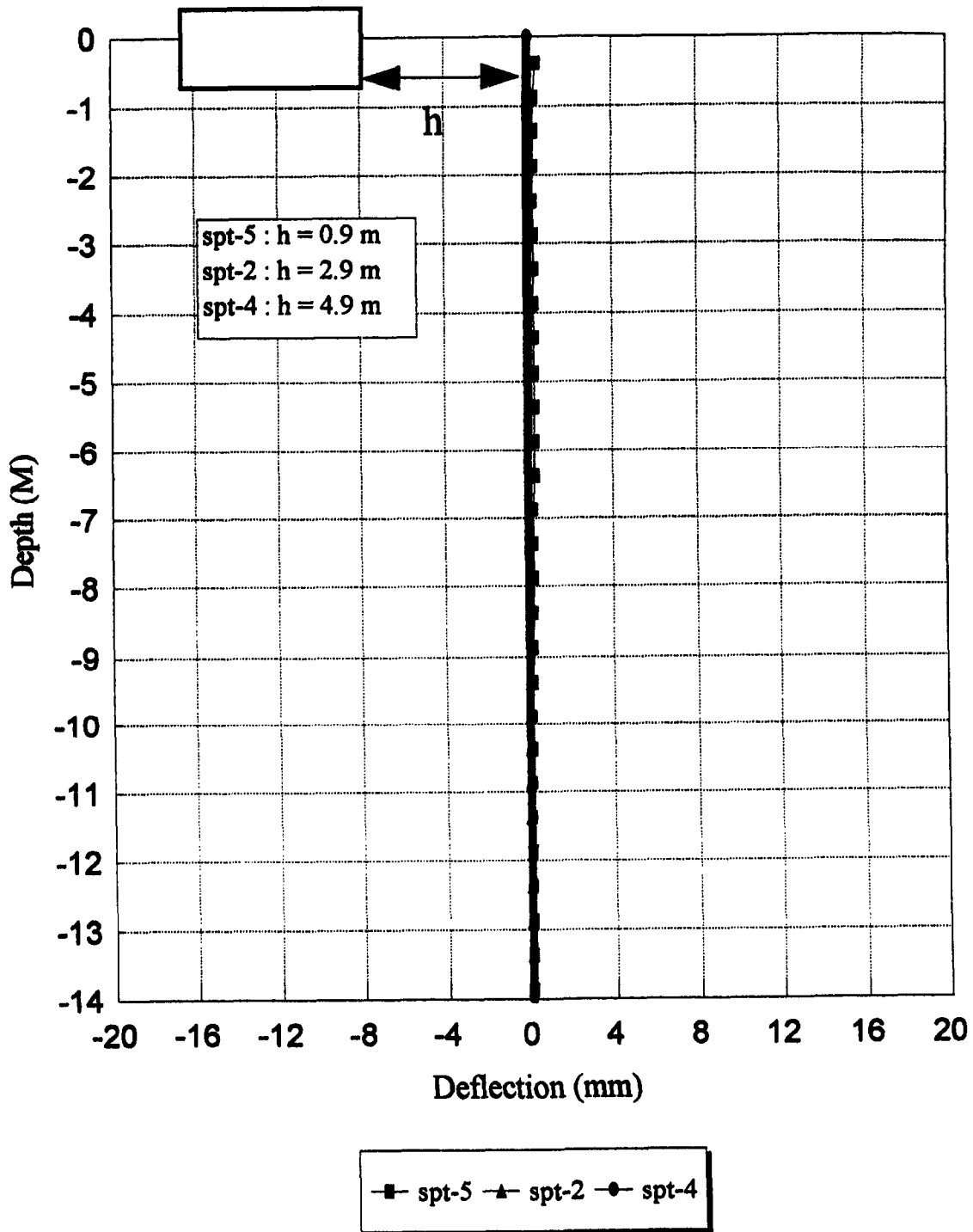


Figure D4: Inclinometer Test - 3.12 MN Creep Load - N-S Direction, 2.5-m Footing

### 7.03 MN Failure Test 2.5 M Footing (North-South)

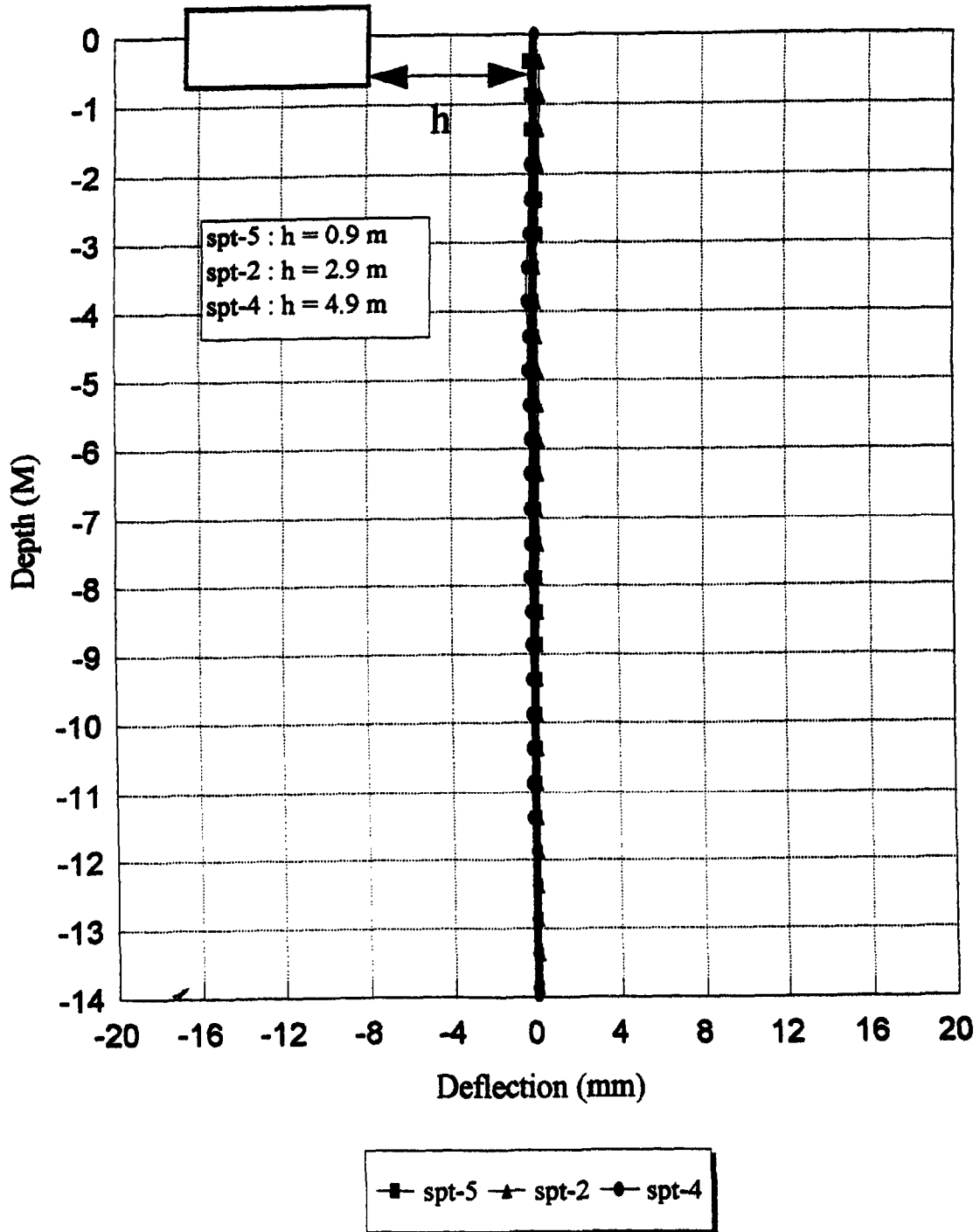


Figure D5: Inclinometer Test -7.03-MN Failure Load - N-S Direction, 2.5-m Footing

### 3.12 MN Creep Test 2.5 M Footing (East-West)

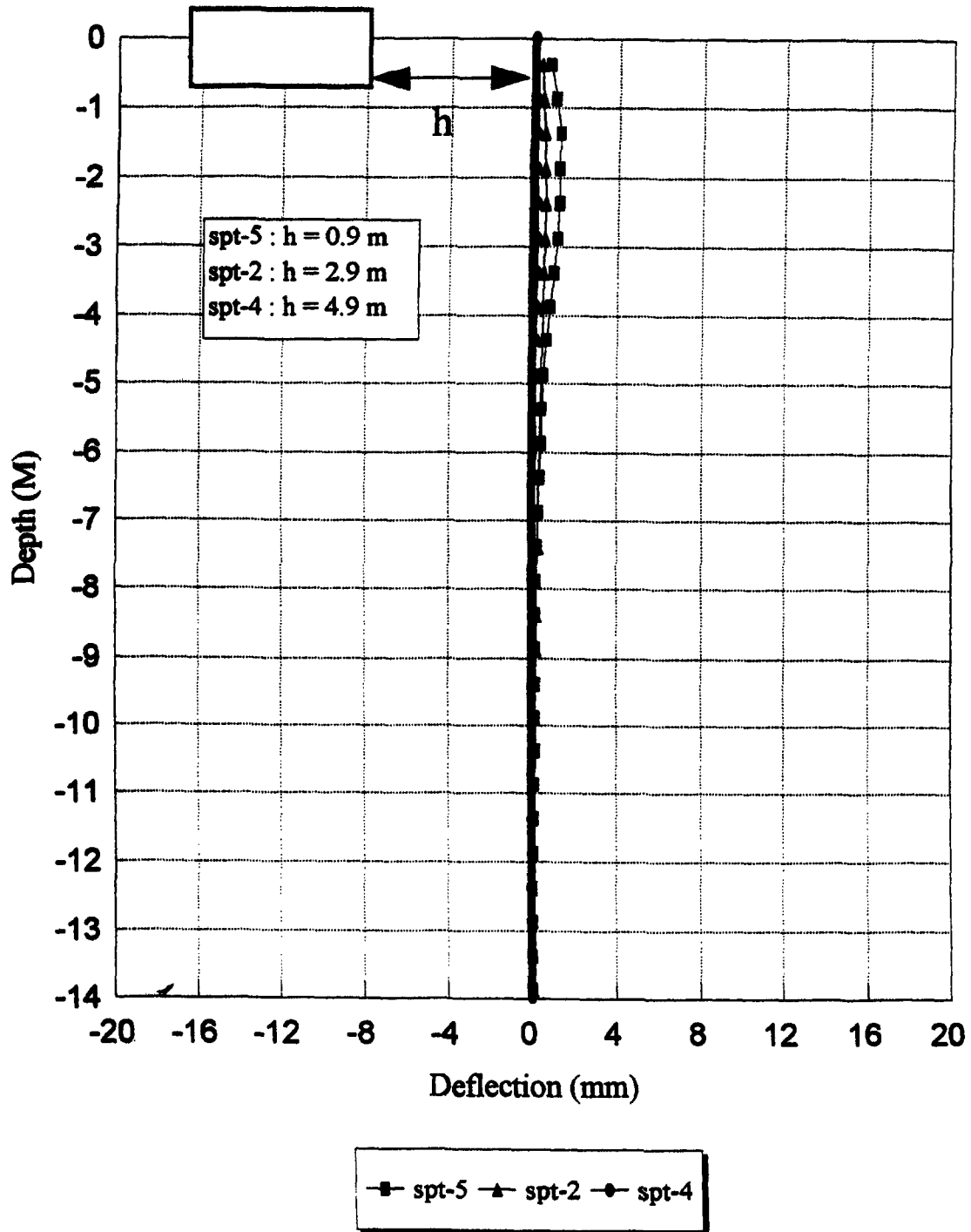


Figure D6: Inclinometer Test -3.12-MN Creep Load - E-W Direction, 2.5-mFooting

## 7.03 MN Failure Test 2.5 M Footing (East-West)

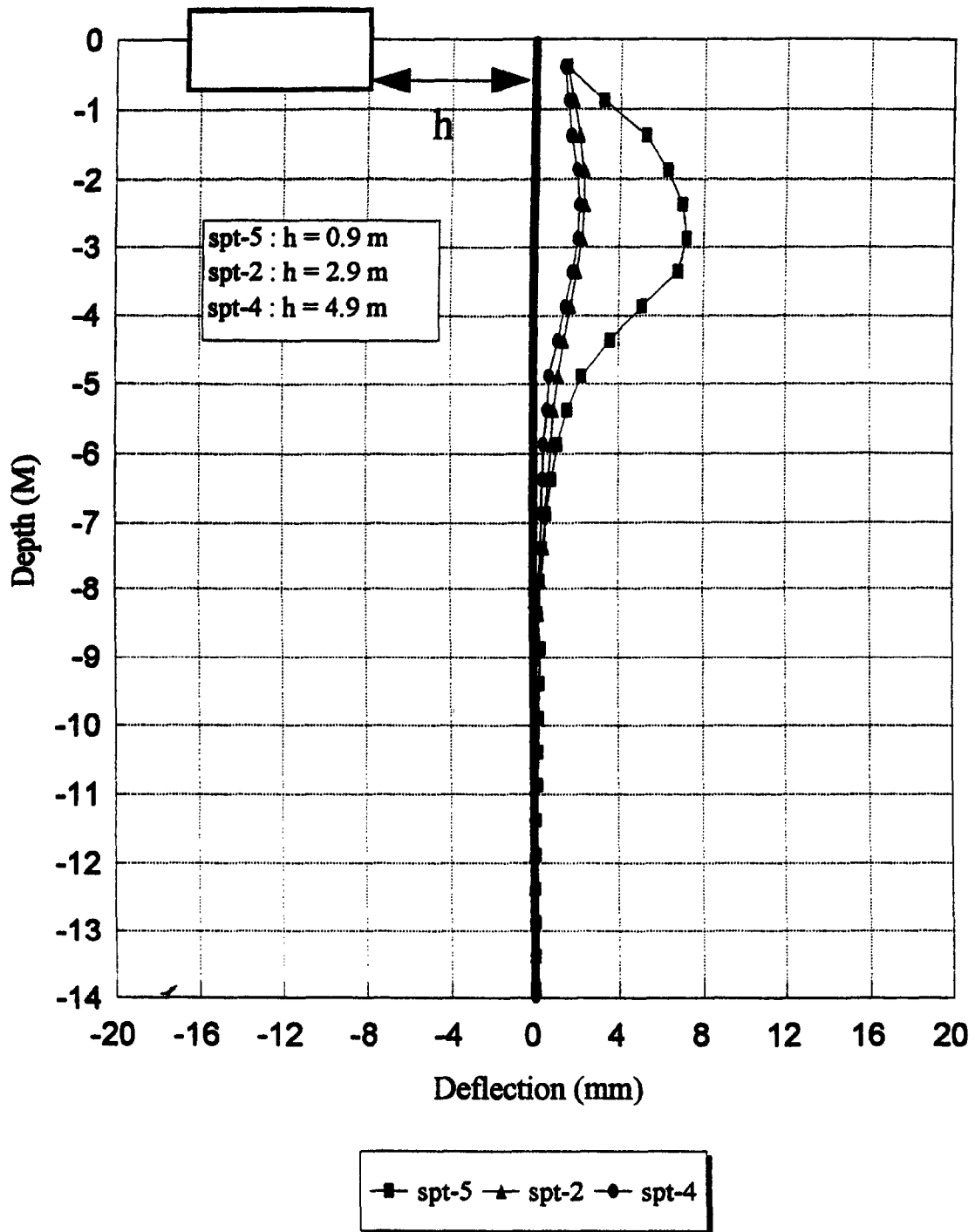


Figure D7: Inclinometer Test -7.03-MN Failure Load - E-W Direction, 2.5-m Footing

# 4.45 MN Creep Test

## 3.0 M Footing - North (North-South)

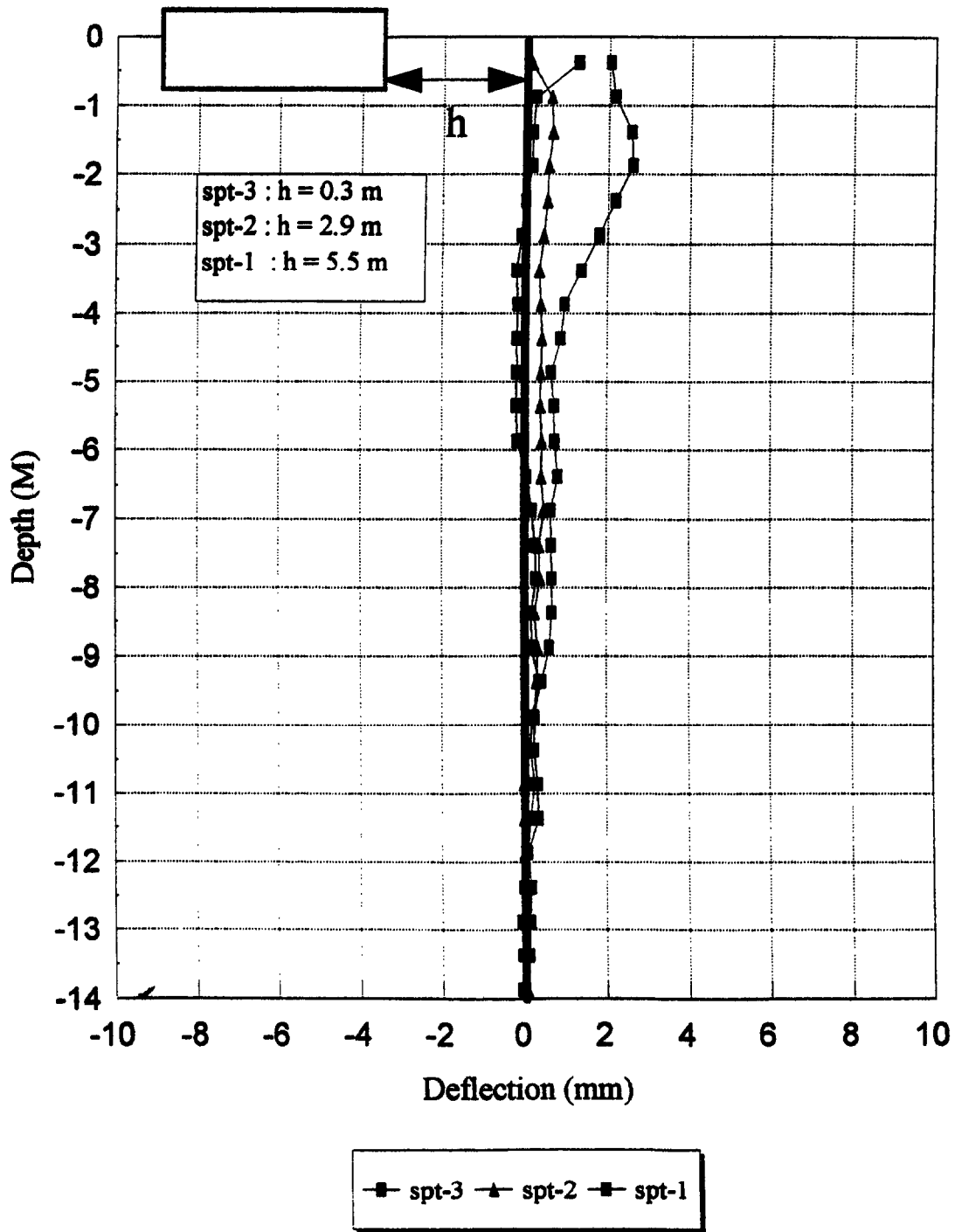


Figure D8: Inclinometer Test -4.45-MN Creep Load - N-S Direction, 3.0-m(s) Footing

# 8.90 MN Failure Test

## 3.0 M Footing - North (North-South)

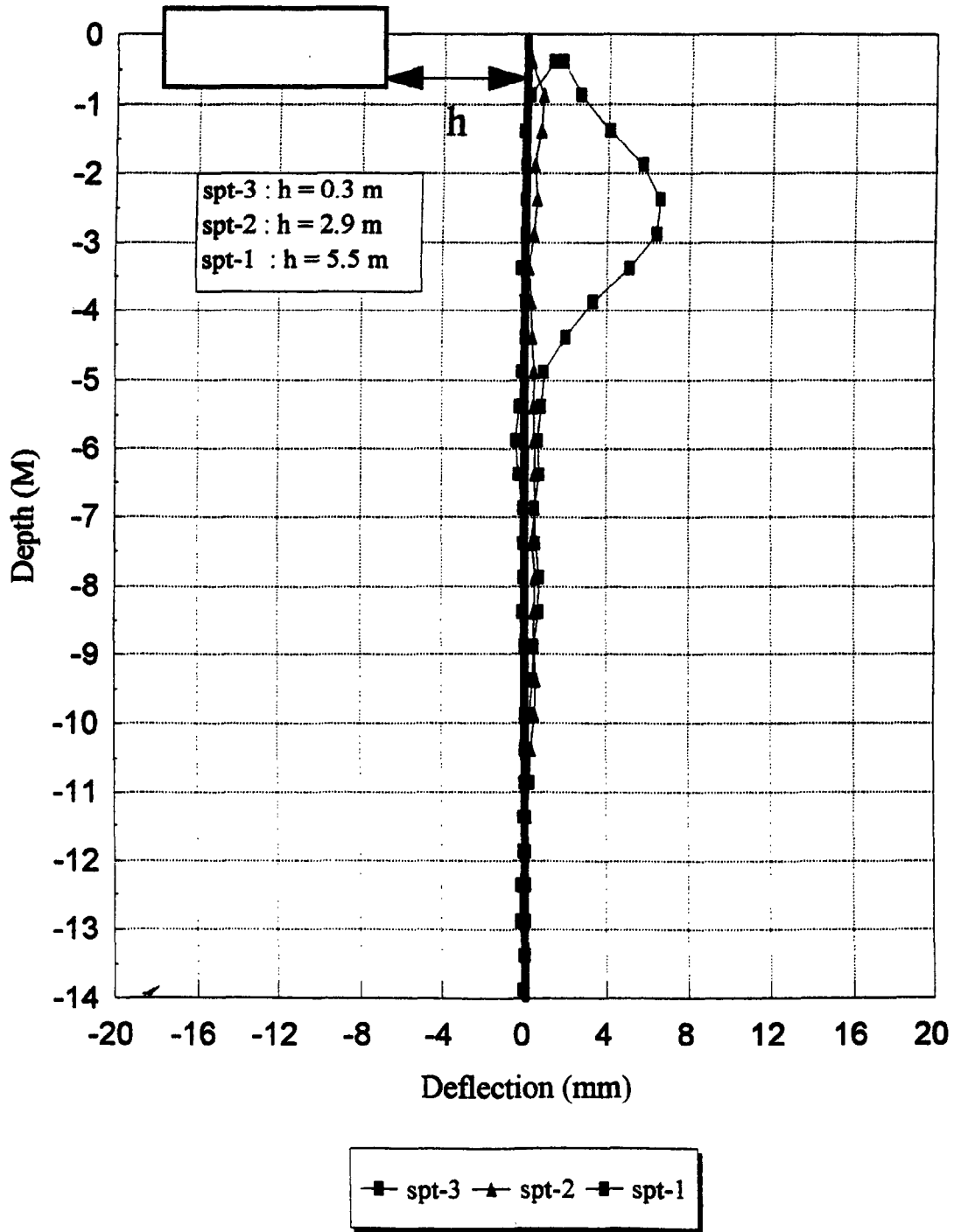
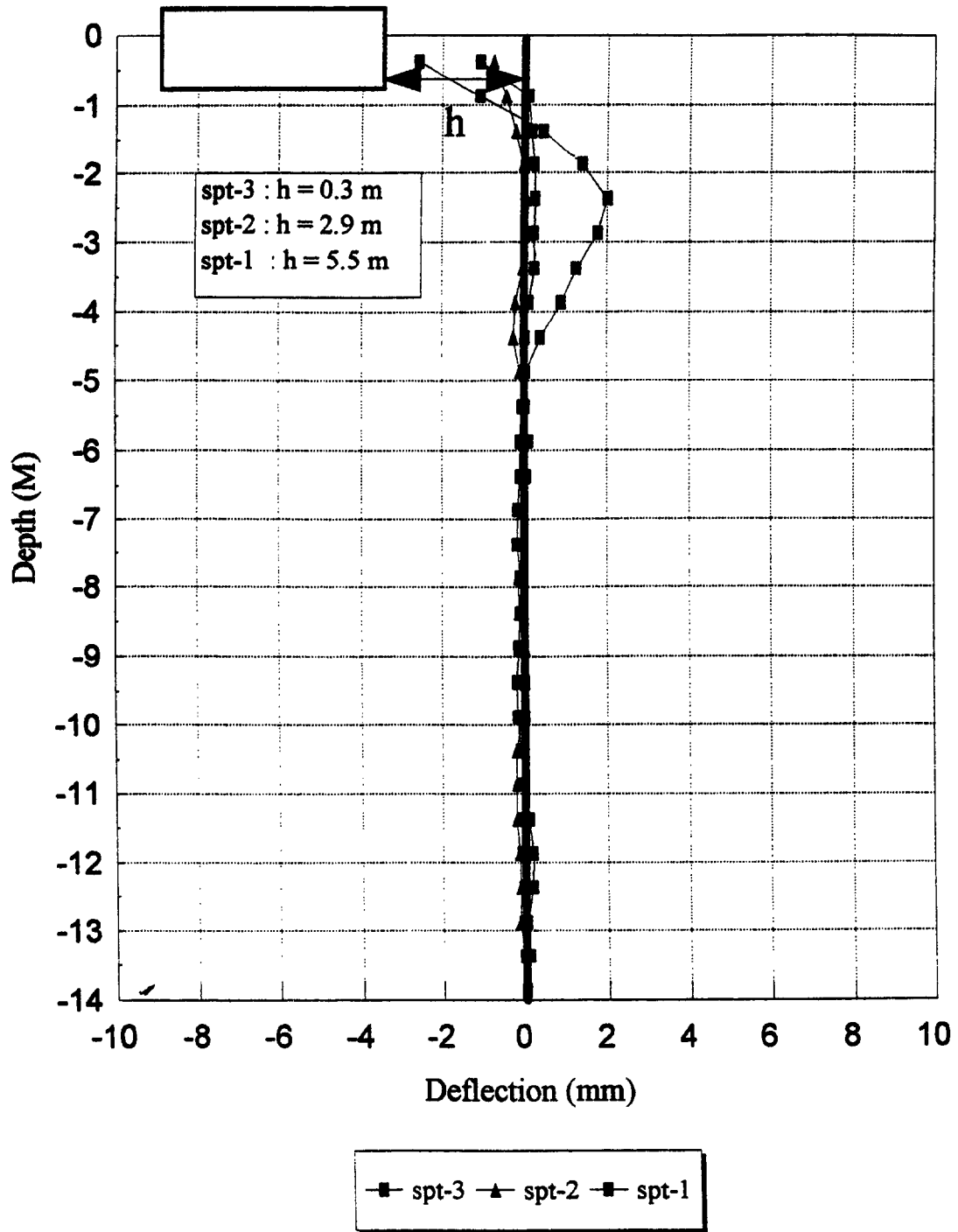


Figure D9: Inclinometer Test -8.90-MN Failure Load - N-S Direction, 3.0-m(n) Footing

**4.45 MN Creep Test**  
**3.0 M Footing - North (East-West)**



**Figure D10:** Inclinometer Test - 4.45-MN Creep Load - E-W Direction, 3.0-m(n) Footing

### 8.90 MN Failure Test 3.0 M Footing - North (East-West)

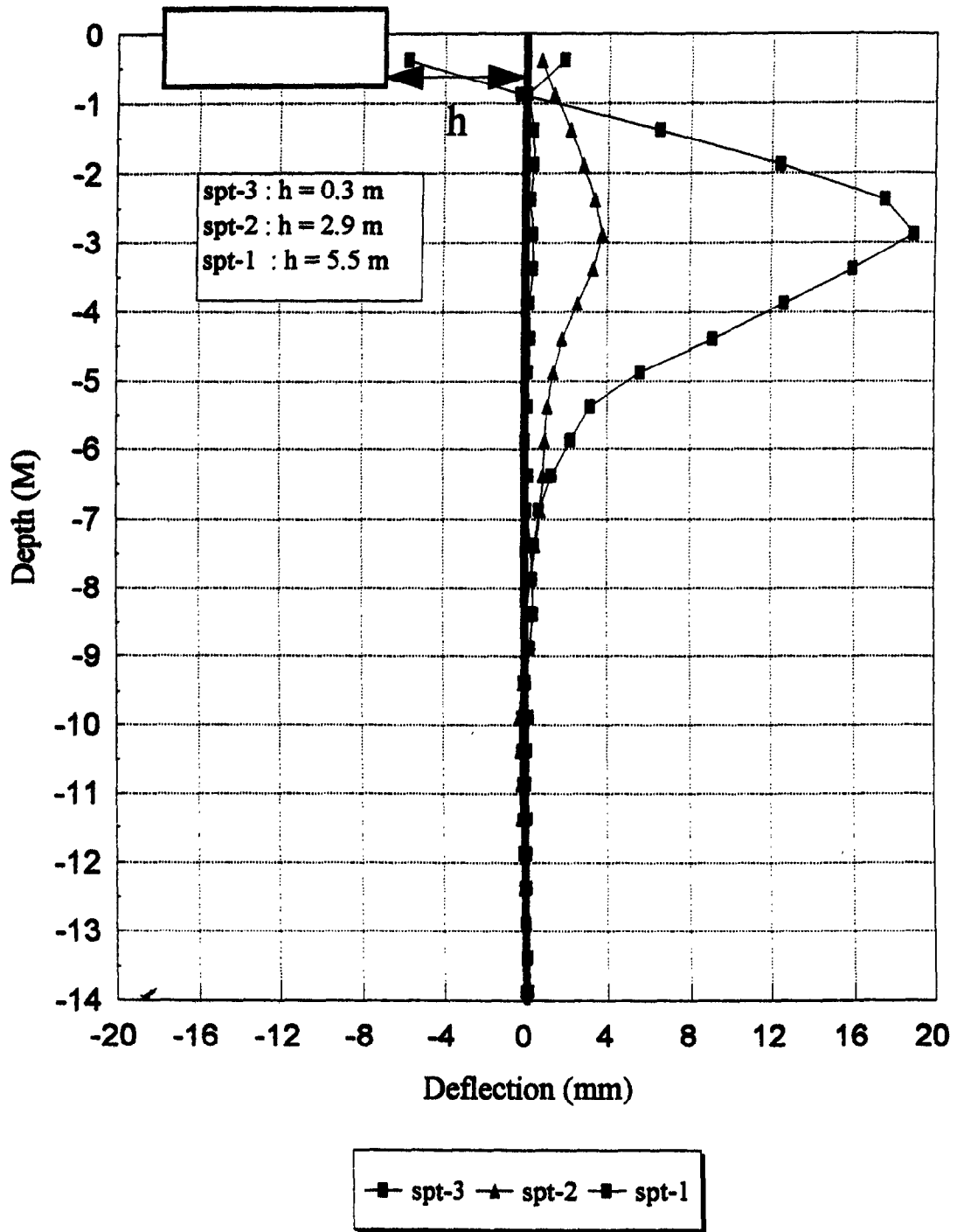


**Figure D11: Inclinometer Test -8.90-MN Failure Load -E-W Direction, 3.0-m(n) Footing**

### 4.45 MN Creep Test 3.0 M Footing - South (North-South)

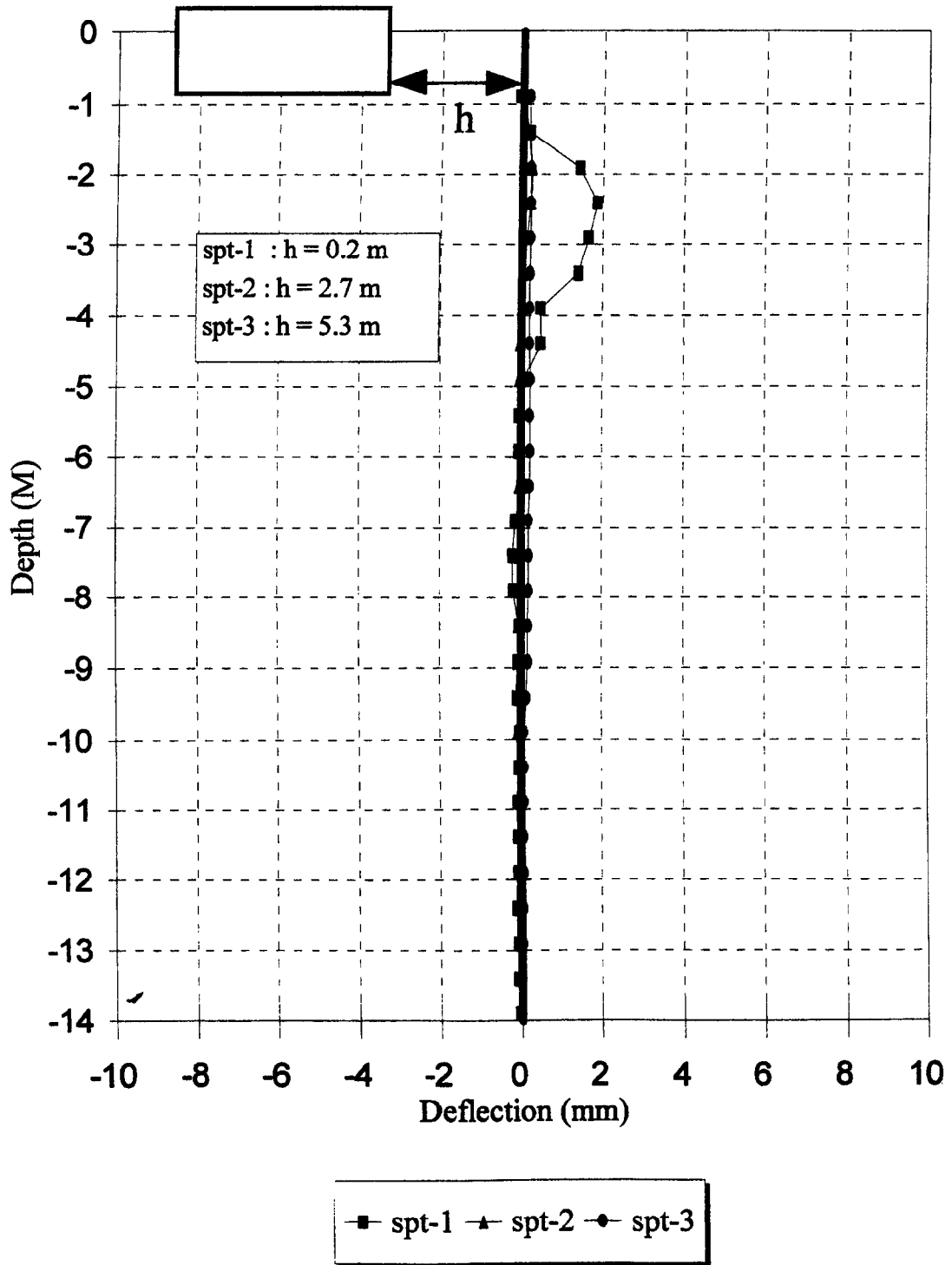


**Figure D12:** Inclinometer Test -4.45-MN Creep Load - N-S Direction, 3.0-m(n) Footing

**8.90 MN Failure Test**  
**3.0 M Footing - South (North-South)**

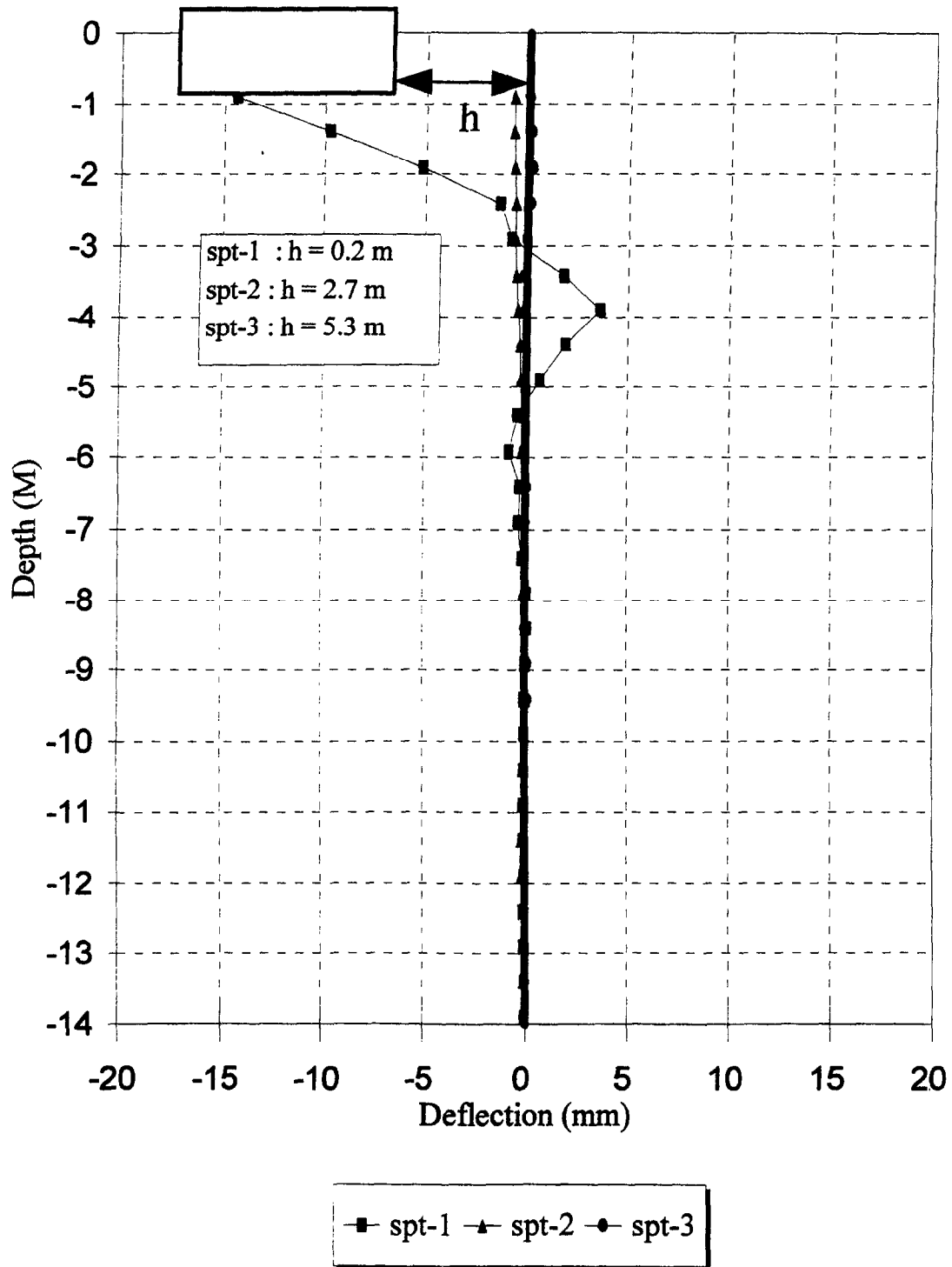


**Figure D13: Inclinometer Test - 8.90 MN Failure Load - N-S Direction, 3.0 m(s) Footing**

### 4.45 MN Creep Test 3.0 M Footing - South (East-West)

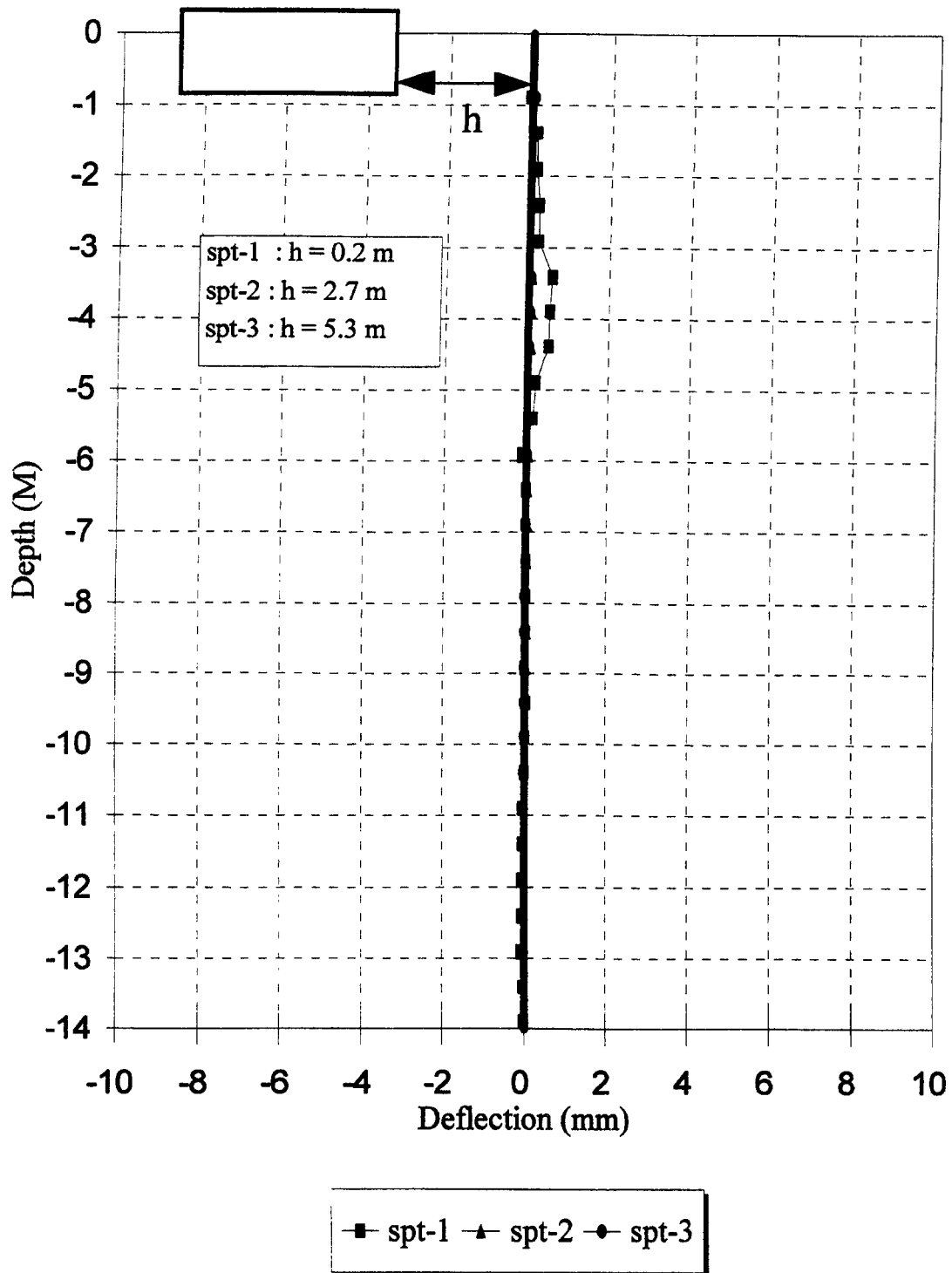


Figure D14: Inclinometer Test -4.45-MN Creep Load - E-W Direction, 3.0-m(s) Footing

# 8.90 MN Failure Test

## 3.0 M Footing - South (East-West)

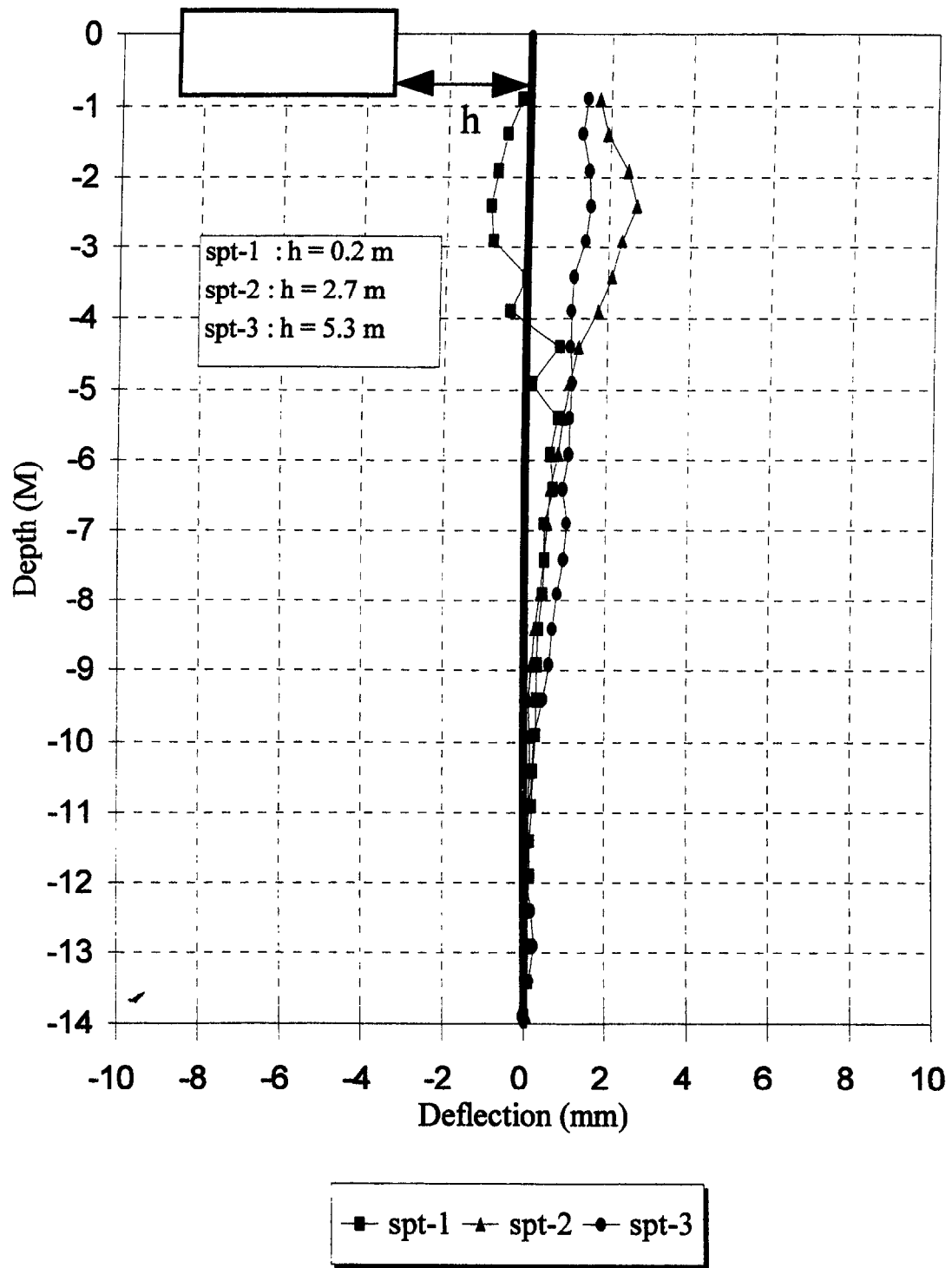
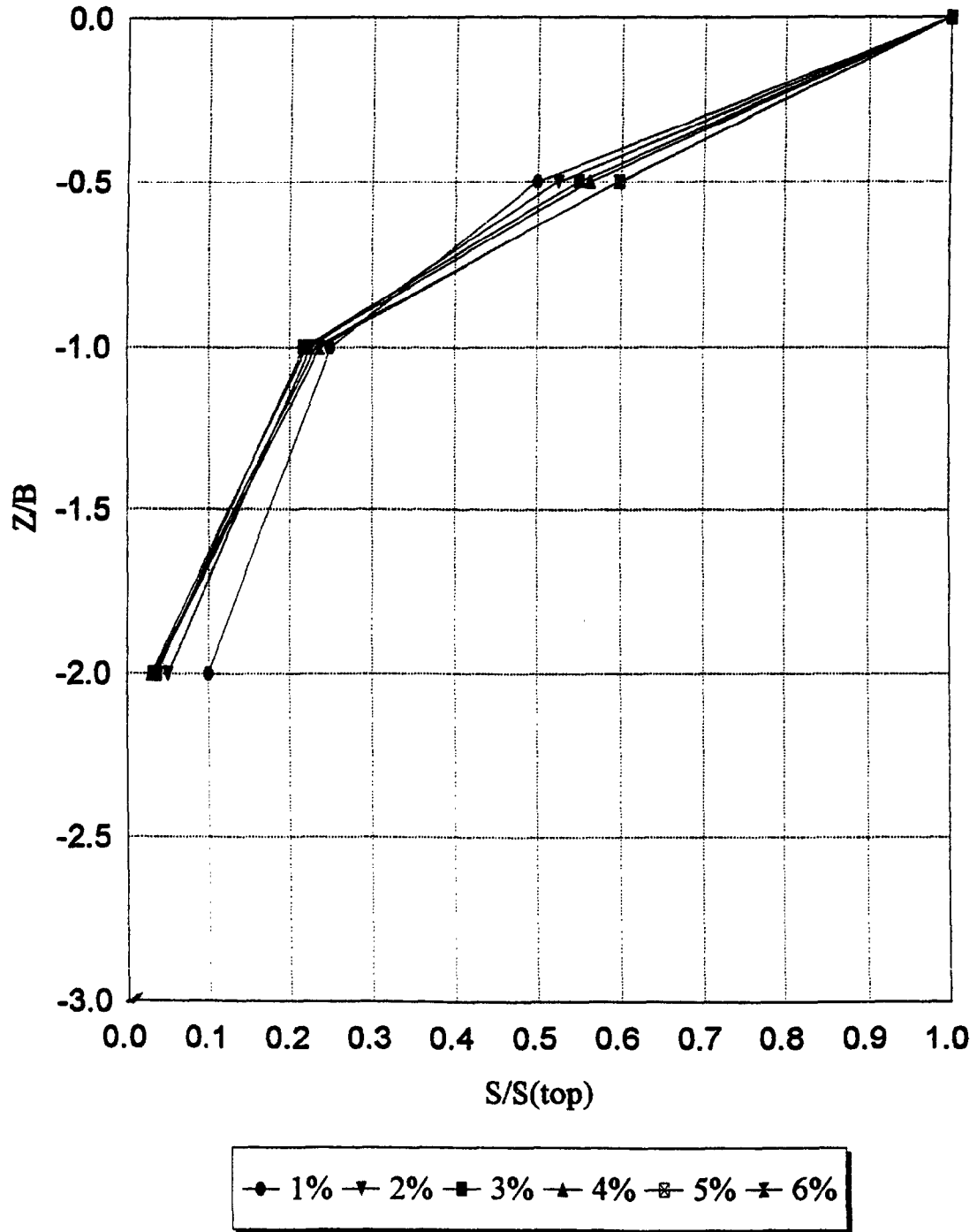


Figure D15: Inclinometer Test - 8.90 MN Failure Load - E-W Direction, 3.0 m(s) Footing

## **APPENDIX E: Telltale Results**

## S/S(top) versus Depth 1.0 M Footing



**Figure E1: Settlement Versus Depth for 1.0-m Footing With Varying Percentages of B**

## S/S(top) versus Depth 1.5 M Footing

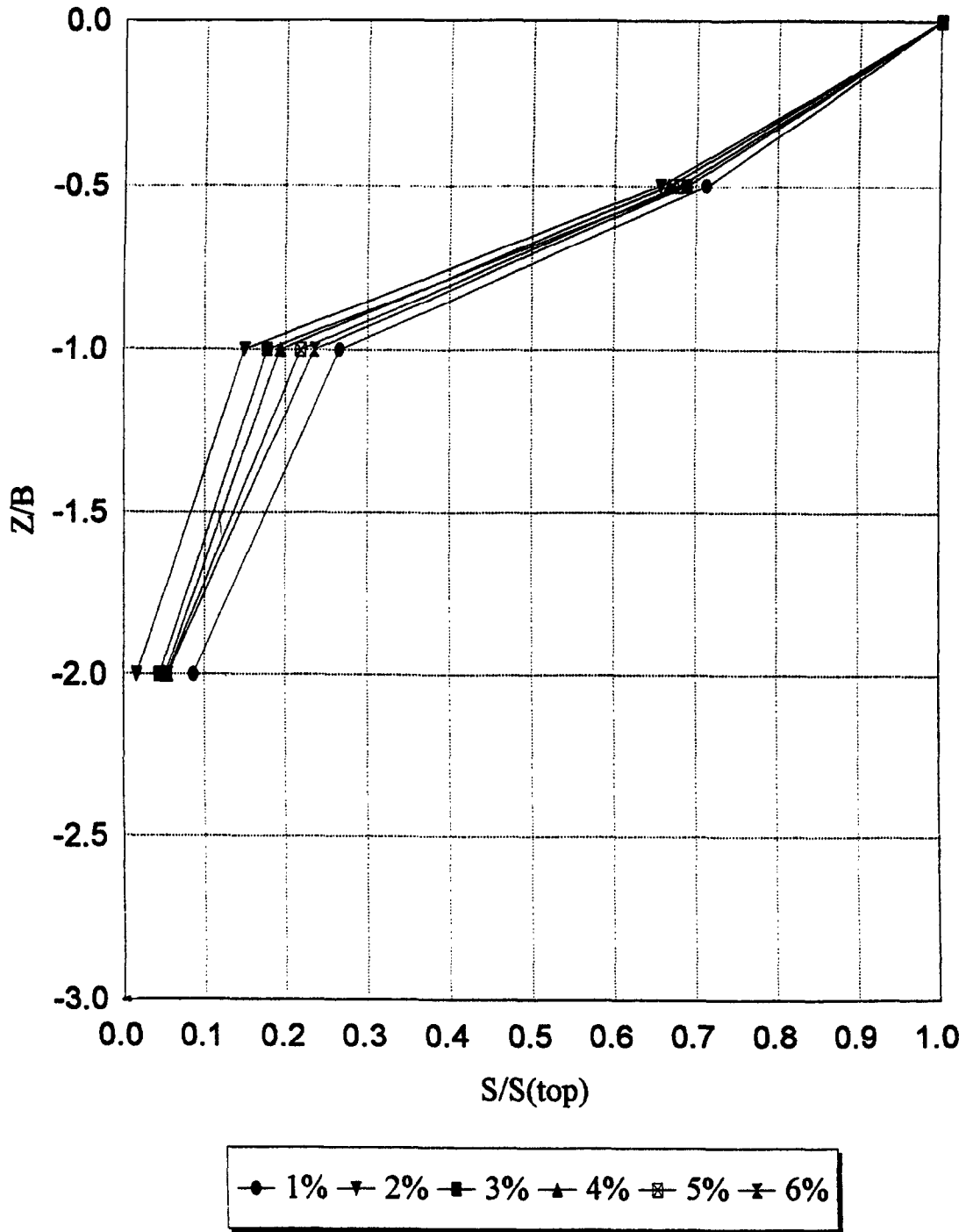


**Figure E2: Settlement Versus Depth for 1.5-m Footing With Varying Percentages of B**

# S/S(top) versus Depth

3.0 M Footing

SOUTH

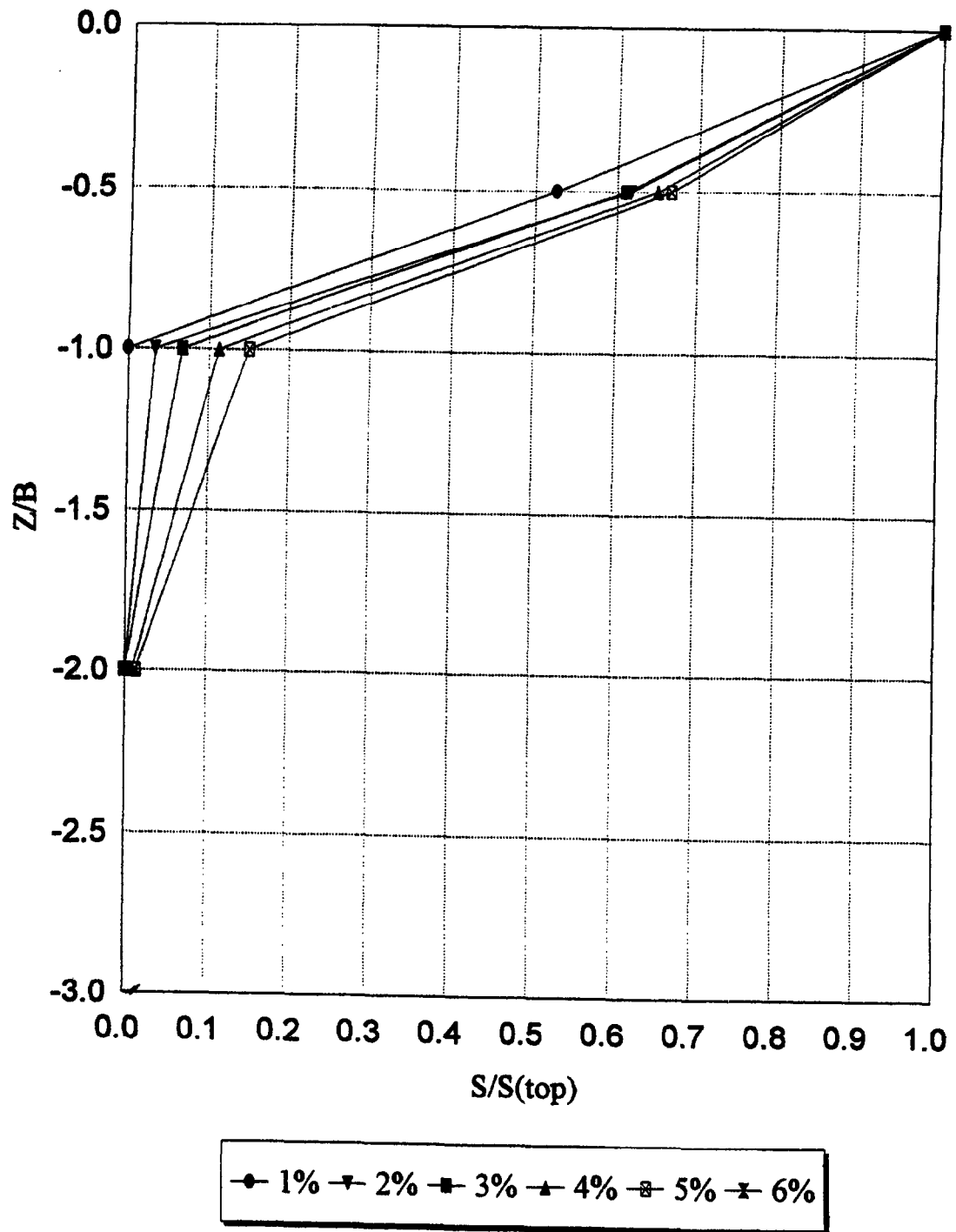


Figure E3: Settlement Versus Depth for 3.0-m(s) Footing With Varying Percentages of B

# S/S(top) versus Depth 3.0 M Footing

NORTH

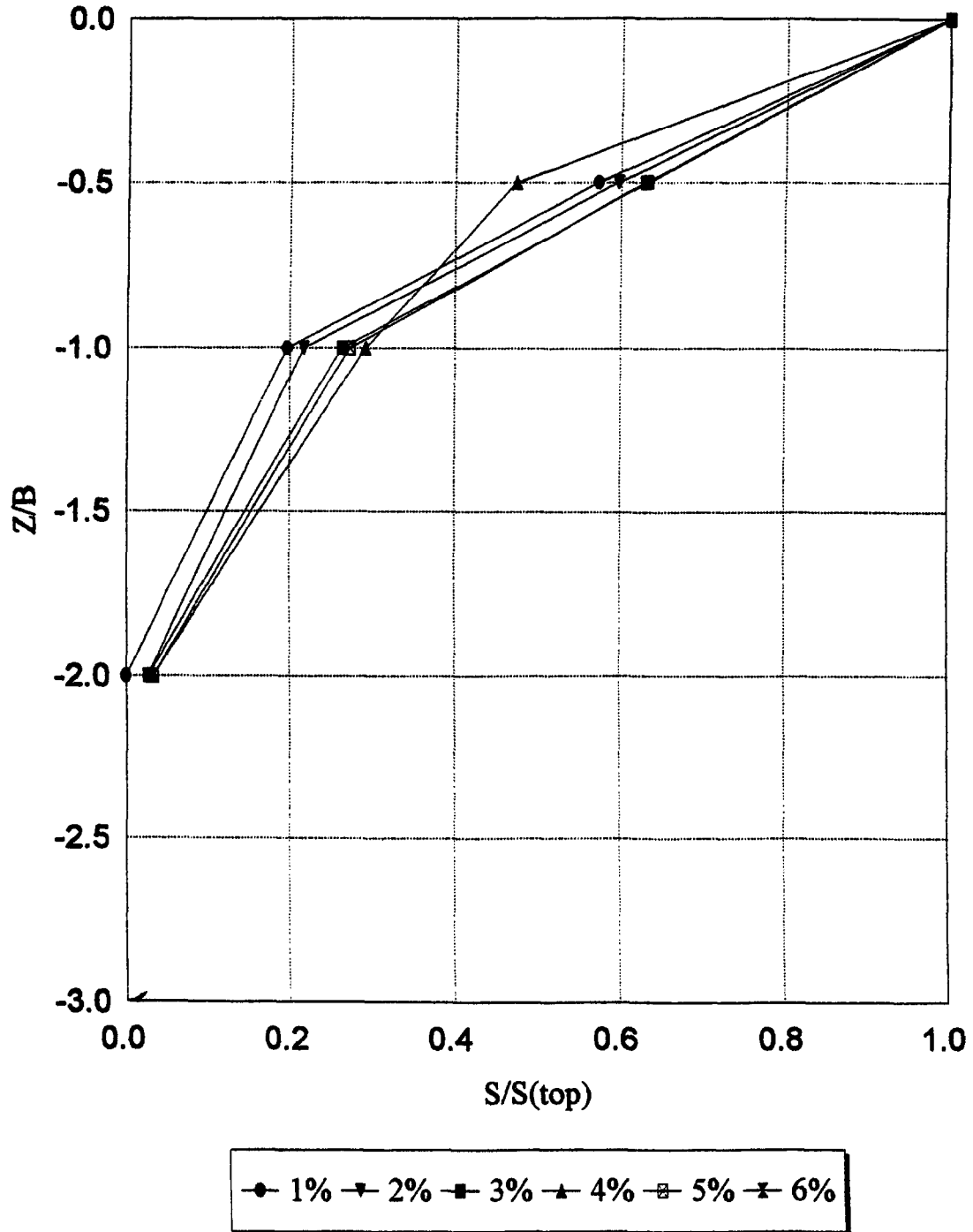


Figure E4: Settlement Versus Depth for 3.0-m(n) Footing With Varying Percentages of B

## REFERENCES

- Amar, S., Baguelin, F., and Canepa, Y. (1984). "Etude experimentale du comportement des fondations superficielles" *Annales de l'ITBTP*, Paris.
- Amar, S., Baguelin, F., and Canepa, Y. (1989). *Shallow Foundation Design Based Upon Static Penetrometer Tests*, Personal communication to J.-L. Briaud.
- Anagnostopoulos, A.G., Papadopoulos, B.P., and Kavvadas, M.J. (1992). "SPT and the Compressibility of Cohesionless Soils", *Proceedings of the 2nd European Symposium on Penetration Testing*, Amsterdam.
- Ballouz, M. and Briaud, J.-L. (1994). *LATWAK: An Impact Test to Obtain the Lateral Static Stiffness of Piles*, Unpublished Report, FHWA Contract No. DTFH61-92-Z-00050. Washington, DC. (1992).
- Ballouz, M., Maxwell J., Briaud, J.-L. (1995). *WAK Tests on 5 Full Scale Footings in Sand*, Unpublished Report, FHWA Contract No. DTFH61-92-Z-00050. Washington, DC. (1992).
- Baus, R.N. (1991) "Data for ASCE Geotechnical Division's Shallow Foundations Committee Data Base" Communication of L. Baus (Department of Civil Engineering, University of South Carolina, Columbia, SC) to J.L. Briaud (Texas A&M University, College Station, TX).
- Bergdahl U., Hult G., Ottosson E. (1985). "Calculation of Settlements of Footings on Sands", *11<sup>th</sup> International Conference on Soil Mechanics and Foundation Engineering*, A.A.Balkema Publishers, Rotterdam, 2167-2170.
- Bowles, J.E. (1988). *Foundation Analysis and Design*, 4th Edition, McGraw-Hill, New York.
- Briaud, J.-L. (1992). *The Presuremeter*, A.A.Balkema Publishers, Brookfield, Vermont.
- Briaud, J.-L. (1993). "The National Geotechnical Experimentation Sites at Texas A&M University: Data Collected Until 1992", *Report to the Federal Highway Administration and the National Science Foundation*, Civil Engineering, Texas A&M University.
- Briaud,, J.-L. (1993a). "Spread Footing Design and Performance", *Federal Highway Administration Workshop at the 10<sup>th</sup> Annual International Bridge Conference and Exhibition*, Pittsburg.
- Briaud, J.-L., and Garland, E. (1985). "Loading Rate Method for Pile Response in Clay" *ASCE Journal of Geotechnical Engineering*, 3(3).

Briaud, J.-L. and Gibbens, R. (1994). "Predicted and Measured Behavior of Five Spread Footings on Sand," *Geotechnical Special Publication No. 41, ASCE Specialty Conference: "Settlement '94"*, ASCE, New York.

Briaud, J.-L. and Lepert, P. (1990). "WAK Test to Find Spread Footing Stiffness," *Journal of Geotechnical Engineering*, ASCE, 116(3), 415-431.

Burland, J.B., and Burbridge, B.C. (1984). "Settlement of Foundations on Sand and Gravel", *Proceedings of the Institute of Civil Engineers, Glasgow and West Scotland Association*, 1325-1379.

Burmister, D.M. (1947). "Discussion in Symposium on Load Tests of Bearing Capacity of Soils" *ASTM STP No. 79*, ASTM, Philadelphia, PA, 139-146.

DeBeer, E. (1965). "Bearing Capacity and Settlement of Shallow Foundations on Sand", *Proceedings, Symposium on Bearing Capacity and Settlement of Foundations*, Duke University, Durham, NC, 315-335.

Dimillio, A. (1994). "FHWA Spread Footing Load Tests at Fairbank 1985 and 1991" Personal Communication from A. Dimillio (HNR-30, FHWA, 6300 Georgetown Pike, McLean, VA 22101) to J.L. Briaud (Texas A&M University, College Station, TX).

Garga, V.K., Quin, J.T. (1974). "An Investigation on Settlements of Direct Foundations on Sand" *Conference on Settlement of Structures*, British Geotechnical Society, Cambridge.

Gibbens, R., and Briaud, J.-L. (1995). *Load Tests on Five Large Spread Footings on Sand and Evaluation of Prediction Methods*, Unpublished Report, FHWA Contract No. DTFH61-92-Z-00050. Washington, DC. (1992).

Gibbs, H.J., Holtz, W.G. (1957). "Research on Determining the Density of Sands by Spoon Penetration Testing", *Proceedings, 4th International Conference on Soil Mechanics and Foundation Engineering*, Vol. 1, London.

Gifford, D.G., Kraemer, S.R., McKown, A.F., Wheeler, J.R. (1989). "Load Settlement Curves, Settlement Observation s-10 Highway Bridges" Communication to F. Yokel (NIST) from Haley & Aldrich (Haley & Aldrich Inc., 238 Main Street, Cambridge, MA 02142).

Gifford, D.G., Perkins, J.R. (1989). "Load Settlement Curves, Settlement Observation s-10 Highway Bridges" Communication to F. Yokel (NIST) from Haley & Aldrich (Haley & Aldrich Inc., 238 Main Street, Cambridge, MA 02142).

- Hansen, J.B. (1970). "A Revised and Extended Formula for Bearing Capacity", Danish Geotechnical Institute, No. 28, Copenhagen.
- Jeanjean, P., and Briaud, J.-L. (1994). *Footings on Sand from Pressuremeter Test*, Unpublished Report, FHWA Contract No. DTFH61-92-Z-00050. Washington, DC. (1992).
- Lockett, L. (1981). "Project I-359-3(5): Load Test at the 15<sup>th</sup> Street Bridge on I-359 Spur, Tuscaloosa County" *Alabama DOT Records*, September 24, 1981, Montgomery.
- Maxwell, J. and Briaud, J.-L. (1991). "WAK Tests on 53 Footings," *Research Report*, Civil Engineering, Texas A&M University.
- Menard, L., and Rousseau, J. (1962). "L'evaluation des Tassements - Tendances Nouvelles", *Sols-Soils*, 1(1), 13-28.
- Meyerhof, G.G. (1951). "The Ultimate Bearing Capacity of Foundations", *Geotechnique*, 2(4), 301-331.
- Meyerhof, G.G. (1963). "Some Recent Research on the Bearing Capacity of Foundations", *CGJ*, Ottawa, Canada.
- Meyerhof, G.G. (1965). "Shallow Foundations", *Journal of the Soil Mechanics and Foundations Division*, 91(SM2), 21-31.
- Meyerhof, G.G. (1983). "Scale Effect of Ultimate Pile Capacity" *Journal of Geotechnical Engineering*, ASCE, 109(6), 797-806.
- Nasr, G., and Briaud, J.-L. (1995). *The Shallow Foundation Data Base: SHALDB(Version 4.0)*, Unpublished Report, FHWA Contract No. DTFH61-92-Z-00050. Washington, DC. (1992).
- NAVFAC, (1982). *Soil Mechanics, Design Manual 7.1*, U.S. Department of Navy, U.S. Government Printing Office, Washington, DC.
- Osterberg J.S. (1947). "Discussion in Symposium on Load Tests of Bearing Capacity of Soils", *ASTM STP 79*, ASTM, Philadelphia, PA, 128-139.
- Palmer L.A. (1947). "Field Loading Tests for the Evaluation of the Wheel Load Capacities of Airport Pavements", *ASTM STP 79*, ASTM, Philadelphia, PA. 9-30.
- Parry, R.H.G. (1971). "A Direct Method of Estimating Settlements in Sands from SPT Values", *Symposium on Interaction of Structure and Foundation*, Foundation Engineering Society, Birmingham.

Peck, R.B., and Bazaraa, A.R.S. (1967). "Settlement of Spread Footings From SPT Values", *Proceedings, Symposium on Interaction of Structure and Foundation*, Foundation Engineering Society, Birmingham, 905-909.

Peck, R.B., Hanson, W.E., and Thornburn, T.H. (1974). *Foundation Engineering*, 2nd Edition, John Wiley & Sons, New York.

Schmertmann, J.H. (1970). Static Cone to Compute Static Settlement of Spread Footings on Sand", *Journal of Soil Mechanics and Foundation Division*, 96(SM3), 1011-1043.

Schmertmann, J.H. (1986). "Dilatometer to Compute Foundation Settlement", *Proceedings of In Situ' 86, Specialty Conference on Use of In Situ Tests and Geotechnical Engineering*, ASCE, New York, 303-321.

Schmertmann, J.H., Hartman, J.P., Brown, P.B. (1978). "Improve Strain Influence Factor Diagrams", *Journal of the Geotechnical Engineering Division*, ASCE, 104(GT8).

Schultze, E., and Sherif, G. (1973). "Prediction of Settlements from Evaluated Settlement Observations on Sand", *Proceedings, 8th International Conference on Soil Mechanics and Foundation Engineering*, Moscow, 225-230.

Seed, H.B., and Reese, L.C. (1957). "The Action of Soft Clay Along Friction Piles", *Transactions of the ASCE*, Paper 2882, 731-764.

Skempton, A.W. (1951). The Bearing Capacity of Clays" *Proceedings of the Building Research Congress*, Institution of Civil Engineers, London, Division I, 180-189.

Skyles, D.L. (1992). "Evaluation of Predicting Shallow Foundation Settlement in Sands from Dilatometer Tests" *Report to FHWA and Masters Thesis*, Department of Civil Engineering, University of Florida, Gainesville.

Terzaghi, K. (1943). Evaluation of Coefficient of Subgrade Reaction, *Geotechnique*, 5(4), 297-326.

Terzaghi, K., and Peck, R.B. (1967). *Soil Mechanics in Engineering Practice*, John Wiley and Sons, Inc., New York.

Vesic, A.S. (1973). "Analysis of Ultimate Loads of Shallow Foundations", *JSMFD*, ASCE, 99(SM1), 45-73.

Vesic, A.S. (1974). *Foundation Engineering Handbook*, Van Nostrand Reinhold Book Co., New York.